

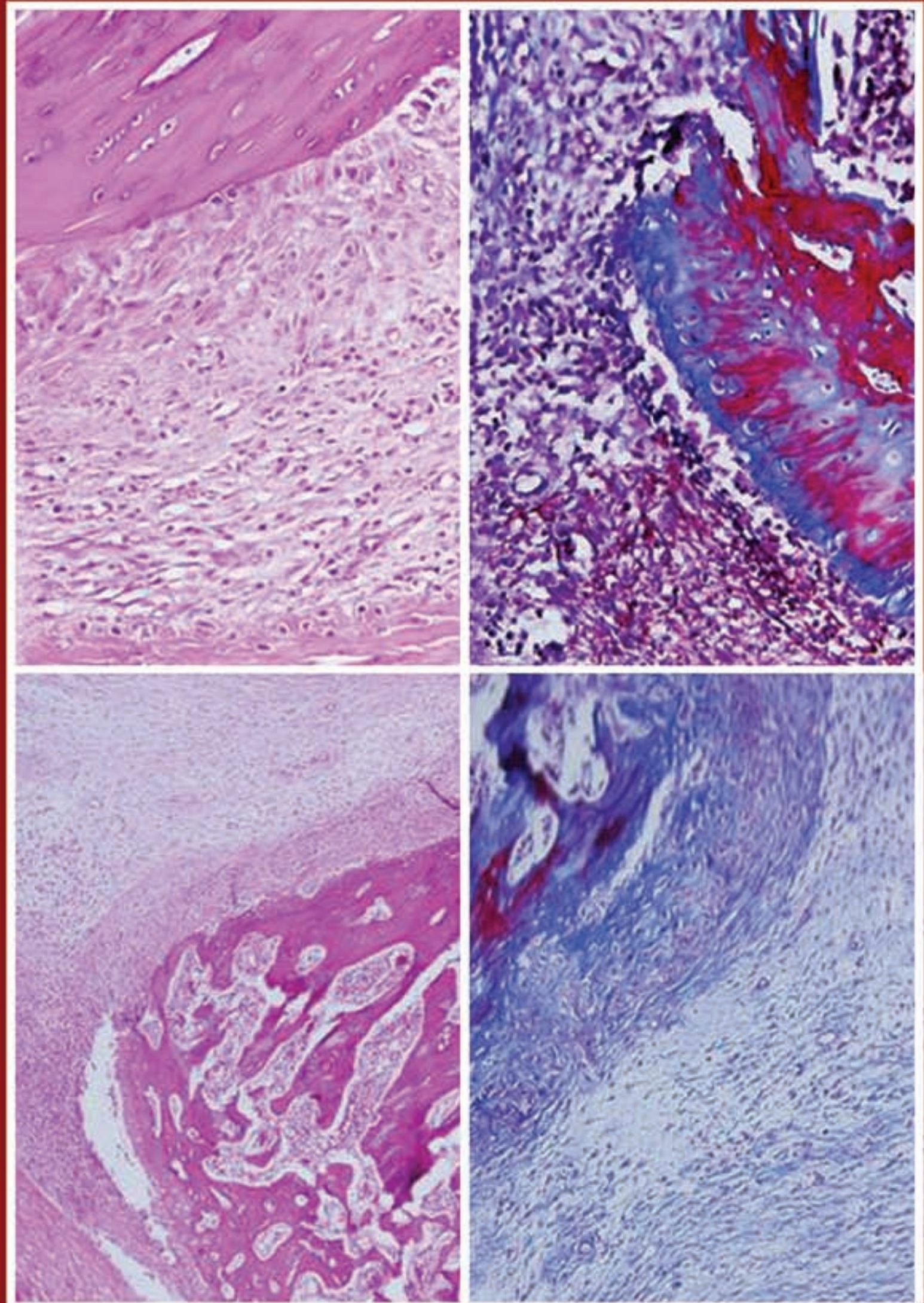
CELL JOURNAL

(Yakhteh)

Vol 25, No 12, December 2023, Serial Number: 119
Pages: 813-882

ISSN: 2228-5806
eISSN: 2228-5814

www.celljournal.org



Aims and Scope: The "Cell Journal (Yakhteh)" is a peer review and monthly English publication of Royan Institute of Iran. The aim of the journal is to disseminate information by publishing the most recent scientific research studies based on medical and developmental biology including cell therapy and regenerative medicine, stem cell biology reproductive medicine, medical genetics, immunology, oncology, clinical biochemistry, neuroscience, and tissue engineering. **Cell J**, has been certified by the Ministry of Culture and Islamic Guidance since 1999 and accredited as a scientific and research journal by HBI (Health and Biomedical Information) Journal Accreditation Commission since 2000 which is an open access journal. **This journal holds the membership of the Committee on Publication Ethics (COPE).**

1. Types of articles

The articles in the field of Cellular and Molecular can be considered for publications in **Cell J**. These articles are as below:

A. Original articles

Original articles are scientific reports of the original research studies. The article consists of English Abstract (structured), Introduction, Materials and Methods, Results, Discussion, Conclusion, Acknowledgements, Author's Contributions, and References (**Up to 40**).

B. Review articles

Review articles are the articles written by well experienced authors and those who have excellence in the related fields. The corresponding author of the review article must be one of the authors of at least three published articles appearing in the references. The review article consists of English Abstract (unstructured), Introduction, Conclusion, Author's Contributions, and References (**Up to 90**).

C. Systematic Reviews

Systematic reviews are a type of literature review that collect and critically analyzes multiple research studies or papers. The Systematic reviews consist of English Abstract (unstructured), Introduction, Materials and Methods, Results, Discussion, Conclusion, Acknowledgements, Author's Contributions, and References (**Up to 90**).

D. Short communications

Short communications are articles containing new findings. Submissions should be brief reports of ongoing researches. The short communication consists of English Abstract (unstructured), the body of the manuscript (should not hold heading or sub-heading), Acknowledgements, Author's Contributions, and References (**Up to 30**).

E. Case reports

Case reports are short discussions of a case or case series with unique features not previously described which make an important teaching point or scientific observation. They may describe novel techniques or use equipment, or new information on diseases of importance. It consists of English Abstracts (Unstructured), Introduction, Case Report, Discussion, Acknowledgements, Author's Contributions, and References (**Up to 30**).

F. Commentary

Commentaries are short articles containing a contemporary issue that is relevant to the journal's scope and also expressing a personal opinion or a new perspective about existing research on a particular topic. The Commentary consists of English Abstract (unstructured), the body of the manuscript (should not hold heading or subheading), Acknowledgements, Author's Contributions, and References (**Up to 30**).

G. Editorial

Editorials are articles should be written in relevant and new data of journals' filed by either the editor in chief or the editorial board.

H. Imaging in biology

Images in biology should focus on a single case with an interesting illustration such as a photograph, histological specimen or investigation. Color images are welcomed. The text should be brief and informative.

I. Letter to the editors

Letter to the editors are in response to previously published **Cell J** articles, and may also include interesting cases that do not meet the requirement of being truly exceptional, as well as other brief technical or clinical notes of general interest.

J. Debate

Debates are articles which show a discussion of the positive and negative view of the author concerning all aspect of the issue relevant to scientific research.

2. Submission process

It is recommended to see the guidelines for reporting different kinds of manuscripts. This guide explains how to prepare the manuscript for submission. Before submitting, we suggest authors to familiarize themselves with **Cell J** format and content by reading the journal via the website (www.celljournal.com). The corresponding author ensures that all authors are included in the author list and agree with its order, and they must be aware of the manuscript submission.

A. Author contributions statements

It is essential for authors to include a statement of responsibility in the manuscript that specifies all the authors' contributions. This participation must include: Conceptualization, Methodology, Software, Validation, Formal analysis, Investigation, Resources, Data Curation, Writing - Original Draft, Writing - Review & Editing, Visualization, Supervision, Project administration, and Funding acquisition. Authors who do not meet the above criteria should be acknowledged in the Acknowledgments section.

B. Cover letter and copyright

Each manuscript should be accompanied by a cover letter, signed by all authors specifying the following statement: "The manuscript has been seen and approved by all authors and is not under active consideration for publication. It has neither been accepted for publication nor published in another journal fully or partially (except in abstract form). **Also, no manuscript would be accepted in case it has been pre-printed or submitted to other websites.** I hereby assign the copyright of the enclosed manuscript to **Cell J**." The corresponding author must confirm the proof of the manuscript before online publishing. It is needed to suggest three peer reviewers in the field of their manuscript.

C. Manuscript preparation

Authors whose first language is not English encouraged to consult a native English speaker in order to confirm his manuscripts to American or British (not a mixture) English usage and grammar. It is necessary to mention that we will check the plagiarism of your manuscript by iThenticate Software. The manuscript should be prepared in accordance with the "International Committee of Medical Journal Editors (ICMJE)". Please send your manuscript in two formats word and PDF (including: title, name of all the authors with their degree, abstract, full text, references, tables and figures) and also send tables and figures separately in the site. The abstract and text pages should have consecutive line numbers in the left margin beginning with the title page and continuing through the last page of the written text. Each abbreviation must be defined in the abstract and text when they are mentioned for the first time. Avoid using abbreviation in the title. Please use the international and standard abbreviations and symbols

It should be added that an essential step toward the integration and linking of scientific information reported in published literature is using standardized nomenclature in all fields of science and medicine. Species names must be italicized (*e.g.*, *Homo sapiens*) and also the full genus and species written out in full, both in the title of the manuscript and at the first mention of an organism in a paper.

It is necessary to mention that genes, mutations, genotypes, and alleles must be indicated in italics. Please use the recommended name by consulting the appropriate genetic nomenclature database, *e.g.*, HUGO for human genes. In another words; if it is a human gene, you must write all the letters in capital and italic (*e.g.*, *OCT4*, *c-MYC*). If not, only write the first letter in capital and italic (*e.g.*, *Oct4*, *c-Myc*). **In addition, protein designations are the same as the gene symbol but are not italicized.**

Of note, Cell J will only consider publishing genetic association study papers that are novel and statistically robust. Authors are advised to adhere to the recommendations outlined in the STREGA statement (<http://www.strega-statement.org>). The following criteria must be met for all submissions:

1. Hardy-Weinberg Equilibrium (HWE) calculations must be carried out and reported along with the P-values if applicable [see Namipashaki et al. 2015 (Cell J, Vol 17, N 2, Pages: 187-192) for a discussion].
2. Linkage disequilibrium (LD) structure between SNPs (if multiple SNPs are reported) must be presented.
3. Appropriate multiple testing correction (if multiple independent SNPs are reported) must be included.

Submissions that fail to meet the above criteria will be rejected before being sent out for review.

Each of the following manuscript components should begin in the following sequence:

Authors' names and order of them must be carefully considered (full name(s), highest awarded academic degree(s), email(s), and institutional affiliation(s) of all the authors in English. Also, you must send mobile number and full postal address of the corresponding author).

Changes to Authorship such as addition, deletion or rearrangement of author names must be made only before the manuscript has been accepted in the case of approving by the journal editor. In this case, the corresponding author must explain the reason of changing and confirm them (which has been signed by all authors of the manuscript). If the manuscript has already been published in an online issue, an erratum is needed. Please contact us via info@celljournal.org in case of any changes (corrections, retractions, erratum, etc.).

Title is providing the full title of the research (do not use abbreviations in title).

Running title is providing a maximum of 7 words (no more than 50 characters).

Abstract must include Objective, Materials and Methods, Results, and Conclusion (no more than 300 words).

Keywords, three to five, must be supplied by the authors at the foot of the abstract chosen from the Medical Subject Heading (MeSH). Therefore; they must be specific and relevant to the paper.

The following components should be identified after the abstract:

Introduction: The Introduction should provide a brief background to the subject of the paper, explain the importance of the study, and state a precise study question or purpose.

Materials and Methods: It includes the exact methods or observations of experiments. If an apparatus is used, its manufacturer's name and address should be stipulated in parenthesis. If the method is established, give reference but if the method is new, give enough information so that another author can perform it. If a drug is used, its generic name, dose, and route of administration must be given. Standard units of measurements and chemical symbols of elements do not need to be defined.

Statistical analysis: Type of study and statistical methods should be mentioned and specified by any general computer program used.

Ethical considerations: Please state that informed consent was obtained from all human adult participants and from the parents or legal guardians of minors and include the name of the appropriate institutional review board that approved the project. It is necessary to indicate in the text that the maintenance and care of experimental animals complies with National Institutes of Health guidelines for the humane use of laboratory animals, or those of your Institute or agency.

Clinical trial registration: All of the Clinical Trials performing in Iran must be registered in Iranian Registry of Clinical Trials (www.irct.ir). The clinical trials performed abroad, could be considered for publication if they register in a registration site approved by WHO or www.clinicaltrials.gov. If you are reporting phase II or phase III randomized controlled trials, you must refer to the CONSORT Statement for recommendations to facilitate the complete and transparent reporting of trial findings. Reports that do not conform to the CONSORT guidelines may need to be revised before peer-reviewing.

Results: They must be presented in the form of text, tables, and figures. Take care that the text does not repeat data that are presented in tables and/or figures. Only emphasize and summarize the essential features of the main results. Tables and figures must be numbered consecutively as appeared in the text and should be organized in separate pages at the end of the manuscript while their location should be mentioned in the main text.

Tables and figures: If the result of your manuscript is too short, it is better to use the text instead of tables & figures. Tables should have a short descriptive heading above them and also any footnotes. Figure's caption should contain a brief title for the whole figure and continue with a short explanation of each part and also the symbols used (no more than 100 words). All figures must be prepared based on cell journal's guideline in color (no more than 6 Figures and Tables) and also in TIF format with 300 DPI resolution.

Of Note: Please put the tables & figures of the result in the results section not any other section of the manuscript.

Supplementary materials would be published on the online version of the journal. This material is important to the understanding and interpretation of the report and should not repeat material within the print article. The amount of supplementary material should be limited. Supplementary material should be original and not previously published and will undergo editorial and peer review with the main manuscript. Also, they must be cited in the manuscript text in parentheses, in a similar way as when citing a figure or a table. Provide a caption for each supplementary material submitted.

Discussion: It should emphasize the present findings and the variations or similarities with other researches done by other researchers. The detailed results should not be repeated in the discussion again. It must emphasize the new and important aspects of the study.

Conclusion: It emphasizes the new and important aspects of the study. All conclusions are justified by the results of the study.

Acknowledgements: This part includes a statement thanking those who contributed substantially with work relevant to the study but does not have authorship criteria. It includes those who provided technical help, writing assistance and name of departments that provided only general support. You must mention financial support in the study. Otherwise; write this sentence "There is no financial support in this study".

Conflict of interest: Any conflict of interest (financial or otherwise) and sources of financial support must be listed in the Acknowledgements. It includes providers of supplies and services from a commercial organization. Any commercial affiliation

must be disclosed, regardless of providing the funding or not.

Of Note: If you have already any patent related to the subject of your manuscript, or you are going to apply for such a patent, it must be mentioned in this part.

References: The references must be written based on the Vancouver style. Thus the references are cited numerically in the text and listed in the bibliography by the order of their appearance. The titles of journals must be abbreviated according to the style used in the list of Journals Indexed in PubMed. Write surname and initials of all authors when there are six or less. In the case of seven or more authors, the names of the first six authors followed by "et al." must be listed. You can download Endnote file for Journal references style: endnote file

The reference of information must be based on the following order:

Article:

Surname(s) and first letter of name & middle name(s) of author(s) .Manuscript title. Journal title (abbr).publication date (year); Volume & Issue: Page number.

Example: Manicardi GC, Bianchi PG, Pantano S, Azzoni P, Bizzaro D, Bianchi U, et al. Presence of endogenous nicks in DNA of ejaculated human spermatozoa and its relationship to chromomycin A3 accessibility. Biol Reprod. 1995; 52(4): 864-867.

Book:

Surname(s) and first letter of name & middle name(s) of author(s).Book title. Edition. Publication place: publisher name; publication date (year); Page number.

Example: Edelman CL, Mandle CL. Health promotion throughout the lifespan. 2nd ed. ST Louis: Mosby; 1998; 145-163.

Chapter of book:

Surname(s) and first letter of name & middle name(s) of author(s).Chapter title. In: Surname(s) and first letter of name & middle name(s) of editor(s), editors. Book title. Edition. Publication place: publisher name; publication date (year); Page number.

Example: Phillips SJ, Whisnant JP. Hypertension and stroke. In: Laragh JH, Brenner BM, editors. Hypertension: pathophysiology, diagnosis, and management. 2nd ed. New York: Raven Press; 1995; 465-478.

Abstract book:

Example: Amini rad O.The antioxidant effect of pomegranate juice on sperm parameters and fertility potential in mice. Cell J. 2008;10 Suppl 1:38.

Thesis:

Name of author. Thesis title. Degree. City name. University. Publication date (year).

Example: Eftekhari Yazdi P. Comparison of fragment removal and co-culture with Vero cell monolayers on development of human fragmented embryos. Presented for the Ph.D., Tehran. Tarbiyat Modarres University. 2004.

Internet references

Article:

Example: Jahanshahi A, Mirnajafi-Zadeh J, Javan M, Mohammad-Zadeh M, Rohani M. Effect of low-frequency stimulation on adenosineA1 and A2A receptors gene expression in dentate gyrus of perforant path kindled rats. Cell J. 2008; 10 (2): 87-92. Available from: <http://www.celljournal.org>. (20 Oct 2008).

Book:

Example: Anderson SC, Poulsen KB. Anderson's electronic atlas of hematology.[CD-ROM]. Philadelphia: Lippincott Williams & Wilkins; 2002.

D. Proofs are sent by email as PDF files and should be checked and returned within 72 hours of receipt. It is the authors' responsibility to check that all the text and data as contained in the page proofs are correct and suitable for publication. **We are requested to pay particular attention to author's names and affiliations as it is essential that these details be accurate when the article is published.**

E. Pay for publication: Publishing an article in **Cell J** requires Article Processing Charges (APC) that will be billed to the submitting author following the acceptance of an article for publication. For more information please see www.celljournal.org.

F. Ethics of scientific publication: Manuscripts that have been published elsewhere with the same intellectual material will

refer to duplicate publication. If authors have used their own previously published work or work that is currently under review, as the basis for a submitted manuscript, they are required to cite the previous work and indicate how their submitted manuscript offers novel contributions beyond those of the previous work. Research and publication misconduct is considered a serious breach of ethics.

The Journal systematically employs iThenticate, plagiarism detection and prevention software designed to ensure the originality of written work before publication. Plagiarism of text from a previously published manuscript by the same or another author is a serious publication offence. Some parts of text may be used, only where the source of the quoted material is clearly acknowledged.

3. General information

A. You can send your manuscript via online submission system which is available on our website. If the manuscript is not prepared according to the format of **Cell J**, it will be returned to authors.

B. The order of article appearance in the Journal is not demonstrating the scientific characters of the authors.

C. **Cell J** has authority to accept or reject the manuscript.

D. Corresponding authors should send the manuscripts via the Online Manuscript Submission System. All submissions will be evaluated by the associated editor in order to check scope and novelty. If the manuscript suits the journal criteria, the associated editor would select the single-blind peer-reviewers. The reviewers of the manuscript must not share information about the review with anyone without permission of the editors and authors. If three reviewers pass their judgments on the manuscript, it will be presented to the associated editor of **Cell J**. In the case of having a favorable judgment on the manuscript, reviewers' comments will be presented to the corresponding author (the identification of the reviewers will not be revealed). After receiving the revision, the associated editor would choose the final reviewer among the previous ones. The final decision will be taken by editor-in-chief based on the final reviewer's comments. The review process takes between 2 to 4 months in **Cell J**. The executive member of journal will contact the corresponding author directly within 3-4 weeks by email. If authors do not receive any reply from journal office after the specified time, they can contact the journal office. Finally, the executive manager will respond promptly to authors' request.

After receiving the acceptance letter, the abstract of the paper would be published electronically. The paper will be in a queue to be published in one Cell J. At last, the corresponding author should verify a proof copy of the paper in order to be published.

The Final Checklist

The authors must ensure that before submitting the manuscript for publication, they have to consider the following parts:

1. The first page of manuscript should contain title, name of the author/coauthors, their academic qualifications, designation & institutions they are affiliated with, mailing address for future correspondence, email address, phone, and fax number.
2. Text of manuscript and References prepared as stated in the "guide for authors" section.
3. Tables should be on a separate page. Figures must be sent in color and also in JPEG (Jpg) format.
4. Cover Letter should be uploaded with the signature of all authors.
5. An ethical committee letter should be inserted at the end of the cover letter.

The Editor-in-Chief: Ahmad Hosseini, Ph.D.

*Cell Journal*_(Yakhteh)

P.O. Box: 16635-148, Iran

Tel/Fax: + 98-21-22510895

Emails: info@celljournal.org

journals@celljournal.org



IN THE NAME OF GOD



Gone But not Forgotten

In the memory of the late Director of Royan Institute,
Founder of Stem Cells Research in Iran and Chairman of
Cell Journal (Yakhteh). May he rest in peace.

Dr. Saeed Kazemi Ashtiani

OWNED:

Royan Institute, Iranian Academic Center for Education Culture and Research (ACECR)

CHAIRMAN:

Hamid Gourabi, Ph.D., (Professor, Royan Institute, Tehran, Iran)

EDITOR IN CHIEF:

Ahmad Hosseini, Ph.D., (Professor, Shahid Beheshti Medical University, Tehran, Iran)

SECTION EDITORS:

Saeid Abroun, Ph.D., Professor, Tarbiat Modares University, Tehran, Iran
Masoud Vosough, M.D., Ph.D., Associate Professor, Royan Institute, Iran
Hoda Madani, M.D., Ph.D., Royan Institute, Iran
Marzieh Ebrahimi, Ph.D., Professor, Royan Institute, Tehran, Iran
Sara Soudi, Ph.D., Associate Professor, Tarbiat Modares University, Tehran, Iran
Sharif Moradi, Ph.D., Assistant Professor, Royan Institute, Tehran, Iran
Sara Pahlavan, Ph.D., Assistant Professor, Royan Institute, Tehran, Iran
Sadaf Vahdat, Ph.D., Assistant Professor, Tarbiat Modares University, Tehran, Iran
Amir Amiri-Yekta, Ph.D., Assistant Professor, Royan Institute, Tehran, Iran
Afagh Alavi, Ph.D., Associate Professor, University of Social Welfare and Rehabilitation Sciences, Tehran, Iran
Seyed Javad Mirnajafi-Zadeh, Ph.D., Assistant Professor, Tarbiat Modares University, Tehran, Iran
Sahar Kiani, Ph.D., Associate Professor, Royan Institute, Tehran, Iran
Marjan Sabaghian, Ph.D., Associate Professor, Royan Institute, Tehran, Iran
Seyyed Abolghasem Ghadami, Ph.D., Alzahra University, Tehran, Iran
Mohammad Kazemi Ashtiani, Ph.D., Royan Institute, Tehran, Iran
Hamed Daemi, Ph.D., Assistant Professor, Royan Institute, Tehran, Iran
Fatemeh Hassani, Ph.D., Assistant Professor, Royan Institute, Tehran, Iran
Mahshid Bazrafkan, Ph.D., Assistant Professor, Avicenna Fertility Center, Karaj, Iran
Alireza Soltanian, Ph.D., Professor, University of Medical Sciences, Hamadan, Iran

EDITORIAL BOARDS:

Saeid Abroun, Ph.D., (Professor, Tarbiat Modares University, Tehran, Iran)
Kamran Alimoghadam, M.D., (Associate Professor, Tehran Medical University, Tehran, Iran)
Alireza Asgari, Ph.D., (Professor, Baghyatallah University, Tehran, Iran)
Mohammad Kazem Aghaee Mazaheri, D.D.S., (Assistant Professor, ACECR, Tehran, Iran)
Mohamadreza Baghaban Eslaminejad, Ph.D., (Professor, Royan Institute, Tehran, Iran)
Gila Behzadi, Ph.D., (Professor, Shahid Beheshti Medical University, Tehran, Iran)
Hossein Baharvand, Ph.D., (Professor, Royan Institute, Tehran, Iran)
Marzieh Ebrahimi, Ph.D., (Professor, Royan Institute, Tehran, Iran)
Mary Familiari, Ph.D., (Senior Lecturer, University of Melbourne, Melbourne, Australia)
Hamid Gourabi, Ph.D., (Professor, Royan Institute, Tehran, Iran)
Jurgen Hescheler, M.D., (Professor, Institute of Neurophysiology of University Zu Koln, Germany)
Ghasem Hosseini Salekdeh, Ph.D., (Professor, Agricultural Biotechnology Research Institute, Karaj, Iran)
Esmail Jabbari, Ph.D., (Associate Professor, University of South Carolina, Columbia, USA)
Suresh Jesuthasan, Ph.D., (Associate Professor, National University of Singapore, Singapore)
Bahram Kazemi, Ph.D., (Professor, Shahid Beheshti Medical University, Tehran, Iran)
Saadi Khochbin, Ph.D., (Professor, Inserm/Grenoble University, France)
Ali Khademhosseini, Ph.D., (Professor, Harvard Medical School, USA)
Kun Ping Lu, M.D., Ph.D., (Professor, Harvard Medical School, Boston, USA)
Navid Manuchehrabadi, Ph.D., (Angio Dynamics, Marlborough, USA)
Hosseinali Mehrani, Ph.D., (Professor, Baghyatallah University, Tehran, Iran)
Marcos Meseguer, Ph.D., (Clinical Embryology Laboratory IVI Valencia, Valencia, Spain)
Seyed Javad Mowla, Ph.D., (Professor, Tarbiat Modares University, Tehran, Iran)
Mohammad Hossein Nasr Esfahani, Ph.D., (Professor, Royan Institute, Tehran, Iran)
Toru Nakano, M.D., Ph.D., (Professor, Osaka University, Osaka, Japan)
Donald Newgreen, Ph.D., (Professor, Murdoch Children Research Institute, Melbourne, Australia)
Mojtaba Rezazadeh Valojerdi, Ph.D., (Professor, Tarbiat Modares University, Tehran, Iran)
Mohammad Hossein Sanati, Ph.D., (Associate Professor, National Institute for Genetic Engineering and Biotechnology, Tehran, Iran)
Eimei Sato, Ph.D., (Professor, Tohoku University, Sendai, Japan)
Andreas Serra, M.D., (Professor, University of Zurich, Zurich, Switzerland)
Abdolhossein Shahverdi, Ph.D., (Professor, Royan Institute, Tehran, Iran)

Michele Catherine Studer, Ph.D., (Institute of Biology Valrose, IBV University of Nice Sophia-Antipolis, France)
Peter Timashev, Ph.D., (Sechenov University, Moscow, Russia)
Daniela Toniolo, Ph.D., (Head, Unit of Common Disorders, San Raffaele Research Institute, Milano, Italy)
Christian van den Bos, Ph.D., Managing Director MARES Ltd, Greven, Germany
Catherine Verfaillie, Ph.D., (Professor, Katholie Universiteit Leuven, Leuven, Belgium)
Gianpaolo Zerbin, M.D., Ph.D., (San Raffaele Scientific Institute, Italy)
Shubing Zhang, Ph.D., (Associate Professor, Central South University, China)
Daniele Zink, Ph.D., (Institute of Bioengineering and Nanotechnology, Agency for Science Technology & Science, Singapore)

EXECUTIVE MANAGER:

Farideh Malekzadeh, M.Sc., (Royan Institute, Tehran, Iran)

EXECUTIVE BOARDS:

Parvaneh Afsharian, Ph.D., (Royan Institute, Tehran, Iran)
Reza Azimi, B.Sc., (Royan Institute, Tehran, Iran)
Reza Omani-Samani, M.D., (Royan Institute, Tehran, Iran)
Elham Amirchaghmaghi, M.D., Ph.D., (Royan Institute, Tehran, Iran)
Leila Daliri, M.Sc., (Royan Institute, Tehran, Iran)
Mahdi Lottfipannah, M.Sc., (Royan Institute, Tehran, Iran)
Faezeh Shekari, Ph.D., (Royan Institute, Tehran, Iran)

ENGLISH EDITORS:

Mitra Amiri Khabooshan, Ph.D., (Monash University, Victoria, Australia)
Sima Binaafar, M. Sc., (Royan Institute, Tehran, Iran)
Saman Eghtesad, Ph.D., (Royan Institute, Tehran, Iran)
Jane Elizabeth Ferrie, Ph.D., (University College of London, London, UK)
Vahid Ezzatizadeh, Ph.D., (Royan Institute, Tehran, Iran)
Farnaz Shapouri, Ph.D., (Memphasys Limited, NSW, Australia)
Kim Vagharfard, M.Sc., (Royan Institute, Tehran, Iran)
Maryam Vatani, M.Sc., (University of Calgary, Canada)

GRAPHIST:

Laleh Mirza Ali Shirvani, B.Sc., (Royan Institute, Tehran, Iran)

PUBLISHED & SPONSORED BY:

Publication of Royan Institute (ACECR)

Indexed in:

1. Thomson Reuters (ISI)
2. PubMed
3. PubMed Central (PMC)
4. National Library Medicine (NLM)
5. Biosis Preview
6. Index Medicus for the Eastern Mediterranean Region (IMEMR)
7. Regional Information Center for Sciences and Technology (RICEST)
8. Index Copernicus International
9. Cambridge Scientific Abstract (CSA)
10. EMBASE
11. Scopus
12. Cinahl Database
13. Google Scholar
14. Chemical Abstract Service (CAS)
15. Proquest
16. Directory of Open Access Journals (DOAJ)
17. Open Academic Journals Index (OAJI)
18. Directory of Research Journals Indexing (DRJI)
19. Scientific Information Database (SID)
20. Iranmedex
21. Islamic World Science Citation Center (ISC)
22. Magiran
23. Science Library Index
24. Biological Abstracts
25. Essential Science Indicators
26. EuroPub

ACECR

Copyright and license information:

The **Cell Journal**^(Yakhteh) is an open access journal which means the articles are freely available online for any individual author to download and use the providing address. The journal is licensed under a Creative Commons Attribution-Non Commercial 3.0 Unported License which allows the author(s) to hold the copyright without restrictions that is permitting unrestricted non-commercial use, distribution, and reproduction in any medium provided the original work is properly cited.

Editorial Office Address (Dr. Ahmad Hosseini):

Royan Institute, P.O.Box: 16635-148,
Tehran, Iran
Tel & Fax: (+9821)22510895
Website: www.celljournal.org
Emails: info@celljournal.org
journals@celljournal.org

Printing Company:

Naghshe e Johar Co.
No. 103, Fajr alley, Tehranpars Street,
Tehran, Iran.



CONTENTS

Systematic Review

- **The Effect of Biomaterials on Human Dental Pulp Stem Cell Neural Differentiation: A Scoping Review**
Maedeh Khatami, Yousef Moradi, Ramyar Rahimi Darehbagh, Donya Azizi, Arash Pooladi, Rojin Ramezani, Seyedeh Asrin Seyedoshohadaei 813

Original Articles

- **Left Barrel Cortical Neurons Activity following Transplantation of Stem Cells into Right Lesioned-Barrel Cortex in Rats**
Mansoureh Sabzalizadeh, Mohammad Reza Afarinesh, Ali Derakhshani, Vahid Sheibani 822

- **Deciphering Role of IncRNA 91H in Liver Cancer: Impact on Tumorigenesis**
Zhiyuan Mo, Zhuangqiang Wang 829

- **SP-8356: A Novel Verbenone Derivative Exerts *In Vitro* Anti-Non-Small Cell Lung Cancer Effects, Promotes Apoptosis via The P53/MDM2 Axis and Inhibits Tumor Formation in Mice**
Lei Yang, Liyi Hu 839

- **The Effects of Lycopene on Modulating Oxidative Stress and Liver Enzymes Levels in Metabolic Syndrome Patients: A Randomised Clinical Trial**
Mahdi Mirahmadi, Malihe Aghasizadeh, Fatemeh Nazifkar, Mahla Ghafarian Choubdari, Reza Assaran-Darban, Shima Tavallaie, Hossein Hatamzadeh, Gordon A Ferns, Mohammad Reza Mirinezhad, Hamed Baharara, Farzin Hadizadeh, Majid Ghayour-Mobarhan 847

- **Clinical Evaluation of Collagen-Induced Arthritis in Female Lewis Rats: A Comprehensive Analysis of Disease Progression and Severity**
Mahnaz Babaahmadi, Nima Makvand Gholipour, Behnoosh Tayebi, Jed Pheneger, Ensiyeh Hajizadeh-Saffar, Mohamadreza Baghaban Eslaminejad, Seyedeh-Nafiseh Hassani 854

- **Association between Genetic Polymorphism of The IncRNA *MIAT* rs1894720 with Ischemic Stroke Risk and IncRNA *MIAT* Expression Levels in The Blood after An Ischemic Stroke: A Case-Control Study**
Tahereh Asadabadi, Mohammad Javad Mokhtari, Mahnaz Bayat, Anahid Safari, Afshin Borhani-Haghighi 863


- **Integrated Bioinformatic Analysis of Differentially Expressed Genes Associated with Wound Healing**
Mansoureh Farhangniya, Farzaneh Mohamadi Farsani, Najmeh Salehi, Ali Samadikuchaksaraei 874

Advisory Board A

Authors Index D

- **Front page of Cell Journal_(Yakhteh): Figure 4A, Page: 859**

The Effect of Biomaterials on Human Dental Pulp Stem Cell Neural Differentiation: A Scoping Review

Maedeh Khatami, M.D.¹, Yousef Moradi, Ph.D.^{2,3}, Ramyar Rahimi Darehbagh, M.D.^{1,4,5,6*} , Donya Azizi, M.D.¹,
Arash Pooladi, M.D., Ph.D.^{6,7,8}, Rojin Ramezani, M.D.¹, Seyedeh Asrin Seyedoshohadaei, M.D.^{9,10}

1. Student Research Committee, Kurdistan University of Medical Sciences, Sanandaj, Iran
2. Social Determinants of Health Research Centre, Research Institute for Health Development, Kurdistan University of Medical Sciences, Sanandaj, Iran
3. Department of Epidemiology and Biostatistics, Faculty of Medicine, Kurdistan University of Medical Sciences, Sanandaj, Iran
4. Nanoclub Elites Association, Tehran, Iran
5. Universal Scientific Education and Research Network (USERN), Sanandaj, Iran
6. Cellular and Molecular Research Centre, Research Institute for Health Development, Kurdistan University of Medical Sciences, Sanandaj, Iran
7. Cancer and Immunology Research Center, Research Institute for Health Development, Kurdistan University of Medical Sciences, Sanandaj, Iran
8. Department of Medical Genetics, Faculty of Medicine, Kurdistan University of Medical Sciences, Sanandaj, Iran
9. Department of Psychiatry, Faculty of Medicine, Kurdistan University of Medical Sciences, Sanandaj, Iran
10. Neurosciences Research Center, Research Institute for Health Development, Kurdistan University of Medical Sciences, Sanandaj, Iran

Abstract

Neural cells are the most important components of the nervous system and have the duty of electrical signal transmission. Damage to these cells can lead to neurological disorders. Scientists have discovered different methods, such as stem cell therapy, to heal or regenerate damaged neural cells. Dental stem cells are among the different cells used in this method. This review attempts to evaluate the effect of biomaterials mentioned in the cited papers on differentiation of human dental pulp stem cells (hDPSCs) into neural cells for use in stem cell therapy of neurological disorders. We searched international databases for articles about the effect of biomaterials on neuronal differentiation of hDPSCs. The relevant articles were screened by title, abstract, and full text, followed by selection and data extraction. Totally, we identified 731 articles and chose 18 for inclusion in the study. A total of four studies employed polymeric scaffolds, four assessed chitosan scaffolds (CS), two utilised hydrogel scaffolds, one investigation utilised decellularised extracellular matrix (ECM), and six studies applied the floating sphere technique. hDPSCs could heal nerve damage in regenerative medicine. In the third iteration of nerve conduits, scaffolds, stem cells, regulated growth factor release, and ECM proteins restore major nerve damage. hDPSCs must differentiate into neural cells or neuron-like cells to regenerate nerves. Plastic-adherent cultures, floating dentosphere cultures, CS, polymeric scaffolds, hydrogels, and ECM mimics have been used to differentiate hDPSCs. According to our findings, the floating dentosphere technique and 3D-PLAS are currently the two best techniques since they result in neuroprogenitor cells, which are the starting point of differentiation and they can turn into any desired neural cell.

Keywords: Biomaterials, Human Dental Pulp Stem Cell, Neural Differentiation

Citation: Khatami M, Moradi Y, Rahimi Darehbagh R, Azizi D, Pooladi A, Ramezani R, Seyedoshohadaei SA. The effect of biomaterials on human dental pulp stem cell neural differentiation: a scoping review. *Cell J.* 2023; 25(12): 813-821. doi: 10.22074/CELLJ.2023.2007711.1375

This open-access article has been published under the terms of the Creative Commons Attribution Non-Commercial 3.0 (CC BY-NC 3.0).

Introduction

The scientific community has placed considerable emphasis on the investigation of stem cells and their therapeutic applications. The pluripotent and multipotent characteristics of stem cells render them indispensable in tissue engineering methodologies, as they facilitate tissue regeneration and repair (1). Dental pulp tissue, which is developed from the neural crest, can now be acquired, separated, and conserved for extended periods of time through non-invasive and innovative techniques, such as retrieval from extracted wisdom teeth and shed deciduous teeth (2). Mesenchymal stem cells, which are a type of stem cells that exist in bone marrow in limited quantities, exhibit mesodermal tissue differentiation and are capable of differentiating into all three

germ layers (3, 4). Multipotent stem cells, known as human dental pulp stem cells (hDPSCs), can be readily extracted from pulp tissue and have the capability to differentiate into diverse cell types, including adipocytes, osteocytes, glial cells, and neural cells because of their heterogeneous character (5). The aforementioned characteristic renders them a non-invasive and ethically sanctioned source of mesenchymal-like stem cells. hDPSCs that originate from neural crest exhibit neuro-ectodermal specification (5, 6). This allows them to generate different neurotrophic factors, like nerve growth factor (NGF) and glial cell line-derived neurotrophic factor, which confer neuroprotective properties (7, 8). It has been shown that hDPSCs express neural markers when transplanted into a rodent brain (9). The results of other



studies demonstrated the differentiation of these hDPSCs into specific kinds of neural cells, including spiral ganglion neuron and inner ear hair cells (10, 11).

Neural cells are fundamental components of the nervous system that enable the propagation of electrical signals. As a result, harm or impairment to these cells can lead to diverse neurological conditions that are contingent on the specific type of neuron affected (2). Various disorders can arise due to impairment in either the central nervous system or peripheral nervous system, including Parkinson's disease, spinal cord injuries, and Alzheimer's disease, among others (12, 13). The treatment of neurodegenerative disorders is a complex process owing to the restricted self-repairing ability of damaged neural cells and their incapacity to regenerate lost cells. Cell-transplant therapy has been investigated as a means to augment endogenous nerve regeneration. hDPSCs present a potential avenue for the restoration of neuronal damage through the application of tissue engineering methodologies, which is due to their capacity to undergo neuronal differentiation and endure harmful conditions associated with lesions (14). Nonetheless, a significant obstacle pertains to the proficient administration of these cells to the intended location and the establishment of a biocompatible milieu for cellular differentiation. The identification of an appropriate biomaterial for the transfer of cells and facilitation of their differentiation into specific cell types is a critical aspect of cell therapy (12, 15).

The integration of scaffolds, cells, and growth factors is a fundamental aspect in the development of structures utilised in tissue engineering (13). Scaffolds have an important effect on cell maintenance, growth, and differentiation, as well as in facilitating cell migration and adhesion by providing a suitable environment. Consequently, it is imperative that they exhibit distinct characteristics, including elevated biocompatibility, biodegradability, absence of toxicity, and lack of inflammatory properties. Scaffolds frequently employed in tissue engineering include chitosan scaffolds (CS), fibrin, collagen, fibronectin, polylactic acid scaffolds (3DP-PLAS), and natural or synthetic silk. Consideration of factors that include, but are not limited to pore size, texture, and mechanical strength, are imperative in the evaluation of these scaffolds. The structures in question are subject to two primary concerns, namely their limited cell-holding capacity and inadequate extracellular matrix (ECM) (7, 14, 16, 17). To mitigate these limitations, a plausible approach involves the incorporation of exogenous biomaterials and the application of biomolecules and proteins to the scaffold. This strategy enhances the scaffold's functionality by creating a more conducive environment that offers ample material and surface area for stem cell proliferation and differentiation. An alternative approach involves the development of an ECM-like architecture that utilises hydrogels or decellularised ECM, which can also provide the necessary substrate and surface (3, 8, 16).

The crucial significance of neural cells lies in their function of propagating electrical impulses throughout the nervous system. Consequently, any aberration in the functioning of these cells may lead to a disrupted nervous

system. Hence, it is evident that a secure and ethically sanctioned approach for the regeneration of neural cells and nerves is imperative. hDPSCs represent a promising avenue for tissue engineering in the context of neuronal injury and neurodegenerative conditions, given their non-invasive acquisition. Therefore, it is imperative to ensure the optimal utilisation and cultivation of these cells. The objective of this investigation is to gather and present scholarly inquiry centred on the development of settings that can proficiently transfer these cells to the designated location and direct their differentiation into the targeted neuronal cells. Since neuro regenerative treatments are a current research concern and are one of the main problems of today's medicine, this study could create a new viewpoint on healing neurodegenerative diseases and their treatments.

Materials and Methods

This scoping review was conducted by following the PRISMA guidelines.

Search strategy and selection

The objective of this scoping review was to identify and assess research studies that centred on the neural differentiation of dental stem cells. We identified 18 studies that were published between 2014 to 2023 after a comprehensive search of the PubMed, Scopus, and Web of Science databases utilising the search flowchart outlined in Figure 1. The reviewed studies were all English. There were no restrictions placed on the search. The search methodology involved manual execution, and all pertinent studies were identified and subjected to a comprehensive review. The inquiry utilised four principal keywords, namely "neural", "differentiation", "dental", and "stem cells", alongside associated keywords derived from MeSH terms. EndNote software was utilised for the purpose of managing the studies and references that were searched. These studies and references were evaluated on the basis of their titles and abstracts. Redundant and non-related research works were identified and eliminated. The identification of duplicate entries was conducted by examining the titles of previously published articles, the year of publication, and the authors. Research relevant to the subject matter was thoroughly scrutinised, and only the outcomes that were relevant to the subject were chosen. Studies related to the topic were independently evaluated and selected by two researchers (MK and DA). The elimination process, which involved exclusion and inclusion criteria, was verified for accuracy by one researcher (RRD).

Exclusion and inclusion criteria

Any study that investigated the neural differentiation of dental stem cells was included in this scoping review. Duplicate citations, studies for which the full text was not available, animal studies, and unrelated outcomes were excluded.

Data collection and extraction

The objective of this scoping review was to identify

and assess research studies related to the topic of this study. The data acquired from the search were input into EndNote software, and an initial compilation of the necessary information was carried out by two researchers (MK and DA) through a review of the titles and abstracts of the articles. We screened 731 English articles published from 1968 to 2023. Animal studies were excluded from the analysis. After screening and finding the studies related to this scoping review, the primary author (MK) examined the full text of 43 studies and chose 18 that had the necessary information for conducting this research.

The data collection was based several key factors: authors and publication year, cell source, study type, biomaterial utilised, impact on differentiation, differentiation review technique, neural expression marker assessment, and resultant neural cell type.

Quality of studies

The first author (MK) assessed the studies and reported the required data according to the Strengthening the Reporting of Observational Studies in Epidemiology (STROBE) statement.

Primary and secondary endpoints

We primarily aimed to evaluate all available literature to identify and introduce the best biomaterial available to differentiate hDPSCs into neural cells based on the data provided by these papers. Our second aim was to evaluate and introduce cultures and growth factors used in this process that were published in these relevant papers.

Results

In the preliminary investigation, we detected 731 articles

in the three databases: PubMed (n=151), Web of Science (n=132), and Scopus (n=448). From these, 290 duplicate papers were detected through automated means and 237 were identified manually. Upon conducting an evaluation of 168 studies based on their titles and abstracts, a total of 43 references were selected for further assessment of their full texts. In the end, a total of 18 articles were deemed eligible for inclusion and subsequent data extraction. Figure 1 contains all of the extracted data. Exclusion criteria were applied to papers that incorporated stem cells obtained from individuals with medical conditions. One article was found to be inaccessible and subsequently excluded.

The biomaterial most commonly utilised in the reviewed literature was the "chitosan porous scaffold", which was featured in a total of four articles. Four studies employed polymeric scaffolds, while two used hydrogel scaffolds. One investigation utilised decellularised ECM, and six studies applied the floating sphere technique during the differentiation process. An article was conducted to compare three protocols for the differentiation of hDPSCs into cholinergic neural cells. All techniques and materials employed were efficacious in generating neural cells or neuron-like cells, and demonstrated at least one positive neuronal expression marker assay.

The extracted data and obtained results are expected to be of tremendous value to researchers globally who are engaged in the exploration of neuron regeneration therapy and cell engineering. We noted advantages and disadvantages for each biomaterial. hDPSCs appear to have the potential to turn into neural cells; however, the resultant cells depend on the techniques and materials used in the media and differentiation process (Table 1).

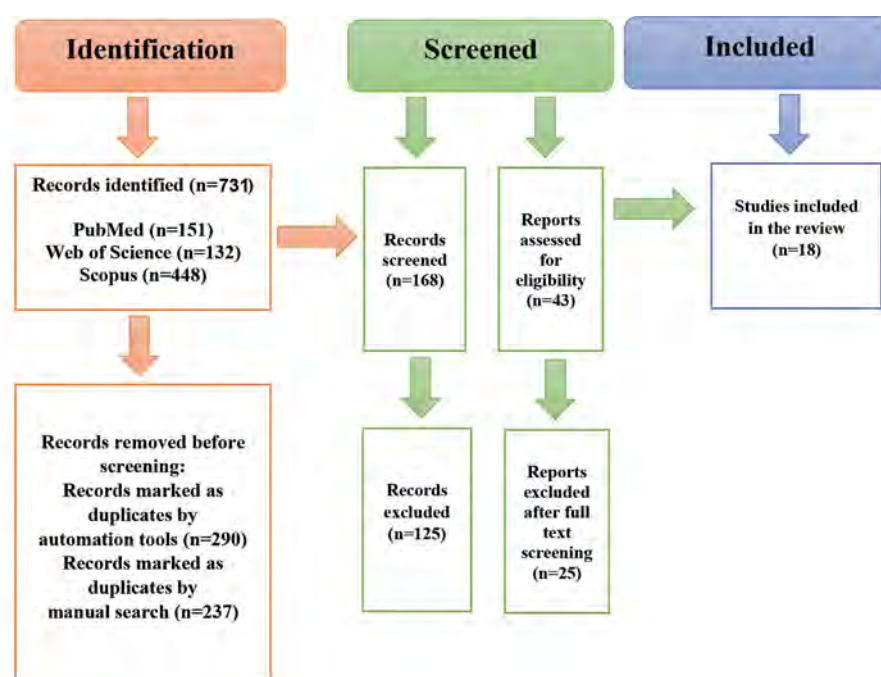


Fig.1: Identification of studies via databases and registers.

Table 1: The effect of biomaterials on hDPSC neural differentiation

Reference	Authors	Year of publication	Cell source	Type of study	Biomaterial		Impact on differentiation	Differentiation review technique	Neuronal expression marker check	Resultant neuron type
					Scaffold	Growth factors/cultures				
(14)	Pineda et al.	2022	hDPSC	<i>In vitro</i>	Nanopatterned poly(lactide-co-caprolactone) (PLCL) scaffolds	Plastic-adherent monolayer cultures, floating dentosphere cultures	Indirect	ICC Flow Cytometry	Neural stem cell marker Nestin, glial markers GFAP, and S100β, and neuronal markers [NeuN and doublecortin (DCX)]	Not mentioned
(3)	Gao et al.	2022	hDPSC	<i>In vitro</i>	TPS-PN plates (poly-N-isopropylacrylamide-co-butyl acrylate coated TPS plates)	rVT, LN, PLO, PBS, PS, DPBS, Trypsin-EDTA, α-MEM, FBS, neurobasal-A, bFGF, EGF, B27, PN	Indirect	Flow cytometry, immunostaining	βIII-tubulin, nestin	Not mentioned
(18)	Drewry et al.	2022	Excluded (due to not being accessible)	-----	-----	-----	-----	-----	-----	-----
(7)	Zheng et al.	2021	hDPSC	<i>In vitro</i>	Chitosan porous scaffolds	Low glucose DMEM, FBS, penicillin, streptomycin	Indirect	Western blot, IF staining, RT-PCR	GFAP, S100β, β-tubulin III	Not mentioned
(16)	Luo et al.	2021	hDPSC	<i>In vitro/ in vivo</i> Sprague-Dawley male rats	GelMA-bFGF hydrogels		Indirect	Immunohistochemical analysis, Western blot	GFAP, β-tubulin III	Not mentioned
(19)	Farhang et al.	2021	hDPSC	<i>In vitro</i>	3D hanging drop technique	Neurobasal media and 10% foetal calf serum containing 20 ng/ml EGF, 40 ng/ml human bFGF (hbFGF), SHH protein	Indirect	ICC	β-tubulin III and NeuN	Not mentioned
(8)	Laudani et al.	2020	hDPSC	<i>In vitro</i>	Decellularized ECM scaffold	FBS, penicillin, streptomycin, and fungizone, trypsin/EDTA, α-MEM, ascorbic acid	Indirect	Cytofluorimetric, IF, SEM, RT-PCR	MAP2, β-III tubulin, neurofilament-heavy (NF-H), VIM, NF-L, PAX6	Not mentioned
(17)	Hsiao et al.	2020	hDPSC	<i>In vitro</i>	3DP-PLAS	-----	Indirect	IF staining	GFAP, nestin, neurofilament-M (NF-M), β-III tubulin, MAP2	Neural precursor cells, neurogenic structures, astrocyte-like cells

Table 1: Continued

Reference	Authors	Year of publication	Cell source	Type of study	Biomaterial		Impact on differentiation	Differentiation review technique	Neuronal expression marker check	Resultant neuron type
					Scaffold	Growth factors/cultures				
(20)	Rafiee et al.	2020	hDPSC	<i>In vitro</i>	Neurosphere technique	20 ng/ml EGF, 20 ng/ml bFGF, and 10 mg/ml heparin/ high-glucose DMEM with 10% FBS	Indirect	Quantitative polymerase chain reaction (qPCR), Western blot, and IF, Immunostaining, Western blot	MAP2, and neurogenin 1 (Ngn1)	Neural progenitor cells
(21)	Goudarzi et al.	2020	hDPSC	<i>In vitro</i>	Neurosphere technique	5% E-CSF	Indirect	ICC, RT-PCR	Nestin, MAP2, Oct4, Sox2, NF-M	Not mentioned
(2)	Kang et al.	2019	hDPSC	<i>In vitro</i>	----- -----	Protocol 1: BME and nerve growth factor (NGF) Protocol 2: D609 Protocol 3: bFGF, SHH, and RA	Indirect	Flow cytometry, cell cycle analyses, RT-qPCR, ICC, analysis of acetylcholine (Ach) secretion in culture media	ChAT, HB9, ISL1, BETA-3, MAP2	Cholinergic neuronal-like cells
(5)	Pisciotta et al.	2018	hDPSC	<i>In vitro</i>	3D floating sphere culture system	EGF, bFGF, DMEM/F12 culture medium, L-glutamine penicillin, streptomycin, B27	Indirect	IF analysis, Western blot, pseudocolour analysis	Nestin, CD271, SOX-10, β -III tubulin, MAP γ	Neural progenitor cells, neural crest stem cells
(6)	Bojnordi et al.	2018	hDPSC	<i>In vitro</i>	Neurosphere technique	bFGF, EGF, B27, N2, poly-L-lysine-coated coverslips	Indirect	Flow cytometry, IF staining	Nestin, NF68, MAP2, β -tubulin	Neuroprogenitor cells, mature neural cells
(12)	Ghasemi Hamidabadi et al.	2017	hDPSC	<i>In vitro</i>	Chitosan-intercalated montmorillonite/PVA nanofibers	Serum-free DMEM/F12 with 2% B27 supplemented with 20 ng/mL bFGF and 20 ng/mL EGF	Indirect	RT-PCR, immunostaining	Oct-4, Nestin, NF-M, NF-H, MAP2, β -III tubulin	Neuron-like cells
(22)	Geng et al.	2017	hDPSC	<i>In vitro</i>	----- -----	Resveratrol, DMEM/F12, 10 ng/ml bFGF, 500 μ M BME and 10% FBS	Indirect	ICC staining, Western blot, RT-PCR	Nestin, Musashi and NF-M	Neuroprogenitor cells
(13)	Zhang et al.	2016	hDPSC	<i>In vitro</i>	Chitosan porous scaffolds	DMEM, FBS, penicillin, streptomycin	Indirect	RT-PCR, Western blot, IF assays	CNPase, MAP2, GFAP	Oligodendrocytes, astrocytes, neural cells

Table 1: Continued

Reference	Authors	Year of publication	Cell source	Type of study	Biomaterial		Impact on differentiation	Differentiation review technique	Neuronal expression marker check	Resultant neuron type
					Scaffold	Growth factors/cultures				
(23)	Martens et al.	2014	hDPSC	<i>In vitro</i>	Collagen hydrogel	Cell suspension, MEM, type I rat tail, sodium hydroxide/ alpha modification (alpha-MEM) FBS, glutamine, penicillin, streptomycin, BME, trans-RA, forskolin, bFGF, platelet-derived growth factor AA (PDGFaa), heregulin-beta-1 (NRG)	Indirect	ICC, ELISA	laminin, p75, GFAP, CD104, nestin	Schwann cell-like phenotype
(15)	Feng et al.	2014	hDPSC	<i>In vitro</i>	3D highly porous CS	Neural induction medium (NIM)-DMEM/F-12 medium, B27, N2, BDNF, NGF, bFGF	Indirect	RT-PCR, Western blot, IF	Nestin, CNPase, MAP2, GFAP	MAP-2+ neural cells, GFAP+ astrocytes and CNP+ oligodendrocytes

hDPSC; Human dental pulp stem cell, FBS; Foetal bovine serum, DMEM; Dulbecco's Modified Eagle medium, bFGF; Basic fibroblast growth factor, EGF; Epidermal growth factor, BME; β -mercaptoethanol, SHH; Sonic hedgehog, RA; Trans-retinoic acid, RT-PCR; Reverse transcription-polymerase chain reaction, IF; Immunofluorescence, ICC; Immunocytochemistry, GFAP; Glial fibrillary acidic protein, MAP2; Microtubule-associated protein 2, CS; Chitosan scaffold, PVA; Poly (vinyl alcohol), and D609; Tricyclodecane-9-yl-xanthogenate.

Discussion

The third stage of nerve conduit development for repairing nerve injuries involves the integration of scaffolds, stem cells, controlled release of growth factors, and ECM proteins. This represents a more advanced iteration of the second generation. According to Luo et al. (16), this particular method has demonstrated efficacy for restoration of substantial nerve damage. Additional research is required to establish the effectiveness and safety of utilising hDPSCs as the stem cell constituent in this approach. Notably, Yang et al. (24) assessed the capability of three different stem cell groups gathered from teeth-dental follicle stem cells (DFSCs), stem cells from apical papilla (SCAPs), and DPSCs to repair a spinal cord injury in rats. Although most dental stem cells secreted nestin and β -III tubulin, interestingly, the DFSCs had better proliferation potential and this indicated their ability to adapt to the environment. It is necessary to determine successful techniques for their proliferation and differentiation into specific cell lineages (4).

According to the literature, hDPSCs have the potential to differentiate in two distinct environments, namely plastic-adherent cultures and floating dentosphere cultures (14). The scaffolds employed in this process of differentiation are subject to modification (13). Scaffolds are utilised as a microenvironment that emulates the function of the ECM in cellular growth and differentiation (15).

CS are frequently utilised in conjunction with diverse growth factors and ECM proteins in these methodologies. The aforementioned scaffold possesses porous properties and can be manipulated into various shapes to facilitate its application in hDPSC neural differentiation. Additionally, it serves as a vehicle for conveying differentiated cells to the site of injury. It has been observed that the combination of CS with hDPSCs leads to an elevated probability of neural differentiation. The crucial attributes of CS are the means pore diameter and elevated swelling efficacy. A pore size of $268.79 \pm 13.25 \mu\text{m}$ is deemed appropriate for neural growth and migration (7, 12, 13, 15).

Research conducted by Zheng et al. (7) involved the integration of CS with basic fibroblast growth factor (bFGF) and ERK/p-ERK to enhance neural differentiation of hDPSCs. bFGF is a biological factor that possesses a brief half-life and necessitates a stable milieu for the purpose of directing the differentiation of stem cells. Nonetheless, the primary limitations of chitosan are its inadequate hydrophilicity and suboptimal thermal and physiochemical characteristics. Ghasemi Hamidabadi et al. (12) have tackled the aforementioned concerns through the amalgamation of organic monmorillonite (OMMT) and chitosan to enhance the physical and thermal characteristics. Additionally, they have incorporated poly(vinylalcohol)(PVA) to augment hydrophilicity. The results revealed that an increased concentration of OMMT (5%) resulted in a greater induction of neural differentiation. Also, another use of chitosan was explored by Mu et al. (25). They assessed the effect of chitosan tubes immersed with DPSCs and stem cell factor (SCF) on facial nerve-vascularised regeneration in rabbits. They reported that the combination of SCF and DPSCs had a positive effect on DPSC migration, activity and proliferation. SCF also provoked DPSCs neural differentiation. The SCF+DPSCs mixture inoculated in chitosan tubes prompted axonal regeneration and remyelination, and restored the function of regenerated nerve.

Polymeric scaffolds represent an alternative approach for the delivery and support of hDPSCs. PLAS are scaffolds that have been used for adhesion of hDPSCs, and the rate of their maturation is influenced by the dimensions of the pores present in these scaffolds. Pores of significant size are conducive to nourishment; although smaller pores offer a greater surface area, they may lead to necrosis. Scaffolds created with emerging technologies, such as 3D printing, have been explored. The width of the gap between struts has been identified as a crucial element in this process (17). Reducing the width of these gaps to 150 μm promotes cellular alignment, and application of poly-L-lysine or alcohol immersion enhances cell adhesion on these structures. Control of the sizes of the pores and gaps provides tremendous advantage for polymeric scaffolds.

Investigation of functionalised nanopatterned PLCL scaffolds showed their ability to enhance the requisite environment for cellular differentiation and migration. The significance of time and temperature are crucial variables during scaffold fabrication and should be duly acknowledged. Various techniques for surface functionalization have been employed to improve cell adhesion, such as plasma and polydopamine (PDA) treatment, graphene oxide (GO), and poly-D-lysine coating. Nonetheless, these techniques may impact the nanotopography of the initial film, and could potentially diminish the surface patterning effect by impeding direct interaction between stem cells and the scaffold surface (14). The ability of resveratrol, a polyphenol, to promote neural differentiation of hDPSCs was also investigated. The results indicated that incubation of cells in 15 μM resveratrol for 12 hours provided the optimum condition

for successful differentiation (22).

Hydrogels are considered a viable approach for creating the necessary microenvironment for growth and viability of the hDPSCs. According to the results by Luo et al. (16), GelMA hydrogels that incorporated 10% bFGF exhibited superior biocompatibility, degradability, pore size, and swellability. The physical characteristics of the hydrogel, such as its pore structure, cross-linking, and overall polymer content have an impact on its properties. These properties, in turn, impact the circulation of nutrients and oxygen in addition to the release of waste materials. The introduction of bFGF into the scaffold facilitates the proliferation and spread of hDPSCs. Another advantage of this biomaterial is its solubility compared to CS.

Martens et al. (23) fabricated a specialised collagen gel using type I collagen extracted from rat tails, which effectively prompted the differentiation of hDPSCs into Schwann cells. The authors generated an engineered neural tissue that facilitated cellular alignment and guidance through the use of collagen, which ultimately promoted the cells to differentiate into Schwann cells.

One potential strategy for achieving hDPSC specialisation is through the replication of the ECM structure. According to Laudani et al. (8), the use of decellularised ECM obtained from stem cells in bone marrow is a viable option for scaffold material in this context. Their study revealed that the morphology and neural marker expression of the resultant cells were favourable and suggestive of differentiated cells with characteristics similar to neural cells. They emphasized that cellular differentiation and adhesion were augmented in this milieu when compared to a glass milieu.

Floating spheres is an alternative method to differentiate hDPSCs into the cells of interest. Conventional adherent techniques potentially disrupt the biological characteristics of cells. However, the 3D floating spheres have been shown to aid in the preservation of fibroblast-like morphology and embryological factors, while simultaneously maintaining differentiation and proliferation capabilities. These spheres are effective in helping hDPSCs differentiate into neural progenitor cells (5, 20). Bojnordi et al. (6) employed the neurosphere methodology in conjunction with poly-L-lysine coverslips to generate fully developed neural cells upon exposure to neural inducers. The neurosphere technique enhances neural crest stem cell marker expression of hDPSCs. Solis-Castro et al. (26) cultured hDPSCs in three different mediums with the sphere technique. They reported that BMP4 has a positive effect in neural marker expression when added to foetal bovine serum (FBS) and OSCFM cultures with this technique. The hanging drop technique is another 3D method. Farhang et al. (19) compared the 3D method with a simple 2D culture and observed that hDPSCs cultured by the 3D hanging drop technique enriched with Sonic hedgehog (SHH) and hbFGF had significantly higher potential for differentiating into cells that express neural markers. Spinal cord fluid is also

effective when combined with the dentosphere process and is another valid method for neural differentiation of hDPSCs (21).

Advanced Dulbecco's Modified Eagle Medium (ADMEM) is a commonly utilised culture medium for the growth and proliferation of hDPSCs. Alterations to this medium have the potential to induce neural differentiation in these cells. A study conducted by Kang et al. (2) compared three distinct protocols for the differentiation of cholinergic neural cells. Protocol I used β -mercaptoethanol (BME) and NGF. Protocol II incorporated tricyclodecane-9-yl-xanthogenate (D609) into the medium, and protocol III combined bFGF, SHH, and retinoic acid (RA) with the medium. The outcomes of all three protocols were comparable; however, protocol III demonstrated a marginally greater secretion of neurotransmitters and elevated expressions of neural markers, which was attributed to the combination of bFGF, SHH, and RA.

A comparative study assessed the efficacy of transplantation of hDPSCs and human dental pulp-derived induced neural cells (DP-iNCs) in the amelioration of functional recovery of mice and the results indicated that the DP-iNCs were more effective than DPSCs. DP-iNCs are better for the niche of the chosen site for transplantation and their ability in angiogenesis is superior to hDPSCs. Hence, hDPSCs appear to be better used in the laboratory for differentiation into the desired cells prior to transplantation (27). The results of studies showed that the additional neurotrophic factor was a pivotal aspect of the treatment of the injured nerve site. Another study showed that the addition of platelet rich plasma to the hDPSCs was effective due to the ability of PRP to provide nutrients, align the anti-inflammatory response, and prevent neuron cells from apoptosis (28).

In addition to cultures and scaffolds, other aspects of cell differentiation should be taken into account. For instance, DPSCs derived from the deciduous teeth of a Down Syndrome patient have a lower level of neural marker expression compared to the control group (29). Also, the cell cycle phase which the DPSC is in has an importance in the differentiation process (30).

Luo et al. (16) transplanted the resultant neural cells into rats. The laboratory results confirmed the success of this experiment. Since no specific research has been conducted directly on humans in this regard, more studies must be conducted to confirm the potential benefit of these stem cells in the clinical setting.

The most common media, growth factors, and cultures used in these studies were: bFGF in nine studies (2, 3, 12, 13, 15, 16, 19, 22, 26); penicillin in five studies (5, 8, 13, 16, 23); and FBS for generating media in five studies (7, 8, 13, 19, 23). The media was approximately the same in all mentioned studies; however, our main focus was scaffolds and we recommend additional studies be conducted to analyse the type of media for differentiating these stem cells into the targeted neural cells.

Diverse methodologies and substances have been investigated to establish ideal conditions for the differentiation of hDPSCs into fully functional neural cells or neuron-like cells. CS, polymeric scaffolds, hydrogels, and ECM mimicking strategies are all involved in enhancing the differentiation process. Our assessment of the cited articles indicates that hDPSCs have the potential to turn into neural cells. The important influencing factor is the technique used to obtain the desired cells. Continued exploration and improvements to these methodologies will further help nerve injury restoration and rejuvenation.

We recommend that more studies, including human clinical trials, should be conducted to confirm the feasibility of these cells in the clinic. It would be helpful to evaluate the media and culture used for differentiating hDPSCs into neural cells or neuron-like cells.

Conclusion

hDPSCs could be used in regenerative medicine to effectively treat nerve damage. Scaffolds, stem cells, regulated growth factor release, and ECM proteins restore major nerve damage. hDPSCs must differentiate into neural cells or neuron-like cells to regenerate nerves. Thus, plastic-adherent cultures, floating dentosphere cultures, CS, polymeric scaffolds, hydrogels, and ECM mimics have been used to differentiate hDPSCs. Studies show that pore size, swelling efficiency, scaffold composition, and growth factors affect hDPSC differentiation and survival. Therefore, due to these traits, many effective nerve injury healing methods have emerged. However, each has advantages and disadvantages. These methods should be improved to maximise nerve damage treatment and safety using hDPSCs. According to our findings, the floating dentosphere technique (e.g., the neurosphere technique) and 3D-PLAS appear to be the two best techniques currently available since they result in neuroprogenitor cells, which are the starting point of differentiation and they can turn into any of the desired neural cells. The most recent published work indicates that the focus is on improving nanopatterned scaffolds and assessing their roles in differentiation of hDPSCs. They are proven to be useful for this purpose.

Acknowledgment

The authors would like to thank the Kurdistan University of Medical Sciences, Sanandaj, Iran and the Student Research Committee at the Kurdistan University of Medical Sciences. There is no financial support and conflicts of interest in this study.

Authors' Contributions

Y.M.; Conceptualization and Methodology. Y.M., R.R.D., A.P.; Validation, Formal analysis, and Supervision. R.R.D.; Project administration, Data curation, and Writing – review and editing. M.K., D.A.; Investigation, Resources, Data curation, Writing – original draft and

Visualisations. R.R., S.A.S.; Validation and Investigation. All authors read and approved the final manuscript.

References

- Biehl JK, Russell B. Introduction to stem cell therapy. *J Cardiovasc Nurs.* 2009; 24(2): 98-103.
- Kang YH, Shivakumar SB, Son YB, Bharti D, Jang SJ, Heo KS, et al. Comparative analysis of three different protocols for cholinergic neuron differentiation in vitro using mesenchymal stem cells from human dental pulp. *Anim Cells Syst (Seoul).* 2019; 23(4): 275-287.
- Gao Y, Tian Z, Liu Q, Wang T, Ban LK, Lee HH, et al. Neuronal cell differentiation of human dental pulp stem cells on synthetic polymeric surfaces coated with ecm proteins. *Front Cell Dev Biol.* 2022; 10: 893241.
- Bongso A, Richards M. History and perspective of stem cell research. *Best Pract Res Clin Obstet Gynaecol.* 2004; 18(6): 827-842.
- Pisciotta A, Bertoni L, Riccio M, Mapelli J, Bigiani A, La Noce M, et al. Use of a 3D floating sphere culture system to maintain the neural crest-related properties of human dental pulp stem cells. *Front Physiol.* 2018; 9: 547.
- Bojnordi MN, Haratizadeh S, Darabi S, Hamidabadi HG. Neural derivation of human dental pulp stem cells via neurosphere technique. *Bratisl Lek Listy.* 2018; 119(9): 550-553.
- Zheng K, Feng G, Zhang J, Xing J, Huang D, Lian M, et al. Basic fibroblast growth factor promotes human dental pulp stem cells cultured in 3D porous chitosan scaffolds to neural differentiation. *Int J Neurosci.* 2021; 131(7): 625-633.
- Laudani S, La Cognata V, Iemmolo R, Bonaventura G, Villaggio G, Saccone S, et al. Effect of a bone marrow-derived extracellular matrix on cell adhesion and neural induction of dental pulp stem cells. *Front Cell Dev Biol.* 2020; 8: 100.
- Arthur A, Rychkov G, Shi S, Koblar SA, Gronthos S. Adult human dental pulp stem cells differentiate toward functionally active neurons under appropriate environmental cues. *Stem Cells.* 2008; 26(7): 1787-1795.
- Adriztina I, Munir D, Sandra F, Ichwan M, Bashiruddin J, Putra IB, et al. Differentiation capacity of dental pulp stem cell into inner ear hair cell using an in vitro assay: a preliminary step toward treating sensorineural hearing loss. *Eur Arch Otorhinolaryngol.* 2022; 279(4): 1805-1812.
- Gonmanee T, Thonabulsombat C, Vongsavan K, Sritanaudomchai H. Differentiation of stem cells from human deciduous and permanent teeth into spiral ganglion neuron-like cells. *Arch Oral Biol.* 2018; 88: 34-41.
- Ghasemi Hamidabadi H, Rezvani Z, Nazm Bojnordi M, Shirinzadeh H, Seifalian AM, Joghataei MT, et al. Chitosan-intercalated montmorillonite/poly(vinyl alcohol) nanofibers as a platform to guide neuronlike differentiation of human dental pulp stem cells. *ACS Appl Mater Interfaces.* 2017; 9(13): 11392-11404.
- Zhang J, Lu X, Feng G, Gu Z, Sun Y, Bao G, et al. Chitosan scaffolds induce human dental pulp stem cells to neural differentiation: potential roles for spinal cord injury therapy. *Cell Tissue Res.* 2016; 366(1): 129-142.
- Pineda JR, Polo Y, Pardo-Rodríguez B, Luzuriaga J, Uribe-Etxebarria V, García-Gallastegui P, et al. In vitro preparation of human Dental Pulp Stem Cell grafts with biodegradable polymer scaffolds for nerve tissue engineering. *Methods Cell Biol.* 2022; 170: 147-167.
- Feng X, Lu X, Huang D, Xing J, Feng G, Jin G, et al. 3D porous chitosan scaffolds suit survival and neural differentiation of dental pulp stem cells. *Cell Mol Neurobiol.* 2014; 34(6): 859-870.
- Luo L, He Y, Jin L, Zhang Y, Guastaldi FP, Albashari AA, et al. Application of bioactive hydrogels combined with dental pulp stem cells for the repair of large gap peripheral nerve injuries. *Bioact Mater.* 2020; 6(3): 638-654.
- Hsiao D, Hsu SH, Chen RS, Chen MH. Characterization of designed directional polylactic acid 3D scaffolds for neural differentiation of human dental pulp stem cells. *J Formos Med Assoc.* 2020; 119(1 Pt 2): 268-275.
- Drewry MD, Dailey MT, Rothermund K, Backman C, Dahl KN, Syed-Picard FN. Promoting and orienting axon extension using scaffold-free dental pulp stem cell sheets. *ACS Biomater Sci Eng.* 2022; 8(2): 814-825.
- Farhang S, Soleimani M, Ostadsharif M, Ghasemi N. Neurogenic induction of human dental pulp derived stem cells by hanging drop technique, basic fibroblast growth factor, and SHH factors. *Dent Res J (Isfahan).* 2021; 18: 57.
- Goudarzi G, Hamidabadi HG, Bojnordi MN, Hedayatpour A, Niapour A, Zahiri M, et al. Role of cerebrospinal fluid in differentiation of human dental pulp stem cells into neuron-like cells. *Anat Cell Biol.* 2020; 53(3): 292-300.
- Geng YW, Zhang Z, Liu MY, Hu WP. Differentiation of human dental pulp stem cells into neuronal by resveratrol. *Cell Biol Int.* 2017; 41(12): 1391-1398.
- Martens W, Sanen K, Georgiou M, Struys T, Bronckaers A, Ameloot M, et al. Human dental pulp stem cells can differentiate into Schwann cells and promote and guide neurite outgrowth in an aligned tissue-engineered collagen construct in vitro. *FASEB J.* 2014; 28(4): 1634-1643.
- Yang C, Li X, Sun L, Guo W, Tian W. Potential of human dental stem cells in repairing the complete transection of rat spinal cord. *J Neural Eng.* 2017; 14(2): 026005
- Mu X, Liu H, Yang S, Li Y, Xiang L, Hu M, et al. Chitosan tubes inoculated with dental pulp stem cells and stem cell factor enhance facial nerve-vascularized regeneration in rabbits. *ACS Omega.* 2022; 7(22): 18509-18520.
- Solis-Castro OO, Boissonade FM, Rivolta MN. Establishment and neural differentiation of neural crest-derived stem cells from human dental pulp in serum-free conditions. *Stem Cells Transl Med.* 2020; 9(11): 1462-1476.
- Matsumura H, Marushima A, Ishikawa H, Toyomura J, Ohyama A, Watanabe M, et al. Induced neural cells from human dental pulp ameliorate functional recovery in a murine model of cerebral infarction. *Stem Cell Rev Rep.* 2022; 18(2): 595-608.
- Hu ZB, Chen HC, Wei B, Zhang ZM, Wu SK, Sun JC, et al. Platelet rich plasma enhanced neuro-regeneration of human dental pulp stem cells in vitro and in rat spinal cord. *Ann Transl Med.* 2022; 10(10): 584.
- Pham TTM, Kato H, Yamaza H, Masuda K, Hirofuji Y, Sato H, et al. Altered development of dopaminergic neurons differentiated from stem cells from human exfoliated deciduous teeth of a patient with Down syndrome. *BMC Neurol.* 2018; 18(1): 132.
- Gnanasegaran N, Govindasamy V, Kathirvaloo P, Musa S, Abu Kasim NH. Effects of cell cycle phases on the induction of dental pulp stem cells toward dopaminergic-like cells. *J Tissue Eng Regen Med.* 2018; 12(2): e881-e893.

Left Barrel Cortical Neurons Activity following Transplantation of Stem Cells into Right Lesioned-Barrel Cortex in Rats

Mansoureh Sabzalizadeh, Ph.D.^{1,2}, Mohammad Reza Afarinesh, Ph.D.^{1,2*} , Ali Derakhshani, Ph.D.³,
Vahid Sheibani, Ph.D.^{1,2*} 

1. Neuroscience Research Center, Institute of Neuropharmacology, Kerman University of Medical Sciences, Kerman, Iran
2. Cognitive Neuroscience Research Center, Institute of Neuropharmacology, Kerman University of Medical Sciences, Kerman, Iran
3. Hydatid Disease Research Center, Kerman University of Medical Sciences, Kerman, Iran

Abstract

Objective: Stem cells (SCs) can improve the functional defects of brain injury. Rodents use their whiskers to get tactile information from their surroundings. The aim of this study was to investigate whether the transplantation of SCs into the lesioned barrel cortex can help neuronal function in the contralateral cortex.

Materials and Methods: Sixteen male Wistar rats (200-230 g) were used in this experimental study. We induced a mechanical lesion in the right barrel cortex area of rats by removing this area by a 3 mm skin punch. Four groups containing one intact group of rats: group 1: control, and three lesion groups, group 2: lesion+un-differentiated dental pulp SCs (U-DPSCs), group 3: lesion+differentiated dental pulp SCs (D-DPSCs), and group 4: cell medium (vehicle) that were injected in the lesion area. Three weeks after transplantation of SCs or cell medium, the rats' responses of left barrel cortical neurons to controlled deflections of right whiskers were recorded by using the extracellular single-unit recordings technique.

Results: The results showed that the neural spontaneous activity and response magnitude of intact barrel cortex neurons in the lesion group decreased significantly ($P < 0.05$) compared to the control group while ON and OFF responses were improved in the D-DPSCs ($P < 0.001$) group compared to the vehicle group three weeks after transplantation.

Conclusion: Transplantation of dental pulp mesenchymal SCs significantly improved the neural responses of the left barrel cortex that was depressed in the vehicle group.

Keywords: Brain Injury, Electrophysiology, Rats, Somatosensory Cortex, Stem Cells

Citation: Sabzalizadeh M, Afarinesh MR, Derakhshani A, Sheibani V. Left barrel cortical neurons activity following transplantation of stem cells into right lesioned-barrel cortex in rats. *Cell J.* 2023; 25(12): 822-828. doi: 10.22074/CELLJ.2023.2007586.1373

This open-access article has been published under the terms of the Creative Commons Attribution Non-Commercial 3.0 (CC BY-NC 3.0).

Introduction

The discrete clustering of its layer IV neurons, collectively known as barrels distinguishes the barrel cortex (1). Each layer IV barrel receives precise sensory information from a single whisker via the thalamus. Extracellular field potential recordings have been used to study this precise structure-function relationship in brain slices (2).

The sensory info integration among the cerebral hemispheres is important for numerous perceptual tasks which need bi-lateral coordination. The right and left somatic sensory cortex function is narrowly linked through the corpus callosum (3). The sensory info integration through the corpus callosum is yet a mystery at the cellular level, however, some new articles have started to discover the interhemispheric

cellular dynamics in the somatosensory system (4). Still, how the number of changes of real-time activity in one cortical area is mirrored in that of its contralateral counterpoint is yet an unsolved question (5). The subcortical pathways from the whiskers on the left and right side of the face are kept quite separate from the periphery to the cortex causing a cortex functional lateralization (6).

Nevertheless, when barrel neurons reply best to contralateral whiskers stimulations, they are also affected by the whiskers on the ipsilateral side of the face as well. Ipsilateral whiskers stimulation induces both local field potential and spikes in the layers of IV and V neurons in the barrel cortex field (7). Cortical neurons' responses to the ipsilateral whiskers are mediated by callosal links since blocking activity in one hemisphere removes all replies in

Received: 22/July/2023, Revised: 29/September/2023, Accepted: 28/October/2023

*Corresponding Address: P.O.Box: 76198-13159, Neuroscience Research Center, Institute of Neuropharmacology, Kerman University of Medical Sciences, Kerman, Iran

Emails: r.afarinesh@kmu.ac.ir, v_sheibani@kmu.ac.ir



Royan Institute
Cell Journal (Yakhteh)

the hemisphere ipsilateral to the stimulated whiskers (8). This may be why, in anesthetized rats, the contralateral intact neuronal activity to the damaged barrel cortex is reduced (9). Also, cerebral cortex lesions generate several complex responses to damage of the brain. Well-reported hypo-excitability impacts caused by cortical lesions consist of extensive hypo-metabolism (10), decreases in blood flow (11), reductions in glucose metabolism (12) and low amplitude of electroencephalogram (EEG) activity (13) in the contralateral along with ipsilateral cortex after damage of the brain. Some of the overall metabolic impacts are observed through extensive areas, while other deficits seem to be limited to areas in the brain connected by their neural links to the damaged areas (14).

To reach functional recovery, injured neuronal network repair and links in the contralateral hemisphere area are needed. A perfect illustration of these therapeutic influences in stem cell (SC) therapy though, has been problematic and infrequently stated before (15). Dental pulp SCs are non-invasive and can be easily isolated from the pulp of adult and postnatal elongated teeth, they can be a suitable option for cell therapy of central nervous system injuries.

SC transplantation could increase axon density and axonal sprouting in the lesion area (16, 17). Several studies highlight the idea that neurotrophic factors released from SC grafts have an important role in the valuable influence of SC transplantation therapy (18-20).

The current research aimed to calculate the effect of SCs therapy on the ON and OFF neuronal response of intact contralateral cortical barrels by the single unit recording technique in rats with a lesioned barrel cortex on the opposite side.

Materials and Methods

Animals

The Kerman Neuroscience Research Center's Research Ethics Committee (IR.KMU.REC.1399.510) gave its approval to the experimental study. Eighteen male adult Wistar rats (200-230 g) were used in this study. The animals had clean cages and were kept in an animal house that was temperature-controlled, well-ventilated, and had free access to a regular diet and water.

Isolation and characterization of DPSC

Isolation and characterization methods were described in our previous study (19). Briefly, the pulp of lower and upper jaw teeth was extracted heterogeneously from 2 Wistar rats (200-300 g). Their pulp tissues were crumbed and then added into a falcon tube containing collagenase I (Serva). Cell cultivation was performed.

As some of these cells exhibited an oval or fibroblast-like shape before neural differentiation, a third passage was used for immunophenotypic analysis to trigger

differentiation. Flow cytometry was used for analyzing the immunophenotypic characterization of cells. After neural differentiation, the cell morphology revealed neuronal-like cells with large, rounded cell bodies and neuron-like processes. SCs were differentiated (19).

Extracellular single-unit recording

Surgery and groups

Sixteen rats were randomly divided into four experimental groups (n=4). After the rats were anesthetized with Ketamine/xylazine (80/10 mg/kg), the head of the rat was fixed in the stereotaxic frame (Stoelting, USA). The right parietal skull was exposed posteriorly (1 to 4 mm) and lateral (4 to 7 mm) to the position of the bregma and was removed by a dental drill. The barrel cortex was cut by a 3-mm skin punch, and then the lesion area was washed with normal saline at 37°C. The skin was stitched and the rats were returned to their cage. See this protocol in our previous study (19).

In this study there was 4 groups. i. Control group was without any surgery or injection, ii. A total of 1×10^6 undifferentiated dental pulp stem cells (lesion+U-DPSC group) in 80 μ l of DMEM, iii. A total of 1×10^6 differentiation dental pulp stem cells (lesion+D-DPSC group) in 80 μ l of DMEM, and iv. Lesion+vehicle group, the rats received 80 μ l of DMEM which was injected directly into the lesion site three days after lesion induction.

Then, the neural activities of the left intact cortical barrels to the right whiskers deflection of rats were recorded by the single-unit recording approach. The number of neurons in each group was as follows: control (n=16 neurons), lesion+vehicle (n=27 neurons), lesion+U-DPSC (n=18 neurons), and lesion+D-DPSC (n=30 neurons).

Each rat was intraperitoneally anesthetized with urethane (1.2 mg/kg), and then the rat's head was fixed in a stereotaxic frame. A dental drill was used to expose and remove the left parietal cortex. Using a servo-controlled heating pad, the body temperature was set to 37°C. Injecting 10% of the initial dose of urethane was used to control the spontaneous movements of whiskers and irregular breathing when changing anesthesia depth. A tungsten microelectrode (1-3 M Ω , FHC) was perpendicularly inserted into the posterior medial field of the barrel cortex by a micro driver (WPI, USA). All units were recorded from depths 600 to 1000 μ m of the cortex. The bandpass of the amplifier was 0.3-10 KHz, a preamplifier amplified the signals. The obtained data were saved on a computer (Science beam, Iran). Neuron electrical activities were considered single units' activity by a signal-to-noise ratios of at least 3:1. An offline sorter of window discriminator was then used to isolate each neuron (8, 21, 22).

Mechanical whisker deflection

A miniature speaker connecting to a glass micropipette (with an inner diameter of 0.68 mm and an outer diameter of 1.2 mm) was used to deflect the whiskers of the right mystacial pad in each rat by a controlled-mechanical whisker deflection.

Then whiskers were cut by 10 mm from the surface of the face. After determining a whisker of D2, the whisker was placed in glass tubes connected to the speaker. The whisker was moved randomly 50 times (23).

A graduated microscope was used to calibrate the amplitude of down-upward (500 μ m) deflections, hold phase (200 ms) and rise time (5 ms). The ON neural response magnitudes (moving the whiskers down from the resting position) and the OFF neural response magnitudes (moving back to the resting position) were recorded. The recorded bin size was adjusted to 1000 ms. By counting the spikes/bin, the unit activity was summed and illustrated as peri-stimulus time histograms (PSTHs) (24, 25).

Statistical analysis

Testing the normality of data distribution was performed using the Kolmogorov-Smirnov test.

All statistical analyzes were performed using SPSS software (version 22, IBM, USA). A one-way ANOVA analysis followed by Bonferroni post hoc test was applied. Data are expressed as mean \pm SEM. A $P < 0.05$ was considered statistically significant.

Results

Spontaneous activity

Spontaneous activity of neurons to the D2 whisker deflection (0-300 ms) is shown in different groups (Fig.1). ANOVA revealed a significant main effect [$F(3, 87) = 10.151, P = 0.0006$] for the spontaneous activity variable. The results showed that a lesion in the right barrel cortex leads to a significant reduction in spontaneous activity in the right intact barrel cortex of the lesion+vehicle group compared to the control group.

The analysis also reported a significant increase in spontaneous activity in the lesion+Un-DPSC compared to the vehicle groups. Results showed that SC therapy cannot restore spontaneous activity to the control level ($P < 0.001$, Fig.1).

A cumulative peri-stimulus time histogram (PSTH) was used to measure and compare neuronal responses in the barrel cortex in the control (n=16 neurons), lesion+vehicle (n=27 neurons), lesion+U-DPSC (n=18 neurons), and Lesion+D-DPSC (n=30 neurons) groups. Figure 2 shows a sample response of cumulative PSTH neurons to PW (D2) deflection.

Response magnitudes

The mean evoked response magnitude of barrel neurons in layer IV of the left hemisphere was analyzed following stimulation on whisker D2.

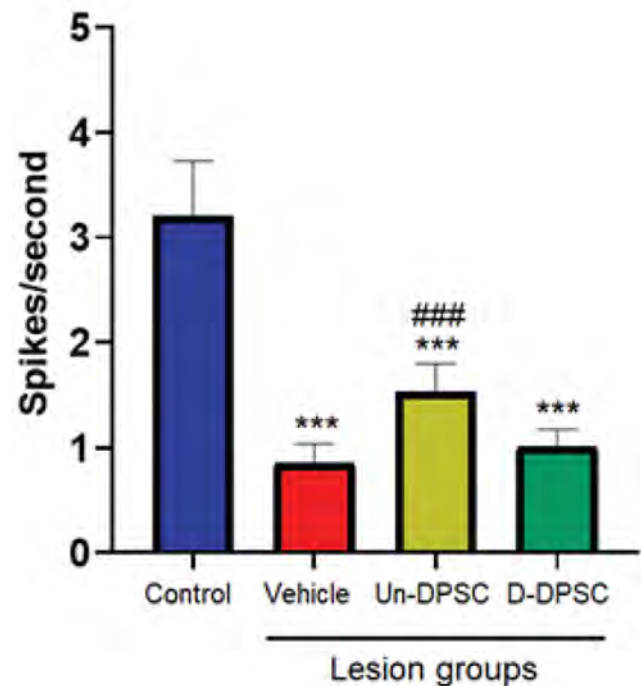


Fig.1: The mean of spontaneous activity of neurons. The spontaneous activity of the left intact cortex of the lesion+Un-DPSC, lesion+D-DPSC, and lesion+vehicle groups were compared to that of the control group. The sign of (*) shows a significant statistical difference between the lesion group and the control group. The sign of (#) shows a significant statistical difference in each group compared with the lesion+vehicle group. Data are expressed as mean \pm SEM. Un-DPSCs; Un-differentiated dental pulp stem cells, D-DPSCs; Lesion+differentiated dental pulp stem cells, ***; $P < 0.001$, and ###; $P < 0.001$.

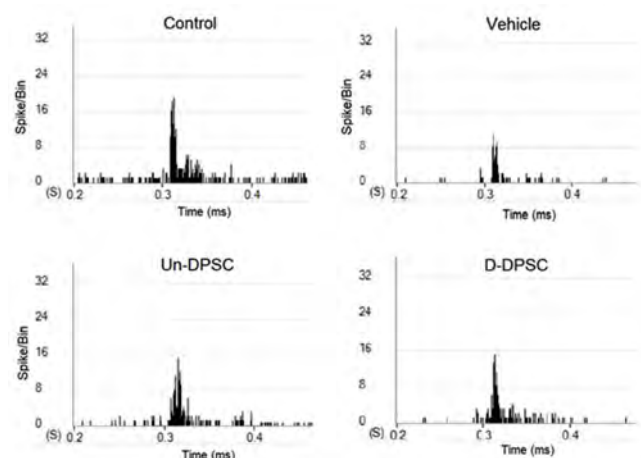


Fig.2: A peri-stimulus time histogram (bin=1 second) showing responses to the whisker of D2 in the control, lesion+vehicle, lesion+Un-DPSC, and lesion+D-DPSC groups. Un-DPSC; Un-differentiated dental pulp stem cell, and D-DPSC; Lesion+differentiated dental pulp stem cell.

ON responses

Analysis of data by One-way ANOVA revealed that there was a main significant effect on the average of the ON response magnitudes of barrel cortical neurons [F (3, 87) =10.151, P=0.000]. Post hoc analysis revealed that the mean of response magnitude in the intact barrel neurons reduced significantly in the lesion+vehicle group (P<0.001) and lesion+Un-DPSC (P<0.01) compared to the control group. The mean of response magnitude revealed a significant increase in the lesion+D-DPSC group compared to the lesion+vehicle group (P<0.01). The mean of response magnitude of the lesion+Un-DPSC group in comparison with the lesion+vehicle group, did not show any significant change (Fig.3).

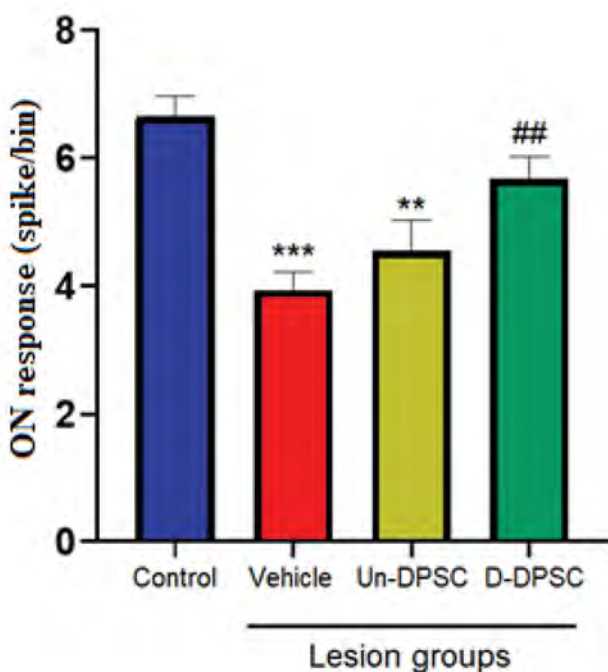


Fig.3: ON responses. ON response magnitudes of the D2 barrel neurons to the whisker deflection in different groups are shown. Data are expressed as mean ± SEM. Un-DPSC; Undifferentiated dental pulp stem cell, D-DPSC; Lesion+differentiated dental pulp stem cell, **, P<0.01, ***, P<0.001, compared to control group, and ##; P<0.01, compared to lesion+vehicle group.

OFF responses

There was a significant effect on the OFF-response magnitudes of barrel cortical neurons [F (3, 87)=8.409, P=0.001]. The mean of OFF response magnitude at the time of stimulation did not show any significant change between the control and the lesion+vehicle groups. When the D2 whisker was deflected, there was a significant increase in the response magnitude of lesion+D-DPSC compared with lesion+vehicle groups (P<0.001). The mean magnitude of the OFF response was not a significant change in the lesion+Un-DPSC compared to the lesion+vehicle group (Fig.4).

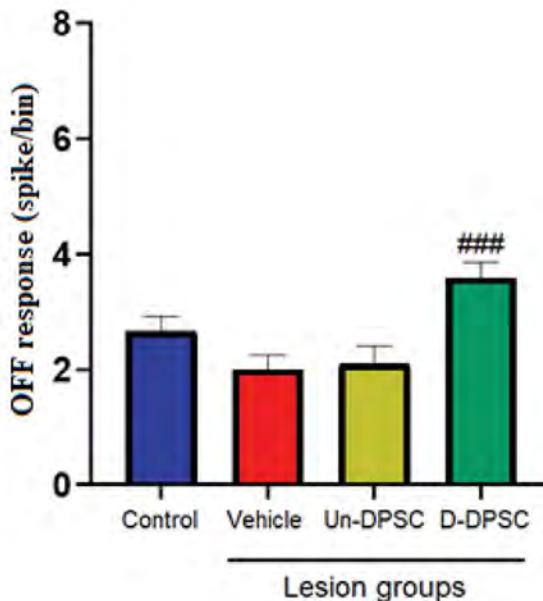


Fig.4: OFF Responses. Magnitudes of the OFF response of the D2 barrel neurons to the whisker deflection in different groups are shown. Data are expressed as mean ± SEM. Un-DPSC; Un-differentiated dental pulp stem cell, D-DPSC; Lesion+differentiated dental pulp stem cell, and ###; P<0.001 compared to lesion+vehicle group.

Latency

Latency ON

There was a main effect on the latency of neuronal responses [F (3, 87)=10.328, P=0.001]. Results revealed that latency in the lesion+vehicle group increased significantly compared to the control group (P<0.01). There was a significant reduction between lesion+Un-DPSC and lesion+D-DPSC in comparison to the lesion+vehicle group (P<0.01, Fig.5).

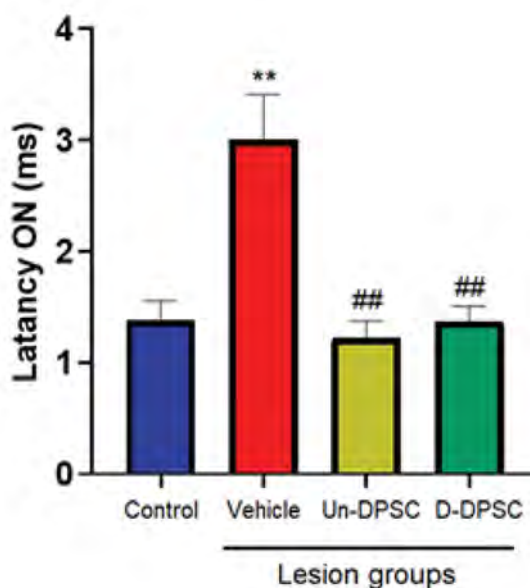


Fig.5: Response latency ON. Response latency of the D2 barrel neurons to the whisker deflection. Data are expressed as mean ± SEM. Un-DPSC; Undifferentiated dental pulp stem cell, D-DPSC; Lesion+differentiated dental pulp stem cell, **, P<0.01, as compared to the control group, and ##; P<0.01, as compared to lesion+vehicle group.

Latency OFF

There was not a main effect on the latency OFF of neuronal responses [$F(3, 87)=1.886, P=0.138$]. There was no significant difference between the control and lesion, and also between the lesion and SCs groups (Fig.6).

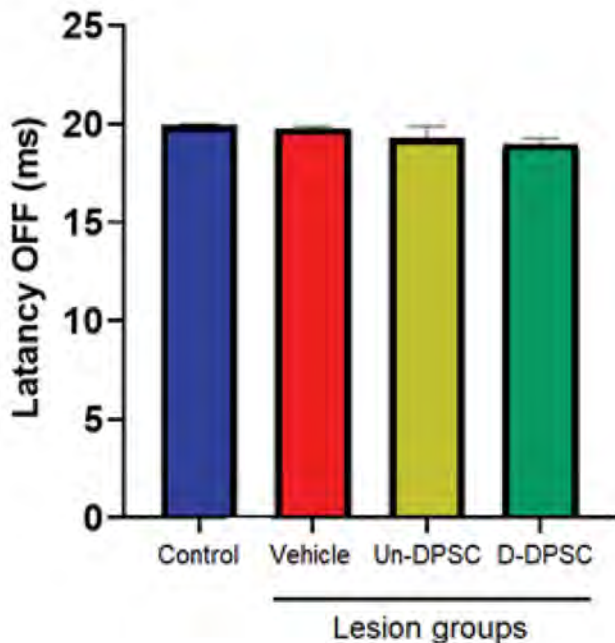


Fig.6: Response latency OFF. Response latency of the D2 barrel neurons to the whisker deflection. Data are expressed as mean \pm SEM. Un-DPSC; Undifferentiated dental pulp stem cell, D-DPSC; Lesion+differentiated dental pulp stem cell.

Discussion

The present study revealed that the spontaneous activity, latency, and features of response magnitude in the barrel cortex opposing the damaged barrel cortex declined compared to the control group's neural activity, three weeks after the unilateral focal lesion in the right barrel cortex. Lesions in the contralateral barrel cortex could change the response patterns of the neural responses of the intact homotopic cortex, which might also influence the animals' behavior (19). This response can improve in the groups that were injected with SCs in the lesioned area compared to the vehicle group three weeks after injection.

Reduced activity in spontaneous and evoked responses after 3 weeks in the lesion group, as well as disorders in the experience-dependent plasticity in the intact barrel cortex neurons following a lesion in the homotopic region in the opposing cerebral hemisphere, have been reported (14) which is consistent with the present study.

Reduced input from the lesioned hemisphere into the intact barrel cortex through the corpus callosum inputs is a possible mechanism for changes due to the lesion (5). According to a chronic study a barrel field cortex, sub-pial aspiration lesion could meaningfully degrade both evoked

activity and background in the barrel field cortex of the contralateral (14).

Still, several types of change, including reactive events, reduced growth factors, and release of neurotransmitters from the lesioned area and also eliminating the activity of ongoing interhemispheric signals originating from the lesioned area can be produced by a cortical lesion. These events are considered the possible modulators for firing features in neurons on the contralateral side (5). Changes in the dendritic morphology and growth factor performance might influence the function and structure of the contralateral barrel cortex of the lesion area (26). Also, the reduced cortical excitability mentioned in this study is probably the result of reduced excitatory neurotransmitter levels in the contralateral cortex (27) which can be investigated in further studies.

Besides, one could argue that thalamocortical projections play a role in improving animal performance (28) as a potential supporter for performance recovery following bilateral or unilateral SI and SII cortex (29).

We observed neural responses improved in both U-DPSC and D-DPSC groups, this improvement was significant in the D-DPSCs group compared to the vehicle group. However, a significant proportion of grafted SCs migrated to the contralateral side of the brain, whether this was lesioned or intact, showing that SCs are attracted by and interact with both reorganization and degeneration regions (30). Behavioral recovery after brain damage can be improved by SC transplantation in animal models but there is no understanding of the functional integration of SC-derived neurons into injured brain circuitry (20).

Because a large part of this area is eliminated by our mechanical lesion, therefore rearrangement of these neuronal barrel clusters by SC injection is far from expected. However, SC transplantation can induce events to enhance performance at the molecular level in the ipsilateral cortex. The ability of DPSCs to provide trophic factors in the peri-lesioned area was proved in our previous study (19).

Regeneration of damaged neuronal axons (31), reduction of apoptosis (32), glial scar (33), and inflammation (34), the release of neuroprotective factors, and the ability to differentiate various cell types, for example, oligodendrocytes, functional neurons, and astrocytes (35) have been considered as feasible mechanisms for functional improvement. Sc therapy may reopen the SII and the contralateral barrel cortex plasticity as well as the plasticity of the remaining barrel cortex that escaped the lesion (19). Still, we do not know the exact mechanism of how the neurons connected to the thalamus and the barrel contralateral cortex. Further investigations are needed to find the exact mechanism.

Transplanted human embryonic SCs in rodents, send axonal projections to extensive brain areas, including the contralateral cortex (19). Following a stroke in rats, axonal projections from intracortical transplanted SC-

derived (36) cortical neurons extend to both contralateral and ipsilateral hemispheres. Whether an activity in the grafted neurons influences sensorimotor function as well as these efferent connections become incorporated into stroke-injured host neural circuitry remains unclear (20). In our previous study, it was shown that transplantation of DPSCs into a lesioned somatosensory (barrel) cortex can facilitate the recovery of function at week 2-4 compared to the vehicle group and affected a range of neuronal markers such as nestin, NeuN, Olig 2, BDNF, neuroigin1 and GFAP in the barrel cortex post-lesion (19). After cortical stroke, transcallosal connections are important and involved in behavioral recovery and spontaneous interhemispheric structural rearrangement. Transcallosal connections of transplanted neurons are likely to participate in this reorganization (37). The results of several recent studies in other experimental models confirm this idea which is in line with our findings, that regeneration of the cortical neural circuitry is probable by cell transplantation in the damaged adult brain (20).

The current study had limitations for recording from the lesioned- barrel cortex and there is a lack of information about how SCs injection can consequently influence neural function.

Conclusion

Injection of D-DPSCs or U-DPSCs into the lesioned barrel cortex area can improve the homologous opposite cortical neural responses. Although the injection of SCs is not expected to reorganize the barrel, the changes in the contralateral barrel cortex could be observed after lesion and SC therapy in neural connections with the area of brain damage.

Acknowledgements

The present study was supported by a research grant from the Council for Development Stem Cells Sciences and Technologies (Grant No.: 82710/11) and by funds from Kerman Neuroscience Research Center (Grant No.: KNRC/EC/95-63). The authors declared no potential conflicts with respect to the research, authorship, and/or publication of this article.

Authors' Contributions

M.R.A., V.Sh.; Conceptualization and Supervision. M.S., M.R.A., V.Sh.; Methodology. M.S., A.D.; Investigation. V.SH.; Funding acquisition. M.S., M.R.A., A.D.; Writing- Reviewing and Editing. All authors read and approved the final manuscript.

References

- Crandall SR, Patrick SL, Cruikshank SJ, Connors BW. Infrabarrels are layer 6 circuit modules in the barrel cortex that link long-range inputs and outputs. *Cell Rep.* 2017; 21(11): 3065-3078.
- Feldmeyer D, Brecht M, Helmchen F, Petersen CC, Poulet JF, Staiger JF, et al. Barrel cortex function. *Prog Neurobiol.* 2013; 103: 3-27.
- Chance SA, Crow TJ. Distinctively human: cerebral lateralisation and language in *Homo sapiens*. *J Anthropol Sci.* 2007; 85: 83-100.
- Ku RY, Torii M. New molecular players in the development of callosal projections. *Cells.* 2020; 10(1): 29.
- Li L, Rema V, Ebner FF. Chronic suppression of activity in barrel field cortex downregulates sensory responses in contralateral barrel field cortex. *J Neurophysiol.* 2005; 94(5): 3342-3356.
- Tsytarev V, Arakawa H, Zhao S, Chédotal A, Erzurumlu RS. Behavioral consequences of a bifacial map in the mouse somatosensory cortex. *J Neurosci.* 2017; 37(30): 7209-7218.
- Sheibani V, Shamsizadeh A, Afarinesh MR, Rezvani ME. Neonatal capsaicin treatment modulates experience-dependent plasticity in the rat barrel cortex. *J Comp Neurol.* 2010; 518(17): 3427-3438.
- Shuler MG, Krupa DJ, Nicolelis MA. Bilateral integration of whisker information in the primary somatosensory cortex of rats. *J Neurosci.* 2001; 21(14): 5251-5261.
- Lu H, Wang L, Rea WW, Brynildsen JK, Jaime S, Zuo Y, et al. Low-but not high-frequency LFP correlates with spontaneous BOLD fluctuations in rat whisker barrel cortex. *Cereb Cortex.* 2016; 26(2): 683-694.
- Nudo RJ. Recovery after damage to motor cortical areas. *Curr Opin Neurobiol.* 1999; 9(6): 740-747.
- Baron JC. Testing cerebral function: will it help the understanding or diagnosis of central nervous system disease? *Ciba Found Symp.* 1991; 163: 250-261.
- Cappa SF, Perani D, Grassi F, Bressi S, Alberoni M, Franceschi M, et al. A PET follow-up study of recovery after stroke in acute aphasics. *Brain Lang.* 1997; 56(1): 55-67.
- Juhász C, Kamondi A, Szirmai I. Spectral EEG analysis following hemispheric stroke: evidences of transhemispheric diaschisis. *Acta Neurol Scand.* 1997; 96(6): 397-400.
- Rema V, Ebner FF. Lesions of mature barrel field cortex interfere with sensory processing and plasticity in connected areas of the contralateral hemisphere. *J Neurosci.* 2003; 23(32): 10378-10387.
- Song M, Mohamad O, Gu X, Wei L, Yu SP. Restoration of intracortical and thalamocortical circuits after transplantation of bone marrow mesenchymal stem cells into the ischemic brain of mice. *Cell Transplant.* 2013; 22(11): 2001-2015.
- Li X, Sundström E. Stem cell therapies for central nervous system trauma: the 4 Ws-what, when, where, and why. *Stem Cells Transl Med.* 2022; 11(1): 14-25.
- Pang QM, Deng KQ, Zhang M, Wu XC, Yang RL, Fu SP, et al. Multiple strategies enhance the efficacy of MSCs transplantation for spinal cord injury. *Biomed Pharmacother.* 2023; 157: 114011.
- Bao X, Wei J, Feng M, Lu S, Li G, Dou W, et al. Transplantation of human bone marrow-derived mesenchymal stem cells promotes behavioral recovery and endogenous neurogenesis after cerebral ischemia in rats. *Brain Res.* 2011; 1367: 103-113.
- Sabzalizadeh M, Afarinesh MR, Esmaeili-Mahani S, Farsinejad A, Derakhshani A, Arabzadeh E, et al. Transplantation of rat dental pulp stem cells facilitates post-lesion recovery in the somatosensory whisker cortex of male Wistar rats. *Brain Res Bull.* 2021; 173: 150-161.
- Palma-Tortosa S, Tornero D, Grønning Hansen M, Monni E, Hajj M, Kartsivadze S, et al. Activity in grafted human iPS cell-derived cortical neurons integrated in stroke-injured rat brain regulates motor behavior. *Proc Natl Acad Sci USA.* 2020; 117(16): 9094-9100.
- Sabzalizadeh M, Mollashahi M, Afarinesh MR, Mafi F, Joushy S, Sheibani V. Sex difference in cognitive behavioral alterations and barrel cortex neuronal responses in rats exposed prenatally to valproic acid under continuous environmental enrichment. *Int J Dev Neurosci.* 2022; 82(6): 513-527.
- Sabzalizadeh M, Afarinesh MR, Esmaeili-Mahani S, Sheibani V. Focal unilateral mechanical lesion in barrel cortex impairs rat's abilities to discriminate textures. *Somatosens Mot Res.* 2021; 38(1): 1-10.
- Shafiei F, Afarinesh MR, Golshan F, Haghpanah T, Sabzalizadeh M, Zangiabadi I, et al. Comparison of pre-pulse inhibition, tactile discrimination learning and barrel cortical neural response in adult male rats following chronic exposure to morphine, methadone and buprenorphine. *Physiol Behav.* 2019; 212: 112694.
- Afarinesh MR, Sheibani V, Arabzadeh S, Shamsizadeh A. Effect of chronic morphine exposure on response properties of rat barrel cortex neurons. *Addict Biol.* 2008; 13(1): 31-39.
- Afarinesh MR, Shafiei F, Sabzalizadeh M, Haghpanah T, Taheri M, Parsania S, et al. Effect of mild and chronic neonatal hypothyroidism on sensory information processing in a rodent model: a behavioral and electrophysiological study. *Brain Res Bull.* 2020; 155: 29-36.
- Madinier A, Quattromani MJ, Sjölund C, Ruscher K, Wieloch T.

- Enriched housing enhances recovery of limb placement ability and reduces aggrecan-containing perineuronal nets in the rat somatosensory cortex after experimental stroke. *PLoS One*. 2014; 9(3): e93121
27. Andrews RJ. Transhemispheric diaschisis. A review and comment. *Stroke*. 1991; 22(7): 943-949.
 28. Tamè L, Braun C, Holmes NP, Farnè A, Pavani F. Bilateral representations of touch in the primary somatosensory cortex. *Cogn Neuropsychol*. 2016; 33(1-2): 48-66.
 29. Gronthos S, Brahim J, Li W, Fisher LW, Cherman N, Boyde A, et al. Stem cell properties of human dental pulp stem cells. *J Dent Res*. 2002; 81(8): 531-535.
 30. Smith SM, Giedzinski E, Angulo MC, Lui T, Lu C, Park AL, et al. Functional equivalence of stem cell and stem cell-derived extracellular vesicle transplantation to repair the irradiated brain. *Stem Cells Transl Med*. 2020; 9(1): 93-105.
 31. Zhang X, Zhou Y, Li H, Wang R, Yang D, Li B, et al. Transplanted dental pulp stem cells migrate to injured area and express neural markers in a rat model of cerebral ischemia. *Cell Physiol Biochem*. 2018; 45(1): 258-266.
 32. Hosseini SM, Farahmandnia M, Razi Z, Delavari S, Shakibajahromi B, Sarvestani FS, et al. Combination cell therapy with mesenchymal stem cells and neural stem cells for brain stroke in rats. *Int J Stem Cells*. 2015; 8(1): 99-105.
 33. Peruzzaro ST, Andrews MMM, Al-Gharaibeh A, Pupiec O, Resk M, Story D, et al. Transplantation of mesenchymal stem cells genetically engineered to overexpress interleukin-10 promotes alternative inflammatory response in rat model of traumatic brain injury. *J Neuroinflammation*. 2019; 16(1): 2.
 34. Hu W, Feng Z, Xu J, Jiang Z, Feng M. Brain-derived neurotrophic factor modified human umbilical cord mesenchymal stem cells-derived cholinergic-like neurons improve spatial learning and memory ability in Alzheimer's disease rats. *Brain Res*. 2019; 1710: 61-73.
 35. Nudi ET, Jacqmain J, Dubbs K, Geeck K, Salois G, Searles MA, et al. Combining enriched environment, progesterone, and embryonic neural stem cell therapy improves recovery after brain injury. *J Neurotrauma*. 2015; 32(14): 1117-1129.
 36. Soma FA, Wang TY, Niclis JC, Bruggeman KF, Kauhausen JA, Guo H, et al. Peptide-based scaffolds support human cortical progenitor graft integration to reduce atrophy and promote functional repair in a model of stroke. *Cell Rep*. 2017; 20(8): 1964-1977.
 37. Carmichael ST, Chesselet MF. Synchronous neuronal activity is a signal for axonal sprouting after cortical lesions in the adult. *J Neurosci*. 2002; 22(14): 6062-6070.
-

Deciphering Role of lncRNA 91H in Liver Cancer: Impact on Tumorigenesis

Zhiyuan Mo, Ph.D., Zhuangqiang Wang, Ph.D.* 

Department of Hepatobiliary Surgery, Shanxi Bethune Hospital, Shanxi Academy of Medical Sciences, Tongji Shanxi Hospital, Third Hospital of Shanxi Medical University, Taiyuan, China

Abstract

Objective: This study aimed to investigate functional role of long ncRNA (lncRNA) 91H in liver cancer tumorigenesis, focusing on its effect on cell proliferation, apoptosis, cell cycle progression, migration, invasion, epithelial-mesenchymal transition (EMT) and *in vivo* tumor growth.

Materials and Methods: In this experimental study, liver cancer tissues and cell lines were analyzed for lncRNA 91H expression using quantitative reverse transcription polymerase chain reaction (qRT-PCR). By employing si-RNA to silence 91H, we aimed to gain a more in-depth understanding of its specific contributions and effects within these cells. Cell proliferation was assessed through the CCK-8 assay, while apoptosis and cell cycle progression were quantified using Annexin V-FITC staining and flow cytometry, respectively. Migration and invasion capabilities of liver cancer cells were assessed through transwell assay. EMT was assessed by analyzing protein expression levels of EMT-associated markers through western blotting. *In vivo* effect of 91H was assessed through xenograft experiments.

Results: Significantly higher levels of lncRNA 91H were observed in the liver cancer tissues and cell lines, than the normal cells. Silencing 91H in liver cancer cells led to a notable reduction of cell proliferation by inducing apoptosis and arresting the cell cycle. Liver cancer cells with decreased 91H expression exhibited diminished migration and invasion abilities, suggesting a role for 91H in promoting these processes. Furthermore, 91H knockdown weakened EMT in liver cancer cells, indicating its involvement in modulating this critical cellular transition. Furthermore, growth of subcutaneous xenograft tumors and weight was effectively suppressed by sh-lncRNA 91H.

Conclusion: Our study strongly supports lncRNA 91H's role in liver cancer progression by enhancing proliferation, migration, invasion, and EMT. Targeting 91H reduced *in vivo* tumor growth, highlighting its potential as a therapeutic liver cancer target. These findings suggest 91H's pivotal role in liver cancer aggressiveness, opening doors for future therapeutic approaches.

Keywords: Apoptosis, Epithelial-Mesenchymal Transition, Liver Cancer, lncRNA 91H, Tumorigenesis

Citation: Mo Zh, Wang Zh. Deciphering role of lncRNA 91H in liver cancer: impact on tumorigenesis. Cell J. 2023; 25(12): 829-838. doi: 10.22074/CELLJ.2023.2010456.1395

This open-access article has been published under the terms of the Creative Commons Attribution Non-Commercial 3.0 (CC BY-NC 3.0).

Introduction

In the recent years, liver cancer has become one of the most overwhelming and highly challenging human health disorders. Neoplastic human malignancies are grouped with the top five human cancers, both in terms of disease prevalence and associated mortality at the global level (1, 2). Liver cancer ranks as the fourth leading global cause of mortality, and the overall incidence of liver cancer has increased over the last two to three decades (3). Liver cancer incidence is anticipated to surge by 55.0%, with a corresponding 56.4% rise in the number of fatalities expected between 2020 and 2040. Moreover, this disease occurs at a comparatively high frequency in East Asian countries (4). However, the incidence of liver cancer has slightly declined in China and Japan (5). Chronic liver infections, such as hepatitis B and C, fatty liver disease, alcohol consumption, and obesity are among some of the commonly reported risk factors for liver cancer (6).

While surgery and liver transplantation are the first-line treatment strategies employed for liver cancer, fewer than 20% of patients qualify for therapy (7). In the rest of cases, localized or systematic chemo- or radiotherapeutic approaches showed limited clinical success and often exhibited metastasis because of the heterogeneous nature of cancer cells (8). In addition, advanced stages of liver cancer are associated with a high risk of recurrence (9). Hence, exploration of liver cancer pathogenesis at the molecular level is necessary for better understanding of its progression and allocation of more effective therapeutic targets.

Long non-coding RNAs (lncRNAs) have gained immense attention with development of the human genome project, and they have received considerable research attention. Classified as the RNA transcripts lacking protein coding potential and comprising more

Received: 30/August/2023, Revised: 19/October/2023, Accepted: 03/December/2023

*Corresponding Address: Department of Hepatobiliary Surgery, Shanxi Bethune Hospital, Shanxi Academy of Medical Sciences, Tongji Shanxi Hospital, Third Hospital of Shanxi Medical University, Taiyuan, China
Email: zhuangqiangwang@126.com



Royan Institute
Cell Journal (Yakhteh)

than 200 nucleotides, lncRNAs have been demonstrated to affect several physiological and pathological aspects of the human body including the growth, progression, and metastasis of cancer (10, 11).

lncRNAs have garnered substantial attention in the recent years, due to their pivotal roles in regulating various cancer pathways and their potential as valuable biomarkers for diagnosing diseases. What was once considered an enigmatic facet of molecular biology has now evolved into a significant area of study, shedding light on the intricate involvement of lncRNAs in virtually all of the fundamental characteristics associated with cancer. Various studies showed that lncRNAs exhibited significant dysregulation in human cancers, including liver cancer, while they were implicated to serve as key prognostic and therapeutic targets (12, 13). Traditionally, cancer research revolved around several well-defined hallmarks of the disease, including sustained proliferation, replicative immortality, evasion of growth suppressors, induction of angiogenesis, resistance to programmed cell death, and the formidable process of metastasis. Notably, lncRNAs have become instrumental in understanding and manipulating these hallmark features. They are now recognized as key orchestrators, exerting a profound influence on each of these facets of cancer progression. For instance, lncRNAs have been found to govern the uncontrolled cell division observed in the sustained proliferation, thereby playing a central role in driving tumor growth. Moreover, they contributed to the cancer cell ability to evade the normal mechanisms that would otherwise halt their relentless growth, thus ensuring replicative immortality. lncRNAs have also been implicated in promoting formation of the new blood vessels, a process known as angiogenesis, which is crucial for the nutrient supplied to the growing tumor. Additionally, they are closely linked to thwarting the programmed cell death or apoptosis, allowing cancer cells to persist and proliferate unchecked. Perhaps one of the most concerning hallmarks of cancer is metastasis, the spread of cancer cells to distant organs and tissues. lncRNAs have been identified as key facilitators in this perilous journey, aiding cancer cells in their escape from the primary tumor and enabling their successful establishment in new sites.

lncRNAs affect diverse signaling pathways in liver cancer cells to regulate their malignant behavior and promote tumorigenesis (14). Significantly, lncRNAs have a pivotal role in modulating the immune response, facilitating liver regeneration, and regulating redox signaling. These functions are of paramount importance in shaping the liver microenvironment and influencing the course of chronic liver diseases. When lncRNAs become dysregulated within these processes, it can trigger chronic hepatitis, abnormal liver growth, and oxidative stress, ultimately paving the way for the onset and advancement of hepatocellular carcinoma (HCC). Certainly, high-throughput technologies like RNA-sequencing and microarrays have unveiled distinct expression profiles of

lncRNAs in HCC tissues compared to noncancerous liver tissues. These findings strongly suggested that biogenesis of the specific lncRNAs underwent dysregulation during development of HCC. Aberrations in lncRNA biogenesis encompassed various processes, including the epigenetic silencing or activation of lncRNAs with tumor-suppressive or promoting roles, transcriptional activation or repression of lncRNAs by specific oncogenic or tumor-suppressive transcription factors, distinct processing patterns that imbue lncRNAs with oncogenic properties, and interactions between lncRNAs, microRNAs or proteins that have an impact on lncRNA stability.

lncRNA 91H exhibited expression patterns during embryonic development and it is typically suppressed after birth, except in the particular tissues, like the mammary gland and uterus. Imprinting modifications, leading to aberrant H19 expression, are associated with developmental disorders. lncRNA 91H is known for its tumor-promoting regulatory role in colorectal cancer (15). Overexpression of 91H has been shown to be associated with the growth and metastasis of hepatocellular, in addition to affecting survival via positive regulation of IGF2 (16). Involvement of H19 in tumorigenesis has been extensively documented, with H19 being consistently overexpressed in the various solid tumors such as prostate, bladder, and breast cancers. In fact, it has been demonstrated that H19 is overexpressed in 73% of the breast cancer tissues compared to the healthy tissues. This study aimed to investigate functional role of 91H in liver cancer. The results indicated that 91H acted as an oncogene in liver cancer and suggested its possible prognostic and therapeutic utility in the future.

Materials and Methods

Patient samples

The current experimental study involved a total of 25 patients (15 male and 10 female, age range of 32-84 years old) diagnosed with liver cancer after obtaining written informed consent. Tumor and adjacent non-tumor liver tissue samples (verified by hospital pathologists) were collected once the patients underwent surgery at the Shanxi Bethune Hospital, Taiyuan, China, but prior to the application of radiotherapy or chemotherapy. The tissues were snap-frozen in liquid nitrogen and stored at -80°C until use. Diagnosis of pathological and metastatic/nonmetastatic stages was performed by three pathologists of the Shanxi Bethune Hospital, Taiyuan, China, who were blinded to the study. This study was approved by the Shanxi Bethune Hospital Ethics Committee (No. 2022521).

Culture and transfection of cell lines

A normal liver epithelial cell line (THLE-3) and four liver tumor cell lines (CSQT-2, Hep3B, Huh-7, and PLC) were obtained from the Chinese Academy of Sciences (Shanghai, China). Dulbecco's modified Eagle's medium (DMEM, HyClone; GE Healthcare Life Sciences, USA) containing 10% fetal bovine serum (FBS, Thermo Fisher Scientific, USA) supplemented with 100 U/ml and 100

mg/ml concentrations of penicillin and streptomycin, respectively (both from Gibco Inc., USA), was used for the culture and maintenance of the cell lines at 37°C with 5% CO₂ in a humidified incubator.

Synthetic small-interfering si-91H (45 nM) and negative control si-NC (45 nM) oligos were acquired from GenePharma Co., Ltd (Shanghai, China). For transfection, the cells were cultured in six-well plates until reaching more than 80% confluence, at which point they were stably transfected with suitable oligos using Lipofectamine® 3,000 reagent (Invitrogen, Thermo Fisher Scientific Inc., USA) according to the manufacturer's guidelines. The cells were harvested 48 hours after transfection.

RNA isolation and quantitative reverse transcription polymerase chain reaction

Total RNA was extracted from the tissues and cell lines using TRIzol reagent (Thermo Fisher Scientific Inc., USA) according to the manufacturer's protocol. Following quantification, using NanoDrop, RNA was reverse-transcribed into cDNA using the RevertAid First Strand cDNA synthesis kit (Thermo Fisher Scientific Inc., USA). To detect relative transcript levels of 91H, quantitative reverse transcription PCR (qRT-PCR) was performed on a QuantStudio 5.0 Real-Time PCR System (Applied Biosystems, Thermo Fisher Scientific Inc., USA) using SYBR™ Green Master Mix (Thermo Fisher Scientific Inc., USA). Relative mRNA expression levels were quantified using 2- $\Delta\Delta C_t$ method and normalized to that of β -actin. The primer sequences used were as follows:

91H-

F: 5'-GCTTGTCAGTAGAGTGCGCC-3'

R: 5'-CATCCAGTTGACCGAGCTTG-3'

β -actin-

F: 5'-CAAGATCATTGCTCCTCCTGA-3'

R: 5'-AGTCCGCCTAGAAGCATTG-3'.

CCK-8 cell proliferation assay

Proliferation of the transfected cancer cells was determined using Cell counting kit-8 (CCK-8, Beyotime Inst. of Biotech., China) according to the manufacturer recommendations. Briefly, 2×10^5 cells were seeded per well in a 96-well plate. After culturing the cells for 0, 24, 48, or 72 hour(s) at 37°C, 15 μ l of CCK-8 reagent was added to each well, followed by incubation for 2 hours at 37°C. Finally, the optical density (OD) at 450 nm (OD₄₅₀) of each well was determined using a spectrophotometer and plotted to generate proliferation curve.

Migration and invasion assays

A24-well BD Matrigel Transwell chamber (BD Biosciences, USA) coated with or without matrigel was used to analyze migration and invasion of the transfected cancer cells. Briefly, 2×10^4 transfected cells were suspended in serum-free DMEM (Gibco, USA) and added to the upper part of the transwell

chamber, whereas 500 μ l of DMEM with 10% FBS was placed in the lower portion of the chamber. After 24 hours of incubation at 37°C, the non-migrating or invading cells were carefully removed with the help of cotton swabs, while those migrating or invading the lower part of the chamber were fixed with methanol (Thermo Scientific, USA) and stained with 0.1% crystal violet (Thermo Scientific, USA). Finally, the cells were visualized and counted manually under a light microscope (100 \times , Olympus, Japan).

Western blotting

To extract total proteins from the cells, we initiated the process by lysing the cells using the radioimmunoprecipitation assay (RIPA) lysis and extraction buffer (Thermo Fisher Scientific, USA), complemented with 1% protease inhibitors (Sigma-Aldrich, USA) to ensure integrity of the proteins during extraction. Following the lysis step, the cell lysates underwent centrifugation to separate cellular components. To quantify presence of the total proteins in the suspension, we employed Bradford's assay, a widely-used method for protein concentration determination. This step allowed us to precisely measure protein content and ensure accuracy in our subsequent analyses.

For separation of proteins, we utilized a 12% sodium dodecyl-sulfate polyacrylamide gel electrophoresis (SDS-PAGE). The separated proteins were then transferred onto polyvinylidene fluoride membranes (Millipore, USA). These membranes were subsequently blocked with 5% skimmed milk for 1.5 hours, serving as a means to prevent non-specific binding during the antibody incubation process. Membranes were probed with the specific primary antibodies like anti-E-cadherin (Sigma-Aldrich, USA) anti- α -catenin, (Thermo Fisher Scientific, USA), anti-N-cadherin (Cell signaling technology, USA), anti-fibronectin (Abcam, USA) and anti-GAPDH (Abcam, USA) overnight at 4°C. The membranes were then incubated with HRP-conjugated secondary antibody (Abcam, USA) and specific protein signals were detected using an Enhanced Chemiluminescence kit (Thermo Fisher Scientific, USA). The acquired signals were quantified with Image J software, and data normalization was achieved by utilizing GAPDH protein.

Flow cytometry

Hep3B and Huh-7 cancer cells, transfected with si-91H or si-NC, were seeded into six-well plates at a density of 5×10^3 cells/well and cultured for 24 hours at 37°C. Afterward, the cells were collected by centrifugation, mixed with 0.025% Triton X-100, and treated with 50 ng/ml-1 propidium iodide (PI, Thermo Fisher Scientific, Fisher) for 25 minutes. A FACSCalibur flow cytometer (BD Biosciences, USA) was used to study cell cycle of the transfected cells.

To study apoptosis, the transfected cells were analyzed using an Annexin V-FITC Apoptosis Detection Kit (Dojindo, China) at room temperature following the manufacturer's instructions. Finally, a FACSCalibur flow cytometer (Becton Dickinson, San Jose, CA, USA) was used to assess apoptosis.

Animal experiment description

A total of 20 male BALB/c nude mice, aged 6-8 weeks and weighting 18 ± 2 g, were procured from Shanxi Academy of Medical Sciences, China. The mice were divided randomly into two groups. In the first group, either Hep3B cells (2×10^6 cells/100 μ l) or Huh-7 cells (2×10^6 cells/100 μ l) were injected subcutaneously (100 μ l/mouse) to establish the tumor xenograft model. Each group consisted of 10 mice. Subsequently, each group was further divided randomly into two subgroups, each containing five mice.

For the purpose of gene silencing, lentivirus carrying a short hairpin RNA (shRNA) targeting lncRNA 91H (sh-lncRNA 91H) were obtained from GenePharma company (China). The lentivirus had a titer of 108 TU/ml and it was administered at a dose of 20 μ l per mouse. As a control, a negative control shRNA (sh-NC), provided by Invitrogen, was also injected. This treatment was carried out weekly for a total of three consecutive weeks. In conclusion of the 28-days period, all nude mice were humanely euthanized. The subcutaneous tumors were then removed, photographed, and weighed for further analysis. All of the experimental procedures adhered to the established guidelines and received approval from the Ethics Committee of Third Hospital of Shanxi Medical University.

Statistical analysis

Graphpad prism 7.0 (GraphPad Software, Inc., San Diego, CA, USA) offline software was used for performing the statistical analysis. The experiments were performed using three replicates and the values given are the representative of mean \pm standard deviation. Student's t test (unpaired, two-tailed) was performed for analyzing the differences between two treatments and $P < 0.05$ difference was considered statistically significant.

Results

91H is overexpressed in liver cancer

qRT-PCR was performed to analyze expression of lncRNA 91H in liver cancer and normal adjacent tissues. The results showed that 91H expression level was significantly higher ($P < 0.05$) in the liver cancer samples than the normal tissue samples (Fig.1A). Interestingly, metastatic liver cancer tissues showed markedly higher ($P < 0.05$) transcript levels of 91H than the matched nonmetastatic cancer tissues (Fig.1B). Moreover, 91H expression level was significantly lower ($P < 0.05$) in tumor tissues corresponding to the stages I and II than that in the stages III and IV of liver cancer (Fig.1C). Expression analysis was also performed in liver cancer cell lines (CSQT-2, Hep3B, Huh-7 and PLC) using THLE-3 and normal liver epithelial cells, as a reference. The cancer cell lines showed significant overexpression ($P < 0.05$) of 91H compared to the normal liver epithelial cells (Fig.1D). The Hep3B and Huh-7 cancer cell lines were shown to express comparatively higher 91H levels among the cancer cell lines, chosen for further studies.

Knockdown of 91H inhibited growth of liver cancer cells

To characterize functional role of 91H in liver cancer, Hep3B and Huh-7 cancer cells were transfected with si-91H to induce 91H knockdown. Using si-NC-transfected cancer cells as a negative control, 91H expressions were downregulated 6.5 and 7.2-fold in si-91H transfected Hep3B and Huh-7 cancer cells, respectively (Fig.2A). Relative proliferation of the 91H downregulating liver cancer cells was studied with respect to the corresponding negative control cells using the CCK-8 assay. Both Hep3B and Huh-7 cancer cells with downregulated 91H showed significantly lower ($P < 0.05$) proliferation than the respective negative control cells (Fig.2B, C).

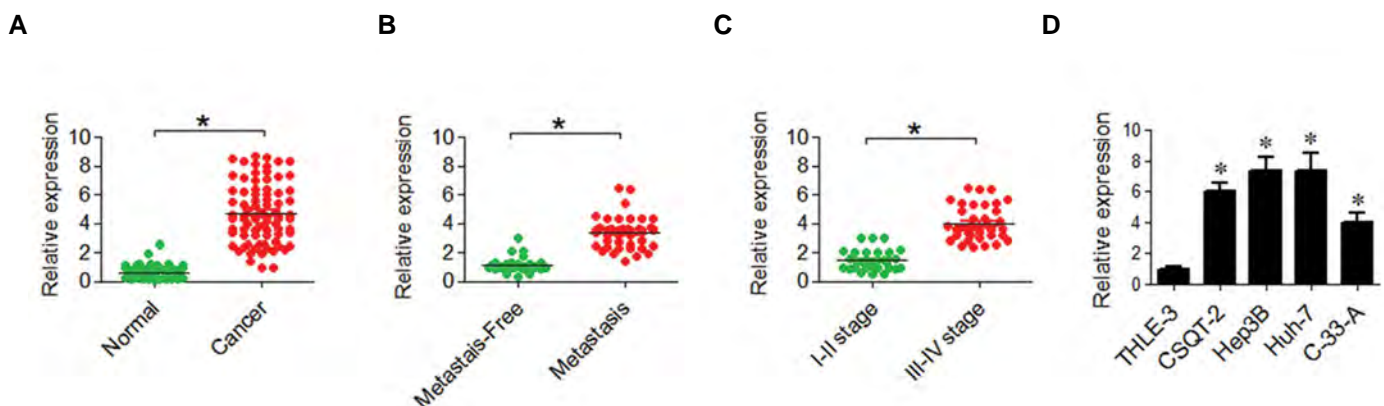


Fig.1: Expression analysis of lncRNA 91H in liver cancer tissues and cell lines. **A.** Comparison of lncRNA 91H expression levels between liver cancer tissues and normal adjacent tissues. Liver cancer tissues exhibited significantly higher expression of 91H compared to normal tissues. **B.** Analysis of 91H expression in metastatic and nonmetastatic liver cancer tissues. Metastatic liver cancer tissues showed markedly higher expression of 91H compared to nonmetastatic tissues. **C.** Assessment of 91H expression in different stages of liver cancer. Tumor tissues corresponding to stage III and IV liver cancer exhibited significantly higher expression of 91H compared to stage I and II tissues. **D.** Evaluation of 91H expression in liver cancer cell lines (CSQT-2, Hep3B, Huh-7, and PLC) compared to THLE-3 normal liver epithelial cells. The cancer cell lines showed significant overexpression of 91H compared to normal liver epithelial cells. Hep3B and Huh-7 cell lines were selected for further study due to their comparatively higher levels of 91H expression. *; $P < 0.05$.

Knockdown of 91H inhibited migration and invasion of liver cancer cells

Transwell assay results demonstrated that knockdown of 91H in the both Hep3B and Huh-7 cells significantly inhibited their migration and invasion abilities, compared to the respective negative control cells. In the invasion

assay, knockdown of 91H led to a significant decrease in the number of invasive cells compared to the negative control group in both cell lines ($P < 0.05$, Fig.3A, B). Similarly, in the migration assay, number of the migratory cells was dramatically reduced in the 91H knockdown group compared to that in the negative control group for the both Hep3B and Huh-7 cells ($P < 0.05$, Fig.3C, D).

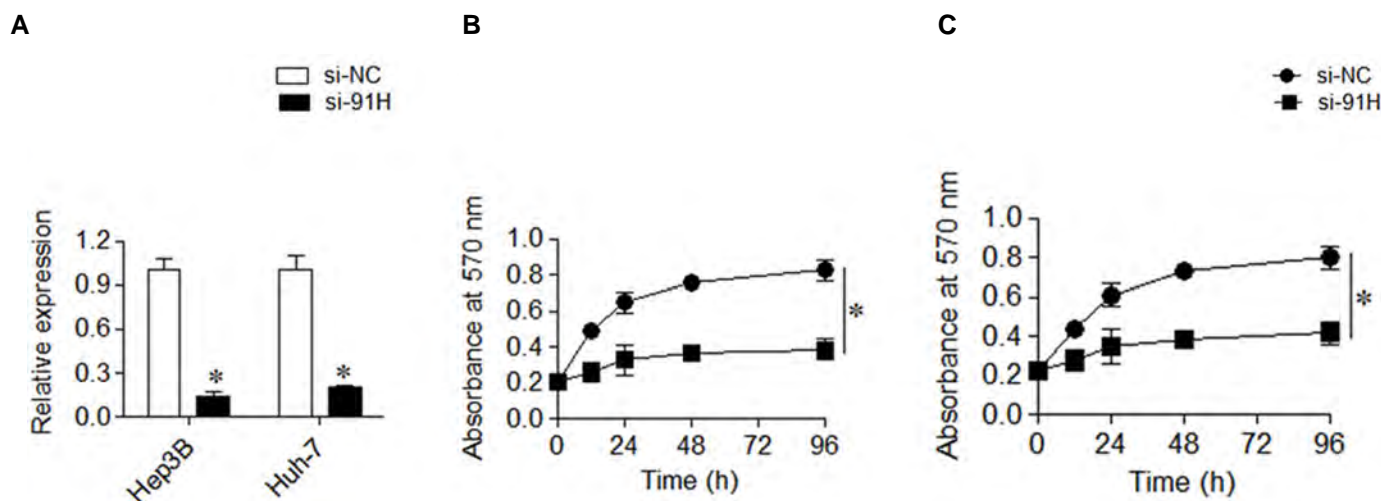


Fig.2: Functional characterization of lncRNA 91H knockdown in liver cancer cells. **A.** Efficiency of lncRNA 91H knock-down in Hep3B and Huh-7 cancer cells. Transfection of si-91H oligos led to a significant downregulation of 91H expression in both Hep3B and Huh-7 cells compared to si-NC-transfected cells, with a fold change of 6.5 and 7.2, respectively. Relative proliferation of liver cancer cells after knockdown of 91H. CCK-8 assays demonstrated that **B.** Hep3B and **C.** Huh-7 cells with downregulated 91H exhibited significantly lower proliferation compared to the respective negative control cells. *; $P < 0.05$ and h; Hours.

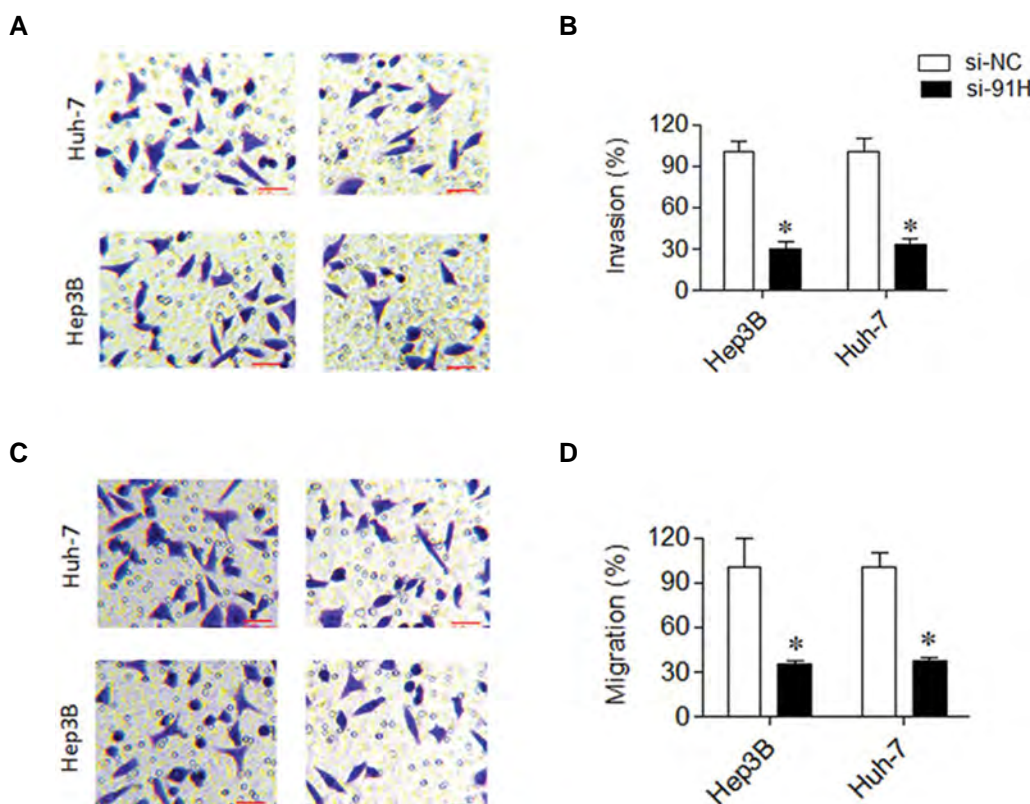


Fig.3: Migration and invasion assay results upon 91H knockdown in Hep3B and Huh-7 cancer cells. **A, B.** Representative images of invasion assays indicating the impact of 91H knockdown on Hep3B and Huh-7 cell invasion. 91H downregulation led to a significant decrease in cell invasion compared to the negative control cells (*; $P < 0.05$). **C, D.** Representative images of migration assays showing the effect of 91H knockdown on Hep3B and Huh-7 cell migration. Knockdown of 91H resulted in a marked reduction in cell migration compared to the negative control cells (*; $P < 0.05$, scale bar: 50 μ m).

Knockdown of 91H weakened the epithelial to mesenchymal transition of liver cancer cells

Our results demonstrated that 91H knockdown in the both Hep3B and Huh-7 cells had a significant impact on the expression of epithelial-to-mesenchymal transition (EMT)-related marker proteins. Downregulation of 91H in Hep3B and Huh-7 cancer cells significantly enhanced ($P<0.05$) expression of epithelial marker proteins (E-cadherin and α -catenin), while it significantly suppressed ($P<0.05$) the intracellular protein levels of mesenchymal markers (N-cadherin and fibronectin), indicating the inhibitory effect of 91H silencing on the EMT of liver cancer cells (Fig.4A-E).

91H silencing induced cell cycle arrest and apoptosis in the host liver cancer cells

To determine mechanism underlying the inhibitory

effects of 91H silencing on the growth, migration, invasion and EMT of liver cancer cells, cell cycle and apoptosis of the Hep3B and Huh-7 cancer cells with downregulated 91H levels were studied with reference to the respective negative control cells, using flow cytometry. The results showed that knockdown of 91H significantly increased relative percentage of the both Hep3B and Huh-7 cancer cells at the G0/G1 transition phase ($P<0.05$), while it significantly decreased ($P<0.05$) relative percentage of the host cells in the S-phase, indicative of G0/G1 cell cycle arrest (Fig.5A, B). Furthermore, relative percentage of apoptotic Hep3B and Huh-7 cancer cells was significantly increased by 91H silencing (Fig.5C, D). The results revealed that knockdown of 91H induced cell cycle arrest and promoted apoptosis to exert tumor-suppressive effects against liver cancer cells.

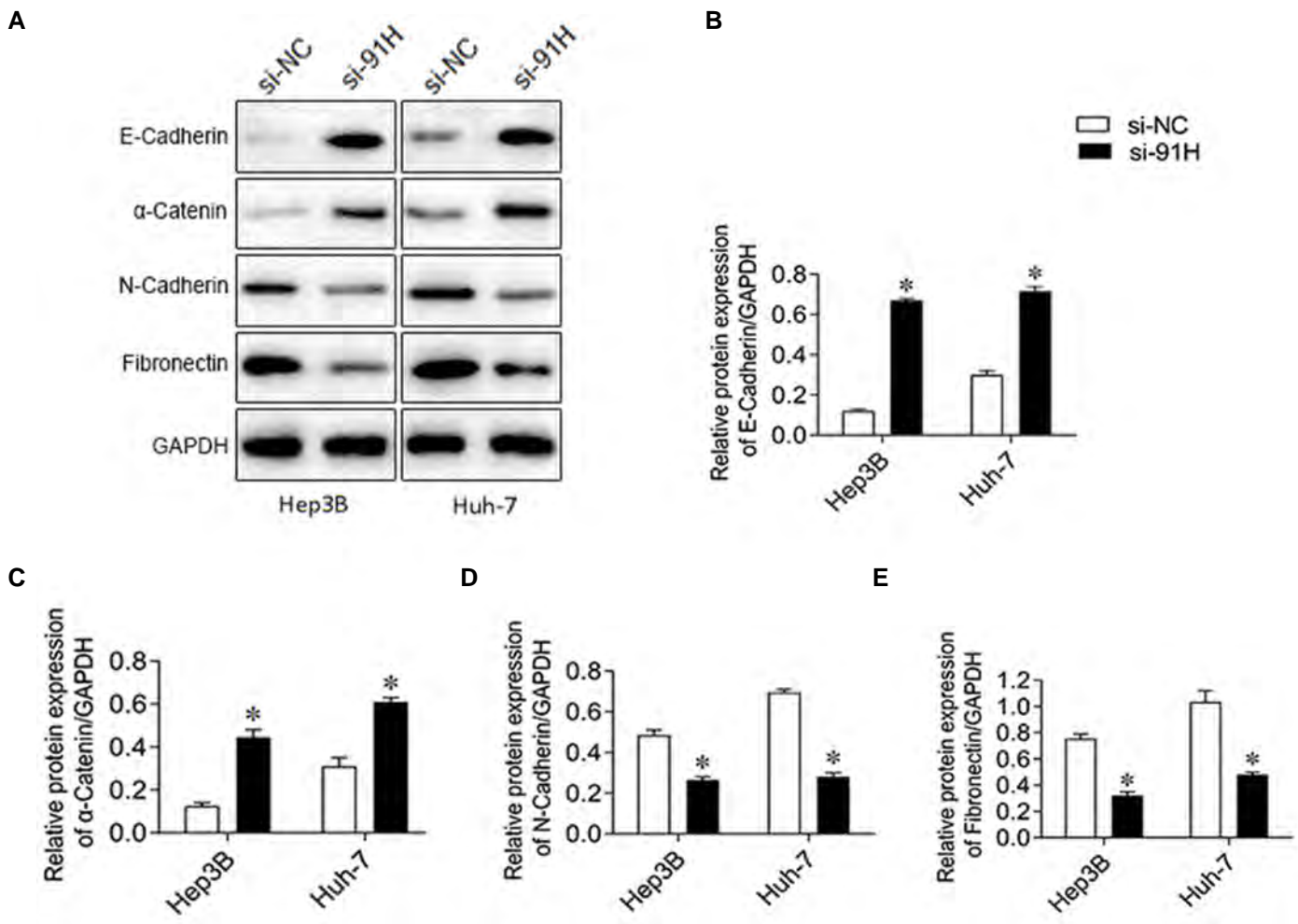
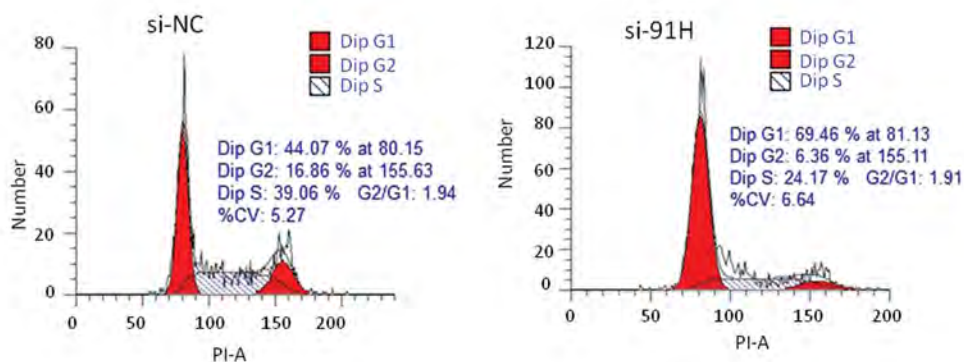
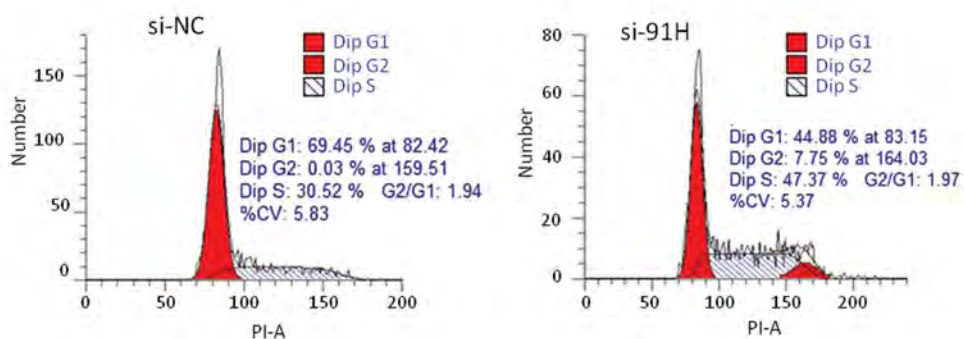


Fig.4: Western blot analysis of epithelial and mesenchymal markers in 91H downregulating Hep3B and Huh-7 cells. **A.** Representative Western blot images showing the protein levels of epithelial markers (E-cadherin and α -catenin) and mesenchymal markers (N-cadherin and fibronectin) in Hep3B and Huh-7 cells with 91H knockdown. Silencing of 91H increased the protein levels of epithelial markers and decreased the levels of mesenchymal markers, suggesting inhibition of the epithelial-to-mesenchymal transition (EMT) in liver cancer cells. **B.** Densitometry analysis of the Western blot for E-cadherin in Hep3B and Huh-7 cells. The protein level of E-cadherin significantly increased upon 91H knockdown compared to the negative control cells ($P<0.05$). **C.** Densitometry analysis of the Western blot for α -catenin in Hep3B and Huh-7 cells. The protein level of α -catenin significantly increased upon 91H knockdown compared to the negative control cells. **D.** Densitometry analysis of the Western blot for N-cadherin in Hep3B and Huh-7 cells. The protein level of N-cadherin significantly decreased upon 91H knockdown compared to the negative control cells. **E.** Densitometry analysis of the Western blot for fibronectin in Hep3B and Huh-7 cells. The protein level of fibronectin significantly decreased upon 91H knockdown compared to the negative control cells. *; $P<0.05$.

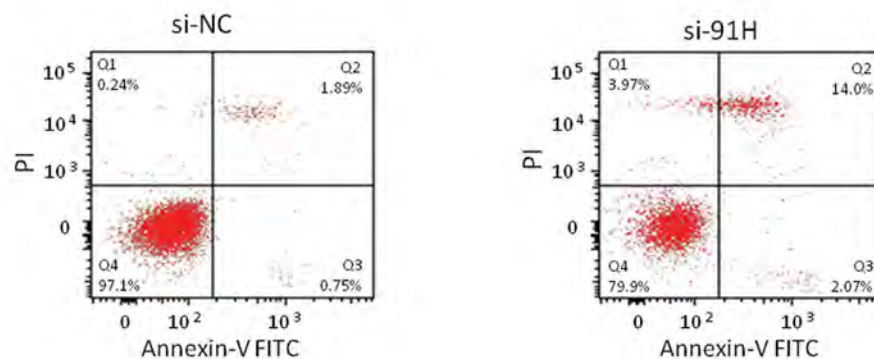
A



B



C



D

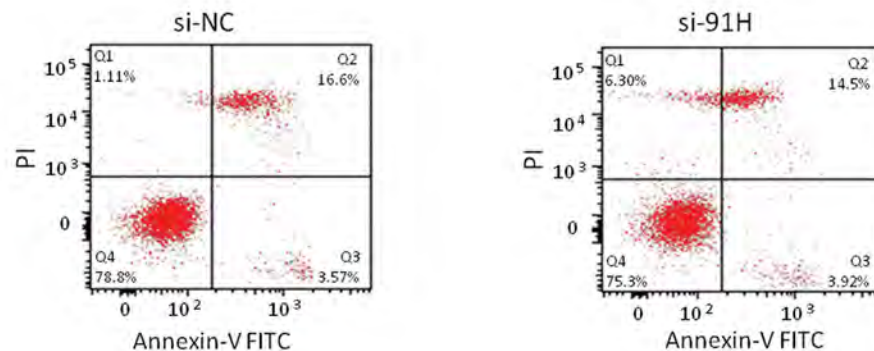


Fig.5: Effects of lncRNA 91H knockdown on cell cycle progression and apoptosis in Hep3B and Huh-7 cancer cells. **A.** Cell cycle analysis of Hep3B cells after 91H knockdown. Flow cytometry revealed a significant increase in the relative percentage of cells at the G0/G1 phase and a decrease in the percentage of cells at the S-phase, indicating G0/G1 cell cycle arrest in 91H downregulating cells compared to the negative control cells. **B.** Cell cycle analysis of Huh-7 cells after 91H knockdown. Flow cytometry revealed increase in the relative percentage of cells at the G0/G1 phase and a decrease in the percentage of cells at the S-phase, indicating G0/G1 cell cycle arrest in 91H downregulating cells compared to the negative control cells. **C.** Representative flow cytometry plots illustrating the apoptotic populations in Hep3B cells after 91H knockdown. Annexin V-FITC/PI staining was used to detect apoptotic cells. The relative percentage of apoptotic cells significantly increased in 91H downregulating cells compared to the negative control cells. **D.** Representative flow cytometry plots illustrating the apoptotic/necrotic populations in Huh-7 cells after 91H knockdown. Annexin V-FITC/PI staining was used to detect apoptotic/necrotic cells. The relative percentage of necrotic cells increased in 91H downregulating cells compared to the negative control cells.

Inhibition of liver cancer growth *in vivo* by silencing lncRNA 91H

To thoroughly investigate impact of lncRNA 91H on liver cancer growth in a live organism context, we utilized nude mouse models, as a platform for our study. In these models, we meticulously measured volume and weight of the formed tumors. Through the implementation of shRNA targeted at lncRNA 91H, we observed a substantial hindrance in tumor development. This intervention led to a remarkable reduction in the both tumor volume and weight, a trend that became evident starting from the 10th day post-treatment in the case of the tumor xenograft

mice injected with Hep3B cells, as compared to the mice treated with sh-NC.

Similarly, in the xenograft mice injected with Huh-7 cells, suppression of lncRNA 91H through shRNA yielded parallel results. Following the 10th day of treatment, a discernible decrease in tumor volume and weight was observed, further highlighting the influence of lncRNA 91H silencing on curbing tumor growth compared to the sh-NC-treated mice. This experimental insight underscored the significant role of lncRNA 91H in promoting liver cancer growth *in vivo* and supported the potential therapeutic avenue of targeting this molecule to impede tumor progression (Fig.6).

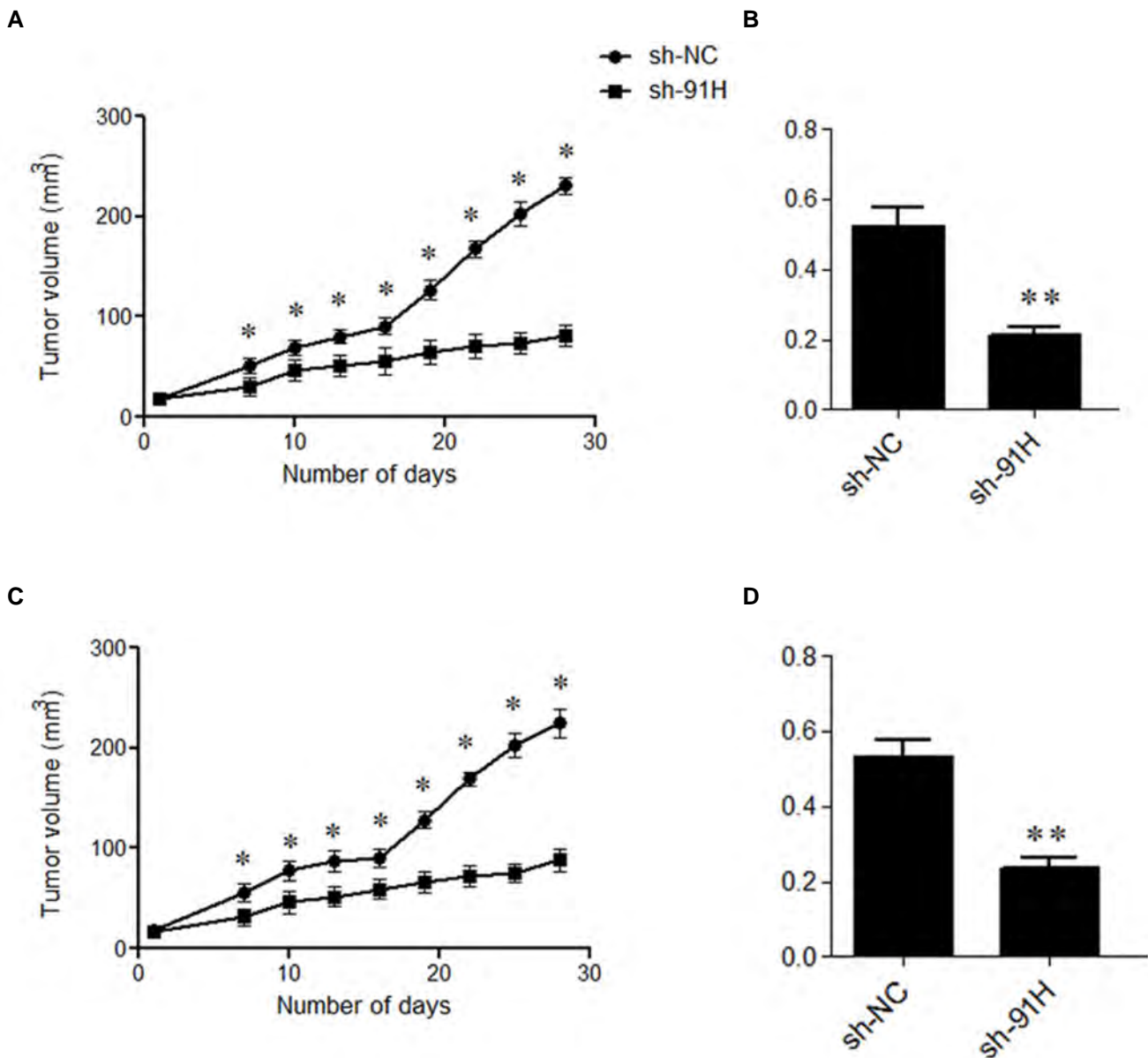


Fig.6: Inhibition of growth by silencing lncRNA 91H. Nude mouse models were utilized to explore the effects of silencing lncRNA 91H on growth. Hep3B cells or Huh-7 cells were subcutaneously injected, followed by treatment with either sh-NC or sh-lncRNA 91H. The subcutaneous tumor volume and tumor weight of **A.** Hep3B cells mouse model and **B.** Huh-7 cells mouse model were plotted. *, P<0.05 and **, P<0.01.

Discussion

In the recent years, there has been an exponential surge in research centered on lncRNAs. The growing body of evidence suggested that lncRNAs exerted a profound influence on various facets of animal cell biology, orchestrating critical processes like cell proliferation, differentiation and apoptosis (17, 18). Perturbed expression of lncRNAs has been closely associated with development and advancement of human cancers, including liver cancer (12, 13). These lncRNAs can function as either oncogenes or tumor suppressors, actively shaping the course of liver cancer tumorigenesis (19, 20). Investigation of the specific regulatory targets of lncRNAs in liver cancer holds the promise of enhancing our understanding of the disease pathogenesis, potentially paving the way for more effective therapeutic strategies against this formidable malignancy.

Previous reports have indicated that ncRNA 91H was upregulated in the various human cancers, with hepatocellular carcinoma, the most prevalent form of liver cancer, being no exception. Furthermore, this upregulation has been linked to the promotion of cancer growth and progression (15, 16). The present study contributes further insight into the functional role of 91H in liver cancer.

Our study revealed that both liver cancer tissues and cells exhibited significantly elevated levels of 91H expression. Importantly, this expression was found to be increased in parallel with the progression of liver cancer and establishment of metastatic lesions. These findings lent support to the prognostic potential of 91H and suggested that it may serve as a predictive marker for liver cancer survival, as previously reported (16, 21). Notably, knockdown of 91H in liver cancer cells resulted in a substantial reduction in their growth, migration and invasion, underscoring its direct involvement in modulating the aggressiveness and malignant behavior of these cancer cells (22).

An analysis of the expression of EMT molecular markers unveiled that downregulation of 91H inhibited EMT in liver cancer cells *in vitro*. EMT is a dynamic cellular process characterized by cytoskeletal rearrangements that underlie transition from an epithelial to a mesenchymal phenotype, enhancing cell motility and, consequently, promoting migration and invasion (23). EMT in cancer cells is characterized by distinct features and plays a pivotal role in fostering characteristics such as stemness, drug resistance and metastasis (24). Therefore, suppression of cancer cell EMT due to 91H knockdown hints at the therapeutic potential of targeting 91H in the context of liver cancer.

Furthermore, our study revealed that inhibition of 91H resulted in cell cycle arrest and induction of apoptosis in liver cancer cells. Similar findings have been reported in relation to silencing H19 (the sense RNA of 91H) in breast cancer cells (25). In summation, this study established that H19, an lncRNA, was upregulated in the both liver

cancer tissues and cell lines and it may represent one of the underlying molecular factors propelling growth, progression, and metastasis of liver cancer.

In our quest to unveil the oncogenic role of lncRNA 91H in liver cancer and its implications for proliferation, migration, invasion, EMT and *in vivo* tumor growth, it is essential to consider the potential molecular mechanisms underlying these effects. While this study primarily focused on the functional outcomes of 91H dysregulation, it is plausible that specific pathways and molecular interactions are at play. One key avenue for investigation involves the potential targets of lncRNA 91H. Identifying downstream genes or proteins regulated by 91H may shed light on its influence on cell proliferation, as well as its role in promoting metastasis and EMT. For instance, prior studies demonstrated modulation of the key EMT-related genes by lncRNAs, and it would be valuable to explore whether 91H similarly impacts these genes in liver cancer cells. Moreover, examining the interaction between 91H and other non-coding RNAs or proteins is of interest. It is conceivable that 91H may act in concert with other molecules to drive its oncogenic effects. Elucidating these interactions can provide insights into the complex regulatory networks that underlie liver cancer progression. The study observation of cell cycle arrest and apoptosis induction following 91H knockdown suggests potential involvement in cell cycle regulation and anti-apoptotic pathways. Investigating these pathways, including cyclins, cyclin-dependent kinases and anti-apoptotic proteins, may provide mechanistic insights into how 91H influences cell proliferation and survival. Furthermore, a deeper exploration of signal transduction pathways, such as PI3K/AKT and MAPK/ERK, which are known to play crucial roles in cancer progression, could reveal whether 91H is connected to these pathways. It is possible that 91H indirectly influences these signaling cascades, impacting cell migration, invasion and EMT in liver cancer.

Limitations of this study include the exclusive reliance on *in vitro* experiments, the study limited clinical sample size, omission of the exploration of potential variations in 91H expression among different populations, absence of long-term patient follow-up, and need for further research to understand 91H molecular mechanisms and translate findings into clinical therapies. Additionally, the study exclusive focus on 91H does not consider other lncRNAs implicated in liver cancer, warranting further comparative research.

Conclusion

The lncRNA 91H was significantly upregulated in liver cancer and its expression was increased with disease progression and metastasis. Silencing 91H expression in liver cancer cells inhibited their growth, migration, invasion and EMT *in vitro*. These inhibitory effects were deduced to result from induction of cell cycle arrest and apoptosis in liver cancer cells. Future investigations should prioritize gaining a deeper understanding of its underlying mechanisms, validate its clinical relevance through larger

patient cohorts and trials, develop therapeutic strategies, explore combination therapies, incorporate it into broader biomarker panels, utilize *in vivo* models and conduct long-term patient follow-up studies. These avenues hold promise for advancing liver cancer research and improving clinical outcomes.

Acknowledgements

This study was supported by Shanxi Province "136 Revitalization Medical Project Construction Funds" from Science and research fund of Shanxi Health Commission (Grant No: 2022043). The authors declare no conflict of interest.

Authors' Contributions

Z.M., Z.W.; Conceptualization and Data curation. Z.M; Investigation. Z.M; Wrote the original draft. Z.W; Wrote, Reviewed, and Edited the manuscript. All authors read and approved the final manuscript.

References

- Anwanwan D, Singh SK, Singh S, Saikam V, Singh R. Challenges in liver cancer and possible treatment approaches. *Biochim Biophys Acta Rev Cancer*. 2020; 1873(1): 188314.
- Wang G, Wang Q, Liang N, Xue H, Yang T, Chen X, et al. Oncogenic driver genes and tumor microenvironment determine the type of liver cancer. *Cell Death Dis*. 2020; 11(5): 313.
- Valery PC, Laversanne M, Clark PJ, Petrick JL, McGlynn KA, Bray F. Projections of primary liver cancer to 2030 in 30 countries worldwide. *Hepatology*. 2018; 67(2): 600-611.
- Liu Z, Jiang Y, Yuan H, Fang Q, Cai N, Suo C, et al. The trends in incidence of primary liver cancer caused by specific etiologies: results from the global burden of disease study 2016 and implications for liver cancer prevention. *J Hepatol*. 2019; 70(4): 674-683.
- Wu J, Yang S, Xu K, Ding C, Zhou Y, Fu X, et al. Patterns and trends of liver cancer incidence rates in Eastern and Southeastern Asian Countries (1983-2007) and Predictions to 2030. *Gastroenterology*. 2018; 154(6): 1719-1728. e5.
- Huang J, Lok V, Ngai CH, Chu C, Patel HK, Thogulva Chandrasekara V, et al. Disease burden, risk factors, and recent trends of liver cancer: a global country-level analysis. *Liver Cancer*. 2021; 10(4): 330-345.
- Strobel O, Neoptolemos J, Jager D, Buchler MW. Optimizing the outcomes of pancreatic cancer surgery. *Nat Rev Clin Oncol*. 2019; 16(1): 11-26.
- Castelli G, Pelosi E, Testa U. Liver cancer: molecular characterization, clonal evolution and cancer stem cells. *Cancers (Basel)*. 2017; 9(9): 127.
- von Felden J, Schulze K, Krech T, Ewald F, Nashan B, Pantel K, et al. Circulating tumor cells as liquid biomarker for high HCC recurrence risk after curative liver resection. *Oncotarget*. 2017; 8(52): 89978-89987.
- Zhang Y, Tang L. The application of lncRNAs in cancer treatment and diagnosis. *Recent Pat Anticancer Drug Discov*. 2018; 13(3): 292-301.
- Nandwani A, Rathore S, Datta M. LncRNAs in cancer: regulatory and therapeutic implications. *Cancer Lett*. 2021; 501: 162-171.
- Wang Y, Zhu P, Luo J, Wang J, Liu Z, Wu W, et al. LncRNA HAND2-AS1 promotes liver cancer stem cell self-renewal via BMP signaling. *Embo J*. 2019; 38(17): e101110.
- Jiao Y, Li Y, Ji B, Cai H, Liu Y. Clinical value of lncRNA LUCAT1 expression in liver cancer and its potential pathways. *J Gastrointest Liver Dis*. 2019; 28(4): 439-447.
- Hu XY, Hou PF, Li TT, Quan HY, Li ML, Lin T, et al. The roles of Wnt/beta-catenin signaling pathway related lncRNAs in cancer. *Int J Biol Sci*. 2018; 14(14): 2003-2011.
- Gao T, Liu X, He B, Nie Z, Zhu C, Zhang P, et al. Exosomal lncRNA 91H is associated with poor development in colorectal cancer by modifying HNRNPk expression. *Cancer Cell Int*. 2018; 18: 11.
- Yi T, Wang T, Shi Y, Peng X, Tang S, Zhong L, et al. Long noncoding RNA 91H overexpression contributes to the growth and metastasis of HCC by epigenetically positively regulating IGF2 expression. *Liver Int*. 2020; 40(2): 456-467.
- Liu X, She Y, Wu H, Zhong D, Zhang J. Long non-coding RNA Gas5 regulates proliferation and apoptosis in HCS-2/8 cells and growth plate chondrocytes by controlling FGF1 expression via miR-21 regulation. *J Biomed Sci*. 2018; 25(1): 18.
- Li J, Tian H, Yang J, Gong Z. Long noncoding RNAs regulate cell growth, proliferation, and apoptosis. *DNA Cell Biol*. 2016; 35(9): 459-470.
- Huo X, Han S, Wu G, Latchoumanin O, Zhou G, Hebbard L, et al. Dysregulated long noncoding RNAs (lncRNAs) in hepatocellular carcinoma: implications for tumorigenesis, disease progression, and liver cancer stem cells. *Mol Cancer*. 2017; 16(1): 165.
- Zhao J, Fu Y, Wu J, Li J, Huang G, Qin L. The diverse mechanisms of mirnas and lncrnas in the maintenance of liver cancer stem cells. *Biomed Res Int*. 2018; 2018: 8686027.
- Deng Q, He B, Gao T, Pan Y, Sun H, Xu Y, et al. Up-regulation of 91H promotes tumor metastasis and predicts poor prognosis for patients with colorectal cancer. *PLoS One*. 2014; 9(7): e103022.
- Vennin C, Spruyt N, Robin YM, Chassat T, Le Bourhis X, Adriaenssens E. The long non-coding RNA 91H increases aggressive phenotype of breast cancer cells and up-regulates H19/IGF2 expression through epigenetic modifications. *Cancer Lett*. 2017; 385: 198-206.
- Yang J, Antin P, Bex G, Blanpain C, Brabletz T, Bronner M, et al. Guidelines and definitions for research on epithelial-mesenchymal transition. *Nat Rev Mol Cell Biol*. 2020; 21(6): 341-352.
- Zhang Y, Weinberg RA. Epithelial-to-mesenchymal transition in cancer: complexity and opportunities. *Front Med*. 2018; 12(4): 361-373.
- Su J, Zhang E, Han L, Yin D, Liu Z, He X, et al. Long noncoding RNA BLACAT1 indicates a poor prognosis of colorectal cancer and affects cell proliferation by epigenetically silencing of p15. *Cell Death Dis*. 2017; 8(3): e2665.

SP-8356: A Novel Verbenone Derivative Exerts *In Vitro* Anti-Non-Small Cell Lung Cancer Effects, Promotes Apoptosis via The P53/MDM2 Axis and Inhibits Tumor Formation in Mice

Lei Yang, Ph.D., Liyi Hu, Ph.D.* 

Department of Clinical Laboratory, People's Hospital of Chongqing Liang jiang New Area, Chongqing, China

Abstract

Objective: Non-small cell lung cancer (NSCLC) stands as a prominent contributor to cancer-related fatalities on a global scale, necessitating the search for novel therapeutic agents. SP-8356, a derivative of (1S)-(-)-verbenone, has shown promise as an anticancer agent in preclinical studies. However, specific mechanisms underlying its effects in NSCLC remain to be elucidated. The aim of this research was to explore the *in vitro* anti-NSCLC effects of SP-8356, elucidate its mechanisms of action, and assess its efficacy in inhibiting tumor formation in a murine model.

Materials and Methods: In this experimental study, NSCLC cell lines were treated with various concentrations of SP-8356. Cell viability and proliferation were assessed using MTT and colony formation assays, respectively. Cell cycle distribution was analyzed by flow cytometry, and apoptosis was evaluated by determining apoptotic protein expression. Western blot analysis was conducted to assess protein expression levels of the both p53 and MDM2. Additionally, we evaluated efficacy of the SP-8356 in inhibiting tumor formation of the nude mouse model.

Results: SP-8356 demonstrated a concentration-dependent inhibition of cell proliferation in the NSCLC cell lines. Flow cytometric analysis showed that SP-8356 led to cell cycle arrest at the G2/M phase, indicating its potential influence on regulating the cell cycle. SP-8356 treatment was associated with the downregulation of CDK1 and Cyclin B1. Additionally, SP-8356 significantly enhanced apoptosis in NSCLC cells. SP-8356 treatment was associated with the downregulation of Bcl-2, while Bax expression was upregulated. Mechanistically, SP-8356 led to accumulation of the p53 protein levels within the NSCLC cells. This accumulation was mediated through inhibition of its negative regulator, MDM2. Using a nude mouse model demonstrated that SP-8356 effectively inhibited tumor formation *in vivo*.

Conclusion: Our findings shed light on the molecular mechanisms underlying anticancer activity of SP-8356 and highlight its potential as a promising therapeutic candidate for NSCLC treatment.

Keywords: Apoptosis, Non-Small Cell Lung Cancer, p53, Proliferation, SP-8356

Citation: Yang L, Hu L. SP-8356: a novel verbenone derivative exerts *in vitro* anti-non-small cell lung cancer effects, promotes apoptosis via the P53/MDM2 axis and inhibits tumor formation in mice. Cell J. 2023; 25(12): 839-846. doi: 10.22074/CELLJ.2023.2008708.1385

This open-access article has been published under the terms of the Creative Commons Attribution Non-Commercial 3.0 (CC BY-NC 3.0).

Introduction

Lung cancer is a leading cause of tumor-related deaths in both men and women (1). Standard treatments like surgery, chemotherapy, and radiotherapy have revolutionized lung cancer treatment (2). Pulmonary neoplasms are broadly divided into non-small cell lung cancer (NSCLC) and small cell cancers; the former represents 80% of all lung cancer cases (3). NSCLC is associated with aberrant protein expression, resulting in extensive proliferation and malignancy (4). A great need has emerged to look for the molecular mechanism related to the NSCLC pathogenesis to improve disease outcomes.

p53 is a tumor suppressor protein, frequently mutated or inactivated in many types of cancer, including NSCLC (5). In NSCLC, p53 mutations are found in approximately 50% of cases, while the majority of mutations occurring

in the DNA binding domain of the protein (6). These mutations can result in the loss of p53 function, leading to accumulation of the DNA damage and promotion of tumor growth and metastasis. In addition to mutations, other mechanisms can also contribute to the inactivation of p53 in NSCLC, such as increased expression of its negative regulator MDM2, which targets p53 for degradation, or alterations in other proteins that regulate p53 activity (7). Loss of p53 function in NSCLC has been associated with a poorer prognosis as well as resistance to chemotherapy and radiation therapy. Therefore, understanding the mechanisms that regulate p53 in NSCLC and developing strategies to restore its function may have important implications for the treatment of this disease.

Natural compounds and their derivatives have become a significant area of interest in drug discovery, due to

Received: 07/August/2023, Revised: 19/September/2023, Accepted: 28/October/2023

*Corresponding Address: Department of Clinical Laboratory, People's Hospital of Chongqing Liang jiang New Area, Chongqing, China

Email: 1811121208@mail.sit.edu.cn



Royan Institute
Cell Journal (Yakhteh)

their diverse pharmacological properties and potential therapeutic applications (8). Among these compounds, (1S)-(-)-verbenone, a naturally occurring monoterpene found in essential oils of various plant species, has been shown to cause promising bioactivities (9). As a result, researchers have synthesized and investigated derivatives of (1S)-(-)-verbenone to enhance its properties and develop novel therapeutic agents (10).

One such derivative is SP-8356, which has garnered attention for its potential pharmacological effects in various areas, including cancer research (11). The unique chemical structure and biological activities of SP-8356 have led to investigating its potential, as an anticancer agent. Preclinical studies have shown encouraging results, indicating that SP-8356 may exhibit significant anticancer properties by targeting specific molecular pathways involved in tumorigenesis (12). The present study was formulated with the aim of exploring role of SP-8356 with respect to the p53 protein in NSCLC cells.

Materials and Methods

Cell culture

In this experimental study, human NSCLC cells (NCI-H460 and A549) and normal human fetal lung fibroblast cell line (MRC-5) were purchased from the Type Culture Collection of the Chinese Academy of Sciences (Shanghai, China). The cells were cultured in appropriate growth media supplemented with 10% fetal bovine serum (FBS, Sigma-Aldrich, USA) and 1% penicillin-streptomycin (Thermo Scientific, USA). The cells were cultured in a humidified incubator at 37°C with 5% CO₂.

Chemicals and reagents

SP-8356, a derivative of (1S)-(-)-verbenone, was synthesized using the previously established methods (13). Stock solutions of SP-8356 were prepared in dimethyl sulfoxide (DMSO) at appropriate concentrations and stored at -20°C.

Cell viability assay (MTT assay)

To assess cell proliferation, NSCLC cells were seeded into 96-well plates at a density of 5000 cells per well and allowed to adhere overnight. The cells were then treated with various concentrations of SP-8356 (5 µM, 10 µM, 15 µM and 20 µM) or vehicle control (DMSO) for 24 hours. Following the specified length of treatment duration, the culture medium was substituted with fresh media containing 0.5 mg/ml of MTT (3-(4,5-dimethylthiazol-2-yl)-2,5-diphenyltetrazolium bromide) and then incubated for an additional 4 hours at 37°C. DMSO was used to dissolve formazan crystals, and the absorbance was determined at 570 nm using a microplate reader.

Colony formation assay

NSCLC cells were plated in 6-well dishes at a sparse density of 200 cells per well and permitted to attach

overnight. Subsequently, the cells were exposed to a range of SP-8356 concentrations (5 µM, 10 µM, 15 µM and 20 µM) or vehicle control (DMSO) for 24 hours. Following the treatment, the existing culture medium was substituted with fresh complete growth media, and the cells were incubated for 14 days to facilitate formation of colonies. The colonies were fixed using methanol and then stained with crystal violet. Count of colonies was conducted manually.

Cell cycle analysis

To explore impact of SP-8356 on the cell cycle, NSCLC cells were exposed to SP-8356 (15 µM) for 24 hours. Following the treatment, the cells were collected, rinsed with phosphate-buffered saline (PBS), fixed in ice-cold 70% ethanol, and preserved at -20°C. Before analysis, the fixed cells were washed with PBS, treated with 50 µl RNase A (from 100 µg/ml stock solution, Sigma-Aldrich, USA), and stained with 200 µl propidium iodide (PI; from 50 µg/ml stock solution, Sigma-Aldrich, USA). A FACS Calibur flow cytometer (BD Biosciences, USA) was used to carry out flow cytometric analysis to ascertain distribution of the cell cycle. BD CellQuest Pro-Software was used for analyzing the results.

Western blotting

To examine the protein expression levels, NSCLC cells were treated with various concentrations of SP-8356 (5 µM, 10 µM, 15 µM and 20 µM) or vehicle control (DMSO) for 24 hours. Following treatment, the cells were lysed using RIPA buffer supplemented with 1X protease (Sigma-Aldrich, USA) and phosphatase inhibitors (prepared from 100X protease/phosphatase inhibitor cocktail; Sigma-Aldrich, USA). Total protein concentration was quantified utilizing a protein assay kit (Pierce™ BCA Protein Assay Kit; Thermo Scientific, USA). Equivalent quantities of protein were segregated through 12% sodium dodecyl sulphate-polyacrylamide gel electrophoresis (SDS-PAGE) and subsequently transferred onto a polyvinylidene fluoride (PVDF) membrane. The membrane was blocked and probed with primary antibodies against anti-CDK1 (ab133327, abcam, USA; 1:1000 dilution), anti-Cyclin B1 (ab32053, abcam, USA; 1:800 dilution), anti-Bax (ab216494, abcam, USA; 1:1000 dilution), anti-Bcl-2 (ab59348, abcam, USA; 1:1000 dilution), anti-p53 (ab131442, abcam, USA; 1:1000 dilution), anti-MDM2 (ab16895, abcam, USA; 1:1000 dilution), and anti-GAPDH (ab8245, abcam, USA; 1:1000 dilution). After rinsing with TBST buffer, the membranes were exposed to peroxidase-conjugated anti-rabbit secondary antibodies (diluted at 1:5000; Hangzhou Multi Sciences [Lianke] Biotech Co., China) at room temperature. Protein signals were detected using an enhanced chemiluminescence (ECL) technique.

Experimental animals

Fifteen male athymic BALB/c nude mice, aged 5-6 weeks, were accommodated in regular cages maintained

at 25°C with a 12-hours light and 12-hours dark cycle. All animal procedures were performed following the protocol approved by People's Hospital of Chongqing Liang jiang New Area (Chongqing, China, PHCL/1231.101). The mice were provided with a standard pellet diet and ad libitum access to water. They were randomly divided into three groups, each containing five animals:

Group I: control mice were received an intravenous injection of isotonic saline (25 ml/kg body weight) along with subcutaneous injection of 2×10^6 A549 cells on one side of the posterior flank.

Group II: nude mice were subcutaneously injected with 2×10^6 A549 cells on one side of the posterior flank, along with an oral low-dose treatment of 10 μ M/kg body weight of SP-8356.

Group III: mice were subcutaneously injected with 2×10^6 A549 cells on one side of the posterior flank, along with an oral high-dose treatment of 10 mg/kg body weight of SP-8356.

At the conclusion of the experimental period on day 19, the mice were anesthetized with ketamine (30 mg/kg body weight) and then euthanized. The tumor tissue was excised, washed with saline, and dried, and its weight was measured. Tumor homogenates (10%) were prepared using a 0.1 M Tris HCl buffer (pH=7.4) and a homogenizer.

To evaluate impact of SP-8356 on tumor cell growth, dimension and weight of the tumors were measured in the mice carrying tumors. Tumor size was calculated using the formula $(L \times S^2) \times 0.5$, where L represented the greatest diameter and S represented the shortest diameter of the tumor. Weight of the tumors was determined by weighing the moist tumor tissue.

Statistical analysis

Data from triplicate or quadruplicate experiments were expressed as mean \pm standard deviation (SD). Statistical significance was determined using appropriate statistical tests, such as Student's t test or one-way analysis of variance (ANOVA), followed by post hoc comparisons. $P < 0.05$ were regarded as statistically significant.

Results

SP-8356 significantly curbed NSCLC cell viability and proliferation

The MTT cell viability assay revealed a notable dose-dependent reduction in cell viability upon treatment with increasing concentrations of SP-8356. The IC_{50} values for A549 and NCI-H460 NSCLC cells were found to be 15 μ M (Fig. 1A).

Furthermore, the inhibitory effect of SP-8356 on cell proliferation was confirmed through a colony formation assay. Treatment with SP-8356 resulted in a significant decrease in the number of colonies formed by NSCLC cells compared to the control group. The concentration-dependent response demonstrated the ability of SP-8356 to impede the clonogenic potential of NSCLC cells (Fig. 1B).

These results collectively highlight the robust inhibitory effects of SP-8356 on the both NSCLC cell viability and proliferation. The findings suggested that SP-8356 was held as a promising therapeutic candidate for combating NSCLC by targeting cell growth and survival pathways. Further investigations are warranted to explore its mechanism of action and potential translational applications for NSCLC treatment.

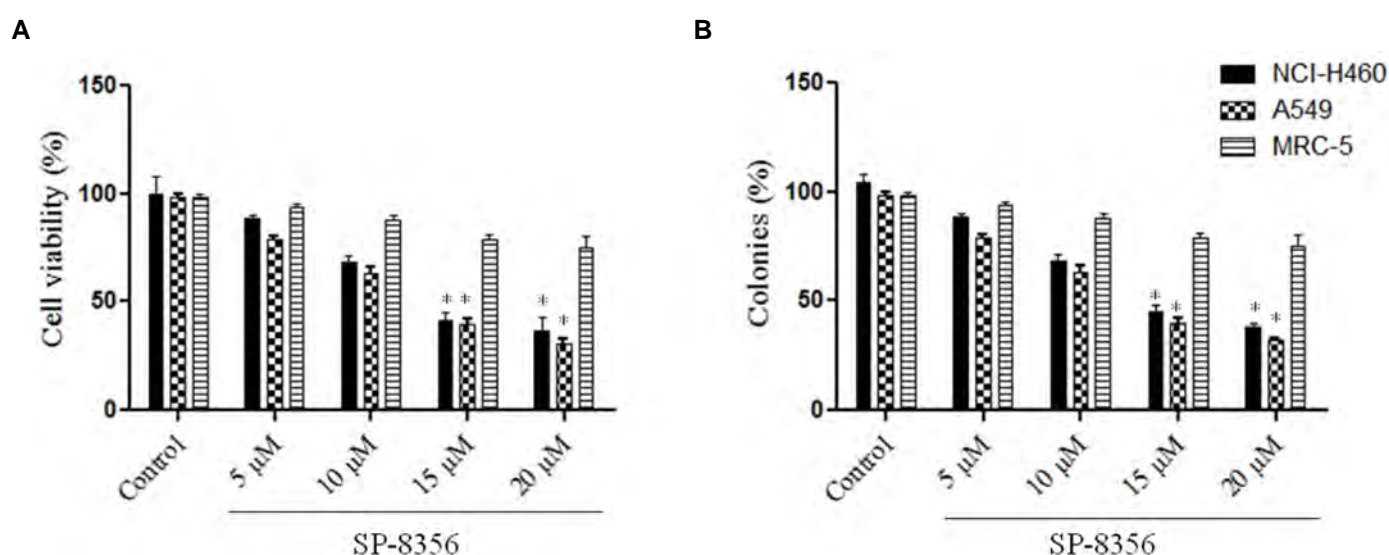


Fig.1: SP-8356 suppresses cell viability and proliferation in NSCLC cells. **A.** MTT cell viability assay illustrates a decline in cell viability that is directly proportional to the rising concentrations of SP-8356, indicating a dose-dependent effect. Treatment with SP-8356 significantly decrease cell viability in NCI-H460 and A549 NSCLC cells compared to MRC-5 cells (control fibroblasts). **B.** Colony formation assay confirms the inhibitory effect of SP-8356 on cell proliferation in NSCLC cells. SP-8356 treatment significantly decrease number of colonies formed by NSCLC cells compared to the control group. The concentration-dependent response highlights the ability of SP-8356 to impede the clonogenic potential of NSCLC cells. The experiments were conducted in triplicate and replicated three times. *, $P < 0.05$ and NSCLC; Non-small cell lung cancer.

SP-8356 regulated G2/M transition

SP-8356 treatment significantly altered the cell cycle progression in NSCLC cells. Flow cytometric analysis demonstrated a rise in the proportion of cells arrested at the G2/M phase, following the SP-8356 treatment in the A549 cells compared to control (Fig.2A, B) and similar results were obtained in NCI-H460 NSCLC cells (Fig.2C, D). Conversely, a significant reduction in the G1 and S phase populations was observed in response to SP-8356 treatment. These findings suggested that SP-8356 triggered G2/M cell cycle arrest in NSCLC cells, implying its potential role in regulating the G2/M transition. These findings collectively suggested that SP-8356 was involved in the regulation of G2/M cell cycle transition in NSCLC cells.

SP-8356 regulated cell cycle and apoptotic associated protein levels

Western blot analysis was performed to evaluate effects

of SP-8356 on cell cycle protein levels in NSCLC cells. Treatment with SP-8356 resulted in notable changes in the expression levels of proteins associated with cell cycle regulation. More specifically, there was a decrease in the expression of CDK1, cyclin B1, and Bcl-2, coupled with an increase in Bax expression observed in the both NCI-H460 (Fig.3A) and A549 (Fig.3B) cell lines. Figure 3C shows densitometry analysis of Figure 3A while as Figure 3D shows densitometry analysis of Figure 3B.

SP-8356 upregulated p53 levels

Treatment with SP-8356 led to a significant upregulation of p53 protein levels in NSCLC cells. Western blot analysis unveiled a significant elevation in p53 expression following SP-8356 treatment in comparison with the control group. Upregulation of p53 was observed in the both A549 and NCI-H460 NSCLC cell lines, indicating a consistent effect of SP-8356 on p53 levels in different cellular contexts (Fig.4).

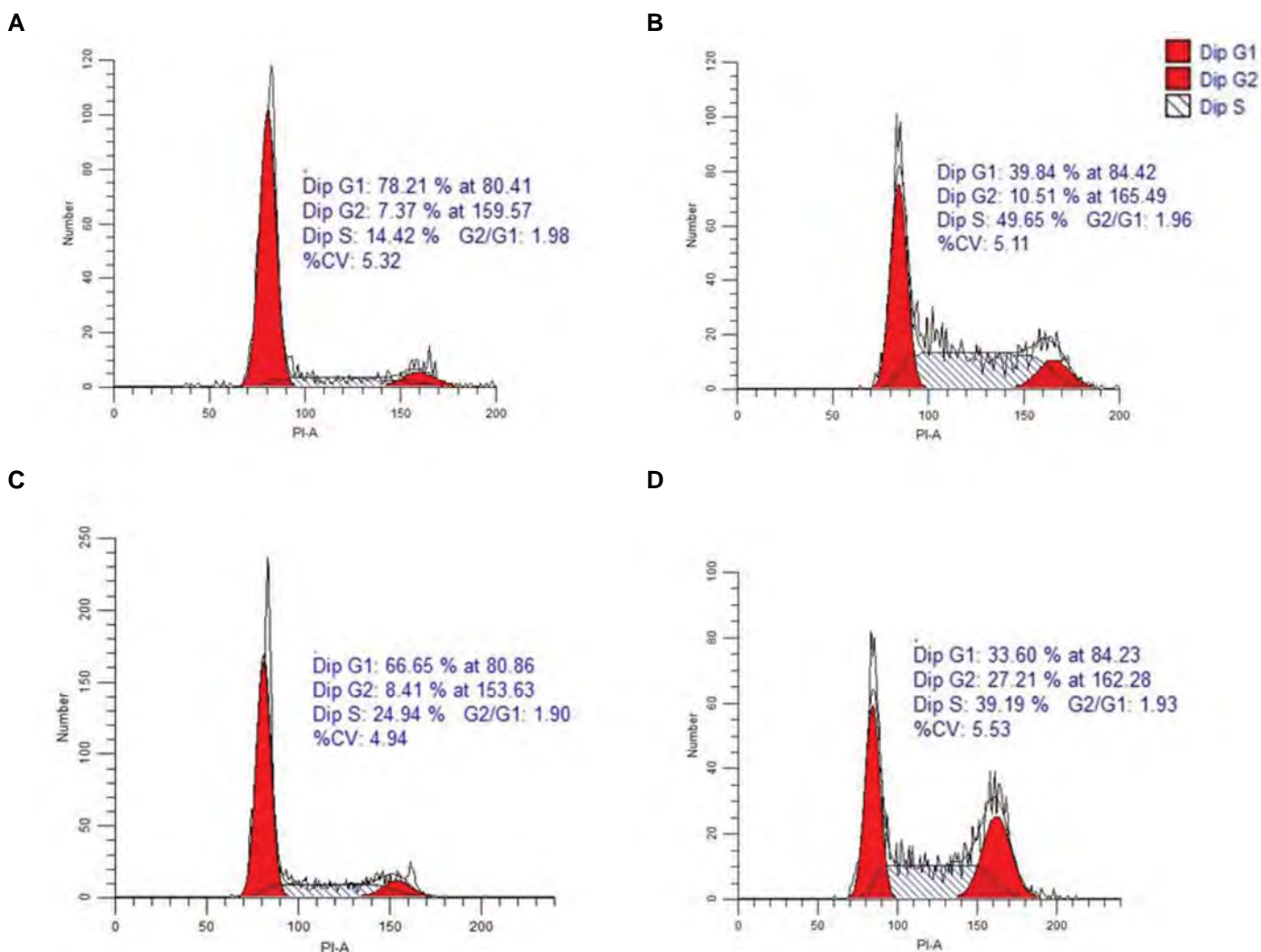


Fig.2: SP-8356 regulates G2/M transition in NSCLC cells. Flow cytometric analysis of cell cycle distribution in NSCLC cells treated with SP-8356. **A.** Untreated NCI-H460 cells, **B.** NCI-H460 cells treated with SP-8356, **C.** Untreated A549 cells, **D.** A549 cells treated with SP-8356. SP-8356 treatment resulted in a notable increase in the percentage of cells arrested in the G2/M phase, as shown by the shift in the cell population towards G2/M in NCI-H460 and A549, compared to respective controls. Conversely, there was a notable decrease in the G1 and S phase populations in response to SP-8356 treatment. NSCLC; Non-small cell lung cancer.

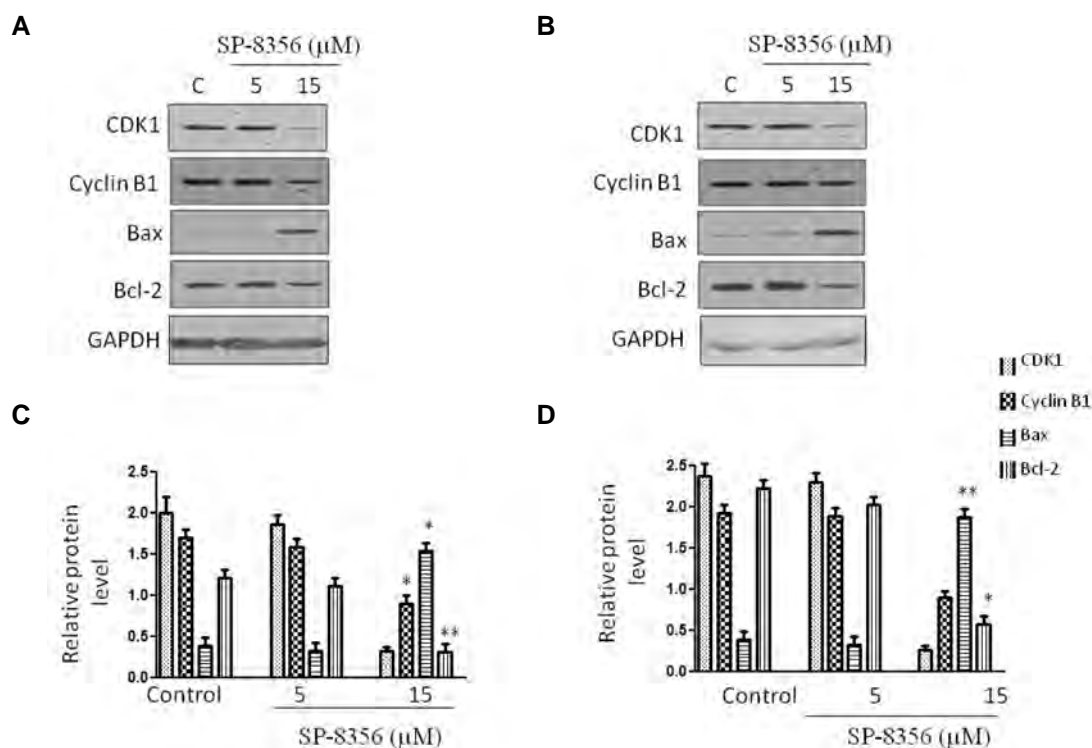


Fig.3: SP-8356 modulates protein levels associated with the cell cycle and apoptosis in NSCLC cells. **A.** Western blot analysis of cell cycle and apoptotic-associated protein levels in NCI-H460 cells treated with SP-8356. **B.** Western blot analysis of cell cycle and apoptotic-associated protein levels in A549 cells treated with SP-8356. Treatment with SP-8356 resulted in notable changes in the expression levels of cell cycle and apoptosis proteins. **C.** Quantitative analysis of western blot “A” using densitometry. **D.** Quantitative analysis of western blot “B” using densitometry. The experiments were conducted in triplicate and replicated three times. *; P<0.05, **; P<0.001, and NSCLC; Non-small cell lung cancer.

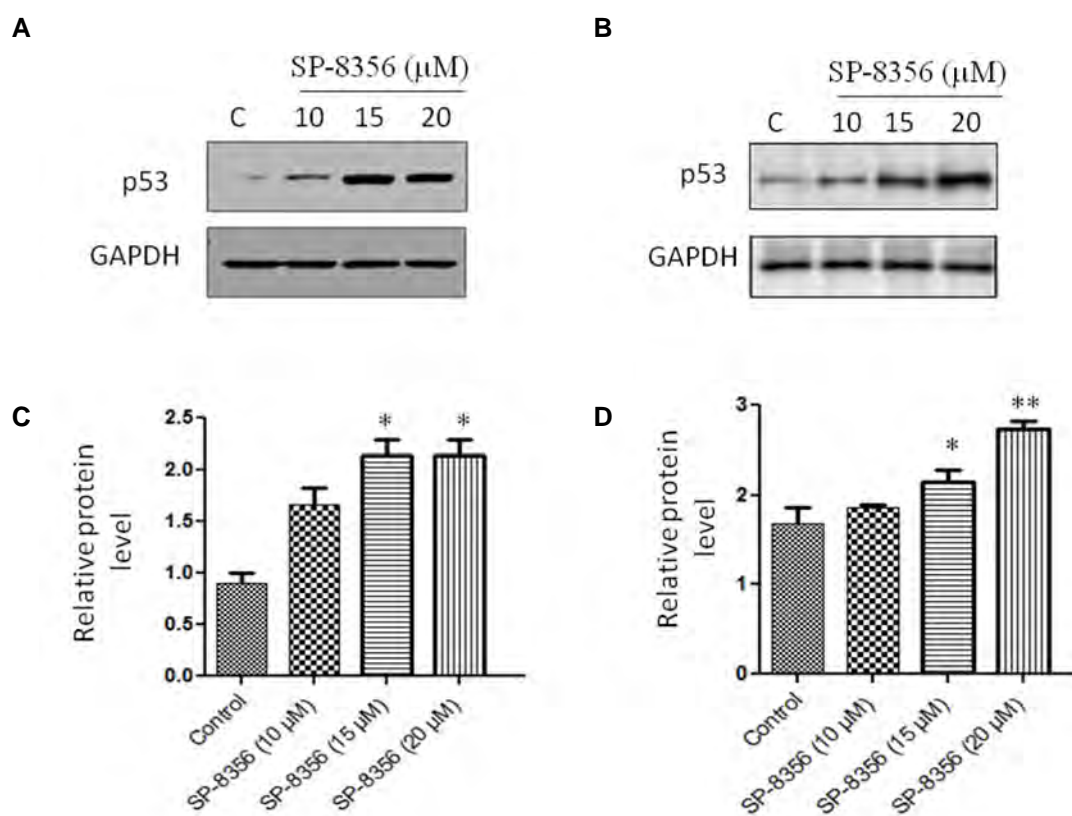


Fig.4: SP-8356 upregulates p53 levels in NSCLC cells. **A.** Expression analysis of p53 protein levels in NCI-H460 cells treated with SP-8356. **B.** Expression analysis of p53 protein levels in A549 cells treated with SP-8356. **C.** Quantitative analysis of western blot “A” using densitometry. **D.** Quantitative analysis of western blot “B” using densitometry. The experiments were conducted in triplicate and replicated three times. *; P<0.05, **; P<0.001, and NSCLC; Non-small cell lung cancer.

SP-8356 acted on p53 through MDM2

To understand the mechanism by which SP-8356 upregulated p53 levels, we investigated its impact on MDM2, a key negative regulator of p53. Western blot analysis revealed that treatment with SP-8356 led to a significant reduction in MDM2 protein expression in NSCLC cells. This downregulation of MDM2 was observed in the both A549 and NCI-H460 NSCLC cell lines (Fig.5).

These findings indicated that SP-8356 acted on p53 through MDM2, inhibiting function of MDM2 and thereby preventing p53 degradation. As a consequence, p53 protein level was increased, leading to its activation and subsequent induction of downstream cellular responses, including cell cycle arrest and apoptosis.

Influence of SP-8356 on tumor size and weight

Impact of SP-8356 on tumor growth inhibition was

evaluated by weighing and measuring tumor size. The results presented in Figure 6A, B clearly demonstrated a notable reduction in tumor size of the both low-dose and high-dose SP-8356-treated groups, compared to the control group.

Furthermore, the high-dose SP-8356-treated group exhibited more significant decrease in tumor size than the low-dose-treated group. Similarly, when examining tumor weight (Fig.1B), both of the low-dose and high-dose SP-8356-treated groups displayed the marked reductions compared to the control group.

Moreover, the high-dose SP-8356-treated group demonstrated a significant decrease in tumor weight compared to the low-dose-treated group. These findings suggested that SP-8356 administration effectively inhibited tumor growth, with higher doses leading to more pronounced effects on the both tumor size and weight.

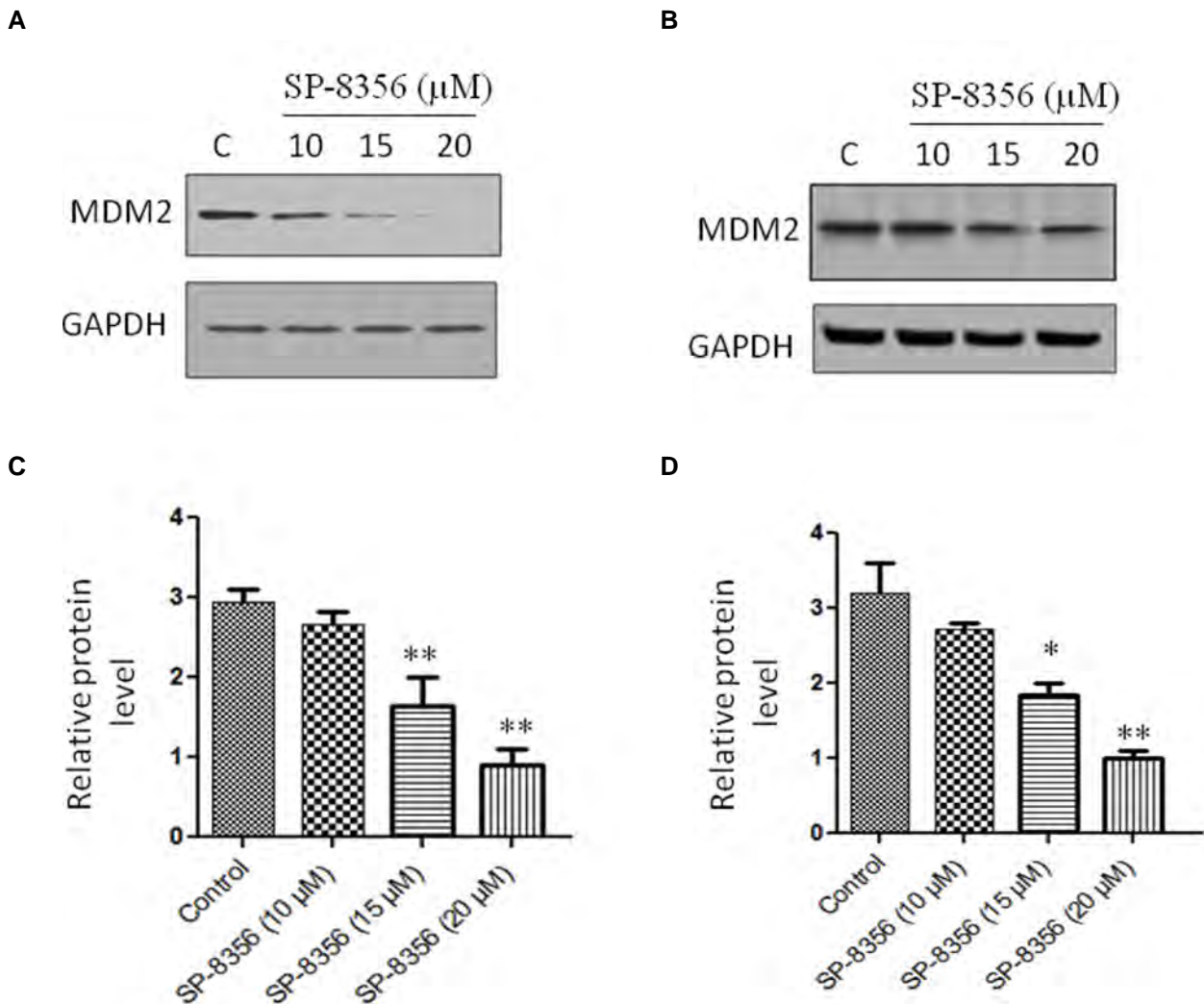


Fig.5: SP-8356 acts on p53 through MDM2. **A.** Expression analysis of MDM2 protein levels in NCI-H460 cells treated with SP-8356. **B.** Expression analysis of MDM2 protein levels in A549 cells treated with SP-8356. **C.** Quantitative analysis of western blot "A" using densitometry. **D.** Quantitative analysis of western blot "B" using densitometry. The experiments were conducted in triplicate and replicated three times. *, P<0.05 and **, P<0.001.

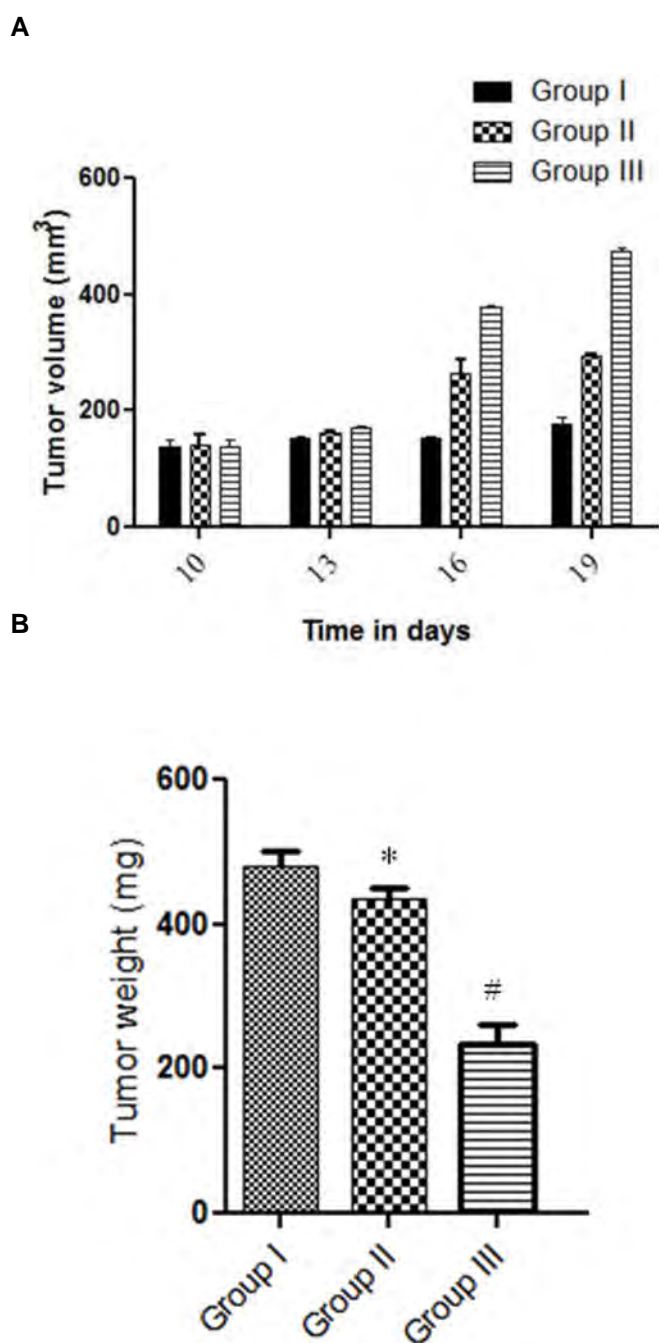


Fig. 6: Effect of SP-8356 on tumor volume and tumor weight. **A.** The graph depicts the impact of SP-8356 treatment on tumor volume. Both of the low-dose (10 μ M) and high-dose (20 μ M) SP-8356-treated groups (groups II and III, respectively) show a significant decrease in tumor volume compared to the control group (group I). **B.** The bar chart illustrates effect of SP-8356 on tumor weight. In the both of low-dose and high-dose SP-8356-treated groups (groups II and III, respectively), tumor weight is markedly decreased compared to the control group (group I). *, $P < 0.01$, when compared to the group I, while as #, $P < 0.05$, when compared to the group II.

Discussion

NSCLC stands as one of the most prevalent and formidable malignancies globally, accounting for a substantial proportion of cancer-related deaths (14). Despite the significant advancements in therapeutic strategies, management of NSCLC remains challenging, necessitating exploration of novel and effective therapeutic

agents (15, 16). In this context, SP-8356, a derivative of (1S)-(-)-verbenone, has emerged as a promising candidate for potential anti-cancer activity in NSCLC cells. The present study investigated anticancer properties of the SP-8356 in NSCLC cells. Our results demonstrated that SP-8356 significantly suppressed cell viability and proliferation in NSCLC cells in a dose-dependent manner, as evidenced by the MTT cell viability assay and colony formation assay, without affecting MRC-5 cells. MRC-5 cells are a type of normal human lung fibroblast cells, often used in research as a representative of non-cancerous, healthy cells. SP-8356 appeared to selectively affect NSCLC cancer cells, specifically without impacting MRC-5 cells. This selectivity could be due to several factors, such as differences in the genetic makeup or signaling pathways between cancer cells and normal cells (17, 18). These findings suggested that SP-8356 had a potent inhibitory effect on NSCLC cell growth, making it a promising candidate for NSCLC treatment.

One of the mechanisms underlying anticancer effects of SP-8356 involves its regulation of the cell cycle progression (10). Flow cytometric analysis revealed that SP-8356 induced G2/M cell cycle arrest in NSCLC cells. G2/M arrest is a critical checkpoint in the cell cycle, where cells are subjected to thorough DNA damage repair before entering mitosis. Ability of SP-8356 to induce G2/M arrest in NSCLC cells may disrupt the uncontrolled cell cycle progression, leading to reduced cell proliferation and increased susceptibility to apoptosis.

Apoptosis is a key process in controlling cellular homeostasis and eliminating damaged or abnormal cells (19). In this study, SP-8356 was found to enhance apoptosis in NSCLC cells, as demonstrated by Annexin V staining and Western blot analysis of apoptotic-associated protein levels. Increase in the pro-apoptotic proteins, like Bax, and decrease in the anti-apoptotic proteins, such as Bcl-2, suggested activation of the intrinsic apoptotic pathway. These findings suggested that SP-8356 can trigger apoptosis in NSCLC cells, contributing to its anticancer effects. Taken together, these results suggested that SP-8356 played role in modulating the G2/M cell cycle transition and induced apoptosis in NSCLC cells. The observed alterations in apoptotic-associated protein levels further supported potential of SP-8356, as a candidate therapeutic agent for inducing cell cycle arrest and promoting apoptosis in NSCLC. Additional research is warranted to uncover the underlying molecular mechanisms and to investigate its therapeutic potential for treating NSCLC.

Upregulation of p53 protein levels was a prominent observation in our study, following the SP-8356 treatment. P53 is a crucial tumor suppressor protein that plays a central role in regulating cell cycle progression, DNA repair, and apoptosis in response to cellular stress (20, 21). The increased levels of p53 in NSCLC cells treated with SP-8356 indicated the compound impacts of p53 expression. Further investigation of the underlying mechanism revealed that SP-8356 acted on p53 through

MDM2, a negative regulator of p53. SP-8356 interfered with the interaction between p53 and MDM2, preventing p53 ubiquitination and subsequent degradation. As a result, p53 level was accumulated within the cells, triggering downstream cellular responses, like cell cycle arrest and apoptosis. The results suggested that SP-8356 was capable to upregulate p53. The increased p53 levels may contribute to the observed anti-cancer effects of SP-8356 in NSCLC cells. Exploring the specific molecular mechanisms through which SP-8356 upregulate p53 expression will yield valuable insights into its potential as a therapeutic agent for NSCLC treatment.

Modulation of the p53-MDM2 axis represented a critical mechanism through which SP-8356 exerted its anticancer effects in NSCLC cells. Disruption of this regulatory pathway enhanced stability and function of p53, promoting its tumor-suppressive activities. The ability of SP-8356 to upregulate p53 and inhibit its ubiquitination highlighted its potential as a targeted therapeutic agent for p53-associated malignancies, including NSCLC. Modulation of the p53-MDM2 axis by SP-8356 highlighted a crucial mechanism underlying its anticancer effects in NSCLC cells. Disruption of this regulatory pathway may represent a promising therapeutic strategy for targeting p53 and promoting tumor suppression. Further investigations into the specific interactions between SP-8356, MDM2, and p53 will provide deeper insights into the molecular mechanisms mediating the compound's impact on p53 regulation and its potential as a novel therapeutic agent for NSCLC treatment.

In conclusion, our study demonstrated that SP-8356, a (1S)-(-)-verbenone derivative, exhibiting potent anticancer properties in NSCLC cells. The compound significantly suppressed cell viability and proliferation, induced G2/M cell cycle arrest, and enhanced apoptosis. Furthermore, SP-8356 upregulated p53 levels by inhibiting its ubiquitination through disruption of the p53-MDM2 interaction. These findings provided valuable insights into the molecular mechanisms that underlie SP-8356 anticancer effects and highlight its potential as a promising therapeutic candidate for NSCLC treatment. Future studies, including *in vivo* investigations and translational research, are warranted to further validate the therapeutic potential of SP-8356 and to advance its development as a targeted therapy for NSCLC patients.

Conclusion

SP-8356, a (1S)-(-)-verbenone derivative, demonstrated potent anticancer effects in NSCLC cells. The compound substantially inhibited cell proliferation, triggered G2/M cell cycle arrest, and fostered apoptosis. Its upregulation of p53 levels via MDM2 inhibition contributed to its anticancer activity. SP-8356 held promise as a targeted therapeutic agent for NSCLC treatment, warranting further investigations for its clinical development.

Acknowledgements

There is no financial support and conflict of interest in this study.

Authors' Contributions

L.Y.; Conceptualization, Methodology, and Investigation. L.H.; Original draft preparation, Statistical analysis, Confirmed the authenticity of the raw data, and Supervision. All authors read and approved the final manuscript.

References

- Sung H, Ferlay J, Siegel RL, Javersanne M, Soerjomataram I, Jemal A, et al. global Cancer Statistics 2020: GLOBOCAN estimates of incidence and mortality worldwide for 36 cancers in 185 countries. *CA Cancer J Clin.* 2021; 71(3): 209-249.
- Wirsdörfer F, de Leve S, Jendrossek V. Combining radiotherapy and immunotherapy in lung cancer: can we expect limitations due to altered normal tissue toxicity? *Int J Mol Sci.* 2018; 20(1): 24.
- Chen Z, Fillmore CM, Hammerman PS, Kim CF, Wong KK. Non-small-cell lung cancers: a heterogeneous set of diseases. *Nat Rev Cancer.* 2014; 14(8): 535-546.
- Tandon N, Goller K, Wang F, Soibam B, Gagea M, Jain AK, et al. Aberrant expression of embryonic mesoderm factor MESP1 promotes tumorigenesis. *EBioMedicine.* 2019; 50: 55-66.
- Baslan T, Morris JP 4th, Zhao Z, Reyes J, Ho YJ, Tsanov KM, et al. Ordered and deterministic cancer genome evolution after p53 loss. *Nature.* 2022; 608(7924): 795-802.
- Saleh MM, Scheffler M, Merkelbach-Bruse S, Scheel AH, Ulmer B, Wolf J, et al. Comprehensive analysis of TP53 and KEAP1 mutations and their impact on survival in localized- and advanced-stage NSCLC. *J Thorac Oncol.* 2022; 17(1): 76-88.
- Ni L, Xu J, Zhao F, Dai X, Tao J, Pan J, et al. MiR-221-3p-mediated downregulation of MDM2 reverses the paclitaxel resistance of non-small cell lung cancer in vitro and in vivo. *Eur J Pharmacol.* 2021; 899: 174054.
- Atanasov AG, Zotchev SB, Dirsch VM, International Natural Product Sciences Taskforce, Supuran CT. Natural products in drug discovery: advances and opportunities. *Nat Rev Drug Discov.* 2021; 20(3): 200-216.
- Perricone M, Arace E, Corbo MR, Sinigaglia M, Bevilacqua A. Bioactivity of essential oils: a review on their interaction with food components. *Front Microbiol.* 2015; 6: 76.
- Mander S, Kim DH, Thi Nguyen H, Yong HJ, Pakh K, Kim EY, et al. SP-8356, a (1S)-(-)-verbenone derivative, exerts in vitro and in vivo anti-breast cancer effects by inhibiting NF-κB signaling. *Sci Rep.* 2019; 9(1): 6595.
- Cui W, Yang D, Chen X, Yu H. SP-8356 (a verbenone derivative) inhibits proliferation, suppresses cell migration and invasion and decreases tumor growth of osteosarcoma: role of PGC-1α/TFAM and AMPK-activation. *Cell J.* 2023; 25(5): 291-299.
- Kim DH, Yong HJ, Mander S, Nguyen HT, Nguyen LP, Park HK, et al. SP-8356, a (1S)-(-)-verbenone derivative, inhibits the growth and motility of liver cancer cells by regulating NF-κB and ERK signaling. *Biomol Ther (Seoul).* 2021; 29(3): 331-341.
- Ju C, Song S, Hwang S, Kim C, Kim M, Gu J, et al. Discovery of novel (1S)-(-)-verbenone derivatives with anti-oxidant and anti-ischemic effects. *Bioorg Med Chem Lett.* 2013; 23(19): 5421-5425.
- Dela Cruz CS, Tanoue LT, Matthay RA. Lung cancer: epidemiology, etiology, and prevention. *Clin Chest Med.* 2011; 32(4): 605-644.
- Bai RL, Chen NF, Li LY, Cui JW. A brand new era of cancer immunotherapy: breakthroughs and challenges. *Chin Med J (Engl).* 2021; 134(11): 1267-1275.
- Pucci C, Martinelli C, Ciofani G. Innovative approaches for cancer treatment: current perspectives and new challenges. *Ecancermedicallscience.* 2019; 13: 961.
- Blagosklonny MV. Selective protection of normal cells from chemotherapy, while killing drug-resistant cancer cells. *Oncotarget.* 2023; 14: 193-206.
- Mansoori B, Mohammadi A, Davudian S, Shirjang S, Baradaran B. The different mechanisms of cancer drug resistance: a brief review. *Adv Pharm Bull.* 2017; 7(3): 339-348.
- Elmore S. Apoptosis: a review of programmed cell death. *Toxicol Pathol.* 2007; 35(4): 495-516.
- Toufektchan E, Toledo F. The guardian of the genome revisited: p53 downregulates genes required for telomere maintenance, DNA repair, and centromere structure. *Cancers (Basel).* 2018; 10(5): 135.
- Marvalim C, Datta A, Lee SC. Role of p53 in breast cancer progression: an insight into p53 targeted therapy. *Theranostics.* 2023; 13(4): 1421-1442.

The Effects of Lycopene on Modulating Oxidative Stress and Liver Enzymes Levels in Metabolic Syndrome Patients: A Randomised Clinical Trial

Mahdi Mirahmadi, M.Sc.¹, Malihe Aghasizadeh, Ph.D.², Fatemeh Nazifkar, B.Sc.³, Mahla Ghafarian Choubdari, B.Sc.³, Reza Assaran-Darban, Ph.D.³, Shima Tavallaie, M.Sc.², Hossein Hatamzadeh, B.Sc.⁴, Gordon A Ferns, Ph.D.⁵, Mohammad Reza Mirinezhad, Ph.D.⁶, Hamed Baharara, Ph.D.⁷, Farzin Hadizadeh, Ph.D.^{1,8*} , Majid Ghayour-Mobarhan, Ph.D.^{2*} 

1. Biotechnology Research Center, Pharmaceutical Technology Institute, Mashhad University of Medical Sciences, Mashhad, Iran
2. International UNESCO Center for Health-Related Basic Sciences and Human Nutrition, Mashhad University of Medical Sciences, Mashhad, Iran
3. Department of Biology, Mashhad Branch, Islamic Azad University, Mashhad, Iran
4. Department of Nutrition, Faculty of Medicine, Mashhad University of Medical Sciences, Mashhad, Iran
5. Brighton & Sussex Medical School, Division of Medical Education, Brighton, UK
6. Department of Medical Genetics, Faculty of Medicine, Mashhad University of Medical Sciences, Mashhad, Iran
7. Department of Clinical Pharmacy, School of Pharmacy, Mashhad University of Medical Sciences, Mashhad, Iran
8. Department of Medicinal Chemistry, School of Pharmacy, Mashhad University of Medical Sciences, Mashhad, Iran

Abstract

Objective: The pathogenesis of metabolic syndrome (MetS) complications involves the excessive production of reactive oxygen species, inflammation, and endothelial dysfunction. Due to Lycopene, a highly unstable structure and its significant effects on modulating the metabolic system, there is a strong need for a formula that can increase its stability. The aim of this study was to develop an approach for encapsulating Lycopene and investigate its effects on inflammatory markers, oxidative stress, and liver enzymes in patients with MetS.

Materials and Methods: This study is a simple randomized, double-blind, objective-based clinical trial that involved eighty subjects with MetS, who were equally and randomly assigned to two groups: one group received 20 mg of Lycopene per day for 8 weeks, and the Placebo group followed the same protocol as the Lycopene group but received a placebo instead of Lycopene. They were called Lycopene and placebo, respectively. During follow-up visits after 4 and 8 weeks, 20 ml of blood was collected for evaluation of liver enzymes and some inflammatory related markers.

Results: Prior to the assignment of volunteers to their respective groups, there were no notable differences in C-reactive protein (CRP), serum liver enzymes, systolic and diastolic blood pressure, or pro-oxidant-antioxidant balance (PAB) between the Lycopene and placebo groups. However, our subsequent analysis revealed a significant reduction in the serum levels of CRP ($P=0.001$) and PAB ($P=0.004$) in the group that received Lycopene. Our encapsulated Lycopene treatment was not associated with a significant difference in serum levels of alanine aminotransferase (ALT), aspartate transferase (AST), or alkaline phosphatase (ALP) between our two groups.

Conclusion: This study investigated the impact of Lycopene on individuals with MetS, revealing a noteworthy modulation effect on PAB and inflammation linked to MetS. However, no significant differences were demonstrated in serum levels of ALT, AST and ALP between the studied group (registration number: IRCT20130507013263N3).

Keywords: Inflammation, Liver Enzyme, Lycopene, Metabolic Syndrome, Oxidative Stress

Citation: Mirahmadi M, Aghasizadeh M, Nazifkar F, Ghafarian Choubdari M, Assaran-Darban R, Tavallaie Sh, Hatamzadeh H, A Ferns G, Mirinezhad MR, Baharara H, Hadizadeh F, Ghayour-Mobarhan M. The effects of lycopene on modulating oxidative stress and liver enzymes levels in metabolic syndrome patients: a randomised clinical trial. Cell J. 2023; 25(12): 847-853. doi: 10.22074/CELLJ.2023.2006158.1353

This open-access article has been published under the terms of the Creative Commons Attribution Non-Commercial 3.0 (CC BY-NC 3.0).

Introduction

Oxidative stress, induced by reactive oxygen species (ROS), is a significant risk factor for cardiovascular disease (CVD) in individuals with metabolic syndrome (MetS) (1). MetS disease, a multifactorial disorder,

is defined by a combination of altered metabolism of glucose, lipids, obesity and/or arterial pressure elevation. The overproduction of ROS may initiate inflammation and endothelial dysfunction, likely through oxidative modification in the liver, thereby may contribute to

Received: 03/July/2023, Revised: 01/October/2023, Accepted: 25/October/2023

*Corresponding Addresses: P.O.Box: 99199-91766, Biotechnology Research Center, Pharmaceutical Technology Institute, Mashhad University of Medical Sciences, Mashhad, Iran

P.O.Box: 99199-91766, International UNESCO Center for Health-Related Basic Sciences and Human Nutrition, Mashhad University of Medical Sciences, Mashhad, Iran

Emails: hadizadehf@mums.ac.ir, ghayourm@mums.ac.ir



Royan Institute
Cell Journal (Yakhteh)

complications associated with MetS (2). Chronic complications linked to MetS risk factors can arise when there's an imbalance in pro-oxidants and antioxidants, particularly when pro-oxidants are in excess (3). The pro-oxidant-antioxidant balance (PAB) affects the interplay between antioxidant activity, oxidative damage, signal pathway activation, and the progression of pathological conditions such as CVD, insulin resistance, and MetS (4). The serum PAB assay is a simple method for evaluation of pro and antioxidant status in a single test, as reported by Alamdari et al. (5). Recent evidence suggested that an increased serum levels of PAB and C-reactive protein (CRP), along with clinical parameters, are independently associated with MetS (6).

Several cross-sectional studies have demonstrated a relationship between MetS and elevated serum liver enzymes, such as alanine aminotransferase (ALT) and aspartate transferase (AST). It seems that an increased activity of liver enzymes can independently predict the progression of MetS, diabetes mellitus, and cardiovascular events (7, 8). Despite some indications, the association between alcohol intake and liver enzyme levels, including γ -glutamyl transferase (GGT), ALT, and AST, has not been conclusively established (9).

Inflammation plays a crucial role in the pathogenesis of diabetes mellitus and atherosclerosis (10). It is hoped that preventing this condition can significantly reduce CVD mortality. Nutraceutical compounds, nutrients, and dietary patterns have been explored for their beneficial properties and therapeutic potential in treating MetS. Although, several nutrients have been considered as a MetS therapeutic approach, no definitive dietary treatment has been established (11).

Nowadays, Lycopene is recognized for its effectiveness in controlling of various diseases such as obesity, diabetes, metabolic syndrome, cardiovascular diseases, infertility, cancers and respiratory disorders (12-14). It's suggested that dietary carotenoids, particularly Lycopene, may play a crucial role in controlling metabolic issues like obesity, hypertension, diabetes, cardiovascular disease, and cancer (15). The structure of Lycopene contains conjugated double bonds that can react with free radicals, making it the most powerful oxygen quencher among natural carotenoids (16). The reactions between Lycopene and ROS depend on various factors, including Lycopene structure, free radical types, and ROS location in the cell membrane, particularly in biological systems (17).

Studies have reported that the use of Lycopene to reduce inflammation and liver disease treatment (18, 19). The bioavailability and absorption of Lycopene are enhanced by trans-to-cis conversion in enterocytes, liver and stomach (20). In the stomach, Lycopene is activated, released from the matrix, internalized into lipid droplets, and then released into the small intestine. Enzymes and bile acids break down the remaining matrix, facilitating the uptake of Lycopene by enterocytes. The majority of Lycopene is packaged

into chylomicrons and secreted into the lymphatic system before being released into the circulation from chylomicrons in the liver. The bioactive properties of Lycopene metabolites are produced through enzymatic or oxidative cleavage in the liver (21).

The anti-inflammatory and antioxidant activities of Lycopene play an important role in the maintenance of the liver normal metabolism (18). There are few clinical trials that examined the effects of Lycopene intervention on patients with MetS. The present study was designed to address to Lycopene effect on MetS patients in Iran.

Materials and Methods

The institutional board of the research and Ethics Committee of Iranian Clinical Trials confirmed in this study (IRCT20130507013263N3), and also, we received the confirmation of the Mashhad University of Medical Sciences (Mashhad, Iran) ethics committee (IR.MUMS.SP.1396.214). This clinical trial was performed in the Qhaem Hospital, (Mashhad, Khorasan Razavi, Iran) and the Clinical Nutrition Department (Mashhad University of Medical Sciences, Mashhad, Iran) between October 2022 and January 2023.

Study participants and eligibility criteria

Participants were recruited by email, face-to-face interviews, social media, and campus-based advertisements. All participants provided their written informed-consent. The study initially had 90 participants. However, during the follow-up period, the number decreased to 80. The main inclusion criteria were: having MetS based on the International Diabetes Federation criteria, which is at least two parameters associated with waist circumference (having a waist circumference higher than 94 cm in men and 80 cm in women), having fasting blood sugar higher than 100 mg/dl or having diabetes, having triglycerides higher than 150 mg/dl, having systolic blood pressure (SBP) of 130 mm Hg or diastolic blood pressure (DBP) higher than 85 mm Hg or using antihypertensive drugs, having HDL less than 40 mg/dl in men and less than 50 mg/dl in women patients who aged between 18-60 years at the beginning of the study (22), and lived in the Mashhad city (Khorasan Razavi, Iran). The detailed exclusion criteria were as follows: having a serious disease requiring active treatment, taking any other herbal supplements, being pregnant or breastfeeding and taking medications that may interact with Lycopene. Figure 1 shows the representative flowchart of the study design.

Study design

This double-blind, randomized and placebo-controlled investigation spanned a duration of 8 weeks. According to previous research (23), we considered 8 weeks as the minimum time of Lycopene intake. The anthropometric parameters were measured during the clinical trial, on initial day and in the 4th and 8th week of the study.

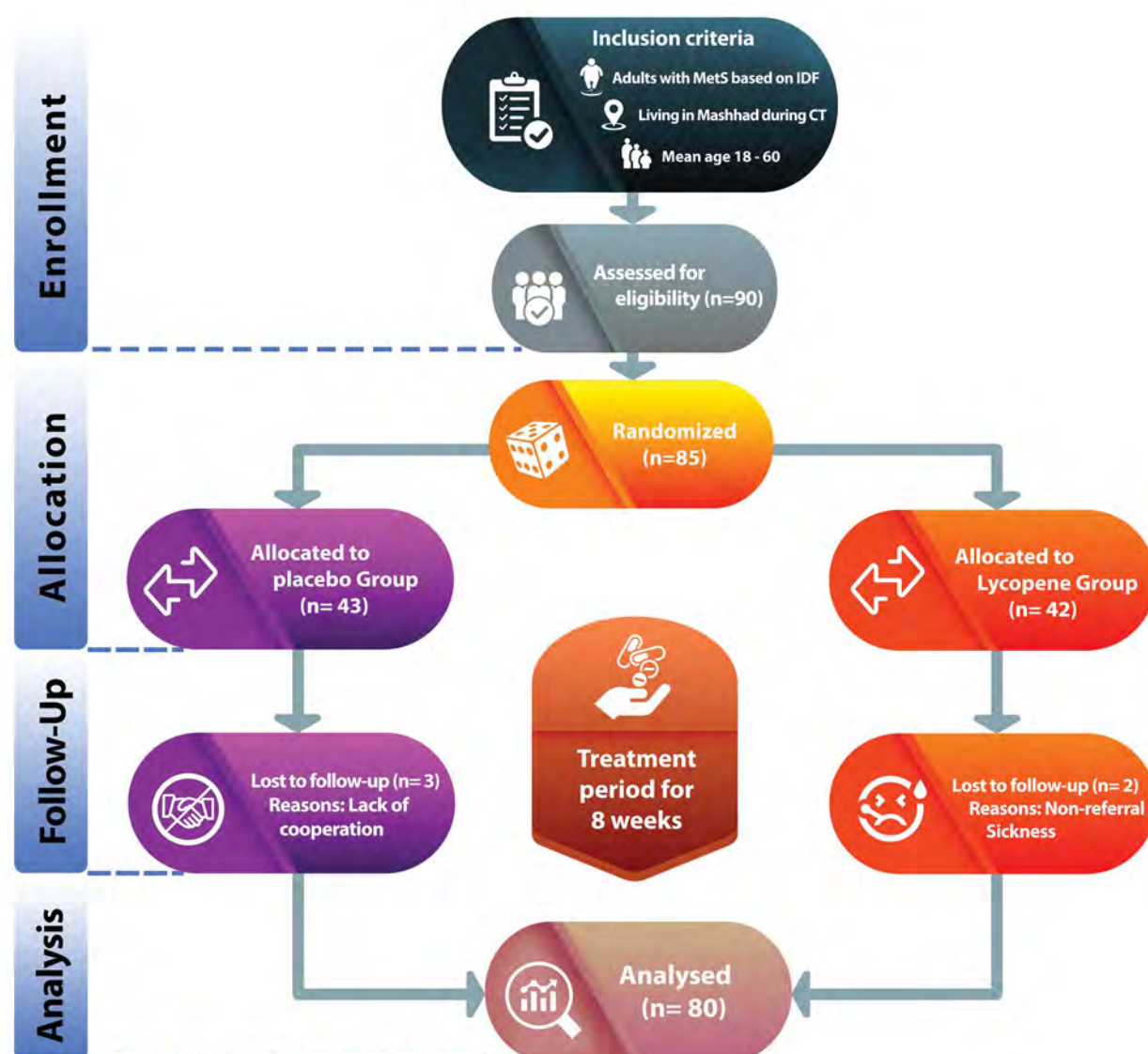


Fig.1: Flowchart of the study.

Interventions

Using SPSS software (version 24.0. Armonk, NY: IBM Corp.), subjects were randomly assigned to either the placebo or intervention groups. Participants chose a sealed envelope containing their random assignment upon entering the trial. All subjects, physicians, care providers, and statisticians were blinded in this study. Also, the placebo group received a preparation that was similar in size, color, and appearance of the treatment group package to maintain blinding. Patients consumed one Lycopene (20 mg) or placebo tablet daily for eight weeks. Assessments were carried out during the fourth and eighth week as a follow-up to determine both the safety and effectiveness. During the trial, evaluations of height, body weight, waist circumference, blood pressure, and body composition were conducted in the first, fourth,

and eighth weeks. After a 12-hour overnight fast, SBP and DBP were measured, and also 20 ml blood of each participant was collected to check fasting blood glucose (FBG) and lipid profile, including triglycerides, low-density lipoprotein cholesterol (LDL-C), high-density lipoprotein cholesterol (HDL-C), total cholesterol, CRP, and PAB, at weeks one and eight. At each follow-up visit, any adverse drug reactions (ADRs) were documented using a standardized report form.

Lycopene extraction and tablet formulation

A modified method was utilized for the extraction of Lycopene and the production of tablets (24-27). Initially, Lycopene was extracted from tomatoes that were heated to a temperature of 37-40°C for three days and dried to achieve a moisture content of about 70-80%.

The tomatoes, which were dried previously, were ground into a powder using a semi-industrial mill. Then they were subjected to an additional 12 hours of drying and then stored in a low-humidity environment to prepare them for the extraction process. Following this, acetone (100014, Merck Milipore, Germany) and ethyl acetate (PHR1481, Sigma-Aldrich, Germany, 1:1, V/V) were introduced to the tomato powder in a 1:4 (W/V) ratio (approximately four times the volume of the powder). Then, the resulting mixture was slowly mixed by a simple butterfly mixer (C9New, Behan laboratory equipments, Iran) for 1-3 hours in a covered and relatively insulated container.

This procedure was performed 3-5 times. Each time, the extract of the powders was separated and filtered, and fresh solvent was added to the container. The separation stage was performed using a modification of previous approaches. A strategy includes using a fabric filter and a device producing a mechanical pressure of more than 1 ton per square meter, the solvents contained in the separated extract and were transferred to a special container. Another method includes the separation of the extract from the powder by using a separator and a vacuum pump.

In our research, we utilized a rotary device to recover the solvent and minimize the volume of the extract, which included acetone, ethyl acetate, and Lycopene. Almost 95% of the solvent was recovered during several stages. A major advantage of this method is the ability to recover and reuse solvents, significantly reducing the high cost of organic solvents. After removing the solvent, 30-35% of the primary extract weight contains the active substance Lycopene. This extract should be restored in a refrigerator at 4°C. To increase the amount of a homogenized Lycopene, the extract was kept at room temperature for a few minutes. To precipitate the Lycopene, cold 96% ethanol was added to the extract with a ratio of 10:1 (W/V). As a result, after centrifugation, the Lycopene was separated from impurities and transferred to another container. The ethanol used in this step was also recovered at a rate of approximately 70-80%. By using the Headspace method (by Gas Chromatography), the residual amount of both of ethyl acetate and acetone in the final extract was also analyzed to determine the presence of the used solvents. In particular, the final extract was analyzed by UV Spectroscopy and the amount of Lycopene was determined based on the standard curve. For the tablet formulation, the extract (25-35% Lycopene) and hexane (104374, Merck Milipore, Germany) (medicinal solvent) were added to the microcrystalline cellulose powder (102331, Merck Milipore, Germany) and mixed (using a simple mixer). After removing the solvent, a powder containing Lycopene was created.

The materials used for extraction and formulation have special properties that help to facilitate the extraction. The Avicel has many properties, including uniform mixing of components, excellent absorption of Lycopene extract, high compressibility and outstanding tablet disintegration properties. Another material that is used in the tablet formulation process is the Aerosil (silicon dioxide). Due

to its crystalline properties, Aerosil has a low density. As a result, a tablet flow is greatly improved during a direct compression (The Aerosil was used in concentration of 1 to 5%). In addition, the polyvinyl pyrrolidone resulted in a better disintegration, higher compressibility and hardening of tablets. Also, the talc powder (IS29000, CP lab safety, USA) was used in the formulation process (2-5%). The use of Aerosil, talc powder, and a special combination of two types of commercial agents (Polyvinylpyrrolidone K30 and Polyvinylpyrrolidone CL) helped the Lycopene maintenance.

Placebo tablets were formulated using identical excipients as the Lycopene tablets, with the only distinction being that Lycopene was substituted with the Avicel, an inert excipient, in the final formulation. Since the final tablets had a red coat, there was no visible difference between the Lycopene-containing tablets and the placebo tablets. One of the goals of this study was to develop a new formulation of Lycopene tablets that would increase the stability of the Lycopene molecule. Therefore, all of the extraction, purification, and drug formulation methods used in this study are novel and have no prior references.

Statistical analysis

Kolmogorov–Smirnov statistical analysis was used to assess normality of the data. For all variables, descriptive statistics were calculated. This includes the mean and standard deviation (represented as mean \pm SD) for data that follows a normal distribution, and the median along with the interquartile range (IQR) for data that does not follow a normal distribution. Normally and non-normally distributed data was analyzed using T student tests and Mann-Whitney, respectively. Normally and non-normally distributed data was analyzed using paired and independent T student tests and Mann-Whitney or Wilcoxon, respectively. Confounding factors such as age and sex were adjusted the analysis of Co-variance (ANCOVA). The $P < 0.05$ was considered statistically significant.

Results

The Table 1 demonstrates the main characteristics of the baseline analysis. Totally, 80 patients who participated in this study were classified as belonging to intervention categories. The mean age of the Lycopene and placebo groups was 44.25 ± 11.25 and 41.75 ± 10.05 years, respectively. There were no significant differences in the levels of CRP, serum liver enzymes, systolic and diastolic blood pressure, and PAB between Lycopene and placebo groups before assigning the patients to the Lycopene and placebo groups.

Comparing the clinical features of our groups ,after 8 weeks of intervention with Lycopene ,we observed some statistically significant differences. The P value of the difference between the Lycopene and placebo groups, after adjusting for confounding factors such as age and sex

was found (Table 2). Interestingly, compared to the initial evaluation, the Lycopene group showed a decrease in the levels of CRP and PAB. However, this reduction was not found to be significant in the placebo group. Additionally,

after adjusting for confounding factors, only the P value of the difference in the PAB level between the two groups remained significant. No significant differences were found in the serum levels of ALT, AST, and ALP between our groups.

Table 1: Baseline features in the study groups

Variable	Lycopene (n=40)	Placebo (n=40)	P value
Gender			0.132
Women	22 (55)	28 (70)	
Men	18 (45)	12 (30)	
Age (Y)	44.25 ± 11.25	41.75 ± 10.05	0.214
Systolic blood pressure (mmHg)	125.00 ± 5.774	134.75 ± 12.790	0.108
Diastolic blood pressure (mmHg)	75.00 ± 12.910	35.628 ± 35.628	0.147
hs-CRP (g/dl)	0.46 ± 0.3	0.44 ± 0.27	0.753
PAB (H.K)	162.30 ± 37.42	172.17 ± 28.72	0.155
ALT (U/L)	22.95 ± 16.35	18.03 ± 7.5	0.519
AST (U/L)	23.13 ± 17.06	17.05 ± 6.2	0.149
ALP (U/L)	123.53 ± 34.92	126.87 ± 48.31	0.836
Non-smoker	35 (87.5)	31 (77.5)	0.408
Exposure-smoker	1 (2.5)	3 (7.5)	
Current smoker	4 (10)	6 (15)	

Data presented as mean ± standard deviations or median (interquartile range) or n (%). Independent sample t test was used where appropriate. PAB; Pro-oxidant-antioxidant balance, ALT; Alanine aminotransferase, AST; Aspartate transferase, ALP; Alkaline phosphatase, and hs-CRP; High-sensitivity C-reactive protein.

Table 2: The effect of Lycopene on CRP and liver enzymes in population study

Variable	Lycopene (n=40)			Placebo (n=40)			P value*
	Baseline	Difference	P value	Baseline	Difference	P value	
hs-CRP (g/dl)	0.46 ± 0.3	-0.14	0.004	0.44 ± 0.27	-0.08	0.141	0.340
PAB (H.K)	162.30 ± 37.42	-29.9	<0.001	172.17 ± 28.72	-10.04	0.098	0.002
ALT (U/L)	22.95 ± 16.35	1.2	0.607	18.03 ± 7.5	1.02	0.439	0.252
AST (U/L)	23.13 ± 17.06	-2.2	0.233	17.05 ± 6.2	1.1	0.146	0.792
ALP (U/L)	123.53 ± 34.92	1.2	0.809	126.87 ± 48.31	9.25	0.226	0.406

The P<0.05 was considered statistically significant. *; P value of difference between in Lycopene and placebo groups after adjusting for confounding factors such as age and sex as co-variant, PAB; Pro-oxidant-antioxidant balance, ALT; Alanine aminotransferase, AST; Aspartate transferase, ALP; Alkaline phosphatase, and hs-CRP; High-sensitivity C-reactive protein. Bold numbers are statistically significant.

Discussion

The mechanism of the high-sensitivity CRP (hs-CRP) reduction by the Lycopene is not only exactly known, but also several hypotheses exist. One of them addressed the Lycopene, as a potent antioxidant, that can prevent the oxidation of LDL and consequently, reduce the inflammatory response in the vascular wall. Another hypothesis is that the Lycopene may affect apolipoprotein B (apo B), one of LDL carriers, and reduce its interaction with a CRP. The CRP, an inflammatory protein, may be involved in tissue damage during a heart attack. Therefore, reducing the interaction of CRP and apo B may lead to lower risk of CVD (28, 29).

The initial question of this study aimed to determine the Lycopene effect on the imbalance of the PAB and hs-CRP in the patient with MetS. The most interesting our finding was that there was a significant difference in PAB levels between our groups, even after adjusting for age and sex. Although, this finding did not align with the previous research. In the study conducted in the United Kingdom with 225 volunteers (94 males and 131 females, aged 40-65 years). They evaluated the Lycopene effects on the modulation of CVD risks after 12 weeks-controlled diet. They considered 3 groups: i. A controlled diet with low consumption of tomato-based food, ii. A high tomato diet (20 to 50 mg Lycopene/day), iii. Controlled diet with Lycopene tablet (10 mg/day). They found that none of the CVD markers, including insulin resistance, sensitivity markers, inflammatory markers, and lipid concentrations, showed significant changes (30). One possible explanation for these results could be the Lycopene low dose used in their study.

As expected, this study found a significant decrease in the hs-CRP levels in the Lycopene group. These results are consistent with Sun and Karin (31) study that showed a daily consumption of Lycopene (29.4 mg/day for one month) reduced the CRP serum level in a population of heart failure patients (23 men, 17 women). Also, Bahcecioglu et al. (32) demonstrated the efficacy of heightened Lycopene intake, derived from tomato products, in ameliorating lipid profiles and inflammatory markers, such as CRP.

Some studies have shown that the Lycopene may be ineffective on liver enzymes and even sometimes have a negative effect on ALT, AST or ALP. The exact mechanism of this process is not clear, but one of the hypotheses is that the Lycopene may affect the activity of other liver enzymes such as CYP450 and cause changes in the metabolism of some drugs. This issue may lead to the liver function dysfunction (33, 34).

The second question this research addressed was the relationship between the Lycopene tablets and liver enzyme serum levels in patients with MetS. We found no difference in the serum level of ALT, AST, and ALP in our groups, which supports the findings of the previous work. In 2020, Negri et al. (35) evaluated the effect of the Lycopene extracts and calorie-restricted regimen in the

obese children with fatty liver. This randomized crossover clinical trial examined 61 obese children with fatty with calorie-restricted regimen alone or with a supplement of Lycopene juice for 2 months. A reduction in the body mass index (BMI), cholesterol, triglycerides, and liver size, was more profound in the Lycopene-supplemented group. They suggested that adding Lycopene to a calorie-restricted regimen could be considered preventive and protective support for an obese child (35).

A randomized intervention trial was designed to determine the Lycopene supplementation effect (7 mg daily for 2 months) on healthy volunteers and CVD patients treated by the Statin. In this study by Seki et al. (36), it was indicated that the mentioned treatment resulted in a 53% improvement in the endothelial-dependent arterial vasodilation for patients, while no effect was observed in healthy volunteers. Furthermore, it was shown that a Lycopene supplementation (20 mg/day for 1 year) led to a decrease in the thickness of the intima-media in the 144 patients with sub-clinical atherosclerosis (37).

While various nutrients have been explored as potential therapeutic approaches for MetS treatment, no definitive dietary treatment has been established. The Lycopene, a carotenoid recognized for its antioxidant properties, is one such nutrient. However, the relationship between a Lycopene intake and MetS risk factors, such as inflammation and insulin resistance, are not well understood. The majority of these studies reported a significant protective association between Lycopene and MetS. However, the specific components of the MetS influenced by the Lycopene varied across studies (38).

While the evidence generally supports a protective relationship between a Lycopene and MetS, further research is needed to understand the mechanisms behind this effect and to establish evidence-based recommendations for the Lycopene intake. Potential challenges of this study may include ensuring that the study duration is sufficient to observe the long-term effects of Lycopene, and maintaining adherence to the assigned Lycopene dietary intake.

Conclusion

In this investigation, we evaluated the effect of Lycopene on the risk status of patients with MetS. Administering daily dosage of 20 mg for 8 weeks resulted in no recorded side effects. Our findings indicate that Lycopene has a modulating effect on PAB and inflammation associated with MetS. Additionally, the encapsulated Lycopene treatment did not yield a significant difference in serum levels of ALT, AST, or ALP between the two groups. These results highlight the Lycopene potential therapeutic value. Further research is essential to validate these findings and explore the mechanisms underlying the observed effects.

Acknowledgements

This project was implemented in collaboration with Mashhad University of Medical Sciences (grant

number: 960774). The authors would like to gratefully acknowledge the contribution of participants in the study. The authors declare that they have no conflicts of interest in this study.




Authors' Contributions

M.M.; Project administration, Methodology, and Original draft preparation. M.A.; Visualization, Software, Writing- Reviewing and Editing. F.N, M.G.C., H.H., H.B.; Visualization and Investigation. R.A.-D.: Conceptualization and Validation. S.T.; Investigation and Formal analysis. G.A.F., M.R.M.; Writing - Review, Editing and Original draft preparation. F.H.; Supervision, Project administration, and Funding acquisition. M.G.-M., Supervision and Project administration. All authors read and approved the final manuscript.

References

- Świątkiewicz I, Wróblewski M, Nuskiewicz J, Sutkowy P, Wróblewska J, Woźniak A. The role of oxidative stress enhanced by adiposity in cardiometabolic diseases. *Int J Mol Sci.* 2023; 24(7): 6382.
- Zafari N, Velayati M, Fahim M, Maftouh M, Pourali G, Khazaei M, et al. Role of gut bacterial and non-bacterial microbiota in alcohol-associated liver disease: Molecular mechanisms, biomarkers, and therapeutic prospective. *Life Sci.* 2022; 305: 120760.
- Zujko ME, Witkowska AM. Dietary antioxidants and chronic diseases. *Antioxidants (Basel).* 2023; 12(2): 362.
- Ghazizadeh H, Saberi-Karimian M, Aghasizadeh M, Sahebi R, Ghazavi H, Khedmatgozar H, et al. Pro-oxidant-antioxidant balance (PAB) as a prognostic index in assessing the cardiovascular risk factors: a narrative review. *Obes Med.* 2020; 19: 100272.
- Alamdari DH, Paletas K, Pegiou T, Sarigianni M, Befani C, Koliakos G. A novel assay for the evaluation of the prooxidant-antioxidant balance, before and after antioxidant vitamin administration in type II diabetes patients. *Clin Biochem.* 2007; 40(3-4): 248-254.
- Ahmadnezhad M, Arefhosseini SR, Parizadeh MR, Tavallaie S, Tayefi M, Darroudi S, et al. Association between serum uric acid, high sensitive C-reactive protein and pro-oxidant-antioxidant balance in patients with metabolic syndrome. *Biofactors.* 2018; 44(3): 263-271.
- Lioudaki E, Ganotakis ES, Mikhailidis DP. Liver enzymes: potential cardiovascular risk markers? *Curr Pharm Des.* 2011; 17(33): 3632-3643.
- Khalesi M, Jafari SA, Kiani M, Picarelli A, Borghini R, Sadeghi R, et al. In vitro gluten challenge test for celiac disease diagnosis. *J Pediatr Gastroenterol Nutr.* 2016; 62(2): 276-283.
- Huang H, Qiu Y, Tang A, Li W, Yao W, Zhong M, et al. The impact of food restriction on liver enzyme levels: a systematic review and meta-analysis. *Nutr Rev.* 2023; 81(8): 939-950.
- Elimam H, Abdulla AM, Taha IM. Inflammatory markers and control of type 2 diabetes mellitus. *Diabetes Metab Syndr.* 2019; 13(1): 800-804.
- Ambroselli D, Masciulli F, Romano E, Catanzaro G, Besharat ZM, Massari MC, et al. New advances in metabolic syndrome, from prevention to treatment: the role of diet and food. *Nutrients.* 2023; 15(3): 640.
- Grabowska M, Wawrzyniak D, Rolle K, Chomczyński P, Oziewicz S, Jurga S, et al. Let food be your medicine: nutraceutical properties of lycopene. *Food Funct.* 2019; 10(6): 3090-3102.
- Andersen LF, Jacobs DR Jr, Gross MD, Schreiner PJ, Dale Williams O, Lee DH. Longitudinal associations between body mass index and serum carotenoids: the CARDIA study. *Br J Nutr.* 2006; 95(2): 358-365.
- Zielinska MA, Hamulka J, Wesolowska A. Carotenoid content in breastmilk in the 3rd and 6th month of lactation and its associations with maternal dietary intake and anthropometric characteristics. *Nutrients.* 2019; 11(1): 193.
- Pandey P, Khan F. A mechanistic review of the anticancer potential of hesperidin, a natural flavonoid from citrus fruits. *Nutr Res.* 2021; 92: 21-31.
- Kelkel M, Schumacher M, Dicato M, Diederich M. Antioxidant and anti-proliferative properties of lycopene. *Free Radic Res.* 2011; 45(8): 925-940.
- Caseiro M, Ascenso A, Costa A, Creagh-Flynn J, Johnson M, Simões S. Lycopene in human health. *Lwt.* 2020; 127: 109323.
- Abenavoli L, Procopio AC, Paravati MR, Costa G, Milić N, Alcaro S, et al. Mediterranean diet: the beneficial effects of lycopene in non-alcoholic fatty liver disease. *J Clin Med.* 2022; 11(12): 3477.
- Xing Y, Ren X, Li X, Sui L, Shi X, Sun Y, et al. Baicalein enhances the effect of acarbose on the improvement of nonalcoholic fatty liver disease associated with prediabetes via the inhibition of de novo lipogenesis. *J Agric Food Chem.* 2021; 69(34): 9822-9836.
- Richelle M, Sanchez B, Tavazzi I, Lambelet P, Bortlik K, Williamson G. Lycopene isomerisation takes place within enterocytes during absorption in human subjects. *Br J Nutr.* 2010; 103(12): 1800-1807.
- Srivastava S, Srivastava AK. Lycopene; chemistry, biosynthesis, metabolism and degradation under various abiotic parameters. *J Food Sci Technol.* 2015; 52: 41-53.
- Oda E. Historical perspectives of the metabolic syndrome. *Clin Dermatol.* 2018; 36(1): 3-8.
- Saawarn N, Shashikanth MC, Saawarn S, Jirge V, Chaitanya NC, Pinakapani R. Lycopene in the management of oral lichen planus: a placebo-controlled study. *Indian J Dent Res.* 2011; 22(5): 639-643.
- Poojary MM, Passamonti P. Extraction of lycopene from tomato processing waste: kinetics and modelling. *Food Chem.* 2015; 173: 943-950.
- Briones-Labarca V, Giovagnoli-Vicuña C, Cañas-Sarazúa R. Optimization of extraction yield, flavonoids and lycopene from tomato pulp by high hydrostatic pressure-assisted extraction. *Food Chem.* 2019; 278: 751-759.
- Zuorro A. Enhanced lycopene extraction from tomato peels by optimized mixed-polarity solvent mixtures. *Molecules.* 2020; 25(9): 2038.
- Periago MJ, Rincón F, Agüera MD, Ros G. Mixture approach for optimizing lycopene extraction from tomato and tomato products. *J Agric Food Chem.* 2004; 52(19): 5796-5802.
- Zamani M, Behmanesh Nia F, Ghaedi K, Mohammadpour S, Amirani N, Goudarzi K, et al. The effects of lycopene and tomato consumption on cardiovascular risk factors in adults: a grade assessment systematic review and meta-analysis. *Curr Pharm Des.* 2023; 29(21): 1671-1700.
- Kim OY, Yoe HY, Kim HJ, Park JY, Kim JY, Lee SH, et al. Independent inverse relationship between serum lycopene concentration and arterial stiffness. *Atherosclerosis.* 2010; 208(2): 581-586.
- Jiang W, Guo MH, Hai X. Hepatoprotective and antioxidant effects of lycopene on non-alcoholic fatty liver disease in rat. *World J Gastroenterol.* 2016; 22(46): 10180-10188.
- Sun B, Karin M. Obesity, inflammation, and liver cancer. *J Hepatol.* 2012; 56(3): 704-713.
- Bahcecioglu IH, Kuzu N, Metin K, Ozercan IH, Ustündag B, Sahin K, et al. Lycopene prevents development of steatohepatitis in experimental nonalcoholic steatohepatitis model induced by high-fat diet. *Vet Med Int.* 2010; 2010: 262179.
- Nosková K, Dovrtělová G, Zendluka O, Strakošová M, Peš O, Juřica J. Lycopene increases metabolic activity of rat liver CYP2B, CYP2D and CYP3A. *Pharmacol Rep.* 2020; 72(1): 156-165.
- Baz L, Algarni S, Al-Thepyani M, Aldairi A, Gashlan H. Lycopene improves metabolic disorders and liver injury induced by a high-fat diet in obese rats. *Molecules.* 2022; 27(22): 7736.
- Negri R, Trinchese G, Carbone F, Caprio MG, Stanzione G, di Scala C, et al. Randomised clinical trial: calorie restriction regimen with tomato juice supplementation ameliorates oxidative stress and preserves a proper immune surveillance modulating mitochondrial bioenergetics of T-Lymphocytes in obese children affected by non-alcoholic fatty liver disease (NAFLD). *J Clin Med.* 2020; 9(1): 141.
- Seki E, Brenner DA, Karin M. A liver full of JNK: signaling in regulation of cell function and disease pathogenesis, and clinical approaches. *Gastroenterology.* 2012; 143(2): 307-320.
- Hadad N, Levy R. The synergistic anti-inflammatory effects of lycopene, lutein, β -carotene, and carnosic acid combinations via redox-based inhibition of NF- κ B signaling. *Free Radic Biol Med.* 2012; 53(7): 1381-1391.
- Senkus KE, Tan L, Crowe-White KM. Lycopene and metabolic syndrome: a systematic review of the literature. *Adv Nutr.* 2019; 10(1): 19-29.

Clinical Evaluation of Collagen-Induced Arthritis in Female Lewis Rats: A Comprehensive Analysis of Disease Progression and Severity

Mahnaz Babaahmadi, Ph.D.^{1,2#}, Nima Makvand Gholipour, B.Sc.^{2#}, Behnoosh Tayebi, Ph.D.^{1,2},
Jed Pheneger, B.Sc.³, Ensiyeh Hajizadeh-Saffar, Ph.D.^{4,5*} , Mohamadreza Baghaban
Eslaminejad, Ph.D.^{2*} , Seyedeh-Nafiseh Hassani, Ph.D.^{2,4*} 

1. Department of Applied Cell Sciences, Faculty of Basic Sciences and Advanced Medical Technologies, Royan Institute, ACECR, Tehran, Iran
2. Department of Stem Cells and Developmental Biology, Cell Science Research Center, Royan Institute for Stem Cell Biology and Technology, ACECR, Tehran, Iran
3. Inotiv, Inc., West Lafayette, IN, USA
4. Advanced Therapy Medicinal Product Technology Development Center (ATMP-TDC), Royan Institute for Stem Cell Biology and Technology, ACECR, Tehran, Iran
5. Department of Regenerative Medicine, Cell Science Research Center, Royan Institute for Stem Cell Biology and Technology, ACECR, Tehran, Iran

Abstract

Objective: The collagen-induced arthritis (CIA) model is the most commonly studied autoimmune model of rheumatoid arthritis (RA). In this study, we investigated the usefulness of collagen type II emulsified in Freund's incomplete adjuvant (CII/IFA) as a suitable method for establishing RA in Lewis rats. The aim of the present study was to present a straightforward and effective method for inducing CIA in rats.

Materials and Methods: In this experimental study, animals were divided into two equal groups (n=5); control and CIA. Five rats were injected intradermally at the base of the tail with a 0.2 ml CII/IFA emulsion. On the seventh day, a 0.1 ml CII/IFA emulsion booster was injected. Arthritis symptoms that arose were evaluated at clinical, histological, radiological, and at protein expression levels to find out if the disease had been induced successfully.

Results: Our finding showed a decreasing trend in the body weight during the RA induction period, while the arthritis score and paw thickness were increased during this period. The results of the enzyme-linked immunosorbent assay (ELISA) for serum samples revealed that the levels of proinflammatory cytokines, interleukin (IL)-1 β , IL-6, IL-17, and tumor necrosis factor (TNF)- α and anti-CII IgG were significantly increased in CIA rats compared to the control group. After CIA induction, the level of anti-inflammatory protein IL-10 was decreased significantly. Radiographic examination of the hind paws showed soft tissue swelling, bone erosion, and osteophyte formation in CIA rats. Additionally, based on histological evaluations, the hind paws of the CIA group showed pannus formation, synovial hyperplasia, and bone and cartilage destruction.

Conclusion: It seems that CII/IFA treatment can be an appropriate and effective method to induce RA disease in Lewis rats. This well-established and well-characterized CIA model in female Lewis rats could be considered to study aspects of RA and develop novel anti-arthritic agents.

Keywords: Clinical Scoring, Collagen-Induced Arthritis, Freund's Incomplete Adjuvant, Rheumatoid Arthritis

Citation: Babaahmadi M, Makvand Gholipour N, Tayebi B, Pheneger J, Hajizadeh-Saffar E, Baghaban Eslaminejad MR, Hassani SN. Clinical evaluation of collagen-induced arthritis in female lewis rats: a comprehensive analysis of disease progression and severity. Cell J. 2023; 25(12): 854-862. doi: 10.22074/CELLJ.2023.2004504.1326

This open-access article has been published under the terms of the Creative Commons Attribution Non-Commercial 3.0 (CC BY-NC 3.0).

Introduction

Rheumatoid arthritis (RA) is a chronic autoimmune disease that primarily affects the joints (1). This systemic disorder has an unknown etiology that affects 1% of the adult population worldwide, making RA one of the most common chronic inflammatory diseases (2, 3). In the RA disorder, the immune

system attacks the synovial membrane of joints, causes the joints to become swollen and painful due to inflammation, thickening of the joint membrane, and fluid accumulation. Over time, this state leads to cartilage and bone destruction, joint deformity, and eventually severe disability (4, 5). The clinical symptoms of the disease negatively affect the patient's

Received: 13/June/2023, Revised: 21/October/2023, Accepted: 30/October/2023

#These authors contributed equally in this study.

*Corresponding Addresses: P.O.Box: 16635-148, Department of Regenerative Medicine, Cell Science Research Center, Royan Institute for Stem Cell Biology and Technology, ACECR, Tehran, Iran

P.O.Box: 16635-148, Department of Stem Cells and Developmental Biology, Cell Science Research Center, Royan Institute for Stem Cell Biology and Technology, ACECR, Tehran, Iran

Emails: en.hajizadeh@royan-rc.ac.ir, eslami@royaninstitute.org, sn.hassani@royan-rc.ac.ir



Royan Institute
Cell Journal (Yakhteh)

quality of life and the ability to work and induce psychological distress. Despite of numerous therapeutic approaches are currently considered to alleviate symptoms, 15-40% of RA patients are resistant to long-term treatments and can become non-responsive to all existing clinical therapies (6). Therefore, suitable *in vivo* models need to assess the safety and efficacy of novel therapies, evaluate the mechanism of action of the drugs, and understand the mechanisms behind the development of the disease.

A Collagen-induced arthritis (CIA) model in mice and rats has been extensively studied because it shares several pathological and immunological features with humans and allows the testing of innovative treatments in preclinical studies (7). Most CIA models are induced by type II collagen (CII), the main protein found in the articular cartilage. Thus, by immunization of some inbreds or outbred rats and mice, an experimental model of autoimmune arthritis can be developed (8). A CII is provided for immunization from animal sources, including pigs, cattle, and chickens (9). To establish arthritis, adjuvants such as Freund's incomplete adjuvant (IFA) accompanied by CII and Freund's complete adjuvant (CFA) with or without collagen are commonly used. In numerous studies, CFA, employed alongside CII as immunological agents, has been utilized for rat modelling, but this approach has its drawbacks (10). The CFA is composed of an emulsion of water and mineral oil containing heat-killed *Mycobacteria*; in contrast, the IFA contains an emulsion of water and non-metabolizable oils (mineral oil) and does not contain any *Mycobacterium* species (7). In a CII-induced establishment in Wistar rats, it was found that when a CFA adjuvant is used to prepare collagen, the immune response, in addition to collagen, is also produced against other *Mycobacterium* antigens, leading to a severe inflammatory response (9, 10).

For the reasons stated, the IFA use in preparing CII/IFA emulsions could be preferable to RA model development, which are similar to human RA in different symptoms of haematology, clinical, histological, and radiology (11).

The aim of the present study was to present a straightforward and effective method for inducing CIA in rats. We opted to utilize an Incomplete Freund's adjuvant (IFA), as an alternative to Complete Freund's adjuvant (CFA), to emulsify a bovine Collagen Type II (CII).

Through the implementation of this immunization procedure, diverse mouse strains exhibited distinct responses, which aligned with their sensitivity to the CIA induction. Ultimately, we sought to determine the most effective CIA model. This approach was aimed at ensuring the model's reliability, marked by high consistency and reproducibility, facilitating comparisons across various research studies. Moreover, we intended for this model to be particularly useful in investigations focused on understanding the etiopathogenetic mechanisms and treatment approaches for RA.

Materials and Methods

Ethical statement

The Royan Institutional Review Board and Institutional

Ethics Committee, (Tehran, Iran) approved this study (IR.ACECR.ROYAN.REC.1398.05). All experimental procedures were conducted under the standard guidelines of the National Institutes of Health guidelines for the Care and Use of Laboratory Animals (eighth edition) (12).

Animals and establishment of an rheumatoid arthritis model

This experimental study in female Lewis rats, because of more susceptibility of female rodents to develop autoimmune complications than males. Lewis rats were purchased from the Pasteur institute Tehran, Iran.

Ten inbred female Lewis rats (200 ± 50 g in weight; 8-10 weeks old) were randomized into equal two groups ($n=5$). Animals of each group were housed in pathogen-free cages (two or three rats in each cage) with free access to standard feed and water, while the diameter of each cage was $27 \times 42 \times 17$ cm. Also, they were kept in an animal laboratory with 12 h of light/dark cycles at $15-24^\circ\text{C}$ and relative humidity of 30-70%.

In accordance with previous studies (10, 13), the CIA model was induced in the animals. Bovine type II collagen (CII, Chondrex, Redmond, WA, USA, 20021) at a concentration of 2 mg/ml was dissolved in 0.05% acetic acid (Merck, Germany, 137000) and emulsified with an equal volume of Freund's incomplete adjuvant (IFA, Thermo Fisher, USA, 77140) using a homogenizer. This process aimed to generate a stable emulsion that would persist as a solid clump, preventing dispersion in water. Briefly, five rats were injected intradermally with a total of 0.2 ml CII/IFA emulsion (1 mg/ml) at the base of the tail, 1-2 cm away from the tail root, and at two sites on the back of rats, for sufficient and consistent drainage to the inguinal lymph nodes. Seven days after primary immunization, a 0.1 ml CII/IFA emulsion booster injection was administered. These rats were then assigned to the model group. The control group did not receive any compound. After 23 days of primary induction, the rats were euthanized, and their sera and paws were harvested for further analysis.

Clinical evaluation of the collagen-induced arthritis animal model

Induction of arthritis in rats was evaluated by body weight changes, paw swelling (characterized by oedema and erythema), and arthritis score from the 7th day of CII/IFA injection until scarification day, the 23rd day of injection. Body weight changes in the rats were measured every two days. The paw swelling was calculated by the thickness of the ankle joints of both hind paws in millimeters using the digital calipers model (Stoelting, USA, 58750). Arthritis scores on the hind paws of each rat were graded from 0 to 4 according to the extent of oedema and erythema of the specific tissues. The severity scores were defined in Table 1. The maximum total score of every arthritic rat was 8 (4 points \times 2 hind paws). The arthritic signs were assessed by two independent investigators every two days and were scored individually using a previously described scoring system (15).

Sample collection

All animals were anaesthetized with a mixture of 50 mg/kg ketamine and 10 mg/kg xylazine (1801020-04, 362845 respectively, both from Alfasan, Woerden, Netherland) then the animals were euthanized with carbon dioxide to perform laboratory assessments. Blood samples were collected via cardiac puncture and immediately centrifuged at 3000 rpm for 10 minutes at 4°C, and the harvested sera were kept at -70°C until the enzyme-linked immunosorbent assay (ELISA). The harvested hind paws were fixed with 10% neutral buffered formalin (Merck, Germany, 104002, pH=7.2).

Enzyme-linked immunosorbent assay

The level of inflammatory cytokines (tumor necrosis factor- α [TNF- α], IL-1 β , IL-17, and IL-6) and immunoregulatory cytokines (IL-10) were detected using the necessary ELISA kits (R&D Systems, USA). The level of anti-CII immunoglobulin was detected using an ELISA kit (Chondrex, USA, 1021T) according to the manufacturer's instructions.

Radiological assessment

Hind paws were radiographed by a conventional X-ray machine (Toshiba, DC-12M) at 45 kV peak, 15 mA and 5 s exposure time. Radiographs were evaluated for different parameters, including soft tissue swelling, bone erosion, and osteophyte formation. These signs were scored blindly by two independent radiologists who were unaware of the treatment assignments on a scale of 0=regular, 1=mild changes, 2=moderate changes, and 3=severe changes (14).

Histological evaluation

The hind paws were decalcified in 10% EDTA (Gibco, USA, 15040) for 28 days at room temperature after being fixed for 48 h in 10% neutral buffered formalin (pH=7.26). Then the tissue samples were embedded in the paraffin (Biooptica, Italy, 087920) and serially sectioned into 5 μ m thick sections. The sections were subjected to hematoxylin, eosin (H&E, Biooptica, Italy, 05-06004, 05-m10003, Biooptica, Italy, respectively) and Masson's trichrome (MT) staining (Sigma, USA, f-7258,). Sections

were observed under the light microscope (Olympus BX51; Olympus, Japan) by an expert pathologist trained in joint pathology and blind to our treatment. Histological analysis was carried out based on bone resorption, cartilage damage, pannus formation, and infiltration of inflammatory cells. The severity of the lesions was determined using a graded scale as follows: 0=no signs of change, 1=mild change, 2=moderate change, and 3=increasing degrees of changes (14).

Statistical analysis

All statistical analyses were performed using the GraphPad Prism 8 (GraphPad Software., La Jolla, California, USA) software. The comparisons of radiology and pathology scores, paw thickness and body weight were performed using a 2-way analysis of variance (ANOVA). Unpaired t test were performed for other variables. Data were expressed as mean \pm standard deviation of the mean (SD), and P<0.05 were considered statistically significant.

Results

Collagen-induced arthritis rats showed clinical signs of rheumatoid arthritis disease

The RA disease progression was assessed based on weight changes, arthritis severity score, and paw thickness. Clinical signs of CIA in the hind paws of rats showed that arthritis established well in animals (Fig.1).

The 23 days after the primary injection, Intense oedema and erythema were observed in the hind paws of the CIA group in comparison with the control group (Fig.1A). Animals in the CIA group showed a trend of mild body weight loss in a time-dependent manner in comparison with the control group (Fig.1B). However, this decreasing trend was insignificant during the model establishment. Erythema and swelling, as disease severity scores, were higher in the CIA group compared to the control group, which was significant at days 15-23 (P<0.001, Fig.1C). The paw thickness, indicative of ankle joint swelling, exhibited a notable increase in the CIA group. This increase was statistically significant from day 17 (P<0.001) through day 23 following the primary induction (P<0.001, Fig.1D).

Table 1: Scoring system for subjective evaluation of arthritis severity

Severity score	Degree of inflammation
0	No evidence of erythema and swelling
1	Erythema and mild swelling confined to the tarsals or ankle joint
2	Erythema and mild swelling extending from the ankle to the tarsals
3	Erythema and moderate swelling extending from the ankle to metatarsal joints
4	Erythema and severe swelling encompassing the ankle, foot, and digits, or ankylosis of the limb

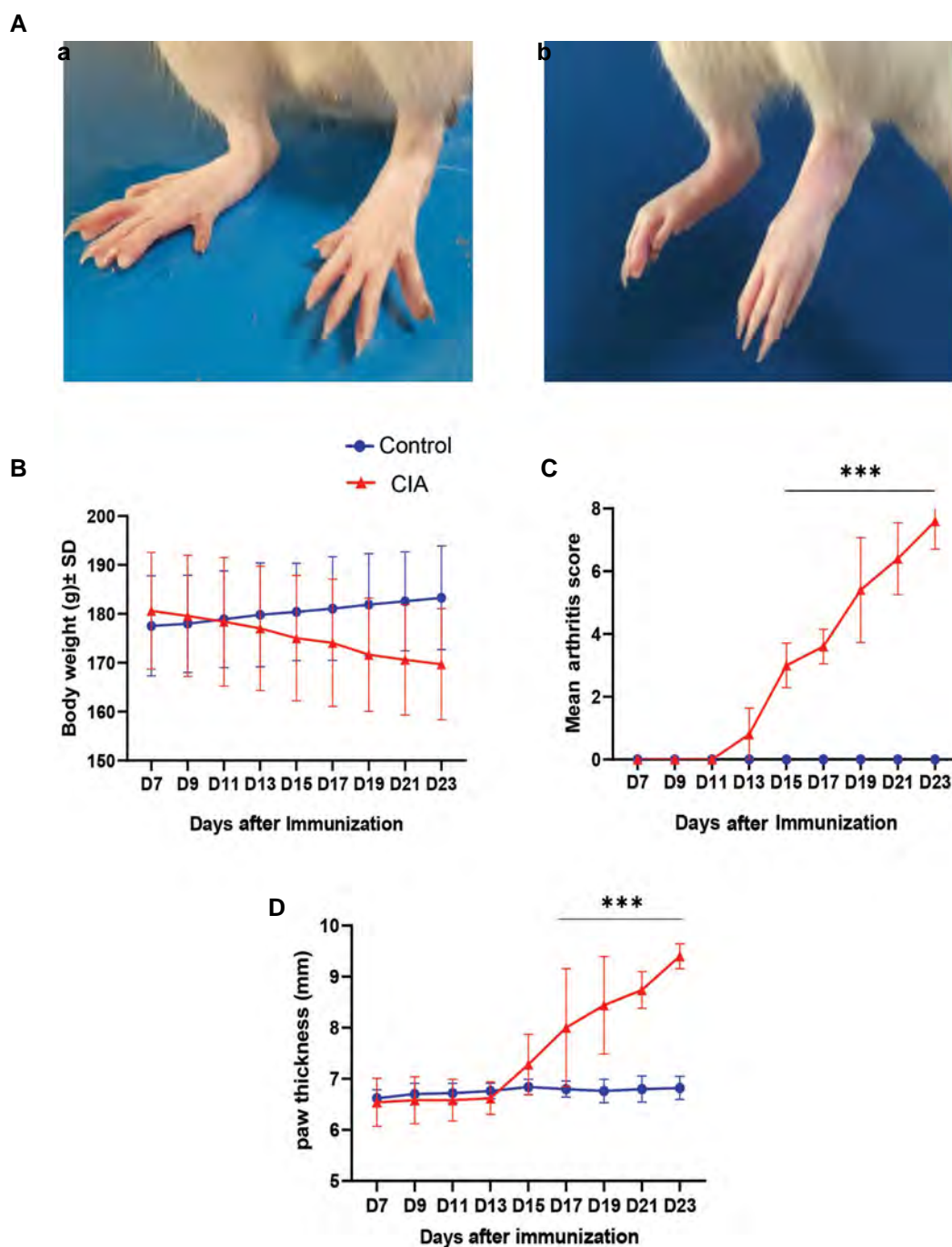


Fig.1: Clinical signs of the CIA induction in rats. **A.** Representative images of the hind paws from the control (a) and CIA (b) groups were taken on the 23rd day after the primary injection of type II collagen emulsified in the incomplete Freund's adjuvant. Intense edema was observed in the hind paws of the CIA group in comparison with the control group. **B.** Body weight changes, **C.** Arthritis scores for hind paws, and **D.** Paw swelling were evaluated in control and CIA groups during the disease induction. All data were presented as the mean \pm standard deviation. The comparisons were performed using two-way analysis of variance (ANOVA, n=5). ***, P<0.001 versus control rats and CIA; Collagen-induced arthritis.

Collagen-induced arthritis rats showed inflammation at the protein expression level

To explore the RA induction in rats, the expression of IL-1 β , IL-6, IL-17, TNF- α as proinflammatory and IL-10 as an anti-inflammatory cytokine was detected by ELISA assay. The protein level of autoreactive antibodies against CII (CII-specific IgG) was also evaluated.

The anti-CII antibody level in the serum of the CIA group was meaningfully higher than those of the control group (P<0.001, Fig.2A).

The expression levels of TNF- α (P<0.001), IL-1 β (P<0.001), IL-6 (P<0.001), and IL-17 (P<0.001) was elevated significantly in the CIA group in comparison with the control group (Fig.2B-E). In addition, the expression

level of IL-10 ($P < 0.001$) in the CIA group was inhibited in comparison with the control group (Fig.2F).

The radiographic features of lateral views of the hind paws in our groups are shown in Figure 3. The radiographic images of the control group revealed normal ankle joints and a higher bone volume than the CIA group (Fig.3A). The severity of RA was radiologically measured the shape and volume of bone. The CIA group exhibited bone erosion and osteophyte formation. Specifically, the joint surfaces had a rough and irregular articular appearance with a diffuse lesion pattern on the articular surface. The radiological scoring of soft tissue swelling ($P < 0.001$), bone erosion (osteolysis) ($P = 0.002$), and osteophyte formation ($P = 0.011$) showed significant differences between our groups (Fig.3B).

Collagen-induced arthritis rats showed symptoms of rheumatoid arthritis disease

The H&E staining of the hind paws of the control group showed a normal articular cartilage with the intact joint space,

and synovial tissue was without any architectural changes (Fig.4A).

The cartilage surface in the CIA group exhibited damages, while the inflammatory mononuclear cells were infiltrated around and inside the cartilage. Granular hard tissue contains an inflammatory tissue with increased fibroblasts and enlarged blood vessels, with signs of bone destruction (Fig.4A). MT staining photographs of hind ankle joints illustrated a normal synovial tissue with typical collagen fibers in the control group. However, the high rate of articular cartilage degradation and extensive fibrosis completely obliterating the joint cavity was observed on the articular surfaces of the joint in the CIA group. In addition, synovial hyperplasia and inflammatory cell infiltration were observed on the articular surface of the joints from the CIA group (Fig.4A). The ankle histopathological score showed significant increases in different parameters, including inflammation, pannus formation, cartilage damage, and bone resorption in the CIA group ($P < 0.0001$, Fig.4B).

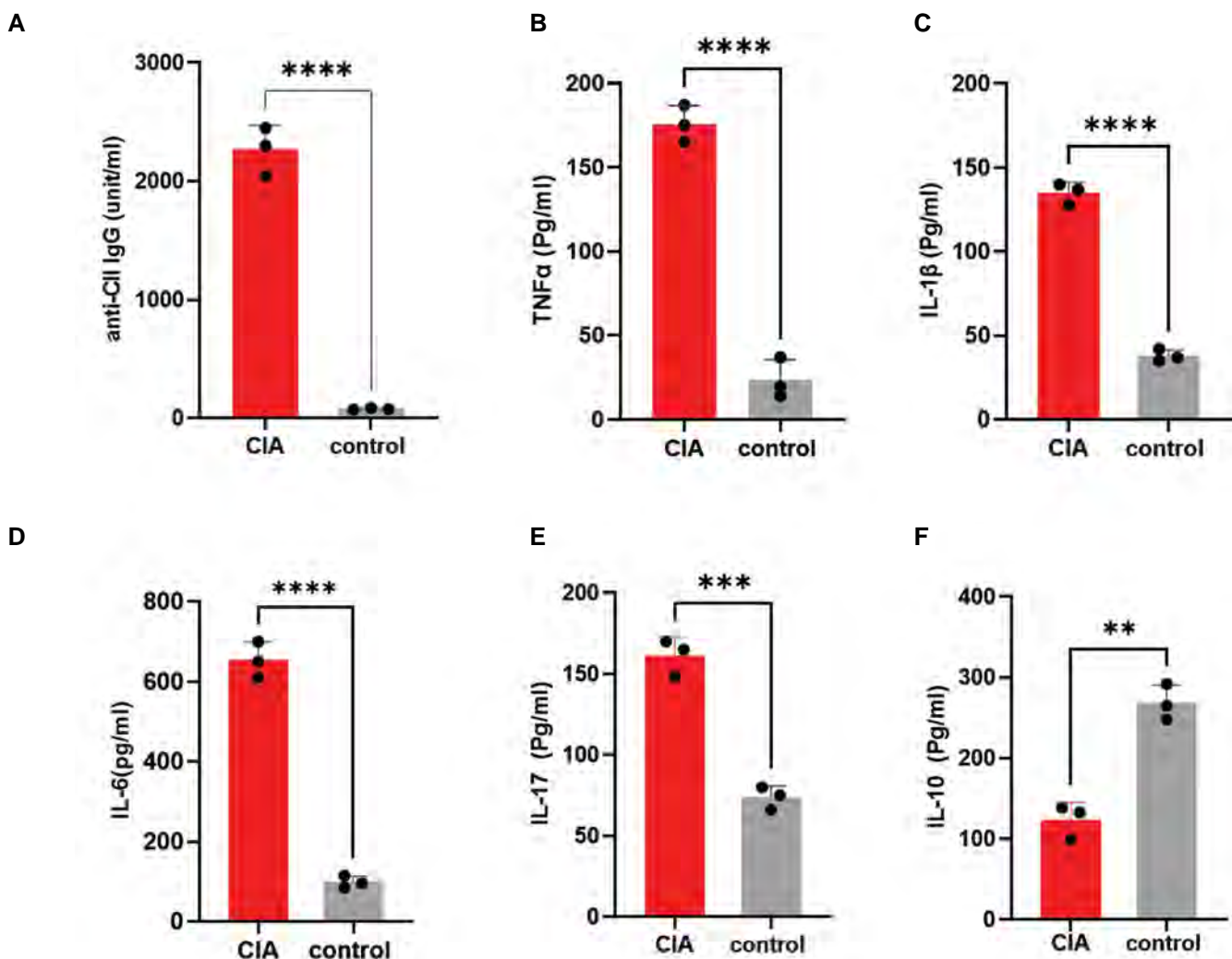


Fig.2: Inflammation produced after CII/IFA injection in rats. **A.** Following CIA induction, the serum levels of anti-CII IgG and **B-E.** Inflammatory cytokines TNF- α , IL-1 β , IL-17, and IL-6 were significantly elevated in the CIA group, and **F.** anti-inflammatory factor IL-10 was decreased in comparison with the control group. All data were presented as the mean \pm standard deviation (n=3). The comparisons were performed using the unpaired t test. *, $P < 0.05$, **, $P < 0.01$, ***, $P < 0.001$, CII/IFA; Collagen type II/Freund's incomplete adjuvant, CIA; Collagen-induced arthritis, TNF- α ; Tumor necrosis factor-alpha, and IL; Interleukin.

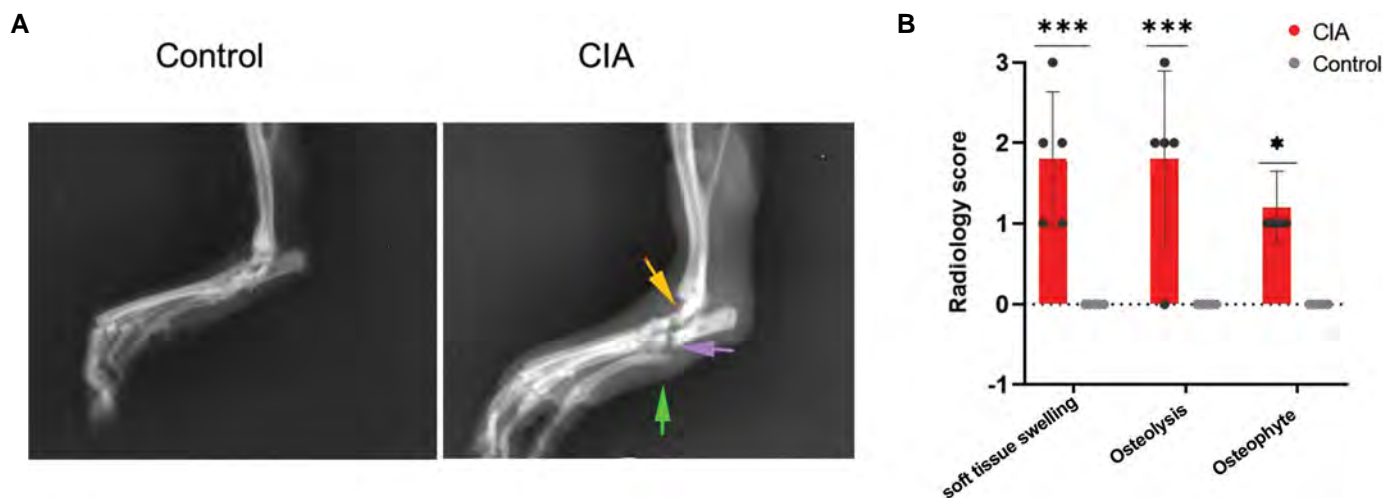


Fig.3: Radiological evaluation of the hind ankle joints. **A.** CIA group had severe soft tissue swelling (green arrow), osteolysis (purple arrow) and periosteal new bone formation (yellow arrow). **B.** Radiological scoring of soft tissue swelling, bone erosion, and osteophyte formation showed significantly increased values in the CIA group in comparison with the control group. All data were presented as the mean ± standard deviation (n=5). The comparisons were performed using two-way analysis of variance (ANOVA). *; P<0.05, ***; P<0.001, and CIA; Collagen-induced arthritis.

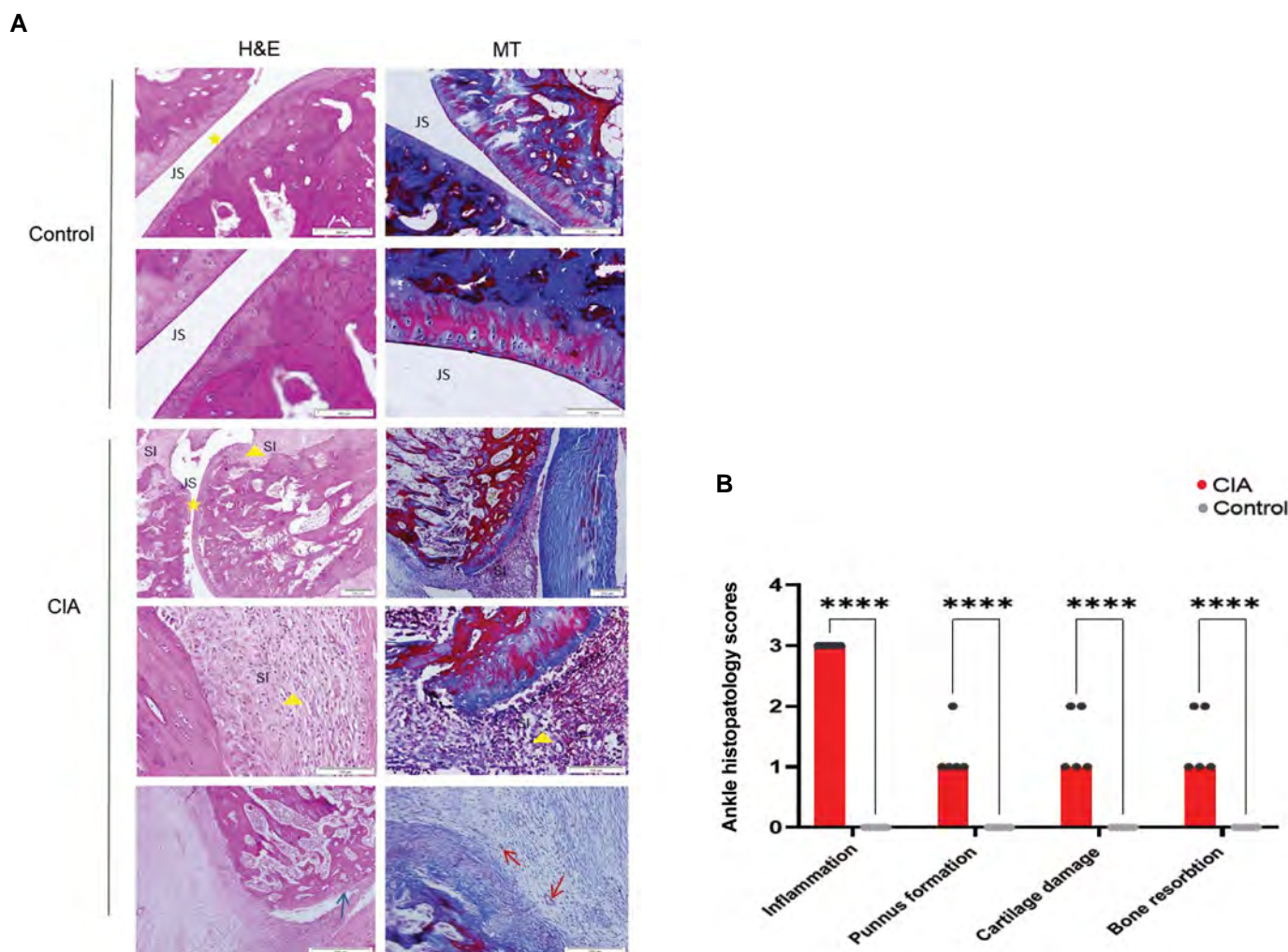


Fig.4: Histological evaluation of the hind ankle joints. **A.** Histological evaluation of the hind ankle joints. H&E and MT staining. The Control group showed an intact articular cartilage, preserved articular space, and typical synovial tissue collagen fibers without any inflammatory infiltration. The CIA group demonstrated synovial hypertrophy with marked mononuclear leukocyte infiltration (inflammation) (triangle), hypervascularity (red arrow) with pannus formation, destruction of the adjacent bone (blue arrow), degenerative changes in articular cartilage with diminished articular space (star). **B.** Histological scores of the rats' ankles in the CIA group showed a significant increase in the inflammation, pannus formation, cartilage damage, and bone resorption changes in comparison with the control group. All data were presented as the mean ± standard deviation (n=5). The comparisons were performed using two-way analysis of variance (ANOVA). ****; P<0.001, CIA; Collagen-induced arthritis, H&E; hematoxylin and eosin, MT; Masson's trichrome, SI; Synovial inflammation, and JS; Joint space.

Discussion

Developing RA animal models may shine the new therapeutic options road. There is a debate regarding the appropriate RA animal models for precise disease characteristics because different models reflect distinct clinical features. These variations could be the result of differences in species, strains, sexes or ages of animals, housing and care refinements, dissimilarity in protocols for arthritis induction, and variation in the materials used for induction such as collagen, lipopolysaccharide, and use of adjuvants such as *Mycobacterium* (16).

Suppose the animal model fails to simulate what is happening in the RA disease. In that case, inaccuracies will occur in finding the underlying biological mechanisms and predicting response to the clinical treatments. One of the most widely used experimental models of autoimmune arthritis CIA which shares several pathological aspects with RA, including synovial hyperplasia, mononuclear cell infiltration, cartilage degradation, and, similar to RA disease in humans, its susceptibility is linked to major histocompatibility complex (MHC) class II molecules (17, 18).

On the other hand, another critical issue is potential harm to animals, i.e., pain, suffering or distress, that should be considered against the possible benefits of each protocol.

Russell and Burch introduced and defined the three Rs (replacement, reduction and refinement) terms, which have become known as 'alternative methods' for minimizing the potential pain, distress and fear in animal research (19). Procedures and materials used to induce arthritis in animals can cause pain and suffering, which may be mild, moderate, or severe, depending on the modelling method, animal acceptance, and type of materials used for disease establishment (9). For this reason, researchers need to consider the conduct to minimize this problem in the animal. Although, there is still a challenging issue. Due to the genetic and physiological differences between humans and animals, and the animal findings need to be fully generalized to the human population (20). There are limitations, therefore preclinical studies are critical and helpful regarding efficacy and safety in the living organism (19). In these viewpoints, we induced the CIA model in female Lewis rats in the present study. In the CIA group, symptoms of arthritis appeared in one or both hind paws from 12th to 14th days and showed a significant difference in swelling of hind paws and arthritis scores from the 17th day in comparison with the control group. We used an inbred strain rat for the CIA establishment because using inbred strains can reduce variability and extremes in responses because they have a more uniform genetic background, which minimizes the effects of genetic variation on experimental outcomes (9). Establishing the CIA model in female rats is imperative because, like humans, females are more receptive to this model (21).

In this study, we used 300 µg bovine CII emulsified in the IFA, and the results showed a successful CIA induction.

The CII immunity depends on the response of tissue-specific T lymphocytes, followed by the stimulation of B cells and the production of large amounts of antibodies against CII. These antibodies specifically bind to conserve epitopes on the type II collagen (CII), including the C1 epitope. They inhibit the CII self-assembly into fibrils, a process that may play a role in the pathogenesis of CIA. In general, the formation of antibodies that target a CII is a pivotal event in the onset and advancement of the CIA within joint tissues. These antibodies also play a role in the development of RA in both human subjects and CIA models (22).

The IFA induces predominantly T helper 2 (Th2) cells through the formation of a depot at the injection site with the stimulation of B cells; this causes the slow release of an antigen. IFAs, organism contamination free, are less toxic, thus, result in a less painful.

In a review study by Noh et al. (23), different models of RA in rodents were compared. It was concluded that in adjuvant-induced arthritis (AIA) models in comparison with the CIA model, the use of CFA adjuvant causes more severe joint damages and extra-articular involvements, such as inflammation in blood vessels, brain and eyes, and bone loss in the axial skeleton, bone marrow hyperplasia and leukocytosis, and enlargement of spleen and lymph nodes. This systemic response is evoked by 'danger' signals available in the CFA. Hence, a CIA could be presumed as an auto-inflammatory rather than an autoimmune situation (24). Therefore, the IFA is preferable to the CFA in creating a CIA model.

Studies revealed that the RA susceptibility in humans and the establishment of a CIA in rodents linked with MHC class II molecules (12), MHC class II regulates B cell activation, proliferation, and differentiation during cognate B cell-T cell interaction (25). In our study, the presence of IgG-specific autoantibodies against CII in the CIA group was significantly increased, confirming B cells' role in the CIA pathogenesis.

According to previous studies, changes in the balance of the inflammatory cytokines towards disease development detected in the joint tissue and serum of RA patients (26, 27). Therefore, in this study, we assessed the expression of cytokines involved in inflammation markers, including IL-1β, IL-6, IL-17, TNF-α, and IL-10. We observed that the levels of proinflammatory cytokines in the CIA model group increased significantly in comparison with the control group. Proinflammatory cytokines play an essential role in the pathogenesis of RA in patients by causing inflammation, synovial hyperplasia, and destruction of cartilage and bone. During the development and progression of the RA, various cells and many cytokines stimulate the production of fibroblast-like synoviocytes (FLSs) and macrophages. Stimulated macrophages release inflammatory mediators, and FLSs secrete cytokines and enzymes, which all are involved in the cartilage and bone degradation (26, 28). The IL-1β and TNF-α increase the proliferation of

synovial membrane cells in the joint, causing it to thicken and decrease the volume of joint fluid. The TNF- α , as a critical regulator of the inflammatory cascade, is a central player in the pathogenesis of RA and is considered for anti-TNF- α biologic (29).

The IL-1 is a crucial mediator of immune responses and is strongly linked to inflammation and joint damages in the RA (30). Therapeutic effects of IL-1 blockade, either through anti-IL-1 antibody or IL-1 receptor antagonist, have been demonstrated in several models of arthritis, such as CIA (29, 31). Another main cytokine in the development of the RA is IL-6, which has an essential effect on the proliferation and differentiation of macrophages, B and T cells, osteoclasts, chondrocytes, and endothelial cells (32-35). Regarding IL-6, there is some evidence of dysregulated overproduction from various animal models of arthritis, including CIA (36). Several strategies have been used to target IL-6 cytokine/signaling in RA patients.

In the CIA model, similar to the pathogenesis of RA in patients, the protein levels of TNF α , IL1 β and IL6 were increased. At the same time, the anti-inflammatory cytokine IL10 was downregulated. The IL-10 is an effector cytokine in mice and humans and is critical in RA pathogenesis (37, 38).

Th17 cells intensify inflammation by the production of IL-17, and elevated serum IL-17 levels are directly related to the severity of RA symptoms in patients (39). The IL-17 can enhance the inflammation and cellular infiltration joint arthritis. Moreover, it mediates bone and cartilage damage, which causes pain and disability in RA patients (40). Thus, the findings in the female Lewis rat CIA model in our study closely resemble the disease characteristics of human RA.

Song et al. (10) induce a simple, specific, and efficient way to induce the CIA model in Wistar rats. They used IFA instead of CFA to emulsify CII, and injected the CII/IFA emulsion into the skin at the base of the tail on the 7th day after the initial immunization. They injected a booster dose of CII/IFA and concluded that this developed CIA model was similar in clinical, hematologic, histopathological, and radiological features to those of humans. In another study, Choudhary et al. (7) used IFA emulsion and autologous collagen to develop severe polyarthritis in Dark Agouti (DA) and Lewis rats. Symptoms of the onset of arthritis were identified two weeks after immunization as paw swelling. As the disease progressed, it eventually led to chronic arthritis, increased inflammatory cytokines, and bone and cartilage destruction (7). Both of these studies confirmed the results of our results.

In our study, in the CIA group, such as RA patients, the IL-10 level declined, which reflects the imbalance between proinflammatory and anti-inflammatory cytokines in the RA pathogenesis. This imbalance might be due to various reasons, such as a specific IL-10 inhibitor, excretion of IL-10, production disruption or increasing degradation.

Alterations in the body weight of animals, paw swelling, and arthritis scores are standard indices used to evaluate arthritis induction and the anti-arthritic effect of drugs in the CIA animal models (37). In the present study, CII/IFA injected rats exhibited weight loss, paw edema and increasing arthritis scores. The histological and radiological findings also confirmed the establishment of arthritis in the CIA model group. These data demonstrated that increased inflammatory cell infiltration in synovial space and extra-articular tissues in CIA animals could be directly related to cartilage and bone destruction.

Conclusion

This study emphasizes the use of IFA/CII emulsion to establish the CIA model in Lewis rats. This model showed a high disease incidence and low variability in clinical symptoms, closely resembling RA progression in humans. Owing to the remarkable consistency of this model when applied to Lewis rats, combined with the exceptionally high acceptance rate among female Lewis rats (approaching 100%), it boasts a notably reduced mortality rate, aligning it with stringent animal welfare principles. The use of this approach in Lewis rats was associated with lower mortality rates. Emphasizing the ethical priority of adhering to the principles of the three Rs (Replacement, Reduction, and Refinement), it is noteworthy that the chosen method for arthritis induction in animals, involving Freund's incomplete adjuvant without mycobacterial antigens, effectively curbs the risk of severe inflammatory reactions and prevents granuloma formation within the animals' vital organs a problem frequently associated with the use of complete adjuvant.

Additionally, it is prudent to recognize that the Dilute Brown non-Agouti (DBA) 1 mouse strain is not universally accessible in all regions. Consequently, the application of this model, which can be established at a more cost-effective rate, represents a significant advantage.

Acknowledgements

The authors sincerely appreciate the efforts of their collaborators at the Royan Advanced Therapy Medicinal Product Technology Development Center (ATMP-TDC) and the Department of Stem Cells and Developmental Biology at Royan Institute, Tehran, Iran. This work was supported by grants from the Royan Stem Cell Technology Company Fund to Seyedeh-Nafiseh Hassani. The authors declare that they have no competing interests.

Authors' Contributions

M.B., N.M.G.; Performed data collection and assembly, data analysis and interpretation, and wrote the manuscript. B.T.; Performed data collection and assembly. J.P.; Developed the study conception and design. M.B.E., E.H.-S., S-N.H.; Conducted the experiments, developed the study conception and design, performed data analysis

and interpretation, and administrative and manuscript proof. All authors read and approved the manuscript.

References

- Jones G, Nash P, Hall S. Advances in rheumatoid arthritis. *Med J Aust.* 2017; 206(5): 221-224.
- Smolen JS, Landewé RBM, Bijlsma JWJ, Burmester GR, Dougados M, Kerschbaumer A, et al. EULAR recommendations for the management of rheumatoid arthritis with synthetic and biological disease-modifying antirheumatic drugs: 2019 update. *Ann Rheum Dis.* 2020; 79(6): 685-699.
- Babaahmadi M, Tayebi B, Gholipour NM, Kamardi MT, Heidari S, Baharvand H, et al. Rheumatoid arthritis: the old issue, the new therapeutic approach. *Stem Cell Res Ther.* 2023; 14(1): 268.
- Bellucci E, Terenzi R, La Paglia GM, Gentileschi S, Tripoli A, Tani C, et al. One year in review 2016: pathogenesis of rheumatoid arthritis. *Clin Exp Rheumatol.* 2016; 34(5): 793-801.
- Angelotti F, Parma A, Cafaro G, Capecchi R, Alunno A, Puxeddu I. One year in review 2017: pathogenesis of rheumatoid arthritis. *Clin Exp Rheumatol.* 2017; 35(3): 368-378.
- Maneiro JR, Souto A, Gomez-Reino JJ. Risks of malignancies related to tofacitinib and biological drugs in rheumatoid arthritis: systematic review, meta-analysis, and network meta-analysis. *Semin Arthritis Rheum.* 2017; 47(2): 149-115.
- Choudhary N, Bhatt LK, Prabhavalkar KS. Experimental animal models for rheumatoid arthritis. *Immunopharmacol Immunotoxicol.* 2018; 40(3): 193-200.
- Yau AC, Holmdahl R. Rheumatoid arthritis: identifying and characterising polymorphisms using rat models. *Dis Model Mech.* 2016; 9(10): 1111-1123.
- Hawkins P, Armstrong R, Boden T, Garside P, Knight K, Lilley E, et al. Applying refinement to the use of mice and rats in rheumatoid arthritis research. *Inflammopharmacology.* 2015; 23(4): 131-150.
- Song HP, Li X, Yu R, Zeng G, Yuan ZY, Wang W, et al. Phenotypic characterization of type II collagen-induced arthritis in Wistar rats. *Exp Ther Med.* 2015; 10(4): 1483-1488.
- Luan J, Hu Z, Cheng J, Zhang R, Yang P, Guo H, et al. Applicability and implementation of the collagen-induced arthritis mouse model, including protocols (Review). *Exp Ther Med.* 2021; 22(3): 939.
- National Research Council (US) Committee for the update of the guide for the care and use of laboratory animals. *Guide for the care and use of laboratory animals.* 8th ed. Washington (DC): National Academies Press (US); 2011.
- Chen J, Li J, Chen J, Cheng W, Lin J, Ke L, et al. Treatment of collagen-induced arthritis rat model by using Notch signalling inhibitor. *J Orthop Translat.* 2021; 28: 100-107.
- Babaahmadi M, Tayebi B, Gholipour NM, Bendele P, Pheneger J, Kheimeh A, et al. Long-term passages of human clonal mesenchymal stromal cells can alleviate the disease in the rat model of collagen-induced arthritis resembling early passages of different heterogeneous cells. *J Tissue Eng Regen Med.* 2022; 16(12): 1261-1275.
- Chen W, Wang J, Xu Z, Huang F, Qian W, Ma J, et al. Apremilast ameliorates experimental arthritis via suppression of Th1 and Th17 cells and enhancement of CD4⁺Foxp3⁺ regulatory T cells differentiation. *Front Immunol.* 2018; 9: 1662.
- Zhao T, Xie Z, Xi Y, Liu L, Li Z, Qin D. How to model rheumatoid arthritis in animals: from rodents to non-human primates. *Front Immunol.* 2022; 13: 887460.
- Miyoshi M, Liu S. Collagen-induced arthritis Models. *Methods Mol Biol.* 2018; 1868: 3-7.
- Ye L, Mingyue H, Feng Z, Zongshun D, Ying X, Xiong C, et al. Systematic review of robust experimental models of rheumatoid arthritis for basic research. *Digital Chinese Medicine.* 2021; 4(4): 262-272.
- Tannenbaum J, Bennett BT. Russell and Burch's 3Rs then and now: the need for clarity in definition and purpose. *J Am Assoc Lab Anim Sci.* 2015; 54(2): 120-132.
- Cavagnaro J, Silva Lima B. Regulatory acceptance of animal models of disease to support clinical trials of medicines and advanced therapy medicinal products. *Eur J Pharmacol.* 2015; 759: 51-62.
- Kim JR, Kim HA. Molecular mechanisms of sex-related differences in arthritis and associated pain. *Int J Mol Sci.* 2020; 21(21): 7938.
- Sun G, Xing C, Zeng L, Huang Y, Sun X, Liu Y. Flemingia flavonoids relieve bone erosion and inflammatory mediators in CIA mice by downregulating NF- κ B and MAPK pathways. *Mediators Inflamm.* 2019; 2019: 5790291.
- Noh ASM, Chuan TD, Khir NAM, Zin AAM, Ghazali AK, Long I, et al. Effects of different doses of complete Freund's adjuvant on nociceptive behaviour and inflammatory parameters in polyarthritic rat model mimicking rheumatoid arthritis. *PLoS One.* 2021; 16(12): e0260423.
- Billiau A, Matthys P. Collagen-induced arthritis and related animal models: how much of their pathogenesis is auto-immune, how much is auto-inflammatory? *Cytokine Growth Factor Rev.* 2011; 22(5-6): 339-344.
- Katikaneni DS, Jin L. B cell MHC class II signaling: a story of life and death. *Hum Immunol.* 2019; 80(1): 37-43.
- Ding Q, Hu W, Wang R, Yang Q, Zhu M, Li M, et al. Signaling pathways in rheumatoid arthritis: implications for targeted therapy. *Signal Transduct Target Ther.* 2023; 8(1): 68.
- Mateen S, Moin S, Shahzad S, Khan AQ. Level of inflammatory cytokines in rheumatoid arthritis patients: Correlation with 25-hydroxy vitamin D and reactive oxygen species. *PLoS One.* 2017; 12(6): e0178879.
- Hamamura K, Lin CC, Yokota H. Salubrinal reduces expression and activity of MMP13 in chondrocytes. *Osteoarthritis Cartilage.* 2013; 21(5): 764-772.
- Sardar S, Andersson Å. Old and new therapeutics for rheumatoid arthritis: in vivo models and drug development. *Immunopharmacol Immunotoxicol.* 2016; 38(1): 2-13.
- Siebert S, Tsoukas A, Robertson J, McInnes I. Cytokines as therapeutic targets in rheumatoid arthritis and other inflammatory diseases. *Pharmacol Rev.* 2015; 67(2): 280-309.
- Shimizu K, Nakajima A, Sudo K, Liu Y, Mizoroki A, Ikarashi T, et al. IL-1 receptor type 2 suppresses collagen-induced arthritis by inhibiting IL-1 signal on macrophages. *J Immunol.* 2015; 194(7): 3156-3168.
- McInnes IB, Buckley CD, Isaacs JD. Cytokines in rheumatoid arthritis - shaping the immunological landscape. *Nat Rev Rheumatol.* 2016; 12(1): 63-68.
- Accortt NA, Bonafede MM, Collier DH, Iles J, Curtis JR. Risk of subsequent infection among patients receiving tumor necrosis factor inhibitors and other disease-modifying antirheumatic drugs. *Arthritis Rheumatol.* 2016; 68(1): 67-76.
- McInnes IB, Schett G. Pathogenetic insights from the treatment of rheumatoid arthritis. *Lancet.* 2017; 389(10086): 2328-2337.
- Uciechowski P, Dempke WCM. Interleukin-6: a masterplayer in the cytokine network. *Oncology.* 2020; 98(3): 131-137.
- Srivastava S, Rasool M. Underpinning IL-6 biology and emphasizing selective JAK blockade as the potential alternate therapeutic intervention for rheumatoid arthritis. *Life Sci.* 2022; 298: 120516.
- Zhang X, Dong Y, Dong H, Zhang W, Li F. Investigation of the effect of phloimoside F on complete Freund's adjuvant-induced arthritis. *Exp Ther Med.* 2017; 13(2): 710-716.
- Chen Z, Bozec A, Ramming A, Schett G. Anti-inflammatory and immune-regulatory cytokines in rheumatoid arthritis. *Nat Rev Rheumatol.* 2019; 15(1): 9-17.
- Ye L, Jiang B, Deng J, Du J, Xiong W, Guan Y, et al. IL-37 Alleviates rheumatoid arthritis by suppressing IL-17 and IL-17-triggering cytokine production and limiting Th17 cell proliferation. *J Immunol.* 2015; 194(11): 5110-5119.
- Robert M, Miossec P. IL-17 in rheumatoid arthritis and precision medicine: from synovitis expression to circulating bioactive levels. *Front Med (Lausanne).* 2019; 5: 364.

Association between Genetic Polymorphism of The lncRNA *MIAT* rs1894720 with Ischemic Stroke Risk and lncRNA *MIAT* Expression Levels in The Blood after An Ischemic Stroke: A Case-Control Study

Tahereh Asadabadi, M.Sc.¹, Mohammad Javad Mokhtari, Ph.D.^{1*} , Mahnaz Bayat, Ph.D.², Anahid Safari, M.D.³, Afshin Borhani-Haghighi, M.D.²

1. Department of Biology, Zarghan Branch, Islamic Azad University, Zarghan, Iran

2. Clinical Neurology Research Center, Shiraz University of Medical Sciences, Shiraz, Iran

3. Stem Cells Technology Research Center, Shiraz University of Medical Sciences, Shiraz, Iran

Abstract

Objective: Genetic aspects can play an essential role in the occurrence and development of ischemic stroke (IS). Rs1894720 polymorphism is one of the eight single nucleotide polymorphisms (SNPs) in the long non-coding RNA (lncRNA) myocardial infarction-associated transcript (*MIAT*) locus. The aim of study is the lncRNA *MIAT* rs1894720 polymorphism decreases IS risk by reducing lncRNA *MIAT* expression.

Materials and Methods: In this case-control study, we studied 232 Iranian patients and 232 controls. The blood samples were collected from patients admitted at different times after stroke symptoms. We enrolled 80, 78, and 74 patients who arrived at the hospital between 0-24, 24-48, and 48-72 hours after the first appearance of symptoms, respectively. DNA genotyping was done by the tetra-primer ARMS-PCR method. Circulating *MIAT* levels were evaluated by real-time polymerase chain reaction (PCR).

Results: The GT genotype of *MIAT* rs1894720 showed a significant association with the risk of IS (OR=3.53, 95% CI=2.13-5.84, P<0.001). *MIAT* expression was higher relative to the control within the first hours after IS. The *MIAT* levels in IS patients with rs1894720 (GT) were significantly lower relative to patients who had the GG and TT genotypes. Linear regression model indicated a significant correlation between *MIAT* expression with atherosclerotic risk factors and types of stroke in IS patients. Receiver operating characteristic (ROC) curve analysis showed that the level of lncRNA *MIAT* after IS could be diagnostic with an area under the curve (AUC) of 0.82. The sensitivity and specificity were 80.17 and 67.24%, respectively (P<0.001).

Conclusion: Our study demonstrated that the *MIAT* rs1894720 polymorphism (GT) might increase the risk of IS in the Iranian population. *MIAT* expression was up-regulated in our IS patients. Hence, it could be a diagnostic biomarker for IS.

Keywords: Biomarkers, Gene Expression, Long Non-Coding RNA

Citation: Asadabadi T, Mokhtari MJ, Bayat M, Safari A, Borhani-Haghighi A. Association between genetic polymorphism of the lncRNA *MIAT* rs1894720 with ischemic stroke risk and lncRNA *MIAT* expression levels in the blood after an ischemic stroke: a case-control study. Cell J. 2023; 25(12): 863-873. doi: 10.22074/CELLJ.2023.2003573.1315

This open-access article has been published under the terms of the Creative Commons Attribution Non-Commercial 3.0 (CC BY-NC 3.0).

Introduction

Ischemic stroke (IS) is the leading cause of permanent or enduring disability in adults worldwide. The patient outcome is influenced by demographics, clinical, and genetic variables (1). The heritability of IS has been estimated at 38%, and several studies demonstrated the critical roles of genetic aspects in the different processes of IS pathophysiology (2).

Thus, clarifying a patient's genetic biology in addition to their epigenetics can help the prediction and prognosis of IS. Approximately 2% of the transcribed RNA in the human genome plays a significant role in protein encoding. Long non-coding RNAs (lncRNAs) are a type of RNA that contain more than 200 nucleotides and do not

have any role in protein synthesis (3). lncRNAs can act as a primary target for treating various disorders. It is used as a new intervention tool for identifying biomarkers and novel treatments for IS (4).

Myocardial infarction-associated transcript (*MIAT*) is a new locus in 22q12.1 identified for myocardial infarction. In addition, *MIAT* with five exons encodes a spliced lncRNA (5). The physiological roles of this gene have been demonstrated in the differentiation of excitatory neurons in the embryonic brain (6). *MIAT* expression has a significant correlation with the risk and progression of different diseases. *MIAT* up-regulation has been demonstrated in patients with IS (7), myocardial infarction (8), and diabetic cardiomyopathy (9). In

Received: 31/May/2023, Revised: 22/October/2023, Accepted: 28/October/2023

*Corresponding Address: P.O.Box: 7341991539, Department of Biology, Zarghan Branch, Islamic Azad University, Zarghan, Iran
Email: mj.mokhtari@iau.ac.ir



Royan Institute
Cell Journal (Yakhteh)

contrast, previous findings showed that down-regulation of *MIAT* expression was associated with schizophrenia, cataracts (10), and diabetic nephropathy (11).

Genetic polymorphisms can affect lncRNA function and expression levels, and can lead to human disease. Single nucleotide polymorphisms (SNPs) are caused by point mutations that affect only one nucleotide within a genetic sequence that gives rise to different alleles (12).

Several SNPs in the *MIAT* locus have a significant association with myocardial infarction (13), and two SNPs in this locus [rs1894720 SNP with minor allele (T) and rs4274 SNP (genotype AA)] are correlated with schizophrenia (14). One SNP, rs1894720 with the GT and TT genotypes, has a significant association with cataracts (10). The rs1894720 polymorphism is one of the several tag SNPs located in the *MIAT* locus. Rao et al. (14) found that *MIAT* SNP rs1894720 increased the risk of paranoid schizophrenia in the minor T allele in a Chinese population. At the same time, its expression was reduced in patients with schizophrenia. Ghapanchi et al. (15) demonstrated that the rs1894720 polymorphism might be associated with an increased risk of salivary gland tumours in the Iranian population. To the best of our knowledge, no further investigation has been conducted into the relationship between *MIAT* polymorphisms and various diseases in the Iranian population. In 2019, Li et al. (10) reported that the *MIAT* rs1894720 polymorphism might be involved in down-regulating *MIAT* expression. They can enhance miR-26b and decrease BCL2L2 expression, leading to an increased incidence of age-related cataracts. The results of an experimental study showed a correlation with the SNP rs1894720 *MIAT* and down-regulation of *MIAT* expression, and an increased risk of age-related hearing loss in dominant, codominant, and recessive genetic models (16).

After IS, cerebral hypoxia acutely alters lncRNA expression profiles so that, in the first 24 hours after a stroke, approximately 3000 lncRNAs are differentially expressed, and alterations in lncRNA expression from 24 hours to 7 days after IS has been reported (17). Zhu et al. (7) reported up-regulation of *MIAT* in IS patients and its correlation with National Institutes of Health Stroke Scale (NIHSS) scores and modified Rankin Scale (mRS).

The receiver operating characteristic (ROC) curve is a probability curve used in binary classification to assess a model's ability to distinguish between positive and negative classes at different threshold levels. The area under the curve (AUC) represents the degree of separability between the classes. The potential marker of *MIAT* expression for IS diagnosis was indicated by ROC curves with 0.84 AUC. Also, *MIAT* expression led to apoptosis of neural cells in IS rats (18), and it has been shown to play a vital role in the development of microvascular dysfunction (9) and

up-regulation of proinflammatory cytokines in diabetes mellitus (19).

Based on the findings from these studies, we selected rs1894720 across the whole *MIAT* locus with the hypothesis that the suppressive effect of this SNP with GT or/and TT genotypes on *MIAT* expression could have a protective impact on IS. In recent years there has been a growing demand for identifying disease-associated SNPs and lncRNAs. This study aimed to explore the relationship between the rs1894720 SNP and lncRNA *MIAT* expression and risk of IS in Iranian patients. We also compared circulating *MIAT* levels in IS patients at different times (0-24, 24-48, and 48-72 hours) after stroke onset, different types of strokes, and various genotypes. The association between *MIAT* expression with clinical characteristics and genotype as well as its potential as a diagnostic marker for IS was also assessed.

Materials and Methods

Study subjects

This was a case-control study of 232 patients and 232 controls conducted from August 2018 to August 2019 at Namazi Hospital, Shiraz, Iran. Recent, initial diagnosis of IS with symptom onset within 24 hours comprised the inclusion criterion. Board certified neurologists obtained the patients' histories, and conducted examinations and assessments to confirm the IS diagnosis. Patient histories involved a thorough interview to gather information about past medical conditions, medications, and family history of neurological disorders. Examinations included a physical exam to assess neurological function, such as muscle strength, reflexes, coordination, and sensory perception. All patients underwent either a brain computed tomography (CT), magnetic resonance imaging (MRI), or both to distinguish the infarction area and exclude the possibility of cerebral haemorrhaging. IS was defined according to the World Health Organization criteria (20). Patients with head trauma, subarachnoid, or intracerebral haemorrhaging were excluded from this study. Patients with vasculitis, arterial dissection, fibromuscular dysplasia, transient ischemic attack, Moyamoya disease, sickle cell disease, different malignancies, or severe inflammation were also excluded.

The control group consisted of a representative sample of the Shiraz population, randomly selected from neighbours who resided closest to the cases and who matched the patients in terms of gender and age. All subjects in this study ranged from 32-90 years of age. Individuals with specific illnesses, brain disorders, or previous strokes were excluded from the control group.

We identified hypertension (Htn) and diabetes mellitus according to defined criteria (21). The stroke severity

was evaluated by NIHSS score at admission, such that increased severity had higher scores (22). The functional outcomes were assessed according to the mRS score at three and six months after admission (blinded to *MIAT* levels). The mRS is a single-item global outcome scale used to assess the functional independence of patients after stroke. Rather than evaluating the observed performance of a specific task, the mRS categorises the patient's level of autonomy based on their ability to perform activities they were able to do before the stroke. The mRS defines seven grades of disability, ranging from 0 to 6. Grade 0 indicates no symptoms, while grade 6 indicates death (23). In our study, we considered an mRS score of 3-6 as an unfavourable functional outcome and the mRS score of 0-2 as a favourable outcome six months after the stroke. IS patients were categorised according to TOAST classification: cardioembolism (CE), small-vessel disease (SVD), large artery atherosclerosis (LAA), other determined aetiology (OD), and undetermined aetiology (UD) (24).

The Islamic Azad University at Kazeroon, Iran Ethics Committee (IR.IAU.KAU.REC.1398.037) approved this study. All participants completed an informed consent (or their proxy respondents) prior to study enrolment. Blood samples were obtained from 232 study patients admitted at three different time points [0-24 (n=80), 24-48 (n=78), and 48-72 (n=74) hours] after onset of initial stroke symptoms.

Rs1894720 single nucleotide polymorphism genotyping and measurement of the *MIAT* lncRNA levels

We used the Favorgen Kit (Taiwan) for DNA extraction. Additionally, the Tetra-ARMS PCR method was employed because it is a fast, inexpensive, and accurate method to assess SNP (25). Primer Express software v.3.0 (Applied Biosystems, Foster City, CA, USA) and the Primer1 program (LAMP web server at: <http://primer1.soton.ac.uk/primer-1.html>) was applied to design and analyse the oligonucleotide primers. The annealing temperature was 65°C for 30 seconds. The following primers were used to detect the rs1894720 polymorphism in the lncRNA *MIAT*.

Forward outer (FO):
5'TTGGAGAACTAGAGGCCTGACAGTCG3'

Reverse outer (RO):
5'TAGGTTAATCACACCATGCAACACTGCC3'

Forward inner (FI):
5'CAATAAATAGGGAAGCAACATGCTTTTAGG3'

Reverse inner (RI):
5'AATCAACCCTAACACATGGACCCCGA3'

SNP was located at chromosome 22:26671261. The size of products included the outer primers (421 bp), G allele (189 bp), and T allele (288 bp). The outer primers are not allele specific and are used to amplify the region that comprises the SNP.

RNA was extracted from whole blood samples with an RNA extraction kit (Favorgen, Taiwan) according to the manufacturer's instructions. RNA samples that had A260/A230 and A260/A280 ratios greater than 1.7 were chosen for cDNA synthesis. The quantitative real-time PCR test was used to measure the level of lncRNA *MIAT*. A Quantstudio 3 Real-time PCR system (Applied Biosystems, Foster City, CA, USA) was used with the following primers:

MIAT-
F: 5'- TCCCATTCCCGGAAGCTAGA -3'
R: 5'- GAGGCATGAAATCACCCCA -3'

We used primers from previous studies for the TATA box-binding protein (*TBP*) (26). Cycle threshold (Ct) values were used to present variations in expression levels. The Ct difference between *TBP* and *MIAT* was shown by Δ Ct. Relative *MIAT* expression level was defined using $2^{-\Delta$ Ct} for each subject.

Statistical analysis

The chi-square test was used to assess Hardy-Weinberg equilibrium (HWE) in the control group. The independent two-sample t-test and a chi-square test were used to evaluate the differences between numeric variables and categorical data, respectively. The association between the risk of IS and *MIAT* polymorphisms was shown by the odds ratio (OR) and corresponding 95% confidence interval (CI). Logistic regression analyses were conducted to evaluate *MIAT* expression levels and clinical parameters between the cases and controls. Analysis of variance (ANOVA) was used to compare the *MIAT* expression levels between different time points after stroke and various types of IS. *MIAT* expression levels are shown as mean \pm SE. Relationships between *MIAT* levels and clinical parameters and genotypes were tested using subgroup analysis and linear regression. We used the Spearman correlation to assess for correlations between stroke severity and *MIAT* levels. Diagnostic and prognostic potential was assessed by ROC curve analysis with AUC serving as a measure of performance. Analysis was performed with SPSS software version 19.0 (IBM SPSS Inc., USA) and GraphPad Prism 5.0 (GraphPad Software, Inc., La Jolla, CA, USA). P<0.05 indicated statistical significance.

Results

Participants' demographic and clinical parameters

The case group included 232 IS patients comprised of 94 females (40.5%) and 138 males (59.5%) who were 32 to 90 years of age (65.90 \pm 14.44 years). Table 1 lists the demographic and clinical characteristics of all subjects. The laboratory results showed a significant difference between the cases and controls in terms of low-density lipoprotein (LDL) and high-density lipoprotein (HDL) levels.

Table 1: Demographic and clinical characteristics of the study participants

Characteristics	IS patients (n=232)	Controls (n=232)	P value
Male	138 (59.48)	138 (59.48)	0.99 ^a
Female	94 (40.51)	94 (40.51)	
Age (Y)	65.90 ± 14.44	65.90 ± 14.44	0.99 ^b
BMI (kg/m ²)	25.99 ± 4.37	26.24 ± 4.48	0.68 ^b
Htn			<0.001 ^a
Yes	134 (57.75)	62 (26.72)	
No	98 (42.24)	170 (73.27)	
Diabetes			0.002 ^a
Yes	72 (31.03)	32 (13.79)	
No	160 (68.96)	200 (86.20)	
Smoking			<0.001 ^a
Yes	70 (30.17)	16 (6.89)	
No	162 (69.82)	216 (93.10)	
Drinking			0.003 ^a
Yes	34 (14.65)	6 (2.58)	
No	198 (85.34)	224 (96.55)	
HLP			0.003 ^a
Yes	82 (35.35)	42 (18.10)	
No	150 (64.65)	190 (81.89)	
TG (mg/dL)	138.72 ± 61.29	135.68 ± 64.03	0.71 ^b
TC (mg/dL)	149.37 ± 67.28	153.71 ± 35.206	0.51 ^b
LDL (mg/dL)	99.61 ± 37.71	84.99 ± 30.41	0.001 ^b
HDL (mg/dL)	49.37 ± 28.8	43.60 ± 10.9	0.04 ^b
TOAST classification			
LAA	68 (29.31)		
SVD	52 (22.41)		
CE	54 (23.27)		
UD	58 (25.00)		
NIHSS (admission)			
≤6	128 (55.17)		
≥7	104 (44.83)		
mRS (3 months)			
0-2	68 (29.31)		
3-6	164 (70.68)		

Data are shown as mean ± standard deviation (SD) or n (%). Htn was defined as systolic blood pressure ≥140 mmHg and/ or diastolic blood pressure ≥90 mmHg or the use of antihypertensive agents. Diabetes mellitus was diagnosed based on the following criteria: two fasting glucose levels >126 mg/dl (7.0 mmol/L) and two hours post-load glucose >200 mg/dl (11.1 mmol/L) or treatment with hypoglycaemic drugs. a; Chi-square test, b; Independent two-sample t test, IS; Ischemic stroke, BMI; Body mass index, TG; Triglycerides, TC; Total cholesterol, LDL; Low-density lipoprotein, HDL; High-density lipoprotein, NIHSS; National Institutes of Health Stroke Scale, mRS; Modified Rankin Scale, LAA; Large artery atherosclerosis, SVD; Small-vessel disease, CE; Cardioembolism, UD; Undetermined, HLP; Hyperlipidaemia, and Htn; Hypertension.

MIAT rs1894720 polymorphism and the risk of ischemic stroke

PCR product size for lncRNA *MIAT* rs1894720 polymorphism was 189 bp for the G allele, 288 bp for the T allele, and 421 bp for the internal control on 2% agarose gel (Fig.1). Allele frequencies and genotypes of the *MIAT* rs1894720 polymorphism were evaluated in both cases and controls (Table 2). We did not find any significant differences in allele frequency of the *MIAT* gene between the case and control groups (P=0.69). In addition, the patients with IS were genotyped as GG (n=28), GT (n=188), and TT (n=16). The GT genotype was associated with a 3.53-fold increase in IS risk in a codominant model (OR=3.53, 95% CI=2.13-5.84, P<0.001). In the dominant model, the GT+TT genotypes were associated with a 2.60-fold higher risk of IS (OR=2.60, 95% CI=1.59-4.25, P<0.001). Also, in the over-dominant model, the GT genotypes were related to a 4.27-fold higher risk of IS (OR=4.27, 95% CI=2.82-6.48, P<0.001). The *MIAT* rs1894720 polymorphism was associated with a 0.24-fold decrease in IS risk in the recessive model (TT vs. GG+GT genotypes) (Table 2). No significant deviations from the HWE were observed in the rs1894720 polymorphism in the control group (P=0.05).

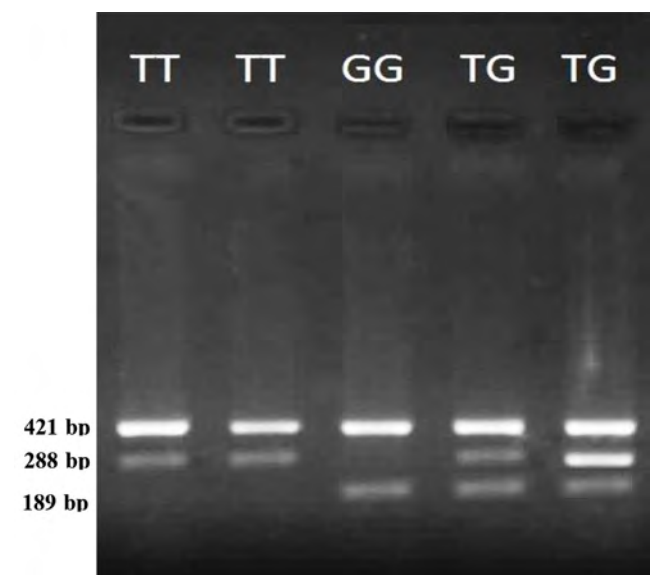


Fig.1: Tetra-primer ARMS-PCR for the detection of lncRNA *MIAT* rs1894720 polymorphism. The product sizes were 189 bp for the G allele, 288 bp for the T allele, and 421 bp for the internal control. lncRNA; Long non-coding RNA.

Alterations in the level of *MIAT* lncRNA in ischemic stroke patients relative to controls

Figure 2A shows a significantly high expression level of *MIAT* in all IS patients relative to controls

(3.08 ± 0.26 vs. 1.05 ± 0.09 , $P < 0.001$). Figure 2B shows significant up-regulation of *MIAT* expression in IS patients compared to the controls at 0–24 hours (2.98 ± 0.43 vs. 1.01 ± 0.16), 24–48 hours (3.61 ± 0.53 vs. 1.1 ± 0.19), and 48–72 hours (2.63 ± 0.38 vs. 1.04 ± 0.13) (all $P = 0.001$). *MIAT* up-regulation remained elevated until 72 hours after stroke onset. There was no significant difference between *MIAT* expression at the three time points [F (2, 113)=1.137, $P = 0.3246$]. Further analysis revealed that *MIAT* expression was significantly ($P < 0.05$) lower in IS patients who had the rs1894720 (GT) polymorphism relative to the GG, TT genotypes, 2.82 ± 0.25 vs. 4.18 ± 0.87 , respectively (Fig.2C). We found significant *MIAT* up-regulation in LAA ($P < 0.001$), SVD ($P < 0.01$), CE ($P < 0.01$), and UD ($P < 0.05$) IS relative to the controls, while there were no significant differences between *MIAT* levels in the four subgroups [F (3, 112)=1.932, $P = 0.12$] (Fig.2D). Logistic regression analysis demonstrated a positive association between *MIAT* expression and the risk of IS. The increase in *MIAT* score remained significant

even after adjusting for related variables of body mass index (BMI), Htn, diabetes, hyperlipidaemia (HLP), alcoholism, and smoking ($P < 0.001$; adjusted OR=1.599; 95% CI=1.21-1.99).

Association of *MIAT* expression with clinical parameters, genotype, and type of stroke

We used subgroup analyses to assess the correlation between *MIAT* expression with clinical parameters and genotype (Table 3). *MIAT* up-regulation was found in the Htn and diabetes subgroups ($P < 0.01$), as well as in the HLP and GT genotype subgroups ($P < 0.05$). However, no significant differences were found regarding sex, age, BMI, NIHSS, mRS, smoking, and alcoholism. In addition, linear regression analysis was employed to identify the association between lncRNA *MIAT* levels and clinical parameters, as well as stroke types, in the cohort of 232 patients (Table 4). There was a significant positive relationship between *MIAT* expression with diabetes ($P = 0.01$), Htn, ($P = 0.005$), drinking ($P = 0.04$), and LAA ($P = 0.01$) in IS patients.

Table 2: Distribution of genotypes, allele frequency of the rs1894720 *MIAT* gene polymorphism and OR with 95% CI in cases and healthy controls

Inheritance	rs1894720	Cases	Controls	OR (95% CI)	P value
Model	Polymorphism	(%)	(%)		
Codominant ^a	GG	28 (12.06)	61 (26.29)	1	
	GT	188 (81.03)	116 (50)	3.53 (2.13-5.84)	<0.001
	TT	16 (6.89)	55 (23.71)	0.63 (0.31-1.29)	0.20
Dominant ^b	GG	28 (12.06)	61 (26.29)	1	
	GT+TT	204 (87.93)	171 (73.71)	2.60 (1.59-4.25)	<0.001
Recessive ^c	GG+GT	216 (93.10)	177 (76.29)	1	
	TT	16 (6.89)	55 (23.71)	0.24 (0.13-0.43)	<0.001
Over-dominant ^d	GG+TT	44 (18.96)	116 (50)	1	
	GT	188 (81.03)	116 (50)	4.27 (2.82-6.48)	<0.001
	G	244 (52.58)	238 (51.29)	1	
	T	220 (47.41)	226 (48.70)	0.94 (0.73-1.22)	0.69

The relationship of each SNP with case/control status was determined by employing unconditional logistic regression analyses. The association between the risk of IS and *MIAT* polymorphisms is shown by OR and the corresponding 95% CI. IS; Ischemic stroke, OR; Odds ratio, CI; Confidence interval, SNP; Single nucleotide polymorphism, ^a; Codominant: Major allele homozygotes vs. heterozygotes, ^b; Dominant: Major allele homozygotes vs. heterozygotes+minor allele homozygotes, ^c; Recessive: Major allele homozygotes+heterozygotes vs. minor allele homozygotes, and ^d; Over-dominant: Major allele homozygotes+minor allele homozygotes vs. heterozygotes.

Spearman correlation of lncRNA *MIAT* with National Institutes of Health Stroke Scale in ischemic stroke

The level of *MIAT* expression in patients showed a positive, nonsignificant correlation with NIHSS scores ($r=0.03$, $P=0.61$). We found a difference in the correlation of *MIAT* expression between IS patients with rs1894720 (GT) and patients with other genotypes (GG, TT). We found a Pearson's correlation coefficient

close to zero in patients with the GT genotype, which indicated no correlation between the variables ($r=0.05$, $P=0.59$) and a positive nonsignificant linear weak correlation in patients with the GG, TT genotype ($r=0.38$, $P=0.07$). In patients with the GT genotype, decreased *MIAT* expression did not have any significant relationship between *MIAT* level and NIHSS score. Patients with the GG, TT genotype and a higher *MIAT* level had a weak positive correlation between *MIAT* level and NIHSS.

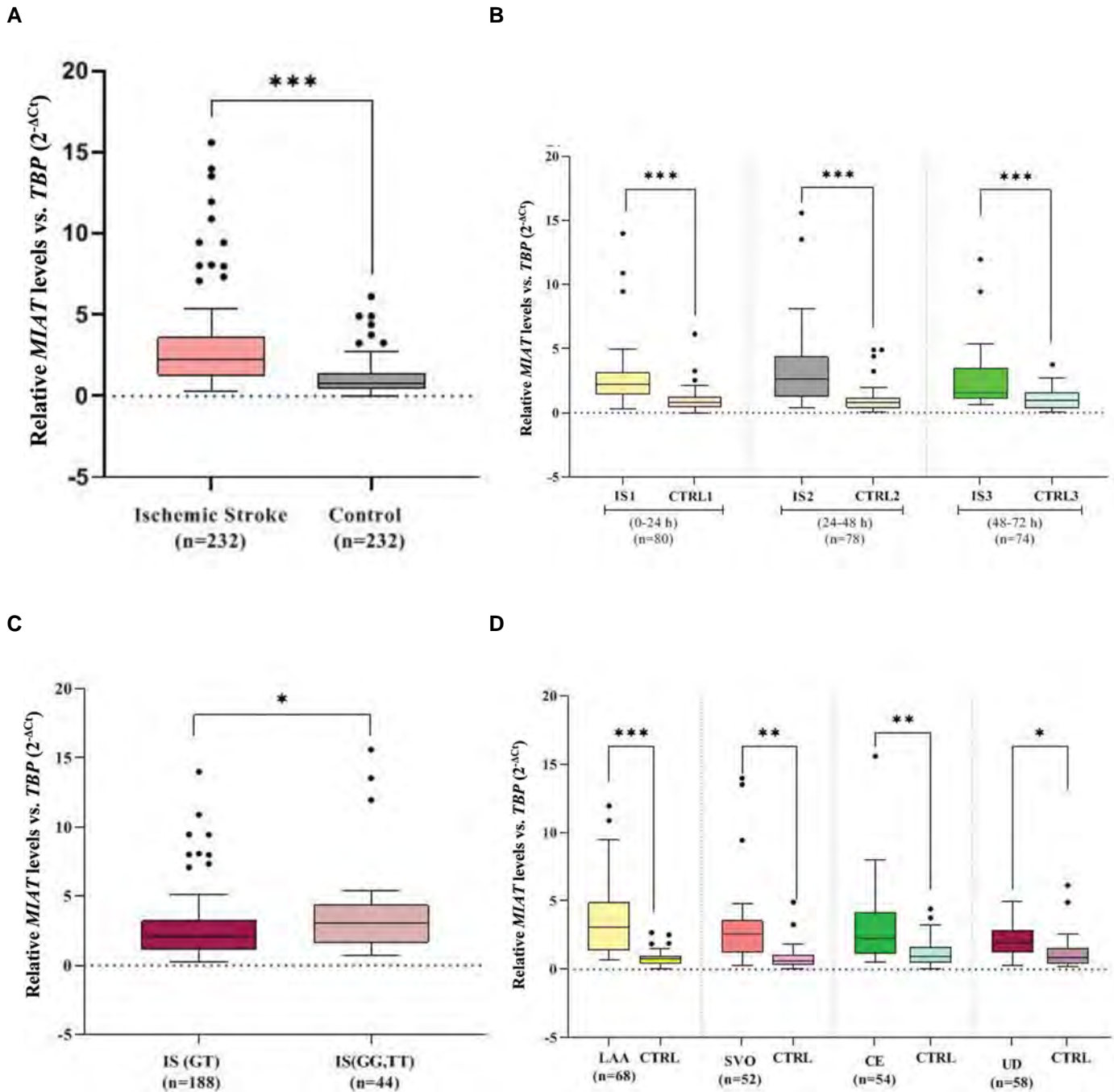


Fig.2: The expression levels of *MIAT* in different subgroups. **A.** Independent Student's t test revealed that in all IS patients, lncRNA *MIAT* levels were significantly higher than in the controls. **B.** At 0-24, 24-48, and 48-72 hours after stroke, the blood levels of lncRNA *MIAT* in IS patients was higher than the age-sex matched controls. There were no significant differences in *MIAT* levels between these three time points. **C.** Comparison of *MIAT* levels between two subgroups of patients with different genotypes GT relative to GG, TT. **D.** *MIAT* levels in the LAA, CE, SVD, and UD groups were significantly higher than in the matched controls. One-Way ANOVA analysis showed no differences among types of strokes. Results are expressed as mean \pm SEM. *, $P < 0.05$, **, $P < 0.01$, ***, $P < 0.001$; IS; Ischemic stroke, lncRNA; Long non-coding RNA, LAA; Large artery atherosclerosis, SVD; Small-vessel disease, CE; Cardioembolism, ANOVA; Analysis of variance, CTRL; Control, UD; Undetermined, SVO; Small vessel occlusion, and h; Hour.

Table 3: Association between clinical parameters and genotype with lncRNA *MIAT* levels in IS patients

Characteristics	Number	Mean \pm SD	t	P value
Sex			0.161	0.82
Male	138	3.12 \pm 2.83		
Female	94	3.03 \pm 2.93		
Age (Y)			0.350	0.93
<70	130	2.86 \pm 2.43		
\geq 70	102	3.36 \pm 3.35		
BMI (kg/m ²)			0.680	0.49
<24	82	3.23 \pm 3.06		
\geq 24	150	2.95 \pm 2.75		
NIHSS			1.513	0.13
\leq 6	128	2.72 \pm 2.16		
\geq 7	104	3.52 \pm 3.51		
mRS (admission)			1.406	0.16
0-2	66	2.94 \pm 1.68		
3-6	166	3.31 \pm 3.19		
mRS (6 months)			0.492	0.62
0-2	148	3.18 \pm 2.98		
3-6	84	2.91 \pm 2.66		
mRS (3 months)			0.550	0.58
0-2	122	2.97 \pm 2.91		
3-6	110	3.27 \pm 2.84		
Smoking			0.233	0.81
Negative	162	3.125 \pm 3.11		
Positive	70	2.98 \pm 2.22		
Alcoholism			1.85	0.06
Negative	198	2.88 \pm 2.53		
Positive	34	4.25 \pm 4.21		
Hypertension			2.47	0.008**
Negative	98	2.33 \pm 1.69		
Positive	134	3.63 \pm 3.38		
HLP			1.88	0.03*
Negative	150	2.41 \pm 1.83		
Positive	82	3.45 \pm 3.24		
Diabetes			2.74	0.007**
Negative	160	2.02 \pm 1.44		
Positive	72	3.56 \pm 3.20		
Genotype			2.029	0.04*
GT	188	2.82 \pm 2.45		
GG, TT	44	4.18 \pm 4.09		

The data were analysed using the Student's t test. P<0.05 indicates statistical significance. IS; Ischemic stroke, lncRNA; Long non-coding RNA, BMI; Body mass index, mRS; Modified Rankin Scale, NIHSS, National Institutes of Health Stroke Scale, and HLP; Hyperlipidaemia.

Table 4: Linear regression analysis for the association between clinical parameters, type of stroke, and genotypes with lncRNA *MIAT* levels in IS patients

Variables	Beta	95% CI	P value
Genotypes	-0.106	-2.081 0.536	0.24
Age (Y)	-0.040	-0.046 0.030	0.68
Sex	0.093	-0.570 1.655	0.33
HLP	0.139	-0.259 1.916	0.13
DM	0.228	0.264 2.544	0.01
Htn	0.254	0.453 2.481	0.005
Smoking	-0.088	-1.726 0.639	0.36
Drinking	0.194	0.060 3.067	0.04
NIHSS	-0.009	-0.086 0.078	0.92
LAA	0.277	0.394 3.083	0.01
SVD	0.176	-0.292 2.704	0.11
CE	0.135	-0.607 2.426	0.23

Linear regression analysis was done. Bold values denote statistical significance at the $P < 0.05$ level. lncRNA; Long non-coding RNA, IS; Ischemic stroke, NIHSS; National Institutes of Health Stroke Scale, Htn; Hypertension, HLP; Hyperlipidaemia, LAA; Large artery atherosclerosis, SVD; Small-vessel disease, CE; Cardioembolism, UD; Undetermined, and DM; Diabetes mellitus.

Diagnostic potential ,prediction of functional outcome, and mortality of *MIAT* expression level in ischemic stroke

The potential diagnostic marker of lncRNA *MIAT* was assessed by ROC curve analysis. The results indicated that *MIAT* is a potential marker with an AUC of 0.82 ± 0.026 (95% CI=0.776-0.881, Fig.S1A, See Supplementary Online Information at www.celljournal.org), with a sensitivity and specificity of 80.17 and 67.24%, respectively ($P < 0.001$). *MIAT* levels showed high diagnostic potential for IS. In our study, patients with an mRS score of 3-6 within six months after stroke were considered to have an unfavourable functional outcome. We did not find a significant predictive prognosis of *MIAT* levels when we analysed the ROC curve for negative outcomes relative to a favourable outcome with an AUC of 0.60 ± 0.05 (95% CI=0.447-0.657, Fig.S1B, See Supplementary Online Information at www.celljournal.org). The sensitivity and specificity were 70.37 and 45.16%, respectively.

At the six month follow-up, 56 cases (24.13%) were deceased. Survivors had lower *MIAT* expression levels than the deceased patients; however, this difference was insignificant. Among other factors, age, BMI, NIHSS score, and mRS score significantly differed between the surviving and deceased patients. *MIAT* expression did not show any significant potential for prediction of six month mortality. The AUC was 0.60 ± 0.06 (95% CI=0.459-0.717, Fig.S1C, See Supplementary Online Information at www.celljournal.org), with a sensitivity and specificity of 90.00 and 35.42%, respectively.

Discussion

This study represents an association of *MIAT* rs1894720 (GT) with a higher risk of IS in Iranian subjects (OR=3.53, 95% CI=2.13-5.84, $P < 0.001$). We observed elevated *MIAT* levels in all of the patients compared to the controls. In contrast, patients with the GT genotype exhibited significantly lower *MIAT* expression levels compared to those with the GG and TT genotypes. The rs1894720 polymorphism is one SNP in the *MIAT* locus, and previous studies have shown an association with *MIAT* down-regulation in the GT and TT genotypes (14, 16). The rs1894720 SNP (GT, TT) in chronic disorders such as schizophrenia and cataracts may be related to a reduction in *MIAT* expression compared to healthy subjects (10, 14). The lower *MIAT* expression in GT patients relative to the GG, TT may be related to the *MIAT* rs1894720 SNP (GT). IS CT an acute neurological disorder, and different factors after cerebral hypoxia acutely and severely alter the expressions of several thousand lncRNAs (17). Cerebral ischemia is an important factor that acutely increases the circulating level of *MIAT* in IS patients (7), while the possible suppressive effect of *MIAT* rs1894720 SNP on *MIAT* expression could reduce *MIAT* levels in IS patients with the GT genotype relative to GG, TT. The suppressive effect of *MIAT* on the expressions of microRNAs-26b and -29b was previously reported (10, 16). *MIAT* expression could be down-regulated due to the GT genotype, and, therefore cause an increase in the expressions of genes that induce neuronal cell death, such as caspase-3, by enhancing miRNA-26b (10). In order to confirm this result, further research needs to be conducted on a larger sample size by analysing plasma microRNAs.

The positive association between *MIAT* expression and cardiovascular diseases [9], as well as atherosclerosis (27), confirms our result about the correlation of lncRNA *MIAT* with LAA stroke. Yan et al. reported the involvement of lncRNA *MIAT* in the pathogenesis of microvascular diseases and angiogenesis (9). lncRNA *MIAT* is highly expressed in atherosclerotic plaque (28). *MIAT*/miR-149-5p/CD47 is a vital macrophage pathway in the growth of necrotic atherosclerotic plaques (29). Therefore, it is possible that the high expression of *MIAT* in atherosclerotic plaques may be down-regulated in subjects with *MIAT* rs1894720 (GT) and this leads to a decrease in the growth of atherosclerotic plaques and the risk of IS. Further investigation in patients with atherosclerosis is needed to confirm this result.

In this study, we demonstrated up-regulated *MIAT* expression after a stroke. Zhu et al. (7), for the first time, showed significant up-regulation in *MIAT* expression levels at 0–24 and 24–48 hours after stroke symptoms. In this study, we evaluated the *MIAT* expression level until 72 hours. The changes in expression levels of different lncRNAs were observed to seven days after a stroke

(17). Yan et al. (9) showed that up-regulation of *MIAT* was associated with retinal neovascularization, vascular leakage, inflammation, and endothelial dysfunction through the miR-150-5p/VEGF network. Endothelial cell injury is the first step in cardiovascular disease (30). Moreover, Vausort et al. (31) reported a correlation in peripheral *MIAT* expression levels with a marker of myocardial infarction. Another study showed that lncRNA *MIAT*, as a profibrotic factor, regulates cardiac fibrosis and cardiac function in myocardial infarction (8). *MIAT* is localized to specific neurons in the nervous system, including the large cortical neurons and the CA1 region of the hippocampus (32). Neurovascular dysfunction and inflammation can be related to IS pathogenesis (33). Additionally, *MIAT* expression was associated with high-sensitivity C-reactive protein (CRP, $r=0.309$, $P<0.001$) as an inflammatory marker in IS patients (7), and neurovascular remodelling in the brain was related to *MIAT* expression (34). These studies indicated that *MIAT* could encourage IS progression.

The up-regulated *MIAT* in our patients showed a non-significant positive correlation with stroke severity, whereas Zhu et al. (7) reported a significant association between lncRNA *MIAT* levels and NIHSS scores. In our research, subgroup analysis and linear regression did not show a significant correlation between *MIAT* and NIHSS score, whereas we found a Pearson's correlation coefficient close to zero in patients with the GT genotype, which indicated the lack of an association between the variables and a positive non-significant linear correlation in GG, TT patients. *MIAT* expression was lower in our GT patients relative to GG and TT. Thus, according to the possible suppressive effect of this SNP on *MIAT* expression, it is possible that in Iranian patients, we could not see a significant positive correlation between *MIAT* expression and NIHSS score. On the other hand, in the Zhu et al. (7) study, 177 patients were within the first 24 hours and only 12 cases were in the 24-48 hours post-stroke onset. Therefore, the positive association between *MIAT* expression and stroke severity in their study mainly belonged to the expression level of *MIAT* at 0-24 hours, and this time may be an optimal time window for expression of *MIAT*. In our study, there were 78 patients within 24 hours of acute IS; more sample sizes are required and that can show a positive association. It seems that this sample size could show a significant elevation in *MIAT* expression relative to the control. In different types of IS stroke, *MIAT* was equally expressed at a high level, and this also supports the results by Zhu et al. (7). In our study, we detected a significant association between *MIAT* expression with types of strokes (LAA) and atherosclerotic risk factors.

In our study, *MIAT* expression may be a potential biomarker for IS diagnosis (AUC=0.82). *MIAT* is highly expressed in neural cells and the peripheral blood of patients, and it could be considered a biomarker for IS (35) and myocardial infarction (36).

The results of recent studies have demonstrated an involvement of lncRNAs in the pathogenesis and progression of human diseases, as well as their critical regulatory functions. Additionally, genetic variations in lncRNAs have been associated with the risk of various diseases. lncRNAs are potential biomarkers for stroke diagnosis because they are relatively stable biomolecules that can withstand various conditions such as pH, extreme temperatures, and enzymatic breakdown. This stability makes them promising as diagnostic markers that can be detected in multiple body fluids, including blood, cerebrospinal fluid, and urine (37). lncRNAs are expressed differently in stroke patients compared to healthy controls and those with other neurological disorders. This differential expression can be used to identify specific lncRNAs that are associated with stroke and can serve as diagnostic markers (38). lncRNAs can be detected in various body fluids without requiring invasive procedures, such as tissue biopsies, which can be uncomfortable and risky for patients (39). Furthermore, many researchers have found that lncRNAs can be good candidates for molecular biomarkers due to high specificity and sensitivity (40).

This study showed that *MIAT* rs1894720 polymorphism correlated with a higher risk of IS. The present results supported our hypothesis and it estimated, for the first time, an association between SNPs in *MIAT* and IS risk. Additional studies in larger populations are needed to confirm these results.

Genetic association research is becoming increasingly important to identify the genetic underpinnings of complex disorders. Advances in genomics have made it possible to stratify patients according to molecular features thought to play important roles in pathogenesis. Therefore, the diagnosis and treatment of a disease may depend on an individual's gene expression pattern. Personalized medicine is particularly important in the field of IS for improving diagnostic and treatment strategies.

This study has certain limitations. More accurate results can be detected with larger sample sizes. In addition, there are other polymorphisms in lncRNA *MIAT* that need to be investigated. We assessed *MIAT* expression without performing a full transcriptome analysis. lncRNA *MIAT* expression levels were detected in whole blood samples, but not in serum, PBMCs or plasma. Therefore, the origin of lncRNA is still unknown. In addition, we did not evaluate the association of inflammatory biomarkers such as CRP, IL-6, and TNF- α with lncRNA *MIAT*.

Conclusion

The use of blood-based biomarkers is a valuable way to evaluate the risk and prognosis of IS. Our study demonstrated that rs1894720 polymorphism (GT) may increase the risk of IS. At different time points, higher levels of *MIAT* expression were found in IS patients compared with controls. Therefore, this study indicates

that the presence of lncRNA *MIAT* in whole blood could be a diagnostic biomarker for IS. Further investigation of the association between this polymorphism and IS in the larger Iranian population is required to validate these findings.

Acknowledgments

The present study was derived from a thesis by Tahereh Asadabadi. There is no financial support and conflict of interest in this study.

Authors' Contributions

T.A.; Performed all of the experiments, data and statistical analysis, and interpreted the data. M.J.M., A.B.-H.; Contributed to the study conception and design, supervised the research and assisted with the study plan. M.B., A.S.; Advised the research and assisted with the research progression. All authors read and approved the final manuscript.

References

- Torres-Aguila NP, Carrera C, Muiño E, Cullell N, Cárcel-Márquez J, Gallego-Fabrega C, et al. Clinical variables and genetic risk factors associated with the acute outcome of ischemic stroke: a systematic review. *J Stroke*. 2019; 21(3): 276-289.
- Nikolic D, Jankovic M, Petrovic B, Novakovic I. Genetic aspects of inflammation and immune response in stroke. *Int J Mol Sci*. 2020; 21(19): 7409.
- Statello L, Guo CJ, Chen LL, Huarte M. Gene regulation by long non-coding RNAs and its biological functions. *Nat Rev Mol Cell Biol*. 2021; 22(2): 96-118.
- Bao MH, Szeto V, Yang BB, Zhu SZ, Sun HS, Feng ZP. Long non-coding RNAs in ischemic stroke. *Cell Death Dis*. 2018; 9(3): 281.
- Shen S, Jiang H, Bei Y, Xiao J, Li X. Long non-coding RNAs in cardiac remodeling. *Cell Physiol Biochem*. 2017; 41(5): 1830-1837.
- Sun C, Huang L, Li Z, Leng K, Xu Y, Jiang X, et al. Long non-coding RNA *MIAT* in development and disease: a new player in an old game. *J Biomed Sci*. 2018; 25(1): 23.
- Zhu M, Li N, Luo P, Jing W, Wen X, Liang C, et al. Peripheral blood leukocyte expression of lncRNA *MIAT* and its diagnostic and prognostic value in ischemic stroke. *J Stroke Cerebrovasc Dis*. 2018; 27(2): 326-337.
- Qu X, Du Y, Shu Y, Gao M, Sun F, Luo S, et al. *MIAT* is a pro-fibrotic long non-coding RNA governing cardiac fibrosis in post-infarct myocardium. *Sci Rep*. 2017; 7: 42657.
- Yan B, Yao J, Liu JY, Li XM, Wang XQ, Li YJ, et al. lncRNA-*MIAT* regulates microvascular dysfunction by functioning as a competing endogenous RNA. *Circ Res*. 2015; 116(7): 1143-1156.
- Li Y, Zhang W, Ke H, Wang Y, Duan C, Zhu Q, et al. Rs1894720 polymorphism is associated with the risk of age-related cataract by regulating the proliferation of epithelial cells in the lens via the signalling pathway of *MIAT*/miR-26b/*BCL2L2*. *Arch Med Sci*. 2020; 18(1): 223-236.
- Ji TT, Qi YH, Li XY, Tang B, Wang YK, Zheng PX, et al. Loss of lncRNA *MIAT* ameliorates proliferation and fibrosis of diabetic nephropathy through reducing *E2F3* expression. *J Cell Mol Med*. 2020; 24(22): 13314-13323.
- Gong J, Liu W, Zhang J, Miao X, Guo AY. lncRNAsNP: a database of SNPs in lncRNAs and their potential functions in human and mouse. *Nucleic Acids Res*. 2015; 43(Database issue): D181-D186.
- Ma R, He X, Zhu X, Pang S, Yan B. Promoter polymorphisms in the lncRNA-*MIAT* gene associated with acute myocardial infarction in Chinese Han population: a case-control study. *Biosci Rep*. 2020; 40(2): BSR20191203.
- Rao SQ, Hu HL, Ye N, Shen Y, Xu Q. Genetic variants in long non-coding RNA *MIAT* contribute to risk of paranoid schizophrenia in a Chinese Han population. *Schizophr Res*. 2015; 166(1-3): 125-130.
- Ghapanchi J, Mokhtari MJ, Zahed M, Ardekani ST, Fattahi MJ, Khademi B, et al. Genetic analysis of lncRNA *H19* (rs217727) and *MIAT* (rs1894720) polymorphisms in patients with salivary gland tumors. *Gene Reports*. 2023; 30: 101724.
- Hao S, Wang L, Zhao K, Zhu X, Ye F. Rs1894720 polymorphism in *MIAT* increased susceptibility to age-related hearing loss by modulating the activation of miR-29b/SIRT1/PGC-1 α signaling. *J Cell Biochem*. 2019; 120(4): 4975-4986.
- Zhu W, Tian L, Yue X, Liu J, Fu Y, Yan Y. lncRNA expression profiling of ischemic stroke during the transition from the acute to subacute stage. *Front Neurol*. 2019; 10: 36.
- Guo X, Wang Y, Zheng D, Cheng X, Sun Y. lncRNA-*MIAT* promotes neural cell autophagy and apoptosis in ischemic stroke by up-regulating *REDD1*. *Brain Res*. 2021; 1763: 147436.
- Qi Y, Wu H, Mai C, Lin H, Shen J, Zhang X, et al. lncRNA-*MIAT*-mediated miR-214-3p silencing is responsible for IL-17 production and cardiac fibrosis in diabetic cardiomyopathy. *Front Cell Dev Biol*. 2020; 8: 243.
- Sedova P, Brown RD, Zvolosky M, Belaskova S, Volna M, Baluchova J, et al. Incidence of stroke and ischemic stroke subtypes: a community-based study in brno, czech republic. *Cerebrovasc Dis*. 2021; 50(1): 54-61.
- Lin CH, Wei JN, Fan KC, Fang CT, Wu WC, Yang CY, et al. Different cutoffs of hypertension, risk of incident diabetes and progression of insulin resistance: a prospective cohort study. *J Formos Med Assoc*. 2022; 121(1 Pt 1): 193-201.
- Zhuo Y, Qu Y, Wu J, Huang X, Yuan W, Lee J, et al. Estimation of stroke severity with National Institutes of Health Stroke Scale grading and retinal features: a cross-sectional study. *Medicine (Baltimore)*. 2021; 100(31): e26846.
- Liu X, Zhou M, Zhao J, Gao Y, Wang Y, Zhou J, et al. Functional independence and disability evaluation in stroke patients: optimal cutoff scores for a pictorial-based longshi scale, barthel index, and modified rankin scale. *Front Neurol*. 2022; 13: 710852.
- Harris S, Sungkar S, Rasyid A, Kurniawan M, Mesiano T, Hidayat R. TOAST subtypes of ischemic stroke and its risk factors: a hospital-based study at Cipto Mangunkusumo Hospital, Indonesia. *Stroke Res Treat*. 2018; 2018: 9589831.
- Zhang S, Dang Y, Zhang Q, Qin Q, Lei C, Chen H, et al. Tetraprimer amplification refractory mutation system PCR (T-ARMS-PCR) rapidly identified a critical missense mutation (P236T) of bovine *ACADVL* gene affecting growth traits. *Gene*. 2015; 559(2): 184-188.
- Rezaei M, Mokhtari MJ, Bayat M, Safari A, Dianatpuor M, Tabrizi R, et al. Long non-coding RNA *H19* expression and functional polymorphism rs217727 are linked to increased ischemic stroke risk. *BMC Neurol*. 2021; 21(1): 54.
- Sun G, Li Y, Ji Z. Up-regulation of *MIAT* aggravates the atherosclerotic damage in atherosclerosis mice through the activation of PI3K/Akt signaling pathway. *Drug Deliv*. 2019; 26(1): 641-649.
- Arslan S, Berkan Ö, Lalem T, Özbilüm N, Göksel S, Korkmaz Ö, et al. Long non-coding RNAs in the atherosclerotic plaque. *Atherosclerosis*. 2017; 266: 176-181.
- Ye ZM, Yang S, Xia YP, Hu RT, Chen S, Li BW, et al. lncRNA *MIAT* sponges miR-149-5p to inhibit efferocytosis in advanced atherosclerosis through CD47 upregulation. *Cell Death Dis*. 2019; 10(2): 138.
- Duan H, Zhang Q, Liu J, Li R, Wang D, Peng W, Wu C. Suppression of apoptosis in vascular endothelial cell, the promising way for natural medicines to treat atherosclerosis. *Pharmacol Res*. 2021; 168: 105599.
- Vausort M, Wagner DR, Devaux Y. Long noncoding RNAs in patients with acute myocardial infarction. *Circ Res*. 2014; 115(7): 668-677.
- Keihani S, Kluever V, Fornasiero EF. Brain long noncoding RNAs: multitask regulators of neuronal differentiation and function. *Molecules*. 2021; 26(13): 3951.
- Karlsson WK, Sørensen CG, Kruuse C. L-arginine and L-NMMA for assessing cerebral endothelial dysfunction in ischaemic cer-

- ebrovascular disease: a systematic review. *Clin Exp Pharmacol Physiol*. 2017; 44(1): 13-20.
34. Jiang Q, Shan K, Qun-Wang X, Zhou RM, Yang H, Liu C, et al. Long non-coding RNA-MIAT promotes neurovascular remodeling in the eye and brain. *Oncotarget*. 2016; 7(31): 49688-49698.
 35. Dykstra-Aiello C, Jickling GC, Ander BP, Shroff N, Zhan X, Liu D, et al. Altered expression of long noncoding rnas in blood after ischemic stroke and proximity to putative stroke risk loci. *Stroke*. 2016; 47(12): 2896-2903.
 36. Azat M, Huojiahemaiti X, Gao R, Peng P. Long noncoding RNA MIAT: a potential role in the diagnosis and mediation of acute myocardial infarction. *Mol Med Rep*. 2019; 20(6): 5216-5222.
 37. Pardini B, Sabo AA, Birolo G, Calin GA. Noncoding RNAs in extracellular fluids as cancer biomarkers: the new frontier of liquid biopsies. *Cancers (Basel)*. 2019; 11(8): 1170. 38.
 38. Ghafouri-Fard S, Shirvani-Farsani Z, Hussen BM, Taheri M, Arefian N. Emerging impact of non-coding rnas in the pathology of stroke. *Front Aging Neurosci*. 2021; 13: 780489.
 39. Tellez-Gabriel M, Heymann D. Exosomal lncRNAs: the newest promising liquid biopsy. *Cancer Drug Resist*. 2019; 2(4): 1002-1017.
 40. Shi T, Gao G, Cao Y. Long noncoding RNAs as novel biomarkers have a promising future in cancer diagnostics. *Dis Markers*. 2016; 2016: 9085195.
-

Integrated Bioinformatic Analysis of Differentially Expressed Genes Associated with Wound Healing

Mansoureh Farhangniya, M.Sc.¹, Farzaneh Mohamadi Farsani, Ph.D.², Najmeh Salehi, Ph.D.³,

Ali Samadikuchaksaraei, M.D, Ph.D.^{4*} 

1. Cellular and Molecular Research Center, Iran University of Medical Sciences, Tehran, Iran
2. Department of Biology, Naghshejahan Higher Education Institute, Isfahan, Iran
3. School of Biological Sciences, Institute for Research in Fundamental Sciences (IPM), Tehran, Iran
4. Department of Medical Biotechnology, Faculty of Allied Medicine, Iran University of Medical Sciences, Tehran, Iran

Abstract

Objective: Wound healing is a complex process involving the coordinated interaction of various genes and molecular pathways. The study aimed to uncover novel therapeutic targets, biomarkers and candidate genes for drug development to improve successful wound repair interventions.

Materials and Methods: This study is a network-meta analysis study. Nine wound healing microarray datasets obtained from the Gene Expression Omnibus (GEO) database were used for this study. Differentially expressed genes (DEGs) were described using the Limma package and shared genes were used as input for weighted gene co-expression network analysis. The Gene Ontology analysis was performed using the EnrichR web server, and construction of a protein-protein interaction (PPI) network was achieved by the STRING and Cytoscape.

Results: A total of 424 DEGs were determined. A co-expression network was constructed using 7692 shared genes between nine data sets, resulting in the identification of seven modules. Among these modules, those with the top 20 genes of up and down-regulation were selected. The top down-regulated genes, including *TJP1*, *SEC61A1*, *PLEK*, *ATP5B*, *PDIA6*, *PIK3R1*, *SRGN*, *SDC2*, and *RRBP7*, and the top up-regulated genes including *RPS27A*, *EEF1A1*, *HNRNPA1*, *CTNNA1*, *POLR2A*, *CFL1*, *CSNK1E*, *HSPD1*, *FN1*, and *AURKB*, which can potentially serve as therapeutic targets were identified. The KEGG pathway analysis found that the majority of the genes are enriched in the "Wnt signaling pathway".

Conclusion: In our study of nine wound healing microarray datasets, we identified DEGs and co-expressed modules using WGCNA. These genes are involved in important cellular processes such as transcription, translation, and post-translational modifications. We found nine down-regulated genes and ten up-regulated genes, which could serve as potential therapeutic targets for further experimental validation. Targeting pathways related to protein synthesis and cell adhesion and migration may enhance wound healing, but additional experimental validation is needed to confirm the effectiveness and safety of targeted interventions.

Keywords: Bioinformatics, Gene, Network-Meta Analysis, Regeneration, Wound Healing

Citation: Farhangniya M, Mohamadi Farsani F, Salehi N, Samadikuchaksaraei A. Integrated bioinformatic analysis of differentially expressed genes associated with wound healing. Cell J. 2023; 25(12): 874-882. doi: 10.22074/CELLJ.2023.2007217.1368

This open-access article has been published under the terms of the Creative Commons Attribution Non-Commercial 3.0 (CC BY-NC 3.0).

Introduction

Wounds are a common occurrence in everyday life and can result from a variety of causes, including trauma, surgery, and chronic conditions such as diabetes. The restoration of tissue integrity and function is an essential process of wound healing, and involves a complex interplay of genes, proteins, and molecular pathways (1). Understanding its molecular mechanisms may develop effective therapeutic interventions, while promoting a successful tissue repair.

Previous studies have demonstrated the potential of using omics data from non-wound healing patients to gain insights into the molecular mechanisms in wound healing and related diseases. By identifying key genes and genetic

variants associated with chronic wounds, researchers can gain a better understanding of the underlying biological processes and potentially develop more effective treatments and therapies for these conditions (2). To gain a better understanding of wound healing processes and ultimately to achieve better methods of wound management and treatment, we need newer and better qualified network-based methods besides laboratory data analysis based on statistical tests.

By doing this study, we can view wounds as distressed molecular networks which arrange the tools for exploring and enhancing the healing process. It leads to improved consideration of the process complication such as (A) the molecular pathways linked to wound healing, (B) the

Received: 17/July/2023, Revised: 28/October/2023, Accepted: 07/November/2023

*Corresponding Address: P.O.Box: 144961-4535, Department of Medical Biotechnology, Faculty of Allied Medicine, Iran University of Medical Sciences, Tehran, Iran

Email: ali.samadi@iums.ac.ir



Royan Institute
Cell Journal
(Yakhteh)

pathway interactions through various stages of wound healing, and also (C) the probability of holding the mechanism of regulatory interactions of wound healing.

Material and Methods

Gene Expression Omnibus datasets

This study is a network-meta analytical study. In this study, we included expression microarray datasets listed in the Gene Expression Omnibus (GEO) of the NCBI official website (<https://www.ncbi.nlm.nih.gov/geo/>) by the end of December 31, 2021. To find datasets reporting the data on expression levels of mRNAs in the wound healing, the following search keywords were used: human wound healing, omics, transcriptomic, genomic, wound repair, regeneration, wound repair, and genetic variation. This search strategy retrieved 7500 datasets. Our inclusion criteria were human subjects and high throughput microarray data. Further, the exclusion criteria were included: i. Samples which had any accompanying disease, ii. Subjects who received any treatments for wound healing, iii. Data derived from a cell line, and iv. Data derived from non-blood samples.

These datasets were manually screened for having data on skin and oral wound healing of human subjects. Manual screening only short-listed 65 datasets. These 65 datasets underwent quality control and were checked against a set of inclusion and exclusion criteria.

Finally, only 9 datasets were selected and included in the present study, which, in total, contained data from 73 patients and 42 healthy controls (a sum of 115 human subjects). The microarray datasets were all obtained from the GPL570, GPL96, and GPL8300 platforms of the GEO

with the origin of skin and oral wounds. Table 1 provides the details of the datasets included in this study.

Data were analyzed using the Robust Rank Aggregation (RRA) method ($|\log_{2}FC| > 1.5$ and an adjusted $P < 0.001$). Rank analysis was used to determine the total number of differentially expressed genes (DEGs). The expression data in our study were quality corrected and quantile normalized using the Affy package implemented in the R programming language (version 4.0.2) (3). The datasets were integrated at mRNA levels using the random effect method (REM) and then up- and down-regulated expressed genes were identified by the MetaDE package in R (version 2.2.1) (4). A principal component analysis was performed on the merged data for normalization in order to exclude heterogeneous data. The MetaQC tool in R (version 0.1.13) (5) was used to assess the studies' quality and consistency.

Data preprocessing and differential expression analysis

Initially, the preprocessing step for raw data were used the Robust MultiArray Averaging (RMA) method in the Oligo package in R (version 1.38.0) (6). According to the Platform annotation data, the probes, that lacked similar gene symbols were deleted. The gene expression value was calculated using the average value of the probes that were mapped to the same gene symbol. Genes with a $|\log_{2}FC| > 1.5$ and an adjusted $P < 0.001$ were identified as DEGs using the Linear Models for Microarray Data (Limma) tool in R (7) $zR\#$. The input data for weighted gene co-expression network analysis (WGCNA) were shared genes from nine datasets (8).

Table 1: Characteristics of selected datasets

No.	Wound healing categories	GEO ID	Platform	Number of subjects	Subjects' group
1	Skin and oral	GSE21648	Affymetrix, GPL96	15	Patients
2	Skin	GSE30355	Affymetrix, GPL570	10	Patients
3	Skin	GSE7890	Affymetrix, GPL570	10	Patients (with no HT)
4	Oral	GSE28914	Affymetrix, GPL570	8	Patients
5	Skin	GSE63107	Affymetrix, GPL570	30	Patients
6	Skin	GSE11919	Affymetrix, GPL570	9	Normal subjects
7	Skin	GSE440	Affymetrix, GPL8300	5	Normal subjects
8	Skin	GSE26487	Affymetrix, GPL8300	10	Normal subjects
9	Skin	GSE427	Affymetrix, GPL8300	18	Normal subjects

GEO; Gene Expression Omnibus, ID; Identification, and HT; Hydrocortisone treatment.

Construction of co-expression modules of datasets by WGCNA

The WGCNA using the WGCNA package in R was undertaken to assess the relative significance expression of genes and their module memberships. Co-expression networks were established in our study using a soft threshold power in order to provide different modules with different expression patterns. The Pearson correlation coefficient was then used to analyze the weighted co-expression connections in the adjacency matrix. The matrix was transformed into the Topological Overlap Matrix (TOM) using a similar function, and then used to assess the co-expression associations between genes. The networks were constructed by grouping numerous genes with comparable co-expression patterns. Consequently, the list of modules related to up- and down-regulated genes and their co-expressed genes were selected.

The protein-protein interaction network

The Search Tool for the Retrieval of Interacting Genes (STRING) version 11.5 (<http://string-db.org/>) (9). The web server was used to acquire the protein-protein interaction (PPI) network. The Cytoscape was used to visualize the PPI network (v3.7.2; <https://cytoscape.org>) (10); The Cytoscape Consortium, San Diego, CA). This phase included a list of the top-ranked up and down-regulated genes and all desired modular genes.

Functional Annotation of differentially expressed genes and desired modules

The EnrichR, an interactive and collaborative *HTML5* gene list enrichment analysis tool, (<https://maayanlab.cloud/Enrichr/>) (2) was used to perform Gene Ontology (GO) and Kyoto Encyclopedia of Genes and Genomes (KEGG) function enrichment analysis on DEGs. We also used linear regression analysis and the Limma package in R software to compare patients' group with the group of normal subjects. After performing this analysis and using Lmfit analysis (Linear Models for Microarray Data) to fit the model in the data for each gene, we obtained an estimate of the regression coefficient of each gene, which was performed using both of eBayes command (11) and Limma package in R software (version 3.18). In the linear regression model, we calculated the correlation coefficient by the concept of $|\logFC| > 1.5$ to compare each gene in the two groups, and the $P < 0.001$ was regarded as statistically significant.

Results

Identification of differentially expressed genes and selection of the top up and down-regulated genes

The final selected data of patients and healthy controls from GPL96 (GSE21648), GPL570 (GSE30355), GSE7890, GSE28914, GSE63107, GSE11919), and GPL8300 (GSE440, GSE26487, GSE427) platforms were entered into this study. In this data, 300 up-regulated and 124 down-regulated genes were identified (Supplementary

1 and 2, See Supplementary Online Information at www.celljournal.org).

The expressions of these genes were significantly different ($|\logFC| > 1.5$ and adjusted $P < 0.001$) between the patient group and healthy control group. Subsequently, we selected 9 down-regulated and 11 up-regulated genes. Down-regulated genes included *TJP1*, *SEC61A1*, *PLEK*, *ATP5B*, *PDIA6*, *PIK3R1*, *SRGN*, *SDC2*, and *RBBP7*. While, up-regulated genes comprised *RPS27A*, *EEF1A1*, *HNRNPA1*, *RAN*, *POLR2A*, *CTNNB1*, *CFL1*, *CSNK1E*, *HSPD1*, *FNI*, and *AURKB*. To assess data distribution following normalization, box plots of gene expression data were depicted (Fig.S1, See Supplementary Online Information at www.celljournal.org). Separate arrays in the box plots exhibited similar medians of expression level, showing that the adjustment was performed correctly. The Figure S1 (See Supplementary Online Information at www.celljournal.org) illustrated box plots of selected gene expression data before and after normalization.

Table 2: Details of co-expressed modules with top up- and down-regulated genes

Co-expressed module	Up or down-regulation	DEGs
Turquoise	Down-regulation	<i>TJP1</i>
	Down-regulation	<i>SEC61A1</i>
	Down-regulation	<i>PLEK</i>
	Down-regulation	<i>ATP5B</i>
	Down-regulation	<i>PDIA6</i>
	Down-regulation	<i>PIK3R1</i>
	Down-regulation	<i>SDC2</i>
	Down-regulation	<i>RBBP7</i>
	Up-regulation	<i>POLR2A</i>
	Up-regulation	<i>CFL1</i>
	Up-regulation	<i>CSNK1E</i>
Blue	Up-regulation	<i>AURKB</i>
	Up-regulation	<i>HNRNPA1</i>
	Up-regulation	<i>CTNNB1</i>
	Up-regulation	<i>HSPD1</i>
Brown	Up-regulation	<i>FNI</i>
	Up-regulation	<i>RPS27A</i>
Yellow	Up-regulation	<i>EEF1A1</i>
	Down-regulation	<i>SRGN</i>

DEGs; Differentially expressed genes.

Weighted gene co-expression network analysis

In this study, a co-expression network was constructed using 7692 shared genes between nine datasets, and the WGCNA package was used to construct co-expression modules. The scale independence and mean connectivity of modules were shown in Figure 1A, B. Generating a TOM, seven modules were identified (Fig.1C). The desired modules were identified according to the merged modules.

Identification of desired modules and establishing the protein-protein interaction network

Among the seven resulting modules described above, co-expressed modules of the 20 top genes of up and down-regulation ($|\logFC| > 1.5$ and adjusted $P < 0.001$)

were identified as desired modules (Table 2). Using the STRING database, the predicted PPI networks of desired modules were created (Fig.2). A PPI network of top up- and down-regulated genes is shown in Figure 3.

Gene Expression and KEGG enrichment analysis of desired modules

The targeted modules were considerably enriched in common GO biological processes, cellular compartments, and molecular functions, according to the GO functional enrichment analysis ($P < 0.05$). The KEGG pathway analysis revealed that most of the enriched genes are in the "Wnt signaling pathway".

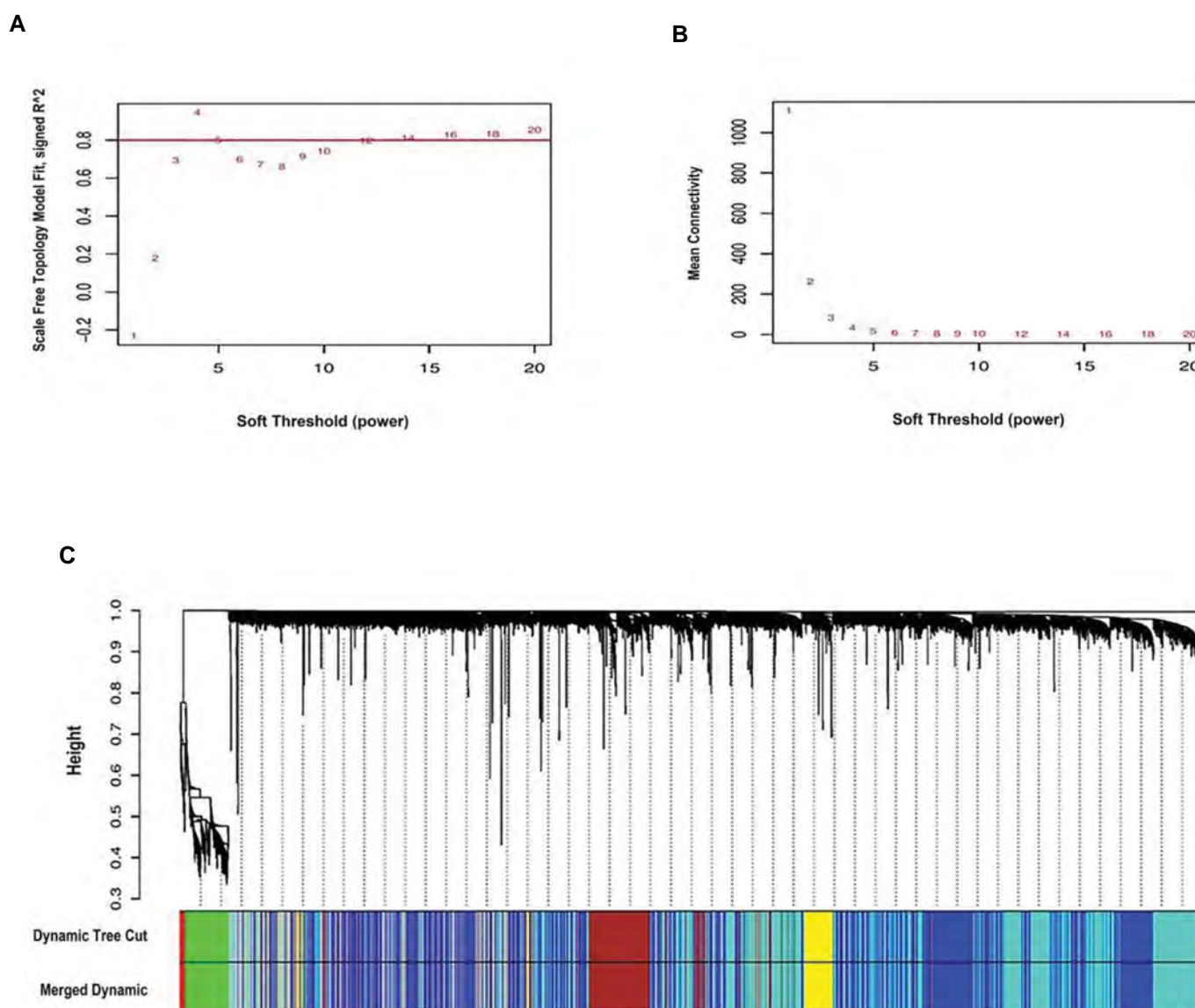
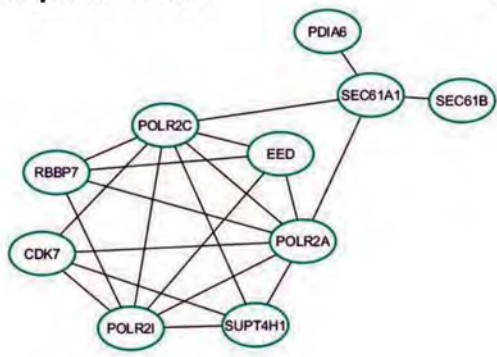
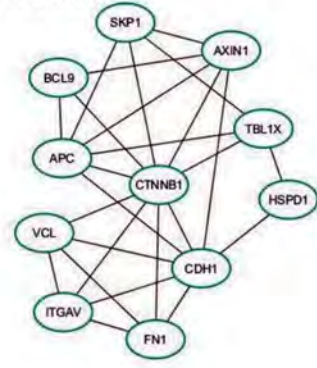


Fig.1: Soft-thresholding power and gene co-expression modules. **A.** WGCNA scale-free fit index analysis for various soft-thresholding powers (β). The appropriate soft-thresholding power=12 was chosen. **B.** Mean connectivity analysis of various soft-thresholding powers. **C.** Using average hierarchical linkage clustering to identify gene co-expression groups. The y-axis represents co-expression distance, and the x-axis represents genes. In the horizontal bar immediately below the dendrogram, modules are represented by different colors, with gray referring to unassigned genes.

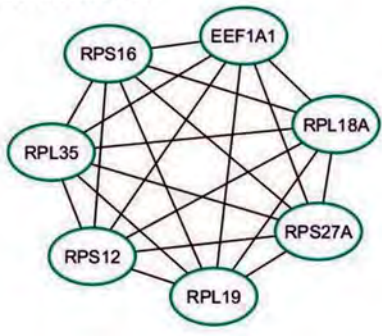
Turquoise module



Blue module



Brown module



Yellow module

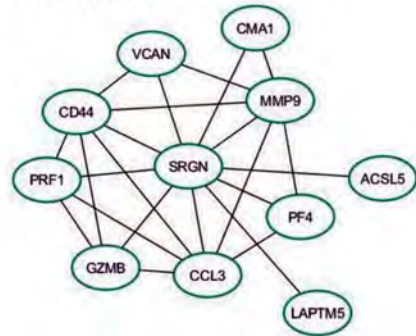


Fig.2: PPI Network. DEGs are presented in each module connecting with lines, which represent interacting proteins. Circles and lines represent genes and the interaction of proteins, respectively. PPI; Protein-protein interaction and DEGs; Differentially expressed genes.

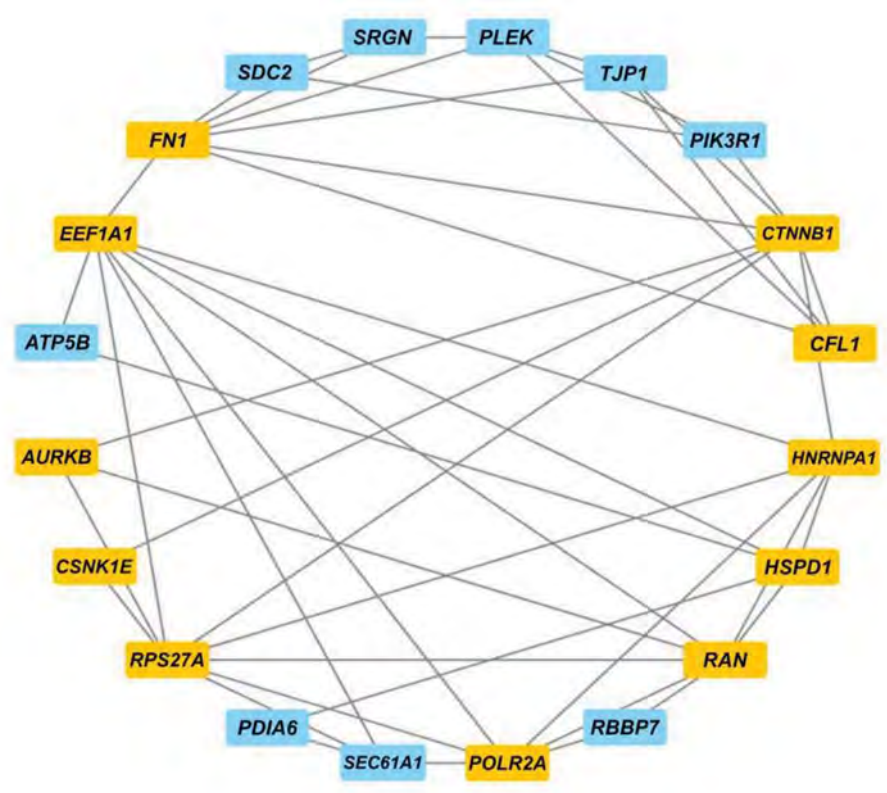


Fig.3: PPI network of top genes. Up-regulated and down-regulated genes are illustrated in yellow and blue colors, respectively. PPI; Protein-protein interaction.

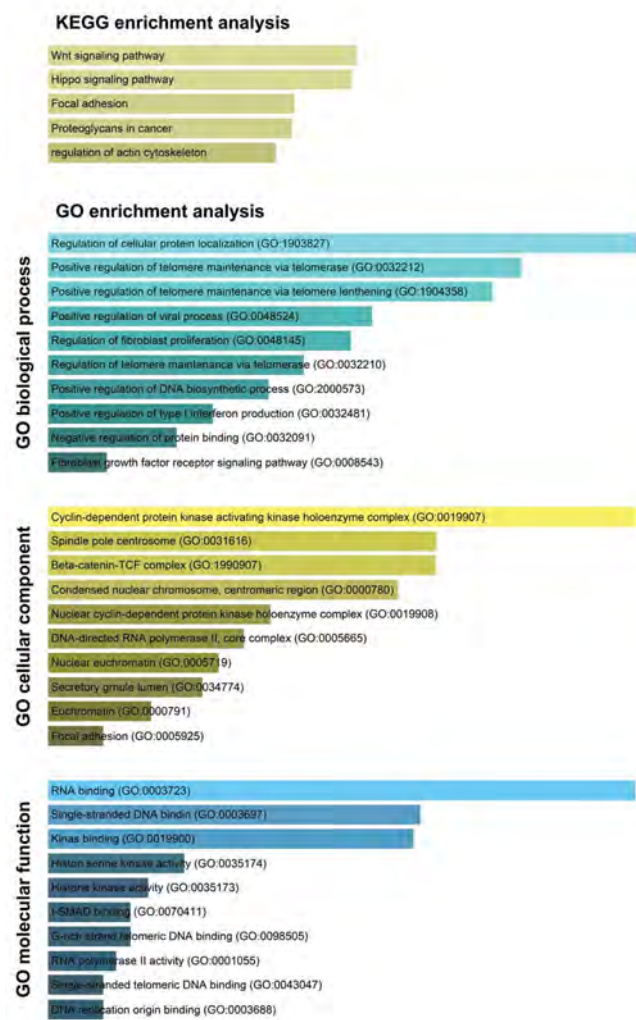


Fig. 4: GO and KEGG findings of the DEGs. The length of each bar shows the level of importance in that category, as determined by the p value. Also, the intensity of color of the bars shows the strength of association with that category. Lower color intensity shows stronger association. GO; Gene Ontology, KEGG; Kyoto Encyclopedia of Genes and Genomes, and DEGs; Differentially expressed genes.

The four desired modules including turquoise, blue, brown and yellow modules were identified for DEGs, resulting from our GO analysis and KEGG findings (Supplementary 3 and 4, See Supplementary Online Information at www.celljournal.org).

Discussion

An acute wound healing is a dynamic process that ultimately leads to the scar development. It seems that there are several signaling pathways and components involved in this process. One of these pathways is the β -catenin-dependent Wnt signaling, which becomes more active after a skin injury and the operation of exogenous Wnt3a (rmWnt3a). Wnt3a promotes the maturation of the wound matrix, re-epithelialization, and the formation of a scar (12). In keratinocytes and fibroblasts, Catenin beta 1 (β -catenin) that coding by *CTNNB1* has different effects, as it restricts the migration of keratinocytes while encouraging the proliferation of fibroblasts. This suggests

that β -catenin may either impede or improve the healing process (13).

Likewise, the *FN1* gene is present at all phases of wound healing. The *FN1* gene provides instructions for making two types of the fibronectin-1 proteins, including soluble plasma fibronectin-1 (pFN1) and insoluble cellular fibronectin-1 (cFN). The pFN1 mainly functions in the early stages of wound healing to aid in forming clots. Platelets, via increased platelet binding site expression, aid in assembling plasma-derived *FN1* into fibrillar matrices. Through locally expressed *FN1* assembly, cellular-derived *FN1* governs the latter phases of a tissue remodeling. The FN1 protein is linked to the collagen III matrices during the granulation stage; the temporary FN1 matrix is then reconstructed into the collagen I matrix, which is surrounded by FN1 (14).

The Cofilin-1 (CFL1) is an actin-remodeling protein that binds to G- and F-actins and induces a pH-sensitive depolymerizing activity that regulates cell motility during tissue repair (15). Both form of the CFL1 protein, including phosphorylated and dephosphorylated, were also detected in platelets, with the latter quantity corresponding to the later phases of platelet aggregation in wound healing, that indicated a newly dephosphorylated CFL1, might play an essential role in the cytoskeletal remodeling that happens during platelet aggregation, a critical step in the early stages of wound healing (16).

Many top-up-regulated genes are strongly associated with one of the four stages of wound healing processes, but in other conditions such as cancer, they are also involved in proliferation. For example, *RPS27a* (ribosomal protein S27a) plays a role in ribosome synthesis and protein post-translational modifications. The *RPS27a* gene has been discovered to have a significant role in a cell proliferation through proliferation stimulation, cell cycle progression control, and apoptosis suppression in leukemia cells (17). The *POLR2A* gene, which encodes the RNA polymerase II subunit A, is strongly associated with cancer development. Studies have demonstrated that *POLR2A* enhances the expression of cyclin and cyclin-dependent kinases (CDKs) at different stages of gastric cancer, suggesting its involvement in promoting cell cycle progression (18). Further studies are required to establish conclusive evidence and its role in wound healing.

In addition, knocking down the *eEF1A1* gene, eukaryotic elongation factor 1A1, has a notable impact on reducing proliferation and activation of apoptosis in Jurkat cells, which may be mediated via the PI3K/Akt/NF- κ B and PI3K/Akt/mTOR signaling pathways (19). Remarkably, *CSNK1E* gene has been identified as a significant contributor to activated β -catenin signaling in cancer, suggesting that it might be a viable therapeutic target for malignancies that contain an active β -catenin protein (20). The heterogeneous nuclear ribonucleoprotein A1 (hnRNP A1) which encoded by *HNRNPA1* gene, is a stress granule protein that plays an important role in the development, proliferation, and metastatic cancer cells

(21). So based on the research, there is a clear relationship between protein biogenesis and wound healing that could be a potential target for therapeutic approaches.

Furthermore, in the present study, nine genes of highest down-regulation rate were identified, including *TJP1*, *SEC61A1*, *PLEK*, *ATP5B*, *PDIA6*, *PIK3R1*, *SDC2*, *RBBP7*, and *SRGN*.

The *PIK3R1* gene is one of the HIF-1 α pathway-associated genes, with a greater expression rate in the skin and the tongue (22). In a next-generation sequencing (NGS) experiment, *PIK3R1* was found to be one of the down-regulated genes in irradiated mouse skin (23). Radiation-induced skin fibrosis is a typical complication of radiotherapy in the clinical practice. In this side effect, *FOXO3* plays a key role as one of the central genes in causing radiation-induced skin fibrosis. Fibrosis is linked to the regulation of the *FOXO3* gene, which plays a role in the P53 pathway and is involved in essential cellular processes such as apoptosis, cell survival, and the regulation of the cell cycle. Additionally, the *PIK3R1* gene can also regulate the expression of *FOXO3* (24).

In this background, the Syndecan-2 a protein in humans is encoded by the *SDC2* gene. *SDC2*, is elevated during fibrosis alike other *SDCs*. It is produced by fibroblasts and stimulated by transforming growth factor β 1 (TGF β 1) and insulin-like growth factor binding protein-3 (25). The *SDC2* is among the up-regulated genes in the axolotl wound healing process, along with *FNI*, *TGF β 1*, and *LTBP3*. It is implicated as a mediator in the TGF β -signaling pathway (26). Similarly, in *SDC2* knock-down mice, the loss of this protein resulted in impaired retinal artery development and vascular branching. In addition, the wound healing was problematic in these mice (27).

Likewise, research has demonstrated that lower gene expression in *SRGN* leads to decreased proliferation and impaired wound healing ability in endothelial cells (28). Also, in a study of a patient with severe congenital neutropenia with the de novo *SEC61A1* mutation, which was reported for the first time, problematic wound healing was addressed as one of the symptoms causes (29). Studies of inflammatory genes and inflammatory processes in wound healing have shown that *PLEK* is one of the central inflammatory genes and acts as a signal transducer in the migration of polymorphonuclear neutrophilic granulocytes to skin lesions which are classified as up-regulated genes in this process (30).

The Tjp (ZO-1) protein, plays a crucial role in wound healing by regulating the assembly and disassembly of tight junctions, as well as promoting cell migration and re-epithelialization (31). In a study that examined expression of genes at 48 hours, 72 hours, and five days after the wound healing process, the *ATP5B* gene, an expression reference gene, showed a minor stability in comparison with other twelve genes (32). The Retinoblastoma Binding Protein 7 (RBBP7), may potentially engage in the early phases of wound healing by serving as a chromatin remodeling factor, which requests additional investigation (33).

Lastly, because of the effects of genes that have not been studied in the wound healing process, including *TJP1*, *SEC61A1*, *PLEK*, *ATP5B*, *PDIA6*, *PIK3R1*, *SRGN*, *SDC2*, *RBBP7*, *RPS27A*, *EEF1A1*, *HNRNP1A1*, *POLR2A*, *CFL1*, *CSNK1E*, *HSPD1*, *FNI*, and *AURKB*, play a crucial role in the cell proliferation by contributing to essential aspects of the cell cycle or the regulatory pathways of the process. While, a cell proliferation refers to the growth and division of cells, it is necessary for the development, maintenance and repair of tissues and organs in the body. Although, additional research is needed, these genes probably play crucial and influential roles in wound healing, with an elevated expression but fine-tuned regulation.

Analyzing these datasets with R software revealed 424 DEGs composed of 300 up-regulated and 124 down-regulated genes between wound samples and normal skin. Several studies have shown that the Wnt gene family can affect wound healing. Wounding can activate Wnt signaling genes in several levels of wound healing. Moreover, Wnt signaling genes are responsible for different stages of skin formation, and this feature makes it a good target for targeting in tissue regeneration studies (34).

Our GO analysis of DEGs demonstrated that a "regulation of cellular protein localization" is one of the mechanisms in wound healing. A targeted localization is a type of regulation that is common in eukaryotes. It is possible for cells to achieve rapid changes in the function of local proteins by particularly redirecting the distribution of a number of existing proteins. Eukaryotic cells have developed sophisticated targeting mechanisms to ensure that proteins are delivered to the correct cellular location. Indeed, essential stages such as the proliferation phase, the supply of protein sources is a priority of wound healing, and any disruption in this process will lead to disruption of it. The enrichment of DEGs in terms such as "positive regulation of telomere maintenance via telomerase" and "positive regulation of telomere maintenance via the telomere lengthening" suggests that any process that stimulates or increases the frequency and extent of the addition of telomeric repeats by telomerase is crucial for effective wound healing. In this aspect, mice with dangerously short telomeres exhibit difficulties with highly proliferative tissue, such as poor wound healing, inflammatory skin lesions, early hair loss, and early hair graying (35). GO and KEGG analyses of up- and down-regulated gene expression showed that the wound healing mechanism is a multidimensional process that comprises multiple signaling pathways and important molecular mechanisms.

Bioinformatics analysis indicated that these genes and pathways could be involved in wound healing processes in several ways. According to GO analysis, the main enrichments of turquoise module related to biological processes include "positive regulation of transcription, DNA-templated", "positive regulation of transcription by RNA polymerase II", "cellular protein modification

process", "mRNA processing" and "positive regulation of nucleic acid-templated transcription" each of which, except for the cellular protein modification process, is somehow related to the transcription process. It is also interesting to note that the blue module enrichment analysis, which is also co-expressed with the majority of up-regulated genes, showed a high overlap in the enrichment of these modular genes with the turquoise module enrichment analysis closely related to the transcription process. During wound healing, several transcription factors coordinately regulate target genes, which vary over time (36), enabling the integration of external stimuli to provide the necessary physiological response. The capacity of numerous transcription factors to bind to these regulatory regions in distinct cell types or respond to stimuli is frequently determined by pre-existing genome-wide chromatin accessibility.

Interestingly, the enrichment analysis of brown module genes suggests that these genes are involved in aspects of the translation process. The most significant pathway related to this module includes "SRP-dependent co-translational protein targeting to membrane". The targeting of proteins to membranes during translation is dependent on two key elements, including the signal-recognition particle (SRP) and the SRP receptor. The SRP is a cytosolic particle that transiently binds to the endoplasmic reticulum signal sequence, the large ribosomal unit, and the SRP receptor in the ER membrane. However, the role of SRPs in the wound healing procedure is closely related to *CELF1*, an RNA-binding protein gene, that is responsible for regulating SRPs. When *CELF1* is depleted in myoblast cells, the wound healing process is disrupted by altering the regulation of SRPs. Comparable abnormalities in a wound healing are found when an SRP subunit imbalance is created by an over-expression of SRP68, which may be a limiting factor in the assembly of functional SRP (37).

After the transcription and translation process, the enrichment of the cellular protein modification process introduces a precise concept. This concept denotes the covalent modification of one or more amino acids in proteins, peptides, and nascent polypeptides (co-translational and post-translational modifications) occurring at the individual cell level. This process is essential in developing tissue specificity for wound healing (38). On the other hand, this protein modification is one of the processes that affect inflammation, which is one of the four main stages of the wound healing process. The post-translational modification (PTM) of the constituents of the inflammatory pathway, for instance Toll-like receptors (TLR) pathways, RIG-I-like receptor (RLR) pathways, NOD-like receptor (NLR) pathways, intracellular DNA sensors, intracellular RNA sensors, and inflammasomes, is critical in the control of these signaling pathways (39). The primary types of a PTM include ubiquitination, phosphorylation, polyubiquitination, methylation, and acetylation, and also, they each serve a particular function in signaling control. A PTM effects a range from the production of pro-inflammatory molecules

to the interaction of adapters and receptors, as well as cell translocation in response to infectious or other damaging agents. One of the main problems disrupting the wound healing process is chronic inflammation. Meanwhile, studies have been conducted on other complications that have been dedicated to down-regulated genes and their effects on inflammatory processes and state that down-regulated genes can affect inflammation (40).

Conclusion

In our analysis of nine wound healing microarray datasets, we identified up- and down-regulated genes and co-expressed modules using WGCNA. DEGs play a role in crucial cellular processes such as transcription, translation, and post-translational modifications. Specifically, we found nine down-regulated genes, including *TJPI*, *SEC61A1*, *PLEK*, *ATP5B*, *PDIA6*, *PIK3R1*, *SRGN*, *SDC2*, and *RBBP7*, as well as ten up-regulated genes: *RPS27A*, *EEF1A1*, *HNRNPA1*, *CTNNB1*, *POLR2A*, *CFL1*, *CSNK1E*, *HSPD1*, *FNI*, and *AURKB*. These discoveries offer valuable insights and potential therapeutic targets for further experimental validation. Targeting pathways related to protein synthesis may enhance cellular activity during wound healing, while interventions aimed at promoting proper cell adhesion and migration could facilitate efficient wound closure. However, additional experimental validation is necessary to confirm the efficacy and safety of any targeted interventions.

Acknowledgements

We are grateful to the Iran University of Medical Sciences that supported this research. There is no conflict of interest in this study.

Authors' Contributions

M.F.; Methodology, Data validation, Formal analysis, Investigation, Data curation, Original draft writing, Review, Editing, and Visualization. F.M.F.; Methodology, Data validation, Formal analysis, Review, Editing. N.S.; Methodology, Data validation, Formal analysis, and Data curation. A.S.; Conceptualization, Project supervision, Project administration, and Funding acquisition. All authors read and approved the final manuscript.

References

1. Tottoli EM, Dorati R, Genta I, Chiesa E, Pisani S, Conti B. Skin wound healing process and new emerging technologies for skin wound care and regeneration. *Pharmaceutics*. 2020; 12(8): 735.
2. Xie Z, Bailey A, Kuleshov MV, Clarke DJB, Evangelista JE, Jenkins SL, et al. Gene set knowledge discovery with enrichr. *Curr Protoc*. 2021; 1(3): e90.
3. Tippmann S. Programming tools: adventures with R. *Nature*. 2015; 517(7532): 109-110.
4. Wang X, Kang DD, Shen K, Song C, Lu S, Chang LC, et al. An R package suite for microarray meta-analysis in quality control, differentially expressed gene analysis and pathway enrichment detection. *Bioinformatics*. 2012; 28(19): 2534-2536.
5. Kang DD, Sibille E, Kaminski N, Tseng GC. MetaQC: objective quality control and inclusion/exclusion criteria for genomic meta-analysis. *Nucleic Acids Res*. 2012; 40(2): e15.

6. Irizarry RA, Hobbs B, Collin F, Beazer-Barclay YD, Antonellis KJ, Scherf U, et al. Exploration, normalization, and summaries of high density oligonucleotide array probe level data. *Biostatistics*. 2003; 4(2): 249-264.
7. Ritchie ME, Phipson B, Wu D, Hu Y, Law CW, Shi W, et al. limma powers differential expression analyses for RNA-sequencing and microarray studies. *Nucleic Acids Res*. 2015; 43(7): e47.
8. Langfelder P, Horvath S. WGCNA: an R package for weighted correlation network analysis. *BMC Bioinformatics*. 2008; 9: 559.
9. Szklarczyk D, Gable AL, Nastou KC, Lyon D, Kirsch R, Pyysalo S, et al. The STRING database in 2021: customizable protein-protein networks, and functional characterization of user-uploaded gene/measurement sets. *Nucleic Acids Res*. 2021; 49(D1):D605-D612.
10. Otasek D, Morris JH, Bouças J, Pico AR, Demchak B. Cytoscape automation: empowering workflow-based network analysis. *Genome Biol*. 2019; 20(1): 185.
11. Smyth GK. limma: Linear models for microarray data. In: Gentleman R, Carey VJ, Huber W, Irizarry RA, Dudoit S, editors. *Bioinformatics and computational biology solutions using R and bioconductor*. Statistics for biology and health. New York: Springer; 2005; 397-420.
12. Carre AL, Hu MS, James AW, Kawai K, Galvez MG, Longaker MT, et al. β -catenin-dependent Wnt signaling: a pathway in acute cutaneous wounding. *Plast Reconstr Surg*. 2018; 141(3): 669-678.
13. Cheon SS, Wei Q, Gurung A, Youn A, Bright T, Poon R, et al. Beta-catenin regulates wound size and mediates the effect of TGF- β in cutaneous healing. *FASEB J*. 2006; 20(6): 692-701.
14. Patten J, Wang K. Fibronectin in development and wound healing. *Adv Drug Deliv Rev*. 2021; 170: 353-368.
15. Condeelis J. How is actin polymerization nucleated in vivo? *Trends Cell Biol*. 2001; 11(7): 288-293.
16. Davidson MM, Haslam RJ. Dephosphorylation of cofilin in stimulated platelets: roles for a GTP-binding protein and Ca²⁺. *Biochem J*. 1994; 301 (Pt 1)(Pt 1): 41-47.
17. Wang H, Yu J, Zhang L, Xiong Y, Chen S, Xing H, et al. RPS27a promotes proliferation, regulates cell cycle progression and inhibits apoptosis of leukemia cells. *Biochem Biophys Res Commun*. 2014; 446(4): 1204-1210.
18. Jiang Q, Zhang J, Li F, Ma X, Wu F, Miao J, et al. POLR2A promotes the proliferation of gastric cancer cells by advancing the overall cell cycle progression. *Front Genet*. 2021; 12: 688575.
19. Huang Y, Hu JD, Qi YL, Wu YA, Zheng J, Chen YY, et al. Effect of knocking down eEF1A1 gene on proliferation and apoptosis in Jurkat cells and its mechanisms. *Zhongguo Shi Yan Xue Ye Xue Za Zhi*. 2012; 20(4): 835-841.
20. Zhu M, Zhang J, Bian S, Zhang X, Shen Y, Ni Z, et al. Circadian gene CSNK1D promoted the progression of hepatocellular carcinoma by activating Wnt/ β -catenin pathway via stabilizing Dishevelled Segment Polarity Protein 3. *Biol Proced Online*. 2022; 24(1): 21.
21. Asadi MR, Rahmanpour D, Moslehian MS, Sabaie H, Hassani M, Ghafouri-Fard S, et al. Stress granules involved in formation, progression and metastasis of cancer: a scoping review. *Front Cell Dev Biol*. 2021; 9: 745394.
22. Chen L, Gajendrareddy PK, DiPietro LA. Differential expression of HIF-1 α in skin and mucosal wounds. *J Dent Res*. 2012; 91(9): 871-876.
23. Yoo H, Kang JW, Lee DW, Oh SH, Lee YS, Lee EJ, et al. Pyruvate metabolism: a therapeutic opportunity in radiation-induced skin injury. *Biochem Biophys Res Commun*. 2015; 460(3): 504-510.
24. Kim J, Choi H, Cho EG, Lee TR. FoxO3a is an antimelanogenic factor that mediates antioxidant-induced depigmentation. *J Invest Dermatol*. 2014; 134(5): 1378-1388.
25. Ruiz XD, Mlakar LR, Yamaguchi Y, Su Y, Larregina AT, Pilewski JM, et al. Syndecan-2 is a novel target of insulin-like growth factor binding protein-3 and is over-expressed in fibrosis. *PLoS One*. 2012; 7(8): e43049.
26. Regős E, Abdelfattah HH, Reszegi A, Szilák L, Werling K, Szabó G, et al. Syndecan-1 inhibits early stages of liver fibrogenesis by interfering with TGF β 1 action and upregulating MMP14. *Matrix Biol*. 2018; 68-69: 474-489.
27. Corti F, Wang Y, Rhodes JM, Atri D, Archer-Hartmann S, Zhang J, et al. N-terminal syndecan-2 domain selectively enhances 6-O heparan sulfate chains sulfation and promotes VEGFA₁₆₅-dependent neovascularization. *Nat Commun*. 2019; 10(1): 1562.
28. Reine TM, Vuong TT, Rutkovskiy A, Meen AJ, Vaage J, Jenssen TG, et al. Serglycin in quiescent and proliferating primary endothelial cells. *PLoS One*. 2015; 10(12): e0145584.
29. Van Nieuwenhove E, Barber JS, Neumann J, Smeets E, Willemssen M, Pasciuto E, et al. Defective Sec61 α 1 underlies a novel cause of autosomal dominant severe congenital neutropenia. *J Allergy Clin Immunol*. 2020; 146(5): 1180-1193.
30. Lundmark A, Davanian H, Båge T, Johannsen G, Koro C, Lundberg J, et al. Transcriptome analysis reveals mucin 4 to be highly associated with periodontitis and identifies pleckstrin as a link to systemic diseases. *Sci Rep*. 2015; 5: 18475.
31. Znalesniak EB, Hoffmann W. Modulation of cell-cell contacts during intestinal restitution in vitro and effects of epidermal growth factor (EGF). *Cell Physiol Biochem*. 2010; 25(4-5): 533-542.
32. Turabelidze A, Guo S, DiPietro LA. Importance of housekeeping gene selection for accurate reverse transcription-quantitative polymerase chain reaction in a wound healing model. *Wound Repair Regen*. 2010; 18(5): 460-466.
33. Pardal AJ, Fernandes-Duarte F, Bowman AJ. The histone chaperoning pathway: from ribosome to nucleosome. *Essays Biochem*. 2019; 63(1): 29-43.
34. Sharma AR, Sharma G, Lee YH, Chakraborty C, Lee SS, Seo EM. Sodium selenite promotes osteoblast differentiation via the WNT/ β -catenin signaling pathway. *Cell J*. 2022; 24(6): 309-315.
35. Nersisyan L, Hopp L, Loeffler-Wirth H, Galle J, Loeffler M, Arakelyan A, et al. Telomere length maintenance and its transcriptional regulation in lynch syndrome and sporadic colorectal carcinoma. *Front Oncol*. 2019; 9: 1172.
36. Aragona M, Dekoninck S, Rulands S, Lenglez S, Mascré G, Simons BD, et al. Defining stem cell dynamics and migration during wound healing in mouse skin epidermis. *Nat Commun*. 2017; 8: 14684.
37. Russo J, Lee JE, López CM, Anderson J, Nguyen TP, Heck AM, et al. The CELF1 RNA-binding protein regulates decay of signal recognition particle mRNAs and limits secretion in mouse myoblasts. *PLoS One*. 2017; 12(1): e0170680.
38. Ho S, Marçal H, Foster LJ. Towards scarless wound healing: a comparison of protein expression between human, adult and foetal fibroblasts. *Biomed Res Int*. 2014; 2014: 676493.
39. Si Y, Zhang Y, Chen Z, Zhou R, Zhang Y, Hao D, et al. Posttranslational modification control of inflammatory signaling. *Adv Exp Med Biol*. 2017; 1024: 37-61.
40. Pathare ADS, Zaveri K, Hinduja I. Downregulation of genes related to immune and inflammatory response in IVF implantation failure cases under controlled ovarian stimulation. *Am J Reprod Immunol*. 2017; 78(1).

Advisory Board of Cell Journal^(Yakhteh)
Vol 25, No 1-12, 2023

A
Abbaspanah B
Abbaszadeh Hojjat-A
Abdi Z
Abdollahi E
Abdollahifar Mohammad A
Abnosi Mohammad H
Abouhamzeh B
Abpeykar Z
Abroun S
Afarinesh Mohammad R
Afshar S
Afzal N
Ahangar P
Ahani A
Ahmad Waza A
Ahmadi H
Ahmadi R
Ajami M
Akhavan Taheri M
Akhlaghpour A
Akram M
Ali F
Alizadeh A
Alizadeh M
Allameh A
Amidi F
Amini P
Amirchaghmaghi E
Amjadi F
ArabZadeh E
Arianmanesh M
Arjmand B
Arkan E
Asadi A
Asadi S
Asaumi R
Ashouri Movassagh S
Ashrafi M
Asl Saeid H
Assadollahi V
Atari F
Azad M
Azimzadeh S

Azizi H
Azizi Z
Azizidoost Sh

B
Babaei F
Babanejad M
Babu S
Baei P
Bagheri F
Bagheri Z
Bagheri-Mohammadi S
Bahadori MH
Baharara J
Baheiraei N
Banaei A
Banan M
Bandarian F
Barabadi Z
Barbakadze T
Basiri M
Bayat M
Bazrafkan M
Bazyar H
Behfar M
Behjati F
Behzadi P
Beigi M
Bhat R
Bidkhorri H
Bordbar S
Borji M
Bozorgi-Zarini A

C
Cheng W
Choudhery M
Ciğerci İ
Colpi GM
Cui Y

D
Daemi H
Dalman A
Dashtizad M
Davoodian N

Delkhosh-kasmaie F
Dey S
Dharamdasani V
Dorgalaleh A
Dormiani K

E
Ebrahimi M
Ebrahimi Sadrabadi A
Ebrahimnejad Gorji K
El-Bialy T
Emadi Bighi M
Emami N
Entezam M
Eskandari N

F
Faghihi F
Fakhri M
Fallahi R
Farazmandfar T
Farghadan M
Farhood B
Fathi-Kazerooni M
Fazeli SAS
Feizi F
Forootan S
Forouzandeh M
Fu W

G
Gerhard H
Ghadami SA
Ghadimi K
Ghaemi M
Ghaffari Mohammad E
Ghaheiri A
Ghanbari E
Gharbi S
Ghasemi H
Ghasemi S
Ghezelayagh Z
Ghezelbash B
Gholami K
Ghorbani M
Ghorbanian MT

Advisory Board of Cell Journal^(Yakhteh)
Vol 25, No 1-12, 2023

Golestan Jahromi M

H

Habibi N

Haghighitalab A

Haghparast A

Haghshenas MR

Hai Y

Haidl G

Haji-Maghsoudi S

Hajizadeh E

Halvaei I

Hashemi J

Hashemi Karoii D

Hashemi M

Hashemi Tayer A

Hassani N

Hassanlou M

Hassanzadeh MA

Hatami M

Heiat M

Hesarakhi M

Hescheler J

Hisayo Nishida F

Homayouni Moghadam F

Hosseini E

Hosseini S

Huang W

I

Igder S

Izadpanah E

J

Jafarian A

Jafarian AH

Jafarinia M

Jafarisani M

Jafarpour S

Jalilian N

Jameie SB

Javad H

Ji W

K

Kaki A

Kalantar SM

Kalantary-Charvadeh A

Kamrani S

Kamyari N

Karami F

Kardar GhA

Karimi S

Karimian M

Kaviani S

Kazemi B

Kazemi M

Kazemi-Sefat GE

Keshavarz H

Khalilabadi R

khamisipour G

Khiaban Tanha B

Khochbin S

khoshzaban A

khosravizadeh Z

Kokaia Z

koohestanian K

Kord-Varkaneh H

Krishnan H

L

Li C

Li H

Lin C

Liu G

lotfi J

Lotfibakhshaiesh N

Luo YH

M

Madani H

Maghami P

Mahmoudi F

Mahmoudian RA

Mahmudi SA

Malekzadeh Shafaroudi M

María-Jimena M

Masjedi M

Mehdizadeh M

Memar R

Mengyu L

Ming M

Mirmosayyeb O

Mirnajafi-Zadeh J

Mirzaeian L

Mofarah ZS

Moghadasali R

Mogharber Bf

Moghimi-Khorasgani A

Moghiseh A

Mohamed Kamel Hala F

Mohammadi M

Mohammadzadeh-Vardin M

Mohazzab A

Montaseri A

Montazersaheb S

Moradi Shabnam Z

Mortaz E

Mosayyebi B

Motalleb GhR

Motevaseli E

Movahedin M

Mozdarani H

Multhoff G

Mutahir Z

N

Nabavi SM

Naderi N

Nagaosa K

Najafi A

Najafi SMA

Naseri M

Nasiri E

Nazemalhosseini-Mojarad E

Nedaeinia R

Nejad Dehbashi F

Nicholson-Roberts TC

Nikbakht M

Niknafs B

Nobakht M

Norizadeh M

Norouzi M

Noruzinia M

Numan Bucak M

O

Obeidi N

Omani-Samani R

Omoruyi F

Advisory Board of Cell Journal^(Yakhteh)
Vol 25, No 1-12, 2023

Omrani MD

P

Pabona John M

Pahlavanneshan S

Pandey A

Pandey S

parsamanesh N

Parvati Sai Arun PV

Pauluhn J

Pérez-Morales R

Piryaei A

Poormoosavi SM

Pouresmaeili F

Pourkhodadad S

Poursafavi Z

Q

Qie S

Qujeq D

R

Rabiei N

Rahbarghazi R

Rahmati S

Rajabi S

Rajabzadeh A

Ramezanali F

Ramezani Farani M

Ramezani M

Ranjbar M

Rathar Y

Razavinasab M

Rehman N

Rezaei N

Rezaei Topraggaleh T

Rezakhani L

Rocio NC

Roshangar L

Rostamian M

Rouhollahi Varnosfaderani S

S

Saadatian Kharajo R

Sabbaghian M

Sadat SM

Sadeghi N

Sagha M

Saheera S

Saki N

Salehi H

Salehnia M

Samadi S

Samadian Z

Samadikuchaksaraei A

Samani F

Satari L

Saylan A

Sellami A

Servatian N

Setayeshmehr M

Shabani R

Shafieyan S

Shahhoseini M

Sharifi S

Shaygannia E

Shekari F

Shiri E

Shirong Z

Shirshahi V

Shokrgozar MA

Soleimani M

Soltani B

Soltani Z

Soltanian AR

Soudi S

Su C

Sudha TYS

Sukyai P

T

Tabatabaei S

Taghiyar L

Taleahmad S

Talebi A

Talebi S

Tamadon A

Tameh Abolfazl A

Tan S

Tavalaee M

Tavana S

Tayebi M

Thakkar U

Timashev P

Torabi S

V

Vahdat S

Vahedi M

Vallian S

Valojerdi MR

Vesali S

Vlachadis N

Vosough M

W

Wang C

Wang W

Wei Y

X

Xiao-Xia H

Y

Yang L

Yang Q

Yang S

Yari S

Yeganeh F

Yekani F

Yousefi Z

Yuchi A

Yun Y

Z

Zahiri R

Zamani M

Zamanian M

Zareen Shaikh S

Zavaran Hosseini A

Zeng M

Zerbini G

Zhang HP

Zhang S

Zhang W

Zhang Y

Zheng N

Zheng Y

Zhou Z

Zou Y

Zununi Vahed S

Index by Authors in Cell Journal^(Yakhteh)
Vol 25, No 1-12, 2023

- A**
- A Ferns G (Page: 847)
- Abbasihormozi Sh (Page: 17)
- Abbasi Kakroodi F (Page: 363)
- Abbaszadeh M (Page: 143)
- Abdollahi E (Page: 688)
- Abedelahi A (Page: 674)
- Abnosi MH (Page: 603)
- Abrari K (Page: 317)
- Abroun S (Pages: 176, 184, 229)
- Abtahi NS (Page: 809)
- Adelipour M (Page: 764)
- Adib M (Pages: 455, 727)
- Afarinesh MR (Page: 822)
- Aflatoonian B (Page: 455)
- Afshar S (Pages: 418, 783)
- Agha Alishiri A (Page: 217)
- Aghajani R (Page: 165)
- Aghamollaei H (Page: 217)
- Aghasizadeh M (Page: 847)
- Aghdami N (Page: 363)
- Ahmadi L (Pages: 110, 307)
- Ahmadraji M (Page: 665)
- Ai F (Page: 391)
- Akbarinehad V (Page: 17)
- Akbarzadeh M (Page: 536)
- Aledavood SA (Page: 51)
- Alipour F (Page: 665)
- Alipour N (Page: 536, 564)
- Alizadeh AA (Page: 790)
- Alizadeh AR (Page: 17)
- Alizadeh Otaghvar H (Page: 300)
- Alizadeh Sh (Page: 1)
- Alizadeh-Fanalou Sh (Page: 427)
- Alosaimi F (Page: 273)
- Alsadat Mahmoudian R (Page: 696)
- Alsafi M (Page: 645)
- Alsahebhosoul F (Page: 110)
- Amini P (Page: 418)
- Aminishakib P (Pages: 363, 407)
- Amiri B (Page: 11)
- Ani M (Page: 165)
- Ani S (Page: 165)
- Anvarinia Y (Page: 327)
- Arab SSh (Page: 62)
- Asadabadi T (Page: 863)
- Asadi M (Page: 1)
- Asgari Y (Page: 633)
- Ashtari F (Page: 307)
- Assaran-Darban R (Page: 847)
- Ataie Fashtami L (Pages: 143, 212, 363)
- Atashi A (Page: 184)
- Attaran N (Page: 51)
- Azadbakht M (Page: 674)
- Azadeh M (Page: 354)
- Azarpira N (Page: 790)
- Azimi Alamouty M (Page: 255)
- Azimi M (Page: 92)
- Azizi D (Page: 813)
- Azizidoost Sh (Page: 764)
- B**
- Babaahmadi M (Pages: 338, 854)
- Babaei N (Page: 102)
- Babajani A (Page: 35)
- Babaloo H (Page: 564)
- Babapour V (Page: 17)
- Baghaban Eslaminejad MR (Pages: 338, 854)
- Bagheri J (Page: 564)
- Baharara H (Page: 847)
- Baharvand H (Pages: 338, 372, 665)
- Bahreini F (Page: 347)
- Bai Q (Page: 801)
- Bajouri A (Page: 143)
- Bakhtiari A (Page: 11)
- Bakhtiarzadeh F (Page: 273)
- Bamdad T (Page: 62)
- Baradaran B (Page: 674)
- Barbakadze T (Page: 247)
- Barzin Tond S (Page: 427)
- Bashash D (Page: 85)
- Basiri M (Pages: 665, 674)
- Bátor J (Page: 247)
- Bayat M (Page: 863)
- Bazgir B (Pages: 135, 513)
- Behdani M (Page: 62)
- Behgozin A (Page: 73)
- Behrangi E (Page: 300)
- Bidkhorri HR (Page: 696)
- Biglar M (Page: 62)
- Bishekolaei R (Page: 354)
- Blourieh T (Page: 363)
- Bo Y (Page: 222)
- Borhani-Haghighi A (Page: 863)
- C**
- Cao W (Page: 613)
- Chavooshi R (Page: 158)
- Chavoshi A (Page: 217)
- Chen J (Pages: 399, 570)
- Chen X (Page: 291)
- Chen Z (Page: 391)
- Cheraghzadeh M (Page: 764)
- Cho KA (Page: 660)
- Cui W (Page: 291)
- D**
- Daemi H (Page: 255)
- Danesh-Doust M (Page: 126)
- Daneshpour MS (Page: 536)
- Darvish Z (Page: 418)
- Davari M (Page: 655)
- Dayani D (Page: 363)

Index by Authors in Cell Journal^(Yakhteh)
Vol 25, No 1-12, 2023

- Dehghani Ashkezari M (Page: 455)
Dehghani F (Page: 790)
Derakhshani A (Page: 822)
Dianatpour M (Page: 790)
Ding B (Page: 222)
Du X (Page: 570)
- E**
- Ebrahimdoost M (Page: 76)
Ebrahimi B (Page: 809)
Ebrahimi E (Page: 338)
Ebrahimi M (Pages: 92, 255)
Eghbali A (Page: 327)
El Agha E (Page: 372)
Emtiazi G (Page: 753)
Entezari M (Page: 102)
Eskandari F (Page: 536)
Eskandari N (Pages: 110, 307, 505)
Eslami N (Page: 772)
Esmaeili Tazangi P (Page: 273)
Etamadifar M (Page: 110)
Etesami E (Page: 45)
- F**
- Fadaei R (Page: 427)
Falak R (Page: 633)
Fallah S (Page: 427)
Fallahnezhad S (Page: 564)
Fan L (Page: 554)
Farbood Y (Page: 764)
Farhadian M (Page: 347)
Farhangniya M (Page: 874)
Farid Mojtahedi M (Page: 427)
Faridi M (Page: 809)
Farshchian M (Page: 696)
Fateh ST (Page: 73)
Fatemi MJ (Page: 281)
Fathi R (Page: 809)
Favaedi R (Page: 45)
- Feng S (Page: 570)
Feng Y (Page: 570)
Firouzi J (Page: 92)
Fu J (Page: 118)
- G**
- Ganji F (Page: 372)
Gao F (Page: 801)
Gao P (Page: 546)
Geranpayeh L (Page: 73)
Ghaeeni S (Page: 461)
Ghaemi F (Page: 92)
Ghafarian Choubdari M (Page: 847)
Ghaffari F (Page: 809)
Ghaffari SH (Page: 85)
Ghaheeri A (Page: 45)
Ghanadian M (Page: 110)
Ghanbari E (Page: 483)
Ghanbari S (Page: 418)
Ghannadian SM (Page: 307)
Ghashghaei Sh (Page: 143)
Ghayour-Mobarhan M (Page: 847)
Ghezelayagh Z (Page: 372)
Gholami M (Pages: 135, 741)
Gholampour MA (Page: 1)
Ghorbanian M (Page: 383)
Ghorbanian MT (Pages: 317, 383)
Ghorbanian Sh (Page: 317)
Ghotbizadeh Vahdani F (Page: 45)
Gohari K (Page: 203)
Golzadeh J (Page: 455)
Gramignoli R (Page: 524)
Gunduz O (Page: 753)
- H**
- Hadizadeh F (Page: 847)
Haghir H (Page: 564)
Hajifathali A (Page: 92)
Hajinasrollah M (Page: 338)
- Hajizadeh-Saffar E (Pages: 338, 854)
Hamed H (Page: 317)
Hashemi B (Page: 158)
Hashemi M (Page: 102)
Hassan M (Pages: 281, 524, 738)
Hassani SN (Pages: 338, 854)
Hassanzadeh H (Page: 696)
Hassanzadeh V (Page: 238)
Hatami Bavarsad N (Page: 783)
Hatamzadeh H (Page: 847)
Hedayati Asl AA (Page: 92)
Heidari D (Page: 513)
Heidarizadi S (Page: 741)
Hezavehei M (Page: 238)
Hosseini Mazinani F (Page: 327)
Hosseini MS (Page: 281)
Hosseini R (Page: 307)
Hosseini-Khannazer N (Pages: 363, 407, 524)
Hou K (Page: 625)
Houjun Z (Page: 264)
Houseini ST (Page: 354)
Hoveizi E (Page: 55)
Hu L (Page: 839)
Hu X (Page: 546)
Huang M (Page: 570)
- I**
- Irajirad R (Page: 126)
Izad M (Page: 717)
Izadi A (Page: 772)
Izadi M (Page: 455)
- J**
- Jadidi Kh (Page: 217)
Jafari R (Page: 505)
Jafarisani M (Page: 505)
Jafarzadeh Esfehiani R (Page: 696)
Jahanbakhsh J (Page: 427)

Index by Authors in Cell Journal^(Yakhteh)
Vol 25, No 1-12, 2023

- Jahangard L (Page: 783)
Jahanshahi A (Page: 273)
Jalili C (Page: 741)
Jamali B (Page: 102)
Jambar Nooshin B (Page: 35)
Jamshidizad A (Page: 655)
Janfada M (Page: 229)
Jangholi A (Page: 790)
Jomehpour M (Page: 229)
Jaroughi N (Page: 363)
- K**
Kaboli S (Page: 633)
Kamali-Dolat Abadi M (Page: 790)
Kang Y (Page: 391)
Kardar GA (Page: 633)
Karimi Darabi M (Page: 764)
Karimi Majd S (Page: 135)
Karimi SA (Page: 783)
Karimi Sh (Pages: 143, 363)
Kashani L (Page: 427)
Kasiri N (Pages: 110, 307)
Kaviani S (Page: 184)
Kazem Arki M (Pages: 363, 407)
Kazemnejad A (Pages: 203, 536)
Kerachian MA (Page: 194)
Keramati Z (Page: 194)
Khademi S (Page: 126)
Khamisipour GhR (Page: 76)
Khani MM (Page: 35)
Khatami M (Page: 813)
Khazaei M (Pages: 483, 496)
Kheirollah A (Page: 764)
Khodarahmian M (Page: 427)
Khodaverdi S (Page: 809)
Khoramipour M (Pages: 363, 407)
Khoshfetrat AB (Pages: 224, 839)
- Xhosravi M (Page: 229)
Xhosronezhad N (Page: 238)
Kiani S (Page: 772)
Kılıç GA (Page: 645)
Kim HJ (Page: 660)
Kompani F (Pages: 1, 85)
Kouhkan A (Page: 17)
Kvergelidze E (Page: 247)
Kwon JY (Page: 660)
- L**
Lai Y (Page: 546)
Li B (Page: 391)
Li H (Page: 570)
Li J (Pages: 222, 391)
Li R (Page: 554)
Li Y (Pages: 447, 570)
Lin H (Page: 625)
Liu J (Page: 546)
Liu L (Page: 447)
Liu Y (Page: 613)
Lotfinia M (Page: 524)
Lou X (Page: 447)
Lubberts E (Page: 300)
Luo CJ (Page: 391)
- M**
Madani H (Page: 363)
Mahaki B (Page: 741)
Mahdavi N (Pages: 363, 407)
Mahi H (Page: 505)
Makvand Gholipour N (Pages: 338, 854)
Mansouri K (Page: 741)
Mansouri P (Page: 300)
Mardpour S (Page: 363)
Masoomikarimi M (Page: 25)
Masoumi F (Page: 655)
Mazaheri F (Page: 455)
- Mehdipour A (Page: 483)
Mehdizadehkashi A (Page: 809)
Mehmandoostli Z (Page: 633)
Mikeladze D (Page: 247)
Mirahmadi M (Page: 847)
Miri-Lavasani Z (Pages: 363, 407)
Mirinezhad MR (Page: 847)
Mirnajafi-Zadeh J (Page: 273)
Mirzaalikhani Y (Page: 772)
Mirzaeian L (Page: 317, 383)
Mo Zh (Page: 829)
Moeinabadi Bidgoli K (Page: 363)
Moadab MA (Page: 790)
Moghadam Sh (Page: 73)
Mohamadi Farsani F (Page: 874)
Mohammadi M (Page: 76)
Mohammadi P (Page: 665)
Mohammadi SA (Page: 76)
Moini A (Page: 427)
Mokarram P (Page: 470)
Mokhber Dezfouli MR (Page: 372)
Mokhtari MJ (Page: 863)
Molazem M (Page: 338)
Moloudi MR (Page: 461)
Momeni S (Page: 51)
Montasser Kouhsari Sh (Page: 717)
Montazerabadi A (Page: 126)
Moradi Marjaneh M (Page: 696)
Moradi N (Page: 427)
Moradi S (Page: 496)
Moradi Y (Page: 813)
Mostafaei F (Page: 338)
Mostafaei Sh (Page: 203)
Motalleb Gh (Page: 194)
Mowla SJ (Page: 300)
Mozdarani H (Page: 688)

Index by Authors in Cell Journal^(Yakhteh)
Vol 25, No 1-12, 2023

Mozdziak P (Page: 317)

N

Naderi M (Page: 217)

Naderi N (Pages: 165, 706)

Najimi M (Page: 738)

Naseh M (Page: 790)

Naseri Mobaraki S (Page: 184)

Nasiri G (Page: 790)

Nasr-Esfahani A (Page: 727)

Nasr-Esfahani MH (Pages: 165, 437,
706, 727)

Nazari F (Page: 603)

Nazeri Z (Page: 764)

Nazifkar F (Page: 847)

Nemati F (Page: 354)

Niasari Naslji A (Page: 17)

Niknafs B (Page: 483)

Niknejad H (Page: 35)

Niknejadi M (Page: 363)

Nikukar H (Page: 45)

Nong XH (Page: 391)

Noorbakhsh F (Page: 25)

Noori A (Page: 372)

Nouri M (Pages: 281, 524)

Nouri S (Page: 753)

Nüssler AK (Page: 738)

O

Obeidi N (Page: 76)

Olfatbakhsh A (Page: 73)

Omid-Shafiei S (Page: 738)

P

Pakdel F (Page: 327)

Pang L (Page: 554)

Pangkahila WI (Page: 591)

Parsa S (Page: 300)

Parsa Sh (Page: 790)

Parvini N (Page: 92)

Pashaei K (Page: 727)

Peng B (Page: 264)

Pezeshki SP (Page: 764)

Phenegar J (Page: 854)

Pirani H (Page: 11)

Pooladi A (Page: 813)

Pourazar A (Page: 307)

Q

Qie S (Page: 613)

R

R Drevet J (Page: 437)

Rabiee F (Page: 706)

Rabiei N (Page: 347)

Rafatpanah H (Page: 696)

Rafeeinia A (Page: 764)

Rahdar A (Page: 194)

Rahimi Darehbagh R (Page: 813)

Rahimpour P (Page: 461)

Rahim-Tayfeh A (Page: 655)

Rahmani M (Page: 437)

Rahmani-Kukia N (Page: 470)

Rahmati M (Pages: 110, 307)

Rajabi S (Page: 372)

Rajabi Zangi A (Page: 655)

Rajaei S (Page: 25)

Ramazanali F (Page: 45)

Ramezani R (Page: 813)

Ranaei A (Page: 217)

Ranjesh MR (Page: 158)

Rashidi I (Page: 741)

Rashidi Z (Pages: 496, 741)

Rezaee Ranjbar Sardari R (Page: 455)

Rezaei N (Pages: 363, 407)

Rezazadeh Valojerdi M (Pages: 579, 809)

Roghanian R (Page: 753)

Roshangar L (Page: 158)

Rostami F (Page: 383)

Rostami R (Page: 427)

Rostami Sh (Page: 85)

S

Saberi S (Page: 203)

Sabzalizadeh M (Page: 822)

Sadeghi E (Page: 579)

Sadeghi N (Page: 165)

Sadeghian Chaleshtori S (Page: 372)

Sadighi Gilani MA (Page: 17)

Safa M (Page: 92)

Safari A (Pages: 255, 863)

Saidijam M (Page: 783)

Salehi M (Page: 25)

Salehi N (Page: 874)

Salehi OR (Page: 11)

Salehi-Najafabadi A (Page: 73)

Salehnia M (Page: 579)

Saliani N (Page: 717)

Samadikuchaksaraei A (Page: 874)

Sanjari MS (Page: 327)

Sarami Forroshani R (Page: 73)

Sargolzaei J (Page: 603)

Sarihi A (Page: 783)

Satarian L (Page: 327)

Sattari A (Page: 354)

Sayadmanesh A (Page: 674)

Sazegar Gh (Page: 564)

Sazgarnia A (Page: 51)

Seifati SM (Page: 455)

Servatian N (Page: 176)

Seydabadi S (Page: 45)

Seyedoshohadaei SA (Page: 813)

Seyedsadr M (Page: 327)

Shafaei H (Page: 674)

Index by Authors in Cell Journal^(Yakhteh)
Vol 25, No 1-12, 2023

- Shafiei R (Page: 753)
Shafiyani S (Page: 363)
Shahhoseini M (Pages: 45, 238)
Shahkarami S (Page: 85)
Shahrabaf MA (Page: 212)
Shahriari E (Page: 783)
Shahverdi AH (Pages: 17, 238)
Shahzadeh Fazeli SA (Page: 176)
Shams MH (Page: 505)
Shamsara M (Page: 655)
Shamsoddini A (Page: 513)
Shanehbandi D (Page: 674)
Shanei A (Page: 51)
Shayan Asl N (Pages: 92, 255)
Sheibani V (Page: 822)
Sheidaei A (Page: 203)
Sheikholeslami-Vatani D (Page: 461)
Shekari F (Pages: 73, 772)
Sheng H (Page: 570)
Shirvani H (Page: 513)
Shojaei A (Page: 273)
Shpichka A (Page: 281)
Soheili ZS (Page: 300)
Soleimani M (Page: 176)
Soltanian AR (Pages: 347, 783)
Sun L (Page: 570)
Sun Y (Page: 801)
Szeberényi J (Page: 247)
- T**
Taghian Dinani H (Page: 706)
Taj Sharghi A (Page: 363)
Tahamtani T (Page: 372)
Tahmasebi F (Page: 564)
Tapak L (Page: 418)
Tavakol Sh (Page: 513)
Tavalaee M (Pages: 437, 706)
- Tavallaie Sh (Page: 847)
Tayebi B (Pages: 338, 854)
Tayebi T (Page: 35)
Tehrani A (Page: 427)
Timashev P (Page: 281)
Toghyani M (Page: 110)
Tong X (Page: 570)
Torabi Sh (Page: 524)
Toufan F (Page: 505)
- V**
Vaezi M (Page: 85)
Vahdat S (Page: 229)
Valipour Motlagh A (Page: 727)
Vaziri Nezamdoost F (Page: 126)
Vosough M (Pages: 143, 212, 281, 363, 407, 524, 738)
- W**
Wahyuniari IAI (Page: 591)
Wahyuningsih KA (Page: 591)
Wang L (Pages: 222, 625)
Wang Sh (Page: 801)
Wang X (Pages: 399, 801)
Wang Y (Pages: 570, 613)
Wang Zh (Page: 829)
Wei W (Page: 391)
Wen Y (Page: 554)
Weta IW (Page: 591)
Widiana IGR (Page: 591)
Woo SY (Page: 660)
Wu J (Page: 447)
- X**
Xiong H (Page: 613)
Xiong XQ (Page: 391)
Xu WX (Page: 118)
- Y**
Yahyaee A (Page: 809)
- Yan C (Page: 613)
Yang D (Page: 291)
Yang L (Page: 839)
Yari K (Page: 674)
Yarmohammadi M (Page: 505)
Yekani F (Page: 73)
Yektadoust E (Page: 665)
Yin J (Page: 399)
Younesian S (Page: 85)
Yousefi Gh (Page: 790)
Yousefi Z (Page: 505)
Yousefi-Najafabadi Z (Page: 633)
Yu H (Page: 291)
Yu M (Page: 118)
Yu Sh (Page: 118)
Yu X (Page: 801)
Yunxia Li (Page: 570)
- Z**
Zahedi AS (Page: 536)
Zamani M (Page: 470)
Zamanian MR (Page: 45)
Zangeneh Motlagh M (Pages: 363, 407)
Zare L (Page: 327)
Zareh-Khoshchereh R (Page: 62)
Zarei-Kheirabadi M (Page: 327)
Zarrabi M (Pages: 281, 524)
Zeng X (Page: 546)
Zhang J (Pages: 391, 447)
Zhang M (Page: 554)
Zhang X (Page: 399)
Zhao T (Page: 554)
Zheng Y (Page: 399)
Zhou Y (Pages: 554, 625)
Zomorodipour A (Page: 655)